

**The role of biofilms in recurrent *Clostridioides difficile*
infection and the interaction of *C. difficile* in
multispecies biofilms**

Charmaine Normington

Submitted in accordance with the requirements for the degree of
Doctor of Philosophy

The University of Leeds
Leeds Institute of Medical Research,
Faculty of Medicine & Health

January, 2020

The candidate confirms that the work submitted is her own, except where work which has formed part of jointly authored publications has been included. The contribution of the candidate and the other authors to this work has been explicitly indicated below. The candidate confirms that appropriate credit has been given within the thesis where reference has been made to the work of others. The jointly authored publication and the contributed work is listed below;

Moura, I.B., Normington, C., Ewin, D. *et al.* Method comparison for the direct enumeration of bacterial species using a chemostat model of the human colon. *BMC Microbiol* 20, 2 (2020).

Author contributions were as follows; design and data analysis (IBM and AMB), data generated (IBM, AMB, CN, DE, EC), drafting of manuscript (IBM, MHW and AMB). Regarding this publication, I (the candidate), assisted in the planning, execution and data generation from the gut model experiments.

Bacterial taxonomic sequencing and bile acid analysis used in Chapters 3 and 4 were performed through Seres Therapeutics proprietary pipelines.

Specifically, I assisted in the execution of the gut model experiments and obtained the samples for analysis. For the bacterial taxonomic sequencing, I performed the DNA extractions, quantification and purifications.

This copy has been supplied on the understanding that it is copyright material and that no quotation from the thesis may be published without proper acknowledgement.

The right of Charmaine Normington to be identified as Author of this work has been asserted by her in accordance with the Copyright, Designs and Patents Act 1988.

© 2020 The University of Leeds and Charmaine Normington

Acknowledgements

Taking on a PhD has been one of the most challenging experiences of my life and I could not have reached this point without the help and support of the people around me. No words can accurately portray my absolute gratitude to you all.

First and foremost, I would like to thank my supervisor, Dr Anthony Buckley. You have been a constant source of inspiration and encouragement. At my lowest points, you were always there to pick up the pieces and encourage me to carry on and forge ahead to the finish line. I have no doubt that I would not be here without your support. I would also like to specifically thank the rest of my supervisory team, Professor Mark Wilcox and Dr Caroline Chilton, for giving me this incredible opportunity and your consistent guidance and support. It has been an absolute pleasure working with you. I gratefully acknowledge the additional funding I received towards my PhD from Seres Therapeutics and the Rosetrees Trust.

The gut model work presented in this thesis was a huge undertaking and would not have been possible without the assistance of the Healthcare Associated Infection Research Group (HCAI) which included Emma Clark, Duncan Ewin, Hannah Harris, Ines Moura, Kate Owen, Sally Pilling, Sharie Shearman and William Spittal. I would like to extend huge thank you to all members for their help and patience, and for creating a fun and friendly environment that made the laboratory work a pleasure. I would like to acknowledge the assistance of Mr Martin Fuller, Astbury Centre for Structural Molecular Biology and Mr Stuart Micklethwaite, Leeds Electron Microscopy and Spectroscopy Centre, The University of Leeds, for all their help in generating the fantastic SEM images used in this thesis.

I would also like to thank Dr Kerrie Davies and Dr Jane Freeman for all their emotional support. Whether it was a shoulder to cry on or a kind word, your help and encouragement was greatly needed and appreciated. To Dr Louissa Macfarlane-Smith (Rust), you never failed to make me smile. Thank you for being a source of comfort, strength and friendship.

To my family. Mom, Dad, David, Sandy and Michelle (Princess Anna), words cannot describe my gratitude. Your support and belief in me was unwavering and I love you all. You made me believe anything was possible, and here we are. My lovely boys, Dale and Ben, thank you for your patience and understanding. And finally, my wonderful hubby, Mr K, you have been my rock and every day I am grateful for you.

Abstract

Clostridioides difficile infection (CDI) is the leading cause of infective antibiotic-associated diarrhoea and is responsible for significant patient morbidity and mortality. Despite appropriate antimicrobial therapy, CDI recurs in approximately 20-30 % of cases, suggesting that *C. difficile* can occupy a protective niche whereby antimicrobial therapy is ineffective. Biofilms represent such a potential niche. We sought to determine the role of biofilms in recurrent CDI (rCDI) and how the sessile community can affect *C. difficile* biofilm formation.

A triple stage chemostat model of the human colon was used to predict the efficacy of a simulated faecal microbiota transplantation (FMT) and two different dosing regimens of a spore consortium, SER-109, to prevent rCDI and to define a role for biofilms in rCDI. Planktonic and biofilm communities were individually analysed using culture-based techniques and bacterial taxonomic sequencing. Bile acid levels were monitored to investigate potential mechanisms of efficacy. A biofilm batch culture assay was used to investigate the influence of biofilm-associated microbiota on *C. difficile* biofilm formation.

Results show that FMT and a triple dose of SER-109 successfully prevented rCDI, potentially due to reducing the levels of primary bile acids through conversion to secondary bile acids. Despite the ability of microbiome therapies to prevent rCDI, they failed to eradicate *C. difficile* from the biofilm, suggesting a risk of future CDI. The biofilm-associated *C. difficile* was able to seed the planktonic phase, resulting in *C. difficile* germination and proliferation, which proved to be sufficient to induce CDI. Biofilm batch culture experiments indicate that commensal biofilm populations can reduce or increase *C. difficile* biofilm formation and growth, which required the presence of viable cells.

We conclude that biofilms provide a protective niche for *C. difficile*, which facilitates CDI recurrence, and that patients undergoing microbiome-based therapies potentially remain at risk of CDI with subsequent antibiotic use.

Table of Contents

Acknowledgements	ii
Abstract	iv
List of Tables	ix
List of Figures	x
Abbreviations	xiii
Chapter 1 Introduction	1
1.1 <i>Clostridium difficile</i>	1
1.1.1 History	1
1.1.2 Clinical manifestations and risk factors	2
1.1.3 CDI recurrence.....	3
1.1.4 Epidemiology.....	5
1.1.5 Pathogenesis	6
1.1.6 Virulence factors	9
1.1.7 Current Diagnosis and Treatment	21
1.1.8 Models used to study CDI	23
1.2 The intestinal microbiota.....	32
1.2.1 Intestinal dysbiosis.....	33
1.2.2 Microbial based therapies	34
1.3 Biofilms.....	39
1.3.1 Biofilm formation and development.....	40
1.3.2 Characteristics of biofilms	49
1.3.3 Methods used in biofilm culture and quantification.....	58
1.4 Rationale	63
1.5 Aims	64
1.5.1 Primary objectives.....	64
Chapter 2 Materials and Methodology	65
2.1 Chemicals and Agars	65
2.2 <i>In vitro</i> gut model experiments	65
2.2.1 Ethical approval.....	65
2.2.2 Participant recruitment and specimen collection	65
2.2.3 Screening of faeces	66
2.2.4 Preparation of the faecal slurry	66
2.2.5 Viability of frozen faeces	67

2.2.6	<i>C. difficile</i> strain.....	67
2.2.7	Spore preparation and purification	67
2.2.8	The <i>in vitro</i> gut model set up	68
2.2.9	Preparation of Gut Model Growth Medium	71
2.2.10	Experimental design.....	73
2.2.11	Sampling planktonic populations.....	74
2.2.12	Sampling biofilm populations.....	75
2.2.13	Matrix-assisted laser desorption/ionisation (MALDI TOF) analysis	76
2.2.14	DNA extraction and taxonomic sequencing of the biofilm	79
2.2.15	Bile acid analysis and quantification.....	80
2.2.16	Cytotoxin assay.....	80
2.2.17	Antimicrobial bioassays.....	83
Chapter 3 Resolution of simulated recurrent CDI using FMT; delineating the sessile and planktonic populations		85
3.1	Background	85
3.1.1	Rationale.....	86
3.2	Methodology.....	87
3.2.1	Experimental design.....	87
3.2.2	Preparation of the FMT faecal slurry	89
3.2.3	Administration of the simulated FMT	89
3.3	Results	92
3.3.1	Viability of frozen faecal slurry.....	92
3.3.2	Planktonic population kinetics	93
3.3.3	Biofilm population kinetics	101
3.4	Discussion	114
Chapter 4 Increased dosing of targeted microbiome therapeutic SER-109 prevents rCDI in an <i>in vitro</i> model of the human gut.		120
4.1	Background	120
4.1.1	Rationale.....	121
4.2	Methodology.....	122
4.2.1	Experimental design.....	122
4.2.2	Preparation of SER-109 spores.	124
4.2.3	Detection of quorum sensing Autoinducer-2 in biofilms	124
4.3	Results	126
4.3.1	Multiple changes to planktonic populations after antibiotic treatment.....	126

4.3.2	Only three doses of SER-109 successfully prevented rCDI.....	126
4.3.3	Increased exposure to cholic acid corresponds with rCDI...	127
4.3.4	Biofilm population diversity increased after multiple SER-109 doses	132
4.3.5	Evidence of AI-2 mediated quorum sensing in biofilms.....	136
4.4	Discussion	141
Chapter 5 Influence of intestinal microorganisms on <i>C. difficile</i> biofilm formation		146
5.1	Background	146
5.1.1	Rationale	147
5.2	Methods.....	148
5.2.1	Bacterial Strains and growth conditions	148
5.2.2	Microbial isolation from the <i>in vitro</i> gut models.....	148
5.2.3	Biofilm assay	151
5.2.4	Semi-quantitative Crystal Violet (CV) assay for total biofilm biomass.....	153
5.2.5	Total viable and spore counts	153
5.2.6	Effect of culture media pH on <i>C. difficile</i> biofilm formation ..	154
5.2.7	Co- and poly culture biofilm assay	154
5.2.8	Co-culture biofilms with cell free supernatants	156
5.2.9	<i>C. difficile</i> cytotoxin testing	158
5.2.10	Scanning Electron Microscopy – sample preparation and biofilm imaging	158
5.2.11	Statistical analysis and graphical software	158
5.3	Results	160
5.3.1	Characterisation of the <i>C. difficile</i> biofilm	160
5.3.2	Impact of pH on biofilm formation.....	163
5.3.3	The effect of microorganisms isolated from the GI tract on <i>C. difficile</i> biofilm formation.....	165
5.3.4	Effect of poly-culture biofilms on <i>C. difficile</i> biofilm formation.....	173
5.4	Discussion	180
Chapter 6 Sessile <i>C. difficile</i> cells can contribute towards recurrent disease		186
6.1	Background	186
6.1.1	Rationale	187
6.2	Materials and Methodology	188

6.2.1	Donor screening and slurry preparation	188
6.2.2	The <i>in vitro</i> gut model set up	188
6.2.3	Experimental design.....	189
6.3	Results	193
6.3.1	Donor model.....	193
6.3.2	Recipient Model (R) and Control Model (C)	197
6.4	Discussion	203
Chapter 7 Conclusions.....		207
7.1	Study limitations and further work	211
References.....		214
Appendix		274

List of Tables

Table 2-1 Composition of the <i>in vitro</i> gut model culture media.	72
Table 2-2 Target microorganisms enumerated from the gut model experiments and appropriate culture media and growth conditions for their isolation.....	78
Table 3-1 Biofilm sampling schedule.	91
Table 3-2 Comparison of the total viable counts of bacteria in the defrosted faecal emulsion used to seed the gut models.....	93
Table 3-3 Peak clindamycin and vancomycin concentrations (mg/L) and corresponding treatment day in model A and model B.	98
Table 4-1 Biofilm sampling schedule of the SER-109 single and triple dose models.	124
Table 5-1 Additional agars used to expand recoveries of sessile populations in the gut models.	149
Table 5-2 Microbial strains used in co- and poly culture experiments, including source, culture conditions and MALDI-TOF analysis score.....	150
Table 5-3 Microbial combinations for poly-culture biofilms.	156

List of Figures

Figure 1-1. The <i>C. difficile</i> recurrence escalator. In patients with CDI, there is an increased risk of further disease recurrence with each subsequent episode of rCDI.....	4
Figure 1-2. <i>C. difficile</i> transmission and pathogenesis in the human gastrointestinal tract.....	8
Figure 1-3. Structure of <i>C. difficile</i> toxins A (tcdA) and B (TcdB).....	10
Figure 1-4. The pathogenicity locus of <i>C. difficile</i>	13
Figure 1-5 Developmental model of biofilm formation.....	41
Figure 1-6 Confocal laser-scanning analysis of stained <i>C. difficile</i> biofilms.....	47
Figure 1-7 Scanning electron microscopy of <i>C. difficile</i> biofilms.....	50
Figure 1-8 Theoretical simulation of the development of phenotypic heterogeneity within biofilms in response to environmental pressure. .	52
Figure 2-1 The Leeds <i>in vitro</i> gut model set-up.....	70
Figure 2-2 Biofilm vessel from the <i>in vitro</i> gut model.....	71
Figure 2-3 The general gut model timeline.....	74
Figure 2-4 Biofilm support structure with multispecies biofilm attached.	75
Figure 2-5 Biofilm sampling procedure.....	76
Figure 2-6 Graphical representation of the cytotoxin assay set up.....	82
Figure 2-7 Image of Vero cell growth and appearance during the cytotoxicity assay.	83
Figure 2-8 Antimicrobial bioassay plate.....	84
Figure 3-1 The <i>in vitro</i> gut model timeline for the rCDI model (A) and the FMT model (B).....	88
Figure 3-2 Simulated faecal microbiota transplantation (FMT) instillation into the triple stage gut model.....	90
Figure 3-3 Enumeration of planktonic anaerobes in (a) the <i>C. difficile</i> recurrence model (model A) and (b) the simulated FMT model (model B).	95
Figure 3-4 Enumeration of planktonic facultative anaerobes in (a) the <i>C. difficile</i> recurrence model (model A) and (b) the simulated FMT model (model B).	96
Figure 3-5 Enumeration of planktonic <i>C. difficile</i> total and spore counts in (a) the <i>C. difficile</i> recurrence model (model A) and (b) the simulated FMT model (model B).	99
Figure 3-6 Biofilm formation in the gut model.....	102

Figure 3-7 Enumeration of biofilm anaerobes in (a) the <i>C. difficile</i> recurrence model (model A) and (b) the simulated FMT model (model B).	104
Figure 3-8 Enumeration of biofilm facultative anaerobes in (a) the <i>C. difficile</i> recurrence model (model A) and (b) the simulated FMT model (model B).....	105
Figure 3-9 Enumeration of <i>C. difficile</i> total and spore counts recovered from the biofilm in models A and B.	108
Figure 3-10 Changes in bacterial taxonomic abundance of the biofilm microbial community at selected time points in the recurrence model (A) and the simulated FMT model (B).....	110
Figure 3-11 Shannon Diversity Index of biofilm samples from model A and model B.....	111
Figure 3-12 Bile acid analysis of the <i>C. difficile</i> recurrence model (A) and the faecal microbiota transplant model (B).....	113
Figure 4-1 The <i>in vitro</i> gut model timeline for SER-109 dosing regimes. ...	123
Figure 4-2 Enumeration of planktonic anaerobes in (a) the single SER-109 dose model and (b) the triple SER-109 dose model.....	128
Figure 4-3 Enumeration of planktonic facultative anaerobes in (a) the single SER-109 dose model and (b) the triple SER-109 dose model.....	129
Figure 4-4 Enumeration of planktonic <i>C. difficile</i> total and spore counts in (a) the single SER-109 dose model and (b) the triple SER-109 dose model.....	130
Figure 4-5 Bile acid analysis of the (a) 1 SER-109 dose model and (b) 3 SER-109 doses model.....	131
Figure 4-6 Enumeration of biofilm anaerobes in (a) the single dose SER-109 model and (b) the triple dosed SER-109 model.....	133
Figure 4-7 Enumeration of biofilm facultative anaerobes in (a) the single dose SER-109 model (b) the triple dosed SER-109 model.....	134
Figure 4-8 Enumeration of <i>C. difficile</i> total and spore counts recovered from the biofilm in the SER-109 gut models.....	135
Figure 4-9 Changes in bacterial taxonomic abundance of the biofilm microbial community at selected time points in the (a) single dose SER-109 model and (b) the triple dosed SER-109 model.....	138
Figure 4-10 Shannon Diversity Index of biofilm samples from the SER-109 triple stage gut models.....	139
Figure 4-11 <i>Vibrio campbellii</i> bioluminescence in response to the presence of Autoinducer-2 molecules in biofilms isolated from gut models dosed with SER-109.....	140
Figure 5-1 The biofilm batch culture assay set up and analysis.....	152
Figure 5-2 Inoculation of the biofilm batch culture experiments for co- and poly-culture assays.....	157
Figure 5-3 Crystal Violet staining and enumeration of <i>C. difficile</i> ribotype 027 strains R20291 and 210 biofilms.....	161

Figure 5-4 Scanning electron microscopy of <i>C. difficile</i> R20291 biofilms grown for 3 days.....	162
Figure 5-5 Crystal violet quantification and enumeration of <i>C. difficile</i> from biofilms formed in medium with different levels of pH.....	164
Figure 5-6 Quantification of mono and co-culture biofilms using the crystal violet assay.....	167
Figure 5-7 Co-culture biofilm experiments between <i>C. difficile</i> and <i>L. rhamnosus</i>	170
Figure 5-8 Co-culture biofilm experiments between <i>C. difficile</i> and <i>B. longum</i>	171
Figure 5-9 <i>C. difficile</i> toxin production in co-culture biofilms.....	172
Figure 5-10 Poly-microbial biofilm culture of <i>C. difficile</i> with <i>B. longum</i> and <i>B. thetaiotaomicron</i>	174
Figure 5-11 Poly-microbial biofilm culture of <i>C. difficile</i> with <i>C. butyricum</i> and <i>M. morgani</i>	176
Figure 5-12 Poly-microbial biofilm culture of <i>Clostridium difficile</i> with <i>S. aureus</i> and <i>Candida albicans</i>	177
Figure 5-13 False-coloured scanning electron microscopy image of 3 day old mono- and poly-microbial biofilms.....	178
Figure 5-14 Poly-microbial biofilm culture of <i>Clostridium difficile</i> with <i>L. rhamnosus</i> and <i>Candida albicans</i>	179
Figure 6-1 The Recipient and Control <i>in vitro</i> gut model set up.	189
Figure 6-2 Model timeline of the biofilm transplant experiment.....	190
Figure 6-3 Diagram of the gut model set-up for the donor model, the recipient model and the control model, illustrating the transplantation of biofilm support structures.....	192
Figure 6-4 Enumeration of planktonic populations in the <i>in vitro</i> Donor gut model.....	195
Figure 6-5 Enumeration of planktonic and sessile <i>C. difficile</i> total and spore counts in the <i>in vitro</i> Donor gut model.....	196
Figure 6-6 Enumeration of planktonic anaerobes in (a) the recipient model and (b) the control model.	199
Figure 6-7 Enumeration of planktonic facultative anaerobes in (a) the recipient model and (b) the control model.....	200
Figure 6-8 Enumeration of planktonic <i>C. difficile</i> total and spore counts in (a) vessel two and (b) vessel three of the recipient model (model R)....	201
Figure 6-9 Enumeration of planktonic <i>C. difficile</i> total and spore counts in (a) vessel two and (b) vessel three of the control model (model C).....	202

Abbreviations

AB	Autoinducer bioassay
ADD	Antibiotic associated disease
AHLs	N-acyl-homoserine lactones
AI-2	Autoinducer-2
AIPs	Autoinducing peptides
APD	Autoprotease domain
AU	Absorbance units
BHI	Brain-heart infusion
CA	Cholic acid
CcpA	Carbon catabolite control protein A
CaDPA	Ca-dipicolinic acid
CAMPS	Cationic antimicrobial peptides
CBA	Columbia blood agar
CCEY	Cefoxitin cycloserine egg yolk agar
CD	<i>C. difficile</i>
CDI	<i>C. difficile</i> infection
C-di-GMP	Cyclic dimeric guanosine monophosphate
CDRN	<i>C. difficile</i> Ribotyping Network
CDT	Binary toxin
CFS	Cell free supernatant
CFU	Colony forming unit
CLE	Cortex lytic enzymes
Clind	Clindamycin
CROPS	Combined repetitive oligopeptides
CSPG4	Chondroitin sulphate proteoglycan 4
CV	Crystal Violet
CWP	Cell wall protein
DCA	Deoxycholic acid
DGC	Diguanylate cyclase
ECM	Extracellular matrix
eDNA	Extracellular DNA
EDTA	Ethylenediaminetetraacetic acid
EHEC	Enterohemorrhagic <i>Escherichia coli</i>
EPS	Extracellular polymeric substances
ESBL	Extended-spectrum beta-lactamase
ESCMID	European Society for Clinical Microbiology and Infectious Disease
EUCLID	European, multicentre, prospective, biannual, point-prevalence study of <i>Clostridium difficile</i> infection in hospitalised patients with diarrhoea
FAA	Fastidious anaerobe agar
FESEM	Field Emission Scanning Electron

	Microscopy
FFT	Faecal filtrate transfers
FMT	Faecal microbiota transplantation
FnBP	Fibronectin-binding protein
FZD	Frizzled
GDH	Glutamate dehydrogenase
GHP	Hydrophilic polypropylene
GI	Gastrointestinal
GTD	Glucosyltransferase domain
GTPases	Guanosine triphosphatases
HCAI	Healthcare Associated Infection Research Group
HIF	1 α - hypoxia-inducible factor 1
HIOs	Human intestinal organoids
HMW-SLP	High molecular weight surface layer protein
HPLC	High-performance liquid chromatography
HTA	Human Tissue Act
IBD	Inflammatory bowel disease
IC	Immunocompromised
IDSA	Infectious Disease Society of America
KO	Knockout
LB	Luria-Bertani
LC-MS	Liquid chromatography-mass spectrometry
LF	Lactose fermenting
LMW-SLP	Low molecular weight surface layer protein
LSR	Lipolysis-stimulated lipoprotein receptor
MALDI-TOF	Matrix-assisted laser desorption ionisation – time of flight
MIC	Minimum inhibitory concentration
MRS	De Man, Rogosa, Sharpe
NAAT	Nucleic acid amplification test
NADPH	Nicotinamide adenine dinucleotide phosphate
NCTC	National Collection of Type Cultures
NHE3	Sodium-hydrogen exchange 3
nCFS	Neutralised cell free supernatant
NOX	Oxidase complex
OGYEA	Oxytetracycline glucose yeast extract agar
Oxo-Bas	Oxo-bile acids
PaLoc	Pathogenicity locus
PBS	Phosphate buffered saline
PDE	Phosphodiesterase
PMC	Pseudomembranous colitis
PSII	Polysaccharide II
PVRL3	Poliovirus receptor-like protein 3
qPCR	Quantitative polymerase chain reaction

qTOF-MS	Quadrupole time-of-flight mass spectrometry
QS	Quorum sensing
rCDI	Recurrent CDI
Redox	Reduction-oxidation
ROS	Reactive oxygen species
rRNA	Ribosomal RNA
RU	Relative units
SCFA	Short-chain fatty acid
SDW	Sterile distilled water
SHEA	Society for Healthcare Epidemiology of America
S-layer	Surface layer
SLPs	Surface layer proteins
SPRE	Surface protein releasing enzyme
SRB	Sulphate-reducing bacteria
T4P	Type IV pili
TA	Toxin/antitoxin systems
TcdA	<i>C. difficile</i> toxin A
TcdB	<i>C. difficile</i> toxin B
TVC	Total viable count
UDP	Uridine diphosphate
Vanc	Vancomycin
VBNC	Viable nonculturable cells
VRE	Vancomycin resistant enterococci
WPR	Weighted pooled rates
WT	Wild type

Chapter 1 Introduction

1.1 *Clostridium difficile*

1.1.1 History

Clostridium difficile was first isolated from the stool of healthy neonates by Hall and O'Toole in 1935. Originally named '*Bacillus difficilis*' due to the difficulty experienced when isolating and culturing the organism, they found that the bacterium was highly pathogenic to animals (Hall and O'Toole, 1935). Hall and O'Toole suggested the pathogenicity of this obligate anaerobe was mediated through the action of a toxin, which was later confirmed by Snyder in 1937 (Snyder, 1937) who further described it as a Gram-positive, spore forming bacillus that produced a heat labile exotoxin. They also observed that this bacterium was found as part of the commensal flora of roughly 10 % of infants, carried asymptotically. However, the link between *C. difficile* and human disease was not established for another four decades.

The earliest reports of pseudomembranous colitis (PMC) occurred in 1983 when Finney, a surgeon at Johns Hopkins Hospital, described a case of 'pseudodiphtheritic enteritis' of the ileum and colon of a patient (Finney, 1983). Subsequently, various reports of a similar nature emerged with the cause attributed to staphylococcal enterocolitis, vascular insufficiency and neonatal necrotizing enterocolitis (Gorbach, 2014). The association between diarrhoea and colitis with antibiotic treatment became apparent in 1973 with cases of pseudomembranous colitis linked to prior use of lincomycin (Scott *et al.*, 1973) and clindamycin (Tedesco *et al.*, 1974). This was further demonstrated using a hamster model of clindamycin-associated colitis, revealing the role of a toxin-producing species of *Clostridium* (Bartlett *et al.*, 1977). Studies on the stool of patients with PMC revealed the cause to be a bacterial produced toxin, which effects could be neutralised by gas-gangrene antitoxin (Larson *et al.*, 1977, Larson and Price, 1977, Bartlett *et al.*, 1978). This neutralising effect was later attributed to *Clostridium sordellii* antitoxin, and hence *C. sordellii* was believed to be the aetiological agent in PMC; however, it could not be recovered from

the stool of patients (Rifkin *et al.*, 1977). *C. difficile* was later isolated in large quantities from patients with antibiotic-associated colitis and was demonstrated to produce a cytotoxin that could be neutralised by *C. sordellii* antitoxin and hereby found to be the aetiological agent in antibiotic-associated diarrhoea and colitis (George *et al.*, 1978a, George *et al.*, 1978b, Bartlett *et al.*, 1979)

C. difficile is now recognised as the leading cause of infective antibiotic-associated diarrhoea in the healthcare setting; however, reports of community acquired CDI rates are increasing (Ofori *et al.*, 2018). Highly resilient spores and recalcitrance to antibiotic treatment has led to the persistence of *C. difficile* infection (CDI) in susceptible patients and healthcare facilities, leading to significant morbidity, mortality and economic burden worldwide. Although officially renamed *Clostridioides difficile* in 2016 (Lawson *et al.*, 2016), *Clostridium difficile* is still the preferred name in current literature and therefore will be referred to as such in this thesis.

1.1.2 Clinical manifestations and risk factors

CDI can present in a variety of disease states, ranging from mild self-limiting diarrhoea to life threatening complications and death. The wide range of clinical manifestations of CDI is a result of host-specific factors (immune status, age and underlying medical conditions) and virulence of the infecting strain. CDI is responsible for between 15-25 % of antibiotic-associated diarrhoea (AAD) (Bartlett and Gerding, 2008) and in the majority of cases symptoms appear a few days after antibiotic use; however, onset may occur concurrently with antibiotic treatment or several weeks following a treatment course (Mogg *et al.*, 1979). Initial symptoms include watery diarrhoea, raised white blood cell counts, raised temperature and fever, hypoalbuminaemia and abdominal discomfort that can rapidly progress to extensive colonic inflammation (Mogg *et al.*, 1979, Bartlett *et al.*, 1980). *C. difficile* is the leading cause of PMC, an advanced stage of CDI, in which lesions of immune cells, necrotic tissue and mucous form plaques that combine in a pseudomembrane, accompanied by fever and leucocytosis (Farooq *et al.*, 2015). In some cases, fulminant colitis occurs, manifesting as acute toxic colitis with colonic and abdominal distension, leading to toxic megacolon, colonic perforation, toxic shock and death (Dallal *et al.*, 2002). Conversely, *C. difficile* may be carried without causing clinical symptoms (asymptomatic carriage).

One of the most significant risk factors for the development of CDI is the use of antibiotics (Spencer, 1998). Antibiotics with the highest risk of predisposing to CDI include ampicillin, amoxicillin, third-generation cephalosporins, clindamycin and fluoroquinolones (de Lalla *et al.*, 1989, Pepin *et al.*, 2005, Vardakas *et al.*, 2012, Leffler and Lamont, 2015). The tendency of certain antibiotics to contribute to the development of CDI could be due to the effect they have on the hosts' microbiome and no activity against *C. difficile*, with increased microbiota disruption linked to increased rates of CDI (Pultz and Donskey, 2005). Advanced age was also highlighted as one of the major risk factors in the development of CDI (McFarland *et al.*, 1999). A prospective population-based analysis in Sweden showed that CDI incidence increased 10 fold over 60 years of age (Karlstrom *et al.*, 1998). Other risk factors for the development of CDI include severe underlying conditions, hospitalisation (especially admittance to the intensive care unit), long-term care facility residence, gastrointestinal (GI) surgery, inflammatory bowel disease, use of gastric acid suppressants, immunosuppression and immunodeficiency (Brown *et al.*, 1990, Fekety and Shah, 1993, McFarland *et al.*, 1999, Rupnik *et al.*, 2009, Vestreinsdottir *et al.*, 2012, Tariq *et al.*, 2017)

1.1.3 CDI recurrence

Despite appropriate antimicrobial therapy, CDI can recur in approximately 20 – 30 % of cases (Kelly and LaMont, 2008, Cornely *et al.*, 2012b). In addition, the risk of further recurrent CDI (rCDI) increases with each subsequent episode (McFarland *et al.*, 1994, McFarland *et al.*, 2002), reaching up to 40 – 60 % (Figure 1-1). rCDI has a significant impact on patients and healthcare resources (Kelly and LaMont, 2008, Wilcox *et al.*, 2017a), with a higher risk of mortality compared to first episode CDI (36 % vs 26 %, $p < 0.001$) (Olsen *et al.*, 2015). rCDI is defined as an additional episode of CDI occurring within 8 weeks of a previous episode (Debast *et al.*, 2014). The majority of recurrences were found to be caused by the same strain isolated in the original episode of CDI, with studies suggesting that in over 80 % of cases, the original strain was responsible for recurrences rather than reinfection with a different strain (Figueroa *et al.*, 2012). More recently, an extended period of 20 weeks instead of the current 8 weeks was proposed to distinguish rCDI with the same strain from reinfection with a different strain (Durovic *et al.*, 2017).

It is believed that rCDI is linked to prolonged intestinal dysbiosis caused by the antibiotics used to treat the initial infection (Kelly and LaMont, 2008). Recurrence rates were similar in patients treated with either metronidazole or vancomycin for their initial episode; whereas fidaxomicin has a significantly lower risk of recurrence, most likely due to the relative narrow spectrum of activity causing less disruption to the microbiota and its anti-sporulation effects (Kelly and LaMont, 2008, Louie *et al.*, 2011, Cornely *et al.*, 2012a, Zhanel *et al.*, 2015). The host's immune response has also been implicated in the risk of developing rCDI, with increased levels of antibodies against either toxin A or toxin B resulting in a protective effect against rCDI (Kyne *et al.*, 2001, Gupta *et al.*, 2016). A human monoclonal antibody against *C. difficile* toxin B (bezlotoxumab) used as an adjunctive therapy alongside standard-of-care therapy, showed a 38 % lower rate of rCDI than that associated with standard-of-care therapy alone (Wilcox *et al.*, 2017b). Interestingly, the human monoclonal antibody against *C. difficile* toxin A (actoxumab) showed no protective effect against rCDI and had no additional benefit when added in combination with bezlotoxumab, suggesting a stronger role for toxin B in CDI in humans.

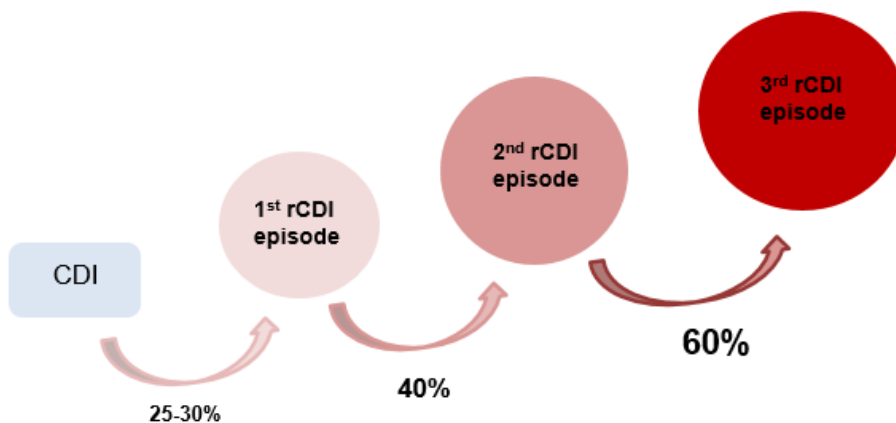


Figure 1-1. The *C. difficile* recurrence escalator. In patients with CDI, there is an increased risk of further disease recurrence with each subsequent episode of rCDI. Initially, there is a 25-30 % risk of recurrence; however, after one episode of rCDI, the risk of another episode increases to 40 % and subsequently rises to a 60 % risk of developing a third episode of rCDI.

1.1.4 Epidemiology

The epidemiology of *C. difficile* in the UK has changed dramatically in the last 10-15 years. During 2003-2004, the first known large outbreak of CDI occurred at the Stoke Manderville Hospital (Buckinghamshire Healthcare NHS Trust), with 174 CDI cases and 19 deaths followed by another outbreak during 2004-2005 of 160 cases with 19 deaths, attributed to the hyper-virulent *C. difficile* ribotype 027 (Smith, 2005). This increased incidence and mortality rate of CDI highlighted the need for closer monitoring of CDI cases and improved infection prevention measures as poor practice in infection control was implicated in both outbreaks. As such, mandatory surveillance and reduction targets for CDI were implemented as well as the *C. difficile* Ribotyping Network (CDRN) to type isolates in order to identify outbreaks and map *C. difficile* epidemiology.

Epidemiological studies since the introduction of *C. difficile* monitoring and surveillance programmes have demonstrated a shifting pattern in ribotype incidence (Freeman *et al.*, 2010). During the years of 2007-2008, 2008-2009 and 2009-2010, ribotype 027 predominated; however, incidence decreased dramatically (55 %, 36 % and 21 %, respectively) (Wilcox *et al.*, 2012), in line with a decrease in overall mortality. This was also accompanied by a reduction in cephalosporin and fluoroquinolone use, indicating improved antibiotic stewardship and prescribing practices that were preventative for CDI.

During 2007-2010, the predominant circulating ribotypes in England included, in order of prevalence, ribotypes 027, 106, 001, 014/020, 015, 002, 078, 005, 023, 016 (Wilcox *et al.*, 2012). Looking at the period from 2008 – 2018, there was a reduction in the prevalence of ribotypes 027, 001 and 106, with compensatory increases in other ribotypes, giving England a more heterogeneous distribution of ribotypes, with predominant ribotypes including 002, 014/020, 015, 005, 023 and 078, levels of which have remained relatively stable for the last approximately 3 years (Public Health England, CDRN 2015-2018 report). The shift from the predominant 027 ribotype to a more diverse occurrence of ribotypes reflects the improved infection prevention and antibiotic prescribing practises and highlights the increasing rate of community onset CDI (Davies *et al.*, 2016) in the UK. A total decrease of 77.9 % in CDI rates from 2007/2008 – 2018/2019 was reported; however, this decrease was mainly seen in the hospital setting as community-onset cases are on the increase and

reportedly constitute 66% of cases, increasing from 57.3 % in 2011/2012 (Public Health England, 2019).

The European, multicentre, prospective, biannual, point-prevalence study of *Clostridium difficile* infection in hospitalised patients with diarrhoea (EUCLID), looked at the distribution of *C. difficile* isolates in Europe which included 19 European countries. They identified 125 distinct ribotypes with considerable inter-country variation in distribution of ribotypes. 027 (19 %) was the predominant strain, followed by 001/072 (11 %) and 014/020 (10 %) and the following contributing ≤ 5 % prevalence: 002, 140, 010, 078, 176 and 018 (Davies *et al.*, 2016). Across Europe, the prevalence of the 027 ribotype has increased over three fold since 2008 with Germany, Hungary, Poland and Romania being most affected, accompanied by a decrease in ribotype diversity (Davies *et al.*, 2016).

1.1.5 Pathogenesis

CDI is mediated through the faecal-oral transmission of spores. *C. difficile* spores are ubiquitous in the environment, especially in healthcare settings (Weber *et al.*, 2013). Spores are incredibly resilient and highly resistant to environmental pressures including high temperatures and standard disinfection procedures (Fawley *et al.*, 2007, Edwards *et al.*, 2016, Dyer *et al.*, 2019). Environmental contamination with *C. difficile* spores, particularly in a hospital setting, is mediated through shedding of spores from symptomatic CDI patients as well as direct transfer to health care workers (Kim *et al.*, 1981, Kaatz *et al.*, 1988, McFarland *et al.*, 1989, Best *et al.*, 2010, Landelle *et al.*, 2014), facilitating the transmission and recurrence of CDI (Figure 1-2). After ingestion, spores can survive the acidic pH of the gastric tract, allowing them to pass into the large intestine (Paredes-Sabja *et al.*, 2014). If the conditions in the intestine are conducive, spores are able to germinate into a vegetative morphotype which then proliferate and produce toxin, resulting in active CDI. Certain strains of *C. difficile* are non-toxigenic and lack the genes required to express the toxins.

The ability of *C. difficile* spores to germinate and colonise the colon is largely dependent on the host microbiota and associated metabolome (Buffie *et al.*, 2015, Theriot and Young, 2015) The intestinal tract is home to a myriad of

microbial populations, and the conservation of these communities is vital in maintaining host health. In a healthy host, the microbiota is able to protect the host against the incursion of pathogens by establishing colonisation resistance and competing for space and nutrients. If there is disruption to the host microbiota, for example antibiotic-induced dysbiosis, this can create an environment conducive to CDI (Theriot *et al.*, 2016). The propensity of *C. difficile* spores to germinate is largely dependent on the presence of certain primary bile acids. Primary bile acids, cholic acid and chenodeoxycholic acid, are derivatives of cholesterol synthesised by the liver and facilitate the absorption of lipids and lipid-soluble vitamins in the intestine. The majority of these bile acids are reabsorbed by the intestine; however, roughly 5 % of these non-reabsorbed primary bile acids undergo 7 α -dehydroxylation by resident anaerobic populations to form the secondary bile acids deoxycholic acid and lithocholic acid (Chiang, 2009). *In vitro*, primary bile acids such as taurocholate together with co-germinants such as glycine, stimulate *C. difficile* spore germination through interactions with the CspC receptor located on the spore coat or outer membrane (Sorg and Sonenshein, 2008, Francis *et al.*, 2013). Conversely, gut microbiota-derived secondary bile acids inhibit spore germination and vegetative growth of *C. difficile* cells. Intestinal dysbiosis, commonly caused by the use of antimicrobials, results in depletion of the populations responsible for the conversion of primary to secondary bile acids, leading to the accumulation of primary bile acids in the intestine, stimulating *C. difficile* germination and outgrowth. In a study assessing levels of bile acids, it was found that primary bile acids were significantly elevated in patients with CDI and rCDI whereas secondary bile acids were elevated in healthy controls (Allegretti *et al.*, 2016).

Germination of *C. difficile* spores is then followed by colonisation and outgrowth, mediated by various adhesion and colonisation factors. *C. difficile* expresses a vast array of virulence factors that aid in survival through the stomach, adhesion to mucosal surfaces and colonisation of the host. Colonisation is facilitated by evasion of the hosts innate defences and the expression of various colonisation factors including fibronectin-binding proteins, cell surface layer proteins and polysaccharides, cell-wall proteins and flagella (Vedantam *et al.*, 2012). Not all patients colonised with *C. difficile* are

symptomatic, but may contribute to the transmission of the disease (Leffler and Lamont, 2015). The symptoms of CDI are mainly attributed to the production of toxins. These toxins cause damage to the host's epithelial cell cytoskeleton, causing disruption to the tight junctions between the cells resulting in fluid loss and a loss of gut barrier integrity (Czepiel *et al.*, 2019).

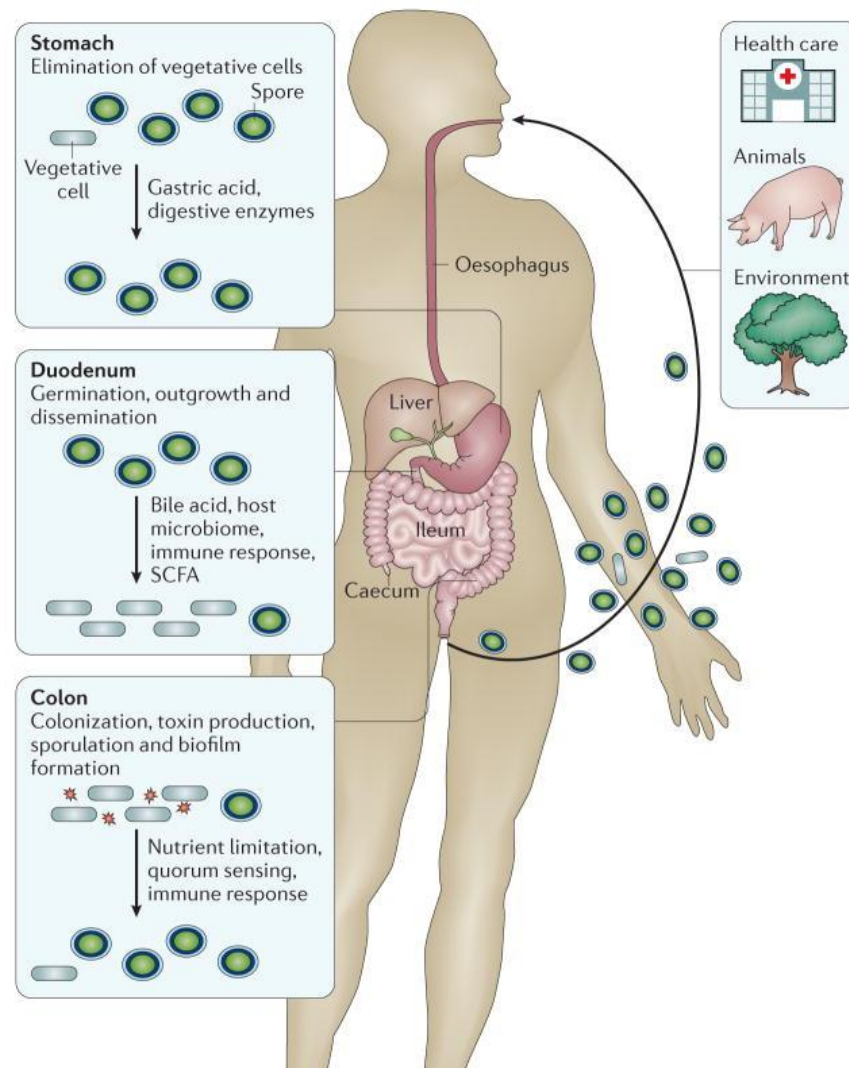


Figure 1-2. *C. difficile* transmission and pathogenesis in the human gastrointestinal tract. The three main sources of *C. difficile* spores are indicated and include health care settings, animal reservoirs and the environment. The life cycle of *C. difficile* is illustrated as well as the influence of host-factors on pathogenesis. Image from Smits *et al.* (2016).

1.1.6 Virulence factors

1.1.6.1 Toxins

The symptoms of CDI are caused by the production of toxins. *C. difficile* can produce up to three toxins, namely enterotoxin toxin A (Tcd A), cytotoxin toxin B (TcdB) and the binary toxin (CDT).

Toxin A and toxin B

TcdA and TcdB belong to the family of large clostridial glucosylation toxins which target the actin cytoskeleton of the hosts' epithelial cells through inactivation of guanosine triphosphatases (GTPases). Historically, TcdA was viewed as the more potent of the two toxins, with administration of purified toxin to rabbit and rodent models eliciting a more toxic effect than that of TcdB (Lyerly *et al.*, 1985, Mitchell *et al.*, 1986, Triadafilopoulos *et al.*, 1987). The reverse was seen in models using human colonic tissue which suggests differences in receptor binding in animal and human models and it was found that TcdB alone is able to induce the phenotype of CDI (Riegler *et al.*, 1995).

TcdA (308 kDa) and TcdB (270 kDa) are highly related, with 48 % identity and 63 % similarity in amino acid sequence (von Eichel-Streiber *et al.*, 1992, Jank and Aktories, 2008, Pruitt *et al.*, 2010). Both toxins are comprised of four major functional domains; an amino-terminal glucosyltransferase domain (GTD) that modifies host Rho-GTPases, a cysteine autoprotease domain (APD), a pore-forming and delivery domain and a combined repetitive oligopeptides (CROPs) domain for receptor binding (Figure 1-3) (Jank and Aktories, 2008, Chumblor *et al.*, 2016).

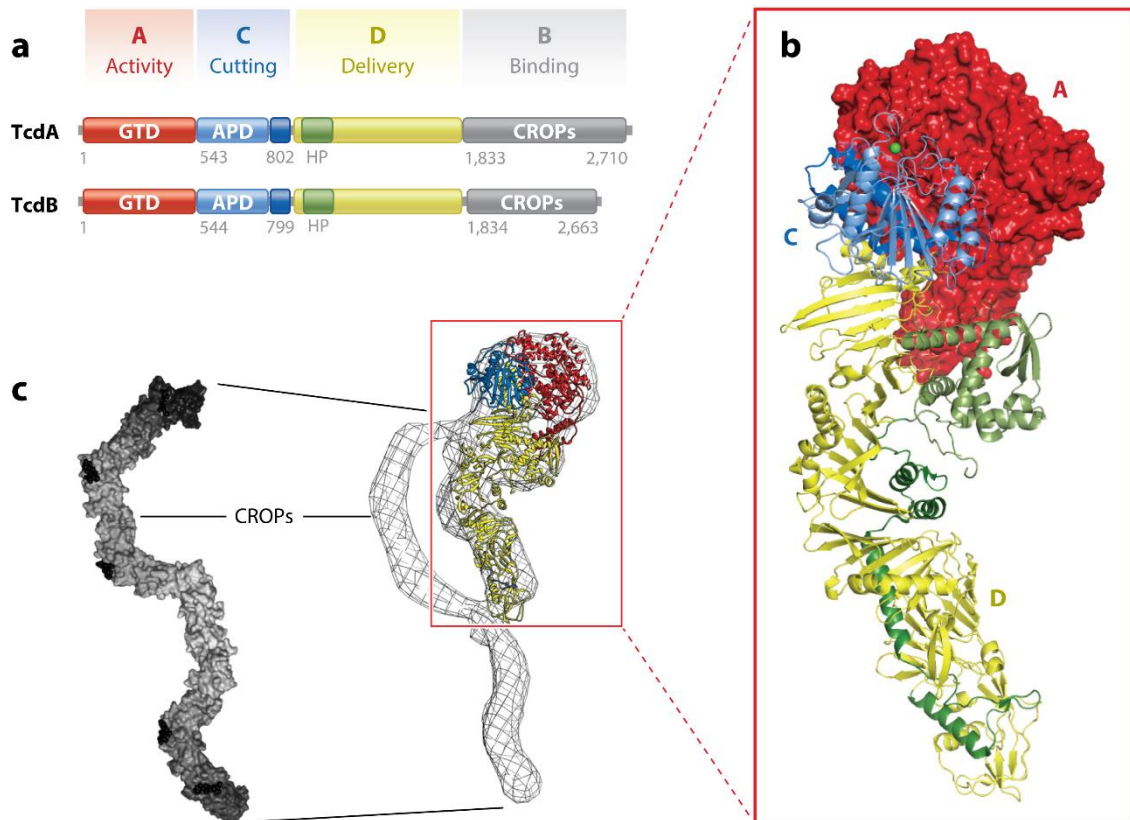


Figure 1-3. Structure of *C. difficile* toxins A (tcdA) and B (TcdB). (a) Gene sequence of *C. difficile* toxin A (TcdA) and toxin B (TcdB), illustrating four domains including the glucosyltransferase (GTD - domain A), the combined repetitive oligopeptides (CROPs, domain B), an autoprotease (domain C) and the delivery/binding (domain D). (b) The crystal structure of domains A, C and D of TcdA and (c) a model of the full toxin. Image from Aktories *et al.* (2017).

Mechanism of action

Once the toxins are secreted, they enter the colonic epithelium via PACSIN2-mediated endocytosis (TcdA) (Chandrasekaran *et al.*, 2016) and clathrin-mediated endocytosis (TcdB) (Papatheodorou *et al.*, 2010). Receptor binding is mainly associated with the CROPs domain which is able to bind carbohydrate residues. Although similar, the CROPs domains for TcdA and TcdB differ in spatial and sequential arrangements, indicating that receptors for the toxins are different (Chaves-Olarte *et al.*, 1997). TcdA receptors identified include GalNAc-(1,3)- β -Gal-(1,4)- β -GlcNAc; Lewis I, X and Y glycan sequences; and glycoprotein gp96 (Tucker and Wilkins, 1991, Teneberg *et al.*, 1996, Smith *et*

al., 1997, Na *et al.*, 2008). Domains other than CROPs have been associated with binding the toxins, as TcdA and TcdB lacking a CROPs domain are still capable of cytotoxic effects, however with less potency (Olling *et al.*, 2011). The receptors identified for TcdB to date include three protein receptors; the poliovirus receptor-like protein 3 (PVRL3) which is expressed on the surface of colon epithelial cells; chondroitin sulphate proteoglycan 4 (CSPG4) which is expressed in the intestinal sub epithelium, indicating that CSPG4 binding occurs once the epithelium is damaged; and the Frizzled (FZD) receptor involved in the Wnt signalling pathway (LaFrance *et al.*, 2015, Yuan *et al.*, 2015, Tao *et al.*, 2016). Acidification of the endosome results in a structural change in the delivery domain, resulting in the translocation of the GTD and APD domains across the membrane (Pruitt *et al.*, 2010). The APD domain then binds eukaryotic inositol-hexakisphosphate (InsP6) which releases the GTD domain into the cytosol through cysteine protease activity (Egerer *et al.*, 2007, Shen *et al.*, 2011).

Once internalised, the GTD domain transfers glucose from uridine diphosphate (UDP) glucose onto Rho proteins at threonine 35 [Rac and cell division control protein 42 (CDC42)] and threonine 37 (Rho A,B and C) (Just *et al.*, 1995a, Just *et al.*, 1995b). Rho proteins are GTP-binding proteins and regulate the cell cytoskeleton and transcription as well as cell-cycle progression and apoptosis (Jaffe and Hall, 2005). Glucosylation of Rho proteins interferes with the ability of Rho to interact with their effector molecules. Cytopathic effects include alterations in the cytoskeleton through the redistribution of actin and the loss of stress fibres leading to alterations in tight junctions, cell shrinkage and disruption to barrier function (Ottlinger and Lin, 1988, Hecht *et al.*, 1992, Nusrat *et al.*, 1995, Nusrat *et al.*, 2001). TcdA and TcdB, through the activation of caspase enzymes and inactivation of RhoA, can induce apoptosis (Hippenstiel *et al.*, 2002, Gerhard *et al.*, 2008).

In addition to direct cytopathic effects, TcdA and TcdB also provoke a significant inflammatory response that leads to tissue damage and necrosis through the induction of pro-inflammatory cytokine IL-1 β . Once the toxins are recognised in the cell, the assembly of a multi-protein complex called the inflammasome is initiated, which is involved in activating inflammation (Ng *et al.*, 2010). They also activate hypoxia-inducible factor 1 (HIF-1 α), a

transcription factor that regulates the expression of genes involved in the immune response (Hirota *et al.*, 2010). At high concentrations, TcdB is able to induce the assembly of the Nicotinamide adenine dinucleotide phosphate (NADPH) oxidase complex (NOX) which leads to the generation of reactive oxygen species (ROS) and tissue necrosis (Farrow *et al.*, 2013).

Regulation of toxin expression

Toxin expression is regulated bidirectionally by environmental and metabolic signals (Bouillaut *et al.*, 2015). Inhibition of toxin production occurs via the carbon catabolite control protein A (CcpA) and the global transcriptional regulator CodY (Dineen *et al.*, 2010) in conditions of high nutrient availability and intracellular levels of GTP, including the presence of glucose or amino acids such as cysteine or proline (Dupuy and Sonenshein, 1998, Karlsson *et al.*, 2000, Antunes *et al.*, 2012). The presence of short-chain fatty acids such as butyrate and sub-inhibitory concentrations of certain antimicrobials are known to stimulate toxin production (Karlsson *et al.*, 2000, Mani *et al.*, 2002, Aldape *et al.*, 2013). Expression of motility-associated sigma factor SigD; sporulation-associated Spo0A; and quorum signalling also influence toxin gene expression (El Meouche *et al.*, 2013, Mackin *et al.*, 2013, Darkoh *et al.*, 2015). Genes encoding these toxins are located in a chromosomal region known as the pathogenicity locus (PaLoc) (Figure 1-4) which is 19.6 kb in length and comprised of five open reading frames (Hammond and Johnson, 1995). In non-toxicogenic strains, this region is replaced by a 115 bp non-coding sequence (Braun *et al.*, 1996). The five genes located on the PaLoc include *tcdA* and *tcdB* which encode toxin A and toxin B respectively; regulatory genes *tcdR* and *tcdC*; and the gene encoding membrane lysis protein *tcdE*. All the genes are transcribed in the same direction, with the exception of *tcdC* which is orientated in the opposite direction (Hammond and Johnson, 1995).

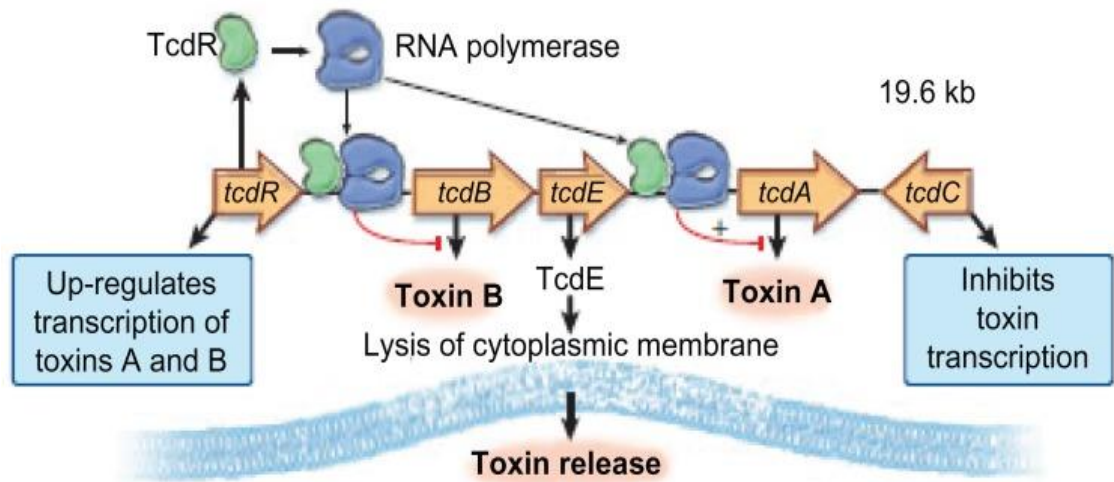


Figure 1-4. The pathogenicity locus of *C. difficile*. Illustration of the 19.6 kb pathogenicity locus encoding a positive transcriptional regulator (*tcdR*), toxin B (*tcdB*), presumed membrane lysis protein (*tcdE*), toxin A (*tcdA*) and a putative negative transcriptional regulator (*tcdC*). Image from Kelly and LaMont (2008).

tcdR encodes an alternative RNA polymerase sigma factor that is critical for the initiation of *tcdA* and *tcdB* expression and acts as a positive regulator of toxin production (Mani and Dupuy, 2001, Mani *et al.*, 2002). *tcdE* encodes a bacteriophage holin-like protein that facilitates the extracellular release of both toxins by forming oligomers in the cytoplasmic membrane (Tan *et al.*, 2001, Govind and Dupuy, 2012). The function of *tcdC* is not fully understood but appears to be involved in repression of toxin production. It was noted that high levels of TcdC and low levels of TcdA, B, D and E were found during early exponential phase, with the reverse seen during stationary phase, suggesting that TcdC negatively regulates the transcription of the other genes (Hundsberger *et al.*, 1997). The identification of an 18 bp deletion in the *tcdC* gene of the epidemic 027 ribotype which led to a functional disruption of the protein, was speculated to be responsible for the hyper production of toxins A and B (Warny *et al.*, 2005, MacCannell *et al.*, 2006). The proposed mechanism of TcdC mediated toxin repression involves the destabilising the TcdR-containing RNA polymerase holoenzyme hereby interfering with its ability to recognise the promoters for *tcdA* and *tcdB* (Matamouros *et al.*, 2007). Further studies into the action of TcdC have provided conflicting results (Carter *et al.*,

2011, Bakker *et al.*, 2012, Cartman *et al.*, 2012), with a *C. difficile* strain 630 containing a mutant *tcdC* gene not displaying significantly different toxin levels when compared to the wild type (Bakker *et al.*, 2012), and a *C. difficile* 027 ribotype strain complemented with a fully functional *tcdC* gene, failed to affect toxin levels (Cartman *et al.*, 2012).

Binary C. difficile transferase toxin

The binary *C. difficile* transferase toxin (CDT) is found in approximately 17-23 % of *C. difficile* strains, notably in 027 and 078 ribotype strains (Eckert *et al.*, 2015) and belongs to the binary actin ADP-ribosylating toxin family (Barth *et al.*, 2004). Presence of CDT in clinical isolates is associated with higher rates of disease recurrence and mortality (Gerding *et al.*, 2014). CDT is encoded by two genes, *cdtA* (48 kDa) and *cdtB* (98.8 kDa) that are located on the binary toxin locus (CdtLoc, 4.3 kb) and transcribe the enzymatic and binding/translocation region of the toxin, respectively (Perelle *et al.*, 1997, Gonçalves *et al.*, 2004). A response regulator gene, *cdtR*, is located upstream of the Cdt A and B operon and acts as a positive regulator of CDT production (Carter *et al.*, 2007). CDT negative strains contain a 2.3 kb deletion in this locus (Stare *et al.*, 2007). The host cell receptor for CDT was identified as the lipolysis-stimulated lipoprotein receptor (LSR) (Papatheodorou *et al.*, 2011). The mechanism of toxin entry is not fully understood; however as the translocation component of this toxin shares similarity with the iota toxin of *C. perfringens*, it is believed that the binding/translocation domain interacts with LSR where it accumulates in lipid rafts, followed by oligomerisation and binding of the enzymatic component. This complex is then internalised in endosomal compartments and acidification of the endosome results in pore formation and translocation into the cytosol (Nagahama *et al.*, 2000, Hale *et al.*, 2004). Translocation of the enzymatic portion of the toxin is dependent on host cell helper proteins including the chaperone protein Hsp90 (Haug *et al.*, 2004) and cyclophilin A (Kaiser *et al.*, 2011). Once in the cytosol, CDT is able to irreversibly ADP-ribosylate G-actin monomers at arginine-177 (Gulke *et al.*, 2001), acting as a capping protein and causing depolymerisation of the actin filament resulting in the destruction of the cell cytoskeleton and cell death (Aktories and Wegner, 1989, Sundriyal *et al.*, 2009).

The ADP-ribosylation of actin by CDT influences the dynamics of the microtubules within the cell. Microtubules growth towards the cell membrane is inhibited by contact with cortical actin; however, the presence of CDT disrupts the capture function of cortical actin, resulting in long protrusions developing from the cells (Siegrist and Doe, 2007). The destruction of the cytoskeleton and development of microtubule protrusions have been shown to increase bacterial adherence and attachment to the cell, and therefore may have a role in colonisation (Schwan *et al.*, 2009).

1.1.6.2 Spores

During nutrient limitation, *C. difficile* forms spores that are metabolically dormant, aero tolerant and highly resilient to environmental pressures including high temperatures and standard disinfection procedures, allowing *C. difficile* to survive and persist in the environment (Sorg and Sonenshein, 2008, Lawley *et al.*, 2009b). Deakin *et al.*, (2012) demonstrated that a sporulation deficient strain of *C. difficile* was unable to persist in the environment or transmit between hosts. Environmental reservoirs of *C. difficile* spores include direct and indirect (hands and shoes) transfer of spores from symptomatic patients in the health care setting, asymptomatic human carriers in the community and hospital setting, zoonotic origins and the food chain (Brown and Wilson, 2018, Ofori *et al.*, 2018, Sheth *et al.*, 2019).

Spore architecture is largely conserved between bacterial species. In the centre lies a partially dehydrated core containing supercoiled DNA bound in acid soluble proteins to protect the DNA and block transcription (Nicholson *et al.*, 1990, Setlow and Setlow, 1993, Moeller *et al.*, 2009). High concentrations of calcium dipicolinic acid are also found in the spore core and contributes to heat resistance in *Bacillus subtilis* (Setlow *et al.*, 2006). This core is surrounded by an inner membrane, a germ cell wall and the spore cortex, the latter containing modified peptidoglycan to facilitate hydrolysis by cortex lytic enzymes (CLE) during germination (Meador-Parton and Popham, 2000, Chirakkal *et al.*, 2002). The spore coat surrounds the cortex and some strains contain an outer exosporium layer which plays a role in adhesion and interaction with the host (Díaz-González *et al.*, 2015).

C. difficile spores are resistant to gastric acid and can survive the passage through the upper GI tract to the small intestine. Here, they come in contact with germinants that act on receptors located in the inner spore membrane, leading to the efflux of monovalent cations and CaDPA and subsequent rehydration of the spore core. Activation of CLEs leads to degradation of the peptidoglycan wall to enable active metabolism of the spore core and facilitates the switch to a vegetative morphotype. Increased sporulation rates have been implicated in the virulence and severity of the epidemic ribotype 027 (Åkerlund *et al.*, 2008, Merrigan *et al.*, 2010); however, this has been disputed with studies finding no significant difference in sporulation rates when compared to other non-epidemic ribotypes (Burns *et al.*, 2010, Sirard *et al.*, 2011). Burns *et al.*, demonstrated high variability in sporulation rates between and within ribotype groups (Burns *et al.*, 2011), highlighting the difficulty in drawing conclusions between sporulation and disease severity.

1.1.6.3 Resistance to the hosts innate defences

Mucosal surfaces are particularly vulnerable to infection, therefore the mucosal immune system is a vital defence against pathogens. The tightly packed epithelial layer of the intestinal tract secretes antimicrobial peptides into the mucous layer, providing a layer of physical and biochemical defence against invading pathogens. In order to colonise host mucosal surfaces in the gut, bacteria must overcome the antimicrobial agents generated by the hosts' innate immune response, including lysozyme and cationic antimicrobial peptides (CAMPs).

Lysozyme is as a peptidoglycan hydrolase secreted at high levels in mucosal surfaces, causing disruption to the bacterial cell wall through cleavage of peptidoglycan at the MurNAc and GlcNAc linkage in the bacterial cell wall. To prevent peptidoglycan hydrolysis, *C. difficile* is able to modify the peptidoglycan in its cell wall to inhibit the action of lysozyme. This is accomplished by N-acetylglucosamine deacetylation of peptidoglycan, mediated by the deacetylase PdaV and regulated by expression of *csfV* gene, encoding the extracytoplasmic sigma factor V (Peltier *et al.*, 2011, Ho *et al.*, 2014). CAMPs are another antimicrobial agent, including cathelicidin antimicrobial peptide and α -definsins. CAMPs mainly target the bacterial cell membrane; however, several different mechanisms of action have been suggested, based on the

individual peptide structure (Bechinger and Gorr, 2017). Resistance of *C. difficile* to CAMPs include the D-alanyl esterification of teichoic acid; mediated by the *dlt* operon, which results in an increased positive charge of the membrane (McBride and Sonenshein, 2011a); and the expression of ABC transporters, the CprABC transporter recognises multiple substrates and is capable of removing CAMPs from the cell (McBride and Sonenshein, 2011b).

1.1.6.4 Adhesins

Adhesion and subsequent colonisation of the GI tract is a precursor to the development of disease. *C. difficile* has been shown to adhere to different cell lines and extracellular matrix (ECM) proteins *in vitro* (Karjalainen *et al.*, 1994, Naaber *et al.*, 1996, Drudy *et al.*, 2001, Cerquetti *et al.*, 2002) and *in vivo* (Borriello *et al.*, 1988b, Spigaglia *et al.*, 2013). Borriello *et al.* (1988) demonstrated enhanced adherence of a virulent toxigenic *C. difficile* strain when compared to a non-virulent toxigenic strain, highlighting the importance of adherence to virulence (Borriello *et al.*, 1988b). Adhesion is mediated by bacterial adhesins that are located on the cell surface. *C. difficile* possesses a proteinaceous cell surface layer (S-layer), which is composed of surface layer proteins (SLPs) connected in a crystal lattice formation. The S-layer is mainly composed of SlpA proteins and the cell wall protein (CWP) family.

Cysteine proteases, Cwp84 and Cwp13, are responsible for the assembly of the S-layer by the cleavage and processing of the precursor molecule SlpA (de la Riva *et al.*, 2011). Cwp84 can also be found in the extracellular fraction and degrades ECM proteins *in vitro*, which could aid in the spread of the bacteria (Janoir *et al.*, 2007). SLPs are composed of two subunits, namely the low-molecular weight S-layer protein (LMW-SLP) and the high-molecular weight S-layer protein (HMW-SLP) (Mauri *et al.*, 1999). SLPs have been shown to facilitate adherence to Hep-2 cells *in vitro*, mediated mainly by the HMW-SLP, with substrates collagen I, thrombospondin and vitronectin identified (Calabi *et al.*, 2002). SlpA has been found to be a major contributor to bacterial adherence, with pre-treatment of host cells with purified SlpA or incubation of vegetative bacteria with anti-SlpA antisera resulting in significantly reduced bacterial attachment (Merrigan *et al.*, 2013). SLPs from 027 and 078 ribotypes demonstrated high variability in LMW-SLP subunit, leading to an increased inflammatory response which could play a role in the hyper-virulence of these

strains (Lynch *et al.*, 2017). Cwps are characterised by the presence of a conserved binding domain CWB2 that, together with polysaccharide II (PSII), anchors the proteins to the bacterial cell surface (Willing *et al.*, 2015). Cwps display high genetic variability in response to immune pressure and hence contribute to the evasion of host defences (Biazzo *et al.*, 2013). Cwp66 has been shown to adhere to Vero cells and its expression is upregulated in response to increased temperatures. With antibodies and adhesion fragments partially inhibiting *C. difficile* adherence during cell binding studies, the role of Cwp66 in bacterial adhesion was demonstrated (Waligora *et al.*, 2001). CwpV, the largest protein of the Cwp family, is composed of a highly variable domain across *C. difficile* strains which mediates the auto-aggregation of *C. difficile* (Reynolds *et al.*, 2011) as well as protection against phage infection (Sekulovic and Fortier, 2015).

The surface-associated fibronectin-binding protein (FnBP) Fbp68 is able to bind soluble and immobilised fibronectin which is a major component of the ECM and potentially acts as a bridge to the host cells. Anti-Fbp68 antibodies were able to partially inhibit *C. difficile* attachment to fibronectin and Vero cells (Hennequin *et al.*, 2003) and pre-treatment of Caco-2 cells with the fibronectin-binding domain of Fbp68 blocked bacterial adhesion (Lin *et al.*, 2011), providing further evidence for the role of Fbp68 in *C. difficile* colonisation. Interestingly, a FnBP mutant demonstrated increased adherence to Caco-2 and HT29-MTX cell lines as well as equivalent faecal shedding and in mouse models when compared to the wild type strain (Barketi-Klai *et al.*, 2011), highlighting the need for further investigation into the role of FnBPs in adherence and colonisation. The collagen-binding protein, CbpA, is another surface-associated protein capable of binding components of the ECM, namely collagen type I and IV. The ability to bind to collagen was indistinguishable between a CbpA knock-out mutant when compared to the wild type (WT) strain (Tulli *et al.*, 2013), indicating that although CbpA is an adhesin, it is not a major adhesin in *C. difficile*. The lipoprotein CD08730 demonstrated adhesive properties to Caco-2. This property was further demonstrated when mutant strain and a WT strain, pre-incubated with specific antibodies, showed a significant reduction in binding (Kovacs-Simon *et al.*, 2014).

1.1.6.5 Secreted proteases

As the secreted component of Cwp84 was found to degrade components of the ECM (Janoir *et al.*, 2007), other secreted proteases have been identified. These are believed to contribute to infection, with the degradation of ECM enabling the spread of bacteria and releasing nutrients. *C. difficile* produces hydrolytic enzymes to degrade connective tissue and include hyaluronidase, chondroitin sulphatase, collagenase and gelatinase (Steffen and Hentges, 1981) and the expression of these have been linked to increased virulence (Seddon *et al.*, 1990). A zinc metalloprotease, CD630_2830 (Zmp1), was identified and found to be capable of cleaving fibronectin and fibrinogen and in doing so destabilising the fibronectin network produced by human fibroblasts (Cafardi *et al.*, 2013). Zmp1 was also found to cleave certain surface adhesins, including the collagen-binding protein CD630_28310, providing a role in the regulation of adherence in *C. difficile* (Hensbergen *et al.*, 2014).

1.1.6.6 Motility

The human intestinal tract is covered by mucus secretions that protect the epithelium and prevent colonisation of the cells; however, bacteria have developed mechanisms to circumvent this and traverse the mucus layer. The flagellum is a complex appendage of the cell surface and is primarily an organelle of motility and chemotaxis; however, other functions have been identified including biofilm formation, adhesion and immune system stimulation (Duan *et al.*, 2013, Haiko and Westerlund-Wikström, 2013). *C. difficile* possesses peritrichous flagella; but the role of flagella in the virulence of *C. difficile* is not well understood. The work from Tasteyre *et al.*, characterised the flagellum of *C. difficile* and found it was comprised of a flagellum subunit (FliC) and a flagellar cap protein (FliD) (Tasteyre *et al.*, 2000, Tasteyre *et al.*, 2001b). Purified FliC, FliD and crude flagella preparations adhered to mouse caecal mucus *in vitro*, revealing a role for flagella in adhesion. Indeed, tissue association in the mouse caecum of a non-flagellated strain was 10-fold lower than that of a flagellated strain (Tasteyre *et al.*, 2001a).

Flagellar gene transcription occurs in a hierarchical order with early-stage genes encoding the basal body assembly and the flagellar alternative sigma factor (SigD). SigD activates late-stage flagellar genes as well as genes

required for post-translational modification of the flagellum (Stabler *et al.*, 2009, El Meouche *et al.*, 2013). SigD has also been linked to TcdA and TcdB expression through the control of *tcdR* transcription. Mutagenesis of *sigD* resulted in a decrease in expression of genes involved in flagellar and toxin regulation (Aubry *et al.*, 2012, El Meouche *et al.*, 2013). More recently, it was found that flagellum and toxin production is subject to phase variation (Anjuwon-Foster and Tamayo, 2017). The DNA invertible element is found upstream of the *sigD* operon, with inversion catalysed by a tyrosine recombinase, RecV (Anjuwon-Foster and Tamayo, 2018).

Evidence suggesting a role for flagella in adherence and colonisation is contradictory, with results comparing the historic *C. difficile* 630 strain showing conflicting results to epidemic 027 R20291. In 2013, Baban *et al.*, (2013) compared the *C. difficile* 630 and R20291 flagellated parent strain to strains in which the flagella were paralysed and strains where the flagella were absent. R20291 flagellar *fliC* and *fliD* mutants adhered less than the WT strain indicating that flagella were necessary for adherence and virulence in R20291 strain but not the 630 strain. R20291 mutants with a paralysed flagellum (the motor proteins of the flagellum were disabled, producing a structurally present but immotile flagella), were able to outcompete *fliC* mutants in colonisation and adherence, indicating that the structural components of flagella are important to *C. difficile* adherence and colonisation, rather than motility (Baban *et al.*, 2013). The contrasting behaviour between the strains highlighted the importance of testing a variety of strains before drawing conclusions. It was also noted that diversity between post-translational modifications of the flagella differ greatly between strains (Twine *et al.*, 2009) and that mutations in these glycosylation modifications can affect motility, colonisation and disease recurrence in mice; indicating that alterations in flagella architecture play a role in virulence (Faulds-Pain *et al.*, 2014). Flagella have also been demonstrated to play a role during *in vitro* biofilm formation, with *fliC* mutants producing less biofilm than the WT strain (Đapa *et al.*, 2013).

In addition to flagella, *C. difficile* was also found to express type IV pili (T4P) that are responsible for swarming and twitching motility but are also associated with adhesion, cell aggregation and biofilm formation (Borriello *et al.*, 1988a, Sebahia *et al.*, 2006, Goulding *et al.*, 2009). The expression of T4P is highly

dependent on intracellular levels of the bacterial second messenger cyclic dimeric guanosine monophosphate (C-di-GMP). In other bacteria, c-di-GMP has been shown to be responsible for the switch from a free living, motile phenotype to a sessile, immobile phenotype. Increased levels of C-di-GMP reduces the expression of flagella and increases the expression of T4P, leading to cell aggregation and biofilm formation (Tamayo *et al.*, 2007). A similar system has been demonstrated in *C. difficile* with increased levels of c-di-GMP associated with increased transcript of the T4P genes (Bordeleau *et al.*, 2015) accompanied by the repression of motility and an increase in cell aggregation (Purcell *et al.*, 2012). Inactivation of the major and minor subunits of pili (PilA1 and PilJ, respectively), results in the absence of pili which significantly reduced cell aggregation in *C. difficile* (Bordeleau *et al.*, 2015). As with flagella, major differences were demonstrated in pilus expression and regulation between the 630 and R20291 strain, with R20291 expressing higher levels on T4P and is therefore capable of surface-associated growth and motility (Purcell *et al.*, 2016). The ability to switch between free-living and sessile phenotypes may have important implications for virulence.

1.1.7 Current Diagnosis and Treatment

According to European guidelines, all unexplained diarrhoea episodes are recommended to be investigated as possible CDI (with the exception of children under 3 years of age) (Crobach *et al.*, 2016). A positive laboratory diagnosis includes a positive result of glutamate dehydrogenase (GDH) and a positive toxin result, or a positive nucleic acid amplification test (NAAT) together with a positive toxin result, from a stool sample. Additional tests include a full blood count, urea and electrolytes as well as lactate and radiology in severe to life-threatening cases. Guidelines for the diagnosis and treatment of CDI and rCDI are available from the European Society for Clinical Microbiology and Infectious Disease (ESCMID) (Debast *et al.*, 2014) and the Infectious Disease Society of America (IDSA) and the Society for Healthcare Epidemiology of America (SHEA) (McDonald *et al.*, 2018b).

In non-severe CDI cases (diarrhoea without features of severe or life-threatening infection), oral vancomycin at 125 mg four times daily for 10 days if symptoms subside, or 14 days should symptoms persist. In severe CDI, characterised by: raised white cell counts of $> 15 \times 10^9/L$, acute kidney injury ($>$

50 % rise in serum creatinine above baseline), temperature > 38.5°C or evidence of severe colitis; treatment includes oral vancomycin at 125 mg four times daily or 200 mg fidaxomicin if antimicrobial treatment is required for other infections or multiple comorbidities. Life-threatening CDI, characterised by: hypotension, partial or complete ileus or toxic megacolon; treatment includes 125 mg NG vancomycin four times daily plus 500 mg IV metronidazole three times daily. There are multiple treatment options for recurrent CDI, including oral fidaxomicin for 10 days or a tapered and pulsed regimen of vancomycin. In cases of multiple recurrences, faecal microbiota transplantation (FMT) is considered.

1.1.7.1 Treatment options for CDI

Initially metronidazole was the drug of choice to treat CDI. A number of studies found equivalent efficacy and recurrence rates of metronidazole to vancomycin for the treatment of CDI (Teasley *et al.*, 1983, Wenisch *et al.*, 1996), and with the emergence of vancomycin resistant enterococci (VRE), the use of vancomycin was discouraged. With the emergence of the hyper-virulent 027 ribotype, with increased disease severity, further studies investigating the efficacy of metronidazole to vancomycin stratified by disease severity found that overall cure rates were 84 % for metronidazole and 97 % for vancomycin. In mild CDI cases, the cure rate was 90 % and 98 % for metronidazole and vancomycin, respectively ($p = 0.36$); whereas, in severe cases the cure rate was 76 % for metronidazole and 97 % for vancomycin ($p = 0.02$). This demonstrated that vancomycin was superior to metronidazole, particularly in the treatment of severe CDI (Zar *et al.*, 2007). In a multinational, randomised, controlled trial, it was found that the clinical success of metronidazole was inferior to vancomycin ($p = 0.02$, 72.7 % vs 81.1 % and $p = 0.059$, 66.3 % vs 78.5 % for severe CDI) (Johnson *et al.*, 2014). It was also found that VRE frequency was similar between patients treated with metronidazole and vancomycin; therefore, vancomycin has replaced metronidazole as the drug of choice for CDI treatment (Sethi *et al.*, 2009).

Fidaxomicin, a more recent option in CDI treatment, was found to be more active against *C. difficile in vitro* than vancomycin, as well as proving to be more selective for *C. difficile* and sparing to the normal gut flora (Ackermann *et*

al., 2004, Finegold *et al.*, 2004, Hecht *et al.*, 2007). Fidaxomicin was found to have equal initial clinical cure efficacy to vancomycin, but was associated with a significantly lower recurrence rate; however, cost-effectiveness of fidaxomicin hinders its use as a first line treatment (Al Momani *et al.*, 2018).

Alternative antimicrobials demonstrating action against *C. difficile* include tigecycline, teicoplanin, ridinilazole and ramoplanin. Non-antimicrobial therapies include immunotherapy (monoclonal antibodies and vaccination), adsorbants to bind toxins and probiotics (Roshan *et al.*, 2018). Microbiome-based therapeutics, including FMT and defined bacterial consortia, are discussed in 1.2.2.

1.1.8 Models used to study CDI

1.1.8.1 *In vivo* models of CDI

Animal models play an important role in understanding disease aetiology. They facilitate the study of host-pathogen interactions, immunological response to pathogens and evaluate the safety, toxicity and efficacy of potential drugs and novel treatments. In contrast to clinical studies, animal model subjects are readily available and provide an opportunity to standardise disease severity and progression. They enable the use of experimental drugs and treatment strategies using invasive tests and extensive tissue sampling; however, there are ethical considerations and study approval can be difficult and time consuming. The animals used are fed the same diet and typically come from an inbred stock, where genetic variation is minimal. This can have an impact on studies especially where the microbiome and/or host factors can affect the disease outcome. This has been shown between the disparity in outcomes from mouse studies and clinical trials (Best *et al.*, 2012, Hutton *et al.*, 2014). Additionally, there are inter-species differences in disease susceptibility and aetiology, making extrapolating results between studies and to humans difficult. Several different animal models have been used to study CDI including hares (Dabard *et al.*, 1979), monkeys (Arnon *et al.*, 1984), prairie dogs (Muller *et al.*, 1987), rabbits (Kelly *et al.*, 1994), rats (Castagliuolo *et al.*, 1997), quails (Butel *et al.*, 1998), guinea pigs (Xia *et al.*, 2000), pigs (Steele *et al.*, 2010), and zebrafish (Hamm *et al.*, 2006); however, the mouse (Chen *et al.*, 2008, Lawley

et al., 2009a, Pawlowski *et al.*, 2010) and hamster (Bartlett *et al.*, 1977, Fekety *et al.*, 1979, Buckley *et al.*, 2011) model of CDI are the most common.

Hamster models – Hamster models, in particular Golden Syrian hamsters, demonstrate many of the clinical characteristics seen in human CDI (Price *et al.*, 1979) and have therefore been used extensively as a model for CDI (Sambol *et al.*, 2001, Goulding *et al.*, 2009, Trzasko *et al.*, 2012, Buckley *et al.*, 2013, Weiss *et al.*, 2014). In hamster models, CDI is induced with the administration of an antimicrobial agent that perturbs the normal gut flora, as seen in humans. This model has been used to elucidate many aspects of CDI and has improved our understanding on the mechanisms of CDI initiation, development, aetiology and treatment. Hamster colonisation studies have demonstrated colonisation resistance of the normal flora to CDI (Wilson *et al.*, 1981, Larson and Welch, 1993) and revealed the presence of toxin specific receptors on colonic epithelium (Rolfe and Song, 1993). They were also crucial in establishing the mechanisms of action of *C. difficile* toxins and their role in virulence and disease (Babcock *et al.*, 2006, Lyras *et al.*, 2009). Hamsters have also been used in CDI induction studies (Larson and Borriello, 1990) and in the evaluation of experimental treatments (Trzasko *et al.*, 2012, Sattar *et al.*, 2015). Despite the extensive use of hamsters in CDI research, there are notable limitations with this model. These include the development of a ‘wet-tail’ phenotype in hamsters instead of diarrhoea, which is a crucial feature of CDI in humans. CDI is also rapidly and uniformly fatal in hamsters if left untreated, which is not consistent with human studies (Sambol *et al.*, 2001, Razaq *et al.*, 2007) and limits the duration of experiments, preventing hamsters being used in colonisation and recurrence studies. There are also distinct histological differences, with the caecum as the site of infection in hamsters whereas the colon is the site of infection in humans (Price *et al.*, 1979). The lack of immunological tools available to study the host immune response is also a major drawback to this model.

Mouse models – The use of mouse models in the study of CDI has increased in line with improved susceptibility models as well as the increased availability and variety of mouse models and mouse-related reagents. Similar to humans, CDI in conventional mice is induced by disrupting the flora with antibiotics (Lawley and Young, 2013) with untreated mice becoming asymptomatic

carriers of *C. difficile* (Lawley *et al.*, 2009a). A number of different mouse models have been described (Collignon, 2010).

Gnotobiotic/ mono axenic mice do not have an associated microbiota and therefore no antibiotic treatment is required to induce CDI. They have been used to investigate the host immune response to infection and the contribution of selected members of the microbiota to *C. difficile* colonisation resistance. They have also been used to identify *C. difficile* genes required for colonisation and virulence (Pawlowski *et al.*, 2010, Reeves *et al.*, 2012, Soavelomandroso *et al.*, 2017). However, the lack of a microbiota in this model is not reflective of the normal condition of humans and animals; therefore, the hosts' immune response to infection may not be accurate or complete and results need to be interpreted with caution. This is particularly true as gnotobiotic mice are known to have an underdeveloped immune system as the microbiota plays an important role in immune homeostasis (Wagner, 2008, Yamamoto *et al.*, 2012).

The antibiotic cocktail mouse model was originally developed to overcome some of the limitations of the hamster model in a species with more immunological tools, providing a more reflective model for CDI in humans. Mice are given a cocktail of antibiotics followed by clindamycin induction and *C. difficile* exposure, and the resulting CDI progression and histological findings closely resemble that of humans (Chen *et al.*, 2008). This model has been used to study colonisation resistance and microbiome studies as well as CDI relapse and recurrence (Chen *et al.*, 2008, Sun *et al.*, 2011); however, mice treated with vancomycin were not as susceptible to relapse as humans and develop a milder form of the disease (Sun *et al.*, 2011).

The single antibiotic mouse model is cheaper than the cocktail model and uses one antibiotic, usually either clindamycin or cefoperazone, to disrupt the microbiota and create an environment susceptible to CDI (Theriot *et al.*, 2011, Buffie *et al.*, 2012). This model has been used to study *C. difficile* asymptomatic carriage and spore transmission (Lawley *et al.*, 2009a); environmental spore contamination and disinfection (Lawley *et al.*, 2010) and microbiota changes during antibiotic treatment and CDI (Buffie *et al.*, 2012). One of the main limitations of this model, as with the other mouse models, is the difference between the mouse and human microbiota and immune factors, which makes extrapolating results difficult. Additionally, mice obtained from

different sources produce different responses to the inducing antibiotic, leading to reproducibility problems. Individual *C. difficile* strain variation leading to different disease outcomes is another notable limitation of these models which makes it difficult to draw conclusions using a single strain (Goulding *et al.*, 2009) as well as reproducibility issues using the same strain which requires dose optimisation to improve the consistency of the outcome (Reeves *et al.*, 2011, Sun *et al.*, 2011). Other mouse models include the humanised microbiota mouse using human-derived faecal microbiota (Collins *et al.*, 2015); and the chimeric mouse model with human intestinal xenografts (Savidge *et al.*, 2003).

1.1.8.1.1 *In vitro* models of CDI

With growing ethical considerations towards animal models, it has been increasingly important to utilise alternative models of disease. The advantages of *in vitro* models include: greater control and flexibility over experiment parameters; they are generally more cost and resource effective and more readily available; a greater number of replicates are achievable; and they eliminate the ethical implications of animal models. *In vitro* CDI models range from simple batch culture to complex, multistage chemostat systems; however, they are unable to model the complexity of animal systems and therefore cannot represent host-related interactions.

Batch culture models - Batch culture models are inexpensive and do not require specialised equipment or specialist knowledge, making them cost and time effective. They offer a large degree of flexibility over experiment parameters and facilitate large numbers of replicates. They also provide an ideal opportunity to compare different strains or substrates run in parallel. They have also been used extensively in gene inactivation technologies, with batch culture providing an easy way to determine the difference between wild type strains and mutants (Aubry *et al.*, 2012, Đapa *et al.*, 2013, Dembek *et al.*, 2015, Jain *et al.*, 2017). Despite these advantages, there are notable limitations to batch culture. The short experimental duration does not reflect the behaviour of *C. difficile* or the microflora *in vivo*, and the depletion of nutrients coupled with the accumulation of waste products can influence observations (Best *et al.*, 2012). Borriello and Barclay (1986) described an *in vitro* batch culture colonisation resistance model. They determined that *C. difficile* growth and toxin production was inhibited when co-cultured in the faecal emulsion from

healthy volunteers but not in faecal emulsions from patients undergoing antibiotic therapy. They also determined the inhibitory effect of the faecal emulsion could be negated by sterilisation of the emulsion and therefore attributing the colonisation resistance demonstrated to the healthy microbiome (Borriello and Barclay, 1986). This experiment was repeated with the caecal contents of hamsters and found that *in vitro* findings correlated closely with *in vivo* hamster models (Larson and Borriello, 1990, Larson and Welch, 1993). Similar batch culture models using faecal emulsions from mice were also used to investigate the effect of different antibiotics on the microbiota and their ability to facilitate or inhibit *C. difficile* growth and toxin production (Pultz and Donskey, 2005). They were also used to determine the effect of fluoroquinolones on colonisation resistance and the subsequent selective pressure on different *C. difficile* epidemic and non-epidemic strains (Adams and Mercer, 2007). Horvat and Rupnik (2018), using batch culture models, demonstrated that dysbiotic faecal microbiota was associated with higher *C. difficile* sporulation frequency and was more affected after co-culture with *C. difficile* than healthy faecal microbiota. In addition to colonisation resistance, batch culture has also been shown to determine the inhibitory effects of putative probiotics on *C. difficile* growth and toxin production (Folkers *et al.*, 2010, Schoster *et al.*, 2013) as well as the activity of novel therapeutics, such as phage cocktails, on *C. difficile* growth in faecal emulsions (Nale *et al.*, 2018).

The continuous culture model – Continuous culture models afford additional flexibility over batch models and facilitates the controlled manipulation of the system. They have longer experimental timescales due to the replenishment of nutrients and removal of waste which allows for a more reflective environment than that seen in batch culture experiments. This enables the profile of the microbiota and *C. difficile* to be investigated in response to environmental changes and treatment interventions. The general protocols for continuous models are well standardised including equipment, methodology and monitoring, leading to more reproducible outcomes that can be compared between studies. They tend to be more expensive and labour-intensive than batch culture systems and often require specialist equipment and training. Continuous culture systems can be single, double or triple staged. Single stage systems represent the earliest and most simple systems.

The first continuous culture system to study CDI was used by Onderdonk in 1979, which was an adaptation from an earlier model (Onderdonk *et al.*, 1976). This single stage model was used to evaluate the changes in *C. difficile* toxin levels in culture media and determined that increased temperature and the presence of sub-inhibitory levels of antibiotics resulted in an increase in toxin production but not an increase in *C. difficile* growth (Onderdonk *et al.*, 1979). The complexity of these models increased with the use of caecal contents from hamsters to seed the model (Wilson *et al.*, 1986). They determined that hamster caecal flora in both the continuous model and transplanted to gnotobiotic mice led to the inhibition of *C. difficile* growth. They later used this model to study nutrient competition between *C. difficile* and the hamster flora (Wilson and Perini, 1988). The use of single stage continuous culture models seeded with human faeces was investigated by Yamamoto-Osaki (1994) where the growth of *C. difficile* was inhibited more strongly with faeces from *C. difficile*-negative patients than *C. difficile* positive patients. They also determined that *C. difficile*-negative faeces contained a greater diversity in microbial populations when compared to *C. difficile*-positive faeces and that colonisation resistance to *C. difficile* may be mediated by the consumption of amino-acids by the microflora rather than the production of inhibitors (Yamamoto-Osaki *et al.*, 1994).

Two stage continuous models were later used to investigate the prebiotic effect of substances on *Bifidobacterium*-mediated inhibition of *C. difficile* (Hopkins and Macfarlane, 2003) and to further study colonisation resistance in environments mimicking the proximal and transverse/distal colon (Fehlbaum *et al.*, 2016). The triple stage continuous model of the human gut is a more complex system, allowing microbiota changes to be monitored in an environment highly reflective of the human gut. This model was used to generate much of the data in this thesis and therefore will be discussed in more detail.

The triple stage continuous gut model – The triple stage gut model used to study CDI was based on the model from Macfarlane *et al.* (1998) which was validated against the microbiological and physico-chemical evaluation of the intestinal contents from human sudden death victims. The model consists of three vessels connected in a weir cascade and top fed with a complex growth

medium at a set flow rate. It was designed to reflect the spatial, nutritional, temporal and physico-chemical properties of the human gut from the proximal colon (vessel one), medial/transverse colon (vessel two) and the distal colon (vessel three) (Macfarlane *et al.*, 1998). The model is inoculated with pooled faecal slurry from healthy volunteers and allowed to equilibrate for a minimum of two weeks. Colonisation resistance in the system is determined with the addition of a *C. difficile* spore preparation, with the failure of these spores to establish colonisation and proliferate confirming microbiota-mediated inhibition of *C. difficile*. This is a crucial step not considered in previous models. From this point the model can be used to evaluate antimicrobial propensity to: induce CDI (Moura *et al.*, 2019); to determine antimicrobial efficacy as a CDI treatment option (Freeman *et al.*, 2007, Baines *et al.*, 2009, Chilton *et al.*, 2014b); to investigate antibiotic dosing regimens (Chilton *et al.*, 2015, Crowther *et al.*, 2016); to evaluate the efficacy of novel interventions (Chilton *et al.*, 2016, Wang *et al.*, 2020); to examine the emergence and transfer of resistance determinants (Saxton *et al.*, 2008, Rooney *et al.*, 2019) and to determine the relative fitness of different *C. difficile* strains (Baines *et al.*, 2013, Crowther *et al.*, 2015). Antibiotics instilled into the model are reflective of a clinical dosing regimen with doses instilled periodically over a number of days to ensure levels achieved are consistent with those found clinically in faeces, which is not seen in other models. Depending on the experiment outcomes, the model can run for a number of months, facilitating daily sampling of microbial populations to generate a profile of the microbiota and *C. difficile* and the subsequent responses to interventions (Chilton *et al.*, 2014a, Crowther *et al.*, 2015, Moura *et al.*, 2019).

Human Intestinal Organoids (HIOs) – organoids are miniature 3D organs grown *in vitro* from adult multipotent stem cells (Ootani *et al.*, 2009, Sato *et al.*, 2009, Sato and Clevers, 2013) or induced pluripotent stem cells (iPSC) (Spence *et al.*, 2011), and cultured in stromal replacement scaffolding that resembles *in vivo* structure and organisation. Organoids provide an advance in the structural and functional complexity of intestinal model systems whilst retaining the ability to modify or influence the genetic and molecular aspect of the system (Hill and Spence, 2016, Wallach and Bayrer, 2017). They form a stable environment in which intestinal tissue function and therapeutic targets can be studied as well

as the study of host-pathogen interactions. The ability to self-renew enables increased research throughput when compared to techniques requiring continuously sourced starting material. Organoids sourced from human material are more applicable to pharmacological research than animal *in vivo* models and *in vitro* batch or continuous models and have been used to study host-bacterial pathologies, such as CDI. One of the main limitations for the use of organoids in CDI research included the inability to co-culture the human cell lines with obligate anaerobic microorganisms; however, it was shown that *C. difficile* could persist for at least 12 hours in the organoids, suggesting the presence anoxic microenvironments suitable for the survival of obligate anaerobic microorganisms (Leslie *et al.*, 2015). Microinjections of *C. difficile* directly into the lumen of the organoid demonstrated *C. difficile* colonisation followed by HIO epithelial cell disruption and the loss of para-cellular barrier function. Similar effects were seen with purified TcdA and absent with a non-toxigenic strain (Leslie *et al.*, 2015). HIOs have also been used to study the effect of *C. difficile* on epithelial cell mRNA expression, with the finding that *C. difficile* can inhibit the expression of the sodium-hydrogen exchanger 3 (NHE3), creating an environment more suitable to *C. difficile* growth (Engevik *et al.*, 2015). HIOs were used to define a role for inflammasomes in CDI pathogenesis with the finding that *C. difficile* toxins induced the expression of caspases 3/7 which lead to apoptosis, a critical early stage host defence against CDI (Saavedra *et al.*, 2018). Using HIOs as a toxicity model, cell death was demonstrated upon exposure to *C. difficile* toxins and Melphalan chemotherapy (Apewokin *et al.*, 2017). Pharmacologic studies using HIOs against CDI have also been considered, with the antibiotic Bacitracin preventing TcdB-mediated disruption of the epithelial cells and the maintenance of cell barrier function (Zhu *et al.*, 2019). Although HIOs offer a clear advantage over other models to study CDI, there are still significant limitations and are discussed in numerous reviews (Zachos *et al.*, 2016, Wallach and Bayrer, 2017, Fair *et al.*, 2018). One of the main limitations is that the organoid lacks certain elements seen in the complete organ and only represent intestinal epithelial cells with potentially important contributions from immune, neural and mesenchymal cells not considered this system; however, the use of iPSC negates some of these restrictions as the HIOs contains both epithelial and mesenchymal cells but

require longer to generate (Spence *et al.*, 2011). There are also practical limitations as HIOs are grown in a 3D shape which makes access to the apical surface difficult resulting in complications of manipulating cells for simple procedures such as microscopy, DNA and mRNA isolation and immunocytochemistry (Zachos *et al.*, 2016, Wallach and Bayrer, 2017, Fair *et al.*, 2018).

1.2 The intestinal microbiota

The indigenous microbiota of the intestinal tract is a diverse microbial community with dynamic interactions that influence the host in healthy and disease states. The microbiota is composed of over 10^{14} microorganisms (Gill *et al.*, 2006) with a collective genome that has more than 100 times the number of genes as the human genome. The microbiota play a significant role in regulating host immunity, maintaining colonocyte homeostasis, metabolism and providing colonisation resistance against pathogen invasion (Bien *et al.*, 2013, Thursby and Juge, 2017). Colonisation resistance was first described by van der Waaij *et al.* (1971) after observations that mice were only colonised by challenges of Enterobacteriaceae after antibiotic-induced disruption to the microbiota. They also noted that anaerobic bacteria were fundamental in colonisation resistance and once antibiotic treatment was removed, colonisation resistance gradually re-established (van der Waaij *et al.*, 1971). Colonisation resistance protects the host against outgrowth of opportunistic pathogens, endogenous pathogens found in low numbers in the GI tract as well as exogenous pathogens. Colonisation resistance mediated by a healthy microbiota includes: competition for nutrients and space, with exogenous organisms unlikely to find uncontested niches and available substrates; metabolic mechanisms including bile acid and short chain fatty acid metabolism; as well as active antagonism in the form of bacteriocins and antimicrobial proteins (Sorbara and Pamer, 2019). The distribution of microorganisms in the intestinal tract is heterogeneous and therefore the mechanisms of colonisation resistance vary according to the spatial organisation of the microenvironments.

Whole-genome shotgun sequencing has revealed a plethora of species isolated from the GI tract with 93.5 % belonging to the phyla Proteobacteria, Firmicutes, Bacteroidetes and Actinobacteria (Hugon *et al.*, 2015). The specific composition of the gut microbiota is highly variable between regions of the gut and between individuals; however, it displays a high degree of functional redundancy and is shaped by both environmental factors and host genetics. Abundant microenvironments of the intestine provide distinct niches for microbes to occupy, with the composition of mucosal communities varying from

luminal contents (Zoetendal *et al.*, 2002, Lavelle *et al.*, 2015). Microbial characterisation of an *in vitro* model simulating luminal and mucosal populations revealed a predominance of Bacteroidetes and Proteobacteria in the luminal content whilst Firmicutes, in particular butyrate-producing *Clostridium* cluster XIVa, preferentially colonised the mucin layer (Van den Abbeele *et al.*, 2013). Perturbation of a healthy microbiota exposes previously unavailable niches and substrates, providing an opportunity for pathogen expansion.

1.2.1 Intestinal dysbiosis

There are a number of different definitions for intestinal dysbiosis, but here it will be described as an imbalance of the microflora and its function (Carding *et al.*, 2015, Lynch and Pedersen, 2016). Intestinal dysbiosis can be caused by a number of factors including drug exposure (in particular antimicrobial agents), stress, radiation and dietary changes. A number of disease states have been linked to intestinal dysbiosis such as inflammatory bowel disease (IBD) (Baumgart and Carding, 2007), metabolic disorders (Ley *et al.*, 2006, Cani *et al.*, 2008), central nervous system related diseases (Lyte *et al.*, 2006), carbapenamase-producing Enterobacteriaceae (CPE) colonisation (Evain *et al.*, 2019) and intestinal infections like CDI (Milani *et al.*, 2016). One of the greatest risk factors of CDI is the use of broad spectrum antibiotics as their use results in dramatic changes to the intestinal microbiota with a decrease in microbial species and functional diversity, creating an environment favourable to colonisation by pathogens, such as *C. difficile* (Khoruts and Sadowsky, 2016). Initial colonisation of *C. difficile* is vital for pathogenesis and therefore the loss of colonisation resistance in the intestinal tract exposes niches previously unavailable to *C. difficile* colonisation, facilitating outgrowth and toxin production. The propensity of an antimicrobial agent to induce CDI is likely related to the effect it has on the host microbiota and *C. difficile* itself. It was found that antimicrobial agents with a broad spectrum increase the risk of inducing CDI when compared to an agent with a narrow spectrum in mice (Pultz and Donskey, 2005). Antibiotic treatment of CDI further perturbs the microbiota, leading to disease relapse, which is reflected in high rates of rCDI (Cornely *et al.*, 2012a, Marsh *et al.*, 2012). The microbiota of patients with recurrent CDI is characterised by reduced community diversity and subsequent

reduced community structure and function, characterised by a reduction in the phylum of Bacteroidetes and Firmicutes, with an increase in Proteobacteria (Chang *et al.*, 2008, Khoruts *et al.*, 2010). Intestinal dysbiosis also leads to metabolic changes in the gut, such as faecal bile acid metabolism. Broad spectrum antibiotics significantly diminish bacterial populations responsible for secondary bile acid metabolism, which are known to inhibit *C. difficile* spore germination. This leads to the accumulation of primary bile acids such as taurocholate and cholate, both being potent *C. difficile* germinants (Sorg and Sonenshein, 2008).

1.2.2 Microbial based therapies

1.2.2.1 Faecal microbiota transplantation (FMT)

Faecal microbiota transplantation (FMT) is a treatment that involves the transplantation of minimally manipulated faeces from a healthy donor to a recipient with the intent of restoring normal gut microbiota composition and function. FMT has been recommended to treat multiply recurrent CDI (Debast *et al.*, 2014). FMT was first described in the 1958 as a treatment for pseudomembranous colitis (Eiseman *et al.*, 1958) and later in the 1983 for CDI (Schwan *et al.*, 1983). A systematic review reported the weighted pooled rate (WPR) clinical cure after a single FMT infusion as 76.1 % (Tariq *et al.*, 2018). It was found that cure rates were lower in randomised trials than open-label studies (WPR: 67.7 % vs 82.7 %), most likely due to patient selection and differences in primary outcomes and study definitions. The randomised trials reported similar cure rates to observational studies after multiple FMT infusions (Tariq *et al.*, 2018). The exact mechanisms underlying the success of FMT are not fully understood; however, the bacterial diversity and functional profile of patient faeces was found to have increased after FMT instillation, reflecting the composition of the donor stool (van Nood *et al.*, 2013, Youngster *et al.*, 2014, Kelly *et al.*, 2016).

1.2.2.1.1 Donor screening, preparation and instillation of stool

Donor eligibility and screening varies between studies; however, in general the donor must be healthy, between 18-50 years of age, have normal bowel movements and to have not taken antimicrobial agents for at least three months, sometime six months, preceding the donation. It is also preferable if a

co-habiting relative of the recipient is able to donate due to the likelihood of a similar microbiota composition due to linked environments. A medical interview and physical examination is conducted and donors excluded if they have a known communicable disease or other systemic or metabolic disease. Donor faeces are screened for parasites and pathogens and general blood work conducted. Routes of administration include the upper GI tract through a nasogastric or nasojejunal tube or gastroscopy (Gough *et al.*, 2011, van Nood *et al.*, 2013); and the lower GI tract using retention enemas (Gough *et al.*, 2011) or colonoscopy (Youngster *et al.*, 2014, Cammarota *et al.*, 2015, Kelly *et al.*, 2016).

1.2.2.1.2 FMT for the treatment of recurrent CDI

Clinical cure rates of 76.1 % (WPR) after a single FMT for rCDI were reported in a systematic review, with lower rates seen in studies including both recurrent and refractory CDI than those with rCDI only (WPR: 63.9 % vs 79 %, $p < 0.001$) (Tariq *et al.*, 2018). It was also found that colonoscopy and oral route were more effective as faecal delivery routes than an enema (Tariq *et al.*, 2018). A randomised open-label controlled trial by van Nood *et al.* (2013) studied three treatment regimes, (1) vancomycin (500 mg 4x daily for 4-5 days) followed by bowel lavage and infusion of FMT through a nasoduodenal tube after antibiotic treatment, n=17, (2) vancomycin (500 mg 4x daily for 14 days), n=13 (3) vancomycin (500 mg 4x daily for 14 days) with bowel lavage on day 4 or 5, n=13. The outcome of the study revealed a 81 % resolution rate for the FMT group (94 % resolution after multiple infusions) and 31 % resolution for the vancomycin only group and 23 % resolution rate for vancomycin treatment followed by bowl lavage. Based on these results, the trial was terminated and the FMT treatment offered off-protocol to the patients in the other arms of the study, achieving an 83 % resolution rate. A pilot study was conducted by Youngster *et al.* (2014) to determine the effectiveness of using a frozen faecal inoculum from unrelated donors for rCDI. A 70 % resolution rate after one FMT treatment was reported and an overall resolution rate of 90 % after retreatment. This demonstrated that using an infusion of unrelated frozen donor stool was efficacious in treating rCDI. A follow up study looking at the oral instillation of a suspension of double encapsulated frozen faecal matter was conducted with an overall resolution rate of 91 % with one or two treatments (Youngster *et al.*,

2016). Another randomised, open-label controlled trial was conducted by Cammarota *et al.* (2015) to evaluate the efficacy of vancomycin treatment followed by FMT instillation versus an extended vancomycin treatment in treating rCDI. Vancomycin treatment followed by FMT instillation returned an overall cure rate of 90 %, whereas vancomycin only had a 26 % cure rate, further illustrating the effectiveness of FMT therapy on rCDI.

In a retrospective series, Kelly *et al.* (2014) investigated the effectiveness and safety of FMT in immunocompromised (IC) patients. IC patients have previously been excluded from FMT studies due to safety concerns; however, the overall resolution rate was reported as 89 % with no deaths or documented infections that occurred as a result of FMT treatment, suggesting that FMT treatment appears to be a safe and effective treatment for rCDI in IC patients. Importantly, two cases of bacteraemia (one of whom died) linked to the transfer of an extended-spectrum beta-lactamase (ESBL) producing *Escherichia coli* following FMT from the same donor have raised major safety concerns (safety alert, FDA).

The mechanisms underlying the success of FMT are likely multifactorial and not fully understood; however, restoration of bile acid metabolism and short-chain fatty acid (SCFA) levels through the reconstitution of a more diverse microbiota have been implicated (McDonald *et al.*, 2018a, Seekatz *et al.*, 2018, Mullish *et al.*, 2019). In contrast, a study using sterile filtrates were effective in the treatment of CDI, indicating that bacterial components and metabolites may be sufficient to reduce the risk of CDI while the normal gut flora is re-established (Ott *et al.*, 2017). Interestingly, analysis of bacteriophages in the filtrate indicated a role for the virome in the efficacy of FMT (Ott *et al.*, 2017). 16S ribosomal RNA (rRNA) was used to determine diversity in patients before and after FMT and the respective donors. The microbial community diversity was consistently low prior to FMT displaying marked dysbiosis characterised by a reduction in the phyla Firmicutes and Bacteroidetes with an increase in Proteobacteria. Post-FMT showed a significant increase in diversity within two weeks, becoming indistinguishable from donor samples and characterised by an increase in Firmicutes; in particular the genus *Blautia*, *Faecalibacterium*, *Roseburia*, *Ruminococcus*; and *Bacteroidetes*; in particular *Bacteroides* and *Parabacteroides*. This was accompanied by the reduction in Proteobacteria;

both Gammaproteobacteria and Betaproteobacteria, in particularly *Enterococcus*, *Escherichia* and *Klebsiella* (van Nood *et al.*, 2013, Youngster *et al.*, 2014, Kelly *et al.*, 2016, Kellingray *et al.*, 2018, Staley *et al.*, 2019).

Adverse events after FMT were generally minor and included patients reporting diarrhoea, abdominal cramps and pain, bloating, constipation, fever, nausea, vomiting, belching and flatulence; however, serious adverse effects have been reported, including death linked directly to FMT from aspiration pneumonia (Baxter *et al.*, 2015, Baxter and Colville, 2016, Wang *et al.*, 2016, Bang *et al.*, 2017), and the transfer of an ESBL producing *E. coli* (safety alert from the FDA). This highlights the safety concerns of FMT and the need to further develop more defined and standardised microbiome-based therapeutics.

1.2.2.2 Other microbiome-based therapies

The success of FMTs have demonstrated that the microbiome can be modulated for an advantageous outcome in CDI; however, the lack of standardisation and potential safety concerns have prompted great interest in defined microbiome based therapies. Using information gathered from FMT experiments, researchers have been able to identify selected populations that may be responsible for the efficacy of the FMT and have strived to create a more defined bacterial consortium or indeed an alternative method of FMT delivery, offering a more standardised procedure.

Targeted restoration of the microbiota has been shown to resolve rCDI in mice (Lawley *et al.*, 2012), generating much interest in the field of targeted microbiome therapies in humans. Rebiotix's RBX2660 works in a similar way to an FMT and is an enema microbiota suspension prepared from a large faecal slurry comprised of 75 stool donations from 17 donors. In a randomised, double-blind, placebo controlled study, 1 dose of RBX2660 proved more effective than the placebo ($p < 0.05$) with an overall response rate of 88.8 % (Dubberke *et al.*, 2018). Further to this study, RBX7455 was produced, which is a lyophilized, orally-administered therapy based on the RBX2260 enema formulation. RBX7455 is in Phase 1 proof-of-concept trial for rCDI with an overall success rate of 90 %, with patients remaining recurrence free at 6 months post treatment (Khanna *et al.*, 2018, Khanna *et al.*, 2019). Another example of lyophilized orally-administered therapies based on faecal-derived

microbiota is the CP101 formulation from Finch Therapeutics. For the treatment of rCDI, CP101 achieved an 88 % success rate with confirmation of phylum-level engraftment of CP101 such that recipients' microbiota composition shifted to that of CP101 (Staley *et al.*, 2017a, Staley *et al.*, 2017b).

A different approach is being taken by Seres Therapeutics in an attempt to produce an effective treatment for rCDI using a more defined bacterial consortium rather than a faecal suspension. SER-109, an oral capsule of a defined mix of spores sourced from faecal donors, achieved 95 % clinical resolution of rCDI in Phase 1 trials (Khanna *et al.*, 2016); however, phase 2 results were in contrast to this with no significant reduction in rCDI. In a post-trial analysis, it was proposed that the lack of SER-109 efficacy in the Phase 2 trial could be due to suboptimal dosing and patient selection issues, with rCDI diagnosed using PCR-based means, which, if not coupled with toxin testing, could incorrectly classify diarrhoea (in the presence of *C. difficile* colonisation) as active rCDI (press release, Seres Therapeutics). SER-109 has entered Phase 3 trials based on these observations. Another Seres Therapeutics product, SER-262, was based on 12 strains of bacterial spores from SER-109 that engrafted in SER-109 patients. SER-262 is produced from *in vitro* fermentation, eliminating the need for faecal donors, reducing the safety concerns surrounding FMTs and a standardised procedure and composition. SER-262 is in Phase 1 clinical trials (ClinicalTrials.gov Identifier: *NCT02830542*). Most microbiome-based therapeutics are based on human faecal specimens and therefore focused on luminal contents alone. Indeed, post-treatment engraftment and microbial composition only looks at luminal populations. The mucosal microbial communities, due to inaccessibility, have been overlooked. Considering the link between biofilms and chronic, relapsing infections (Bjarnsholt, 2013), the need to study the composition of the biofilm communities and their potential role in rCDI is evident.

1.3 Biofilms

The association of biofilms with chronic infection has been well demonstrated (Donlan and Costerton, 2002, Hall-Stoodley and Stoodley, 2009, Bjarnsholt, 2013), therefore biofilm formation could play an important role in CDI, in particularly CDI recurrence, where the biofilm could protect *C. difficile* cells from host defences and antimicrobial therapy, as well as preventing its removal from the gut with the luminal flow. *C. difficile* has been shown to form robust biofilms *in vitro* (Dawson *et al.*, 2012, Donelli *et al.*, 2012, Đapa *et al.*, 2013, Semenyuk *et al.*, 2014) and *in vivo* (Buckley *et al.*, 2011, Semenyuk *et al.*, 2015) in mouse and hamster models. A biofilm is regarded as a complex community of microbial cells embedded in a self-produced matrix of extracellular polymeric substances (EPS) (Costerton *et al.*, 1995, de Vos, 2015, Coenye *et al.*, 2020). The matrix is mainly comprised of polysaccharides, extracellular DNA and proteins; however, non-cellular materials may also be found depending on the environment in which the biofilm formed (Percival *et al.*, 2011). They are ubiquitous in nature and are believed to be the predominant mode of bacterial growth. The clinical implications of biofilms have been extensively reviewed (Donlan, 2001a, Hall-Stoodley *et al.*, 2004) with an estimated 65 % of all hospital infections being associated with biofilms (Costerton *et al.*, 1999, Potera, 1999, Donlan, 2001b). Biofilms present in hospital wards on medical devices and equipment act as reservoirs for pathogens leading to the spread of infection. Biofilms protect pathogens from the hosts' immune response and act as a barrier to certain antimicrobial agents, contributing to disease persistence and recurrence (Costerton *et al.*, 1995, Bjarnsholt, 2013) resulting in significant patient morbidity and mortality as well as economic burden.

The study of anaerobic bacteria in intestinal biofilms is poorly understood due to the invasive nature of mucosal sampling and the lack of suitable *in vitro* models, therefore the role of biofilms in CDI has not been fully elucidated. Due to the inaccessibility of the mucosal communities in healthy individuals, the majority of the data on these populations comes from biopsy samples from patients with GI disorders with results potentially influenced by antimicrobial therapy and colonic washing prior to the procedure. In these studies, it has become clear that microbial populations adherent to the colonic mucosa are

heterogeneous in their distribution along the colon, taking advantage of microhabitats and selective metabolic niches. The community profile of the sessile populations were revealed to be significantly different from those obtained from faecal specimens (Zoetendal *et al.*, 2002, Macfarlane and Dillon, 2007). Although not anatomically reflective, *in vitro* biofilm studies of microorganisms isolated from the GI tract provide data on potential biofilm forming capabilities and mechanisms.

1.3.1 Biofilm formation and development

The ability of *C. difficile* to form a biofilm *in vitro* was first demonstrated by Donelli *et al.* (2012) using crystal violet staining and Field Emission Scanning Electron Microscopy (FESEM). Further studies revealed that the amount of biofilm produced was strain dependent, with hyper virulent strains forming a larger biofilm (Đapa *et al.*, 2013, Piotrowski *et al.*, 2017). Many studies have since focused on the mechanisms underpinning *C. difficile* biofilm formation *in vitro* using a combination of microscopy and biofilm batch cultures. During *in vivo* studies, *C. difficile* has been shown to adhere to the epithelial mucosa in hamster (Borriello *et al.*, 1988b) and mouse models (Spigaglia *et al.*, 2013). *In vivo* evidence for biofilm formation of *C. difficile* was demonstrated by clumps or aggregates of *C. difficile* cells associated with damaged tissue, the epithelial barrier and within the mucus layer (Lawley *et al.*, 2009a, Spencer *et al.*, 2014, Soavelomandroso *et al.*, 2017). Semenyuk *et al.* (2015) demonstrated that *C. difficile* was present as a minority member of a multispecies community located in the outer mucus layer in the caecum and colon of a mouse model, providing evidence of interactions of *C. difficile* with multispecies biofilms. Evidence of *C. difficile* biofilm formation in the human GI tract has not yet been demonstrated; however, cells have been shown to adhere to human intestinal epithelial lines *in vitro* (Drudy *et al.*, 2001, Spigaglia *et al.*, 2013) and Lyra *et al.* (2012) detected *C. difficile* together with common GI tract microorganisms in a mucosal biopsy sample. This evidence suggests the potential for *C. difficile* to form biofilms or be incorporated into existing biofilms in the GI tract.

The transition from unicellular planktonic organisms to diverse surface-bound multicellular communities requires a highly regulated developmental pathway in response to bacterial and environmental signals. Through advances in molecular and imaging techniques, many of the mechanisms of biofilm

formation have been identified. Although complex, biofilm development follows a regulated path and is generally accepted as consisting of four stages (Palmer and White, 1997, Sauer *et al.*, 2002) namely initial reversible attachment, irreversible attachment, co-aggregation/maturation and dispersal/detachment (Figure 1-5). These stages form part of a biofilm life-cycle with detached cells reverting back to a planktonic phenotype. Bacteria within each stage are phenotypically distinct from cells in other developmental stages (Sauer *et al.*, 2002) and it is possible for all four stages to occur simultaneously in mature biofilms. The cells within biofilms display altered gene expression profiles in each stage, creating a community of cells fundamentally different from planktonic cells, capable of rapidly responding and adapting to changing internal and external conditions (Donlan, 2002).

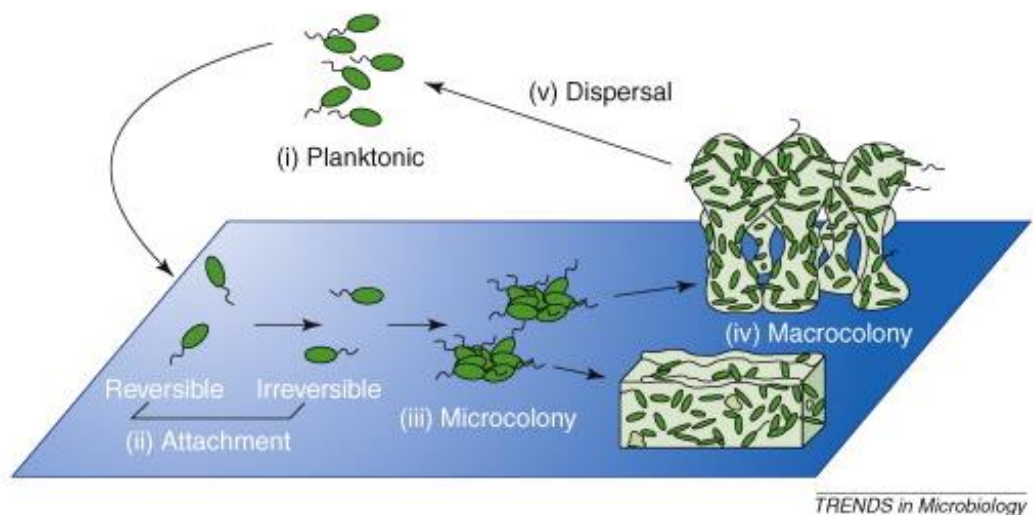


Figure 1-5 Developmental model of biofilm formation. Through microscopic analysis of predominantly Gram negative bacteria, *Pseudomonas aeruginosa* in particular, this developmental model was established. It illustrates the formation of a biofilm as a life-cycle, with transitions through distinct developmental stages. These stages include the attachment of planktonic (i) bacteria to a surface (ii), aggregation and microcolony formation (iii), biofilm maturation to a macrocolony (iv) and dispersal or dissemination back to a planktonic state (v). Image from Monds and O'Toole, 2009.

1.3.1.1 The biofilm life-cycle

The establishment of a biofilm is a multifactorial process consisting of phases that contain both conserved and species-specific events. The first step in biofilm formation is attachment to a surface. Zobell (1943) first proposed that adherence was a two-step sequence involving initial reversible attachment followed by irreversible attachment. In order for bacteria to attach to a surface, they need to be in close proximity to the surface and this is mediated by Brownian motion, gravitation, diffusion or intrinsic motility of the organism.

Biofilm formation is initiated through the non-specific interaction of planktonic bacteria with a substratum in response to environmental conditions. Non-specific binding involving hydrophobic and electrostatic interactions often occurs between a bacteria and an abiotic surface, whereas specific molecular mechanisms characteristic to the surface of the cell are involved in adhesion to living tissue (Percival *et al.*, 2011) such as hydrophobicity, the presence of flagella, fimbriae, lipopolysaccharide (LPS) and the production of EPS (Donlan, 2002). Using phase-contrast microscopy, O'Toole and Kolter (1998a) determined that planktonic cells attach as a dense monolayer to the substratum, followed by microcolony formation. This initial attachment is reversible as some cells may only attach transiently. Motile bacteria generally have a competitive advantage, using flagella to overcome some of the repulsive forces and align the bacteria in close proximity to the surface. A mutant defective for flagella biosynthesis in *Pseudomonas aeruginosa* was unable to make stable interactions with an abiotic surface resulting in few adherent cells (O'Toole and Kolter, 1998a) and a significant reduction in biofilm formation under flow conditions when compared to the flagellated wild type (Sauer *et al.*, 2002). The role of flagella in biofilm formation is not restricted to initial binding, with investigations indicating an architectural role for flagella in biofilms with consequences throughout the biofilm life-cycle in *E. coli* (Domka *et al.*, 2007, Serra *et al.*, 2013). In *C. difficile*, a flagella mutant produced less biofilm than the wild type strain; however, this effect was only seen in later stages of biofilm development indicating a role for flagella in *C. difficile* biofilm maturation (Đapa *et al.*, 2013).

Irreversible attachment is characterised by specific interactions of the microorganism with the conditioning film, which is formed by the adsorption of

molecules to the substrate that influences adhesion (Lorite *et al.*, 2011). These interactions are facilitated by the presence of cell-surface adhesions, such as pili, and stimulate various signalling pathways regulated by intra and extracellular signals leading to biofilm formation (O'Toole and Kolter, 1998b). A role for T4P in stabilising interactions with the surface and other cells was demonstrated when a *P. aeruginosa* mutant defective for T4P biosynthesis was able to form a sparse monolayer of planktonic cells adhered to the surface but failed to aggregate and form microcolonies (O'Toole and Kolter, 1998a). T4P-mediated twitching motility was also found to be necessary for cells to migrate along a surface to recruit other cells into aggregates, indicating a role for T4P early on in the developmental pathway. A *C. difficile* pilin *pilA1* mutant, defective for T4P production, formed an initial biofilm with significantly reduced mass and thickness when compared to the wild type. Biofilm forming ability was restored upon complementation, indicating a role for T4P in early *C. difficile* biofilm formation (Maldarelli *et al.*, 2016, Purcell *et al.*, 2016). RNA sequencing also revealed an altered gene expression profile for T4P when *C. difficile* was grown in a biofilm, compared to planktonic growth (Maldarelli *et al.*, 2016). Đapa *et al.* (2013) also found a role for a mature S-layer in early *C. difficile* biofilm formation while investigating a mutated *cwp84* gene. The *cwp84* gene encodes a surface protease that is involved in maturation of the S-layer in *C. difficile*. The *cwp84* deletion mutant showed no defect in planktonic growth in strain R20291; however, a dramatic reduction in biofilm accumulation was seen (Đapa *et al.*, 2013). The opposite was seen in strain 630 as this mutant displayed an increase in biofilms formation (Pantaleon *et al.*, 2015). Both strains encode different proteins that are involved in S-layer maturation and therefore express different protein arrays on the immature S-layer (Biazzo *et al.*, 2013), indicating that the contribution of the S-layer to biofilm formation is strain specific.

During biofilm maturation, cell clusters become progressively layered with the majority of the cells displaced from the substratum. Characteristic of the maturation stage is biofilm differentiation resulting in a complex architecture consisting of mature community encased in EPS. The greatest difference in protein expression is seen in the maturation stage when compared to planktonic cells with approximately 50 % of proteins upregulated in a mature *P.*

aeruginosa biofilm with 36 % of the detectable proteins displaying a 6 fold or higher change in regulation (Sauer *et al.*, 2002). It was also found that protein patterns were significantly different from the reversible binding stage with the *de novo* expression of over 100 proteins.

In the final stage of biofilm development, cell clusters undergo alterations in their structure as a result of the dispersion/detachment of bacteria from the interior to the bulk phase. Dispersion facilitates the recolonization of biofilms when there is nutrient limitation or an accumulation of waste products. Dawson *et al.* (2012) demonstrated the ability of *C. difficile* biofilms to detach from an abiotic surface as a free-floating aggregate, which could have consequences in CDI. The dispersion of bacteria from biofilms has vast implications for clinical settings (Nickel *et al.*, 1994, Lindsay and von Holy, 2006, Percival and Suleman, 2014) and public health (Zottola and Sasahara, 1994, Lau and Ashbolt, 2009), with links to infection dissemination and persistence. Stoodley *et al.* (2001) investigated the detachment of cells from a mixed species biofilm comprised of *P. aeruginosa*, *Pseudomonas fluorescens*, *Klebsiella pneumoniae* and *Stenotrophomonas maltophilia*, and reported the dissemination of large cell clusters containing enough cells to exceed the minimum infective dose of many biofilm-forming pathogens. Cells from a biofilm may be dispersed passively through erosion and sloughing or actively in response to quorum sensing (QS) signals and/or nutrient levels or shedding from actively growing cells. Detachment of biofilm aggregates offer a fitness advantage in establishing new biofilms over planktonic cells in environments with high competition for nutrients.

The release of cells is facilitated by the degradation of the EPS believed to be initiated by the concentration of an inducer molecule resulting in the expression of matrix-degrading enzymes (Stoodley *et al.*, 2002). Examples of matrix polymer-degrading enzymes include the surface protein releasing enzyme (SPRE) of *Streptococcus mutans* (Lee *et al.*, 1996) and alginate lyase of *P. aeruginosa* (Boyd and Chakrabarty, 1994) with overexpression leading to the disruption of the EPS and the subsequent release of cells from the biofilm. Cell-density-dependent regulation and QS homoserine lactones have also been implicated in cell dispersal through the activation of matrix-degrading enzymes (Allison *et al.*, 1998, Stoodley *et al.*, 2002).

1.3.1.2 Biofilm structure

The extracellular matrix of a biofilm is composed of water, environmental components such as host molecules, and self-produced EPS consisting of: polysaccharides, proteins, nucleic acids and lipids (Di Martino, 2018). The function of the EPS is to provide mechanical stability to biofilms and mediates their adhesion to surfaces whilst providing protection against biocides, antibiotics, host immune responses and UV radiation (Flemming and Wingender, 2010). The formation of the EPS matrix creates a unique environment that facilitates the transition to a biofilm mode of growth. The exact composition of the EPS is dependent on the environment in which it forms and the organisms present, therefore varies greatly in its physical and chemical properties. The EPS is able to incorporate large amounts of water into its structure through hydrogen bonding which protects the embedded cells from desiccation and is responsible for over 90 % of the dry mass of a biofilm (Donlan, 2002). The EPS is able to immobilise biofilm cells and keeps them in close proximity to enable interactions to occur such as cell-to-cell communication through quorum sensing, horizontal gene transfer and the development of synergistic cooperation (Flemming and Wingender, 2010). The matrix is able to retard the diffusion of extracellular enzymes enabling cells to metabolise particulate nutrients, serving as an external digestive system, allowing nutrients to be sequestered and utilised. It also keeps the contents of lysed cells available as a source of nutrients and serves as a genetic archive.

The EPS facilitates the formation of extensive 3D networks with differing chemical gradients, generating biodiversity by forming a range of different habitats within a single biofilm. It provides physical structures that separate micro-domains harbouring different biochemical environments that are modified in response to changing external and internal conditions (Lawrence *et al.*, 2007). The structure of the EPS is also influenced by the interaction of non-microbial particles from the host or the environment, which may become embedded in the matrix. This is evident during infective endocarditis when microcolonies develop in a matrix of EPS, fibrin and platelets leading to the development of a fibrin capsule that protects the bacteria from the host immune response (Durack, 1975).

The presence and purpose of extracellular DNA (eDNA) within the EPS has been extensively reviewed by Montanaro *et al.* (2011) and Okshevsky and Meyer (2015). Altruistic autolysis of small sub-populations and fratricidal differentiation of attacker and target cells are the main mechanisms responsible for the release of DNA into the matrix. The presence of eDNA in the matrix plays an important role in the initial attachment of bacteria and stabilises the matrix structure. It also acts as a dynamic gene pool facilitating the rapid spread of virulence and antibiotic resistance genes through horizontal gene transfer to naturally competent organisms. DNA is also anionic and therefore has the ability to chelate cations and restricts the diffusion of cationic antimicrobial agents. Investigations on the composition of EPS of *C. difficile* has revealed the presence of eDNA, polysaccharides and proteins (Đapa *et al.*, 2013, Semenyuk *et al.*, 2014). Differential polysaccharide staining of *C. difficile* biofilms revealed different polysaccharide compositions on the surface of cells and the intracellular regions (Figure 1-6).

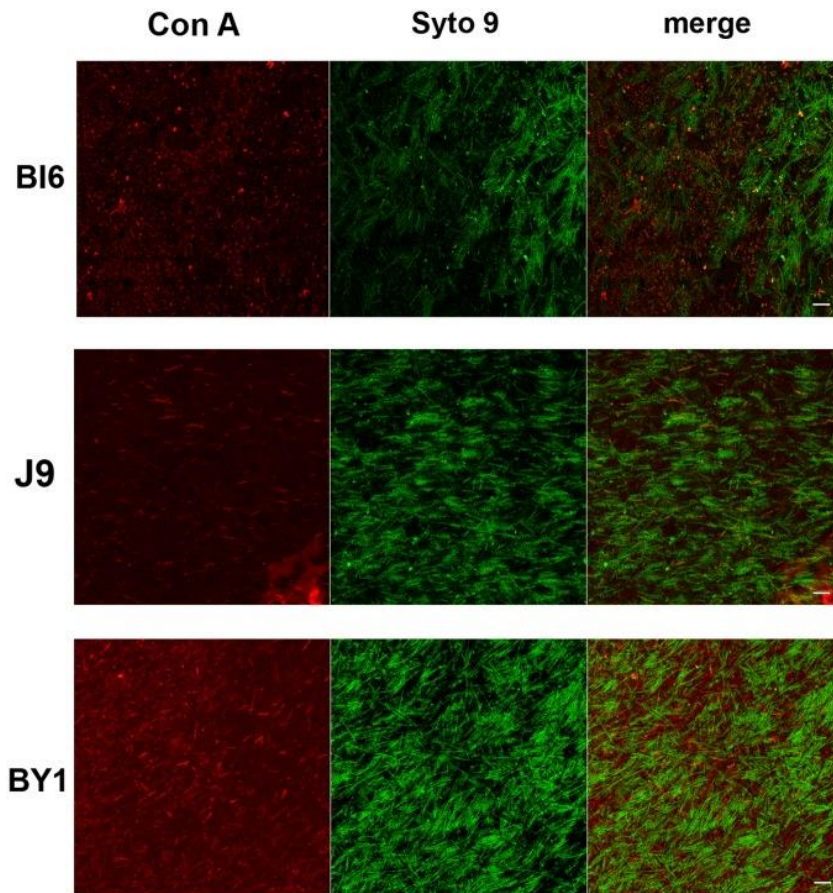


Figure 1-6 Confocal laser-scanning analysis of stained *C. difficile*

biofilms. *C. difficile* strains B16 (top panels), J9 (middle panels) and BY1 (bottom panels) were stained with the polysaccharide stain concanavalin A-Texas Red (left panels) and the nucleic acid stain Syto-9 (middle panels) (middle, Syto-9, green) and imaged separately (left and middle panels) and together (right panels). Image from Semenyuk *et al.*, 2014.

1.3.1.3 Genetic determinants for *C. difficile* biofilm formation

C-di-GMP can regulate cellular pathways through a number of mechanisms including regulation of gene expression through directly binding to riboswitches or modulation of transcription factors or allosteric regulation of enzymes (Sudarsan *et al.*, 2008, Valentini and Filloux, 2016). Levels of c-di-GMP are regulated by the enzymes diguanylate cyclase (DGC) responsible for its synthesis, and c-di-GMP specific phosphodiesterase (PDE) responsible for its breakdown (Simm *et al.*, 2004). In a study by Bordeleau *et al.* (2011), *C. difficile* was found to express an unusually high assortment of functional DGCs and PDEs, indicating that c-di-GMP was an important and well conserved signalling

system. They also found that increased levels of c-di-GMP resulted in reduced flagella expression whilst increasing the expression of adhesins (Bordeleau *et al.*, 2011). Ectopic expression of genes regulating c-di-GMP levels demonstrated reduced motility and cell aggregation associated with high c-di-GMP levels (Purcell *et al.*, 2012). Later it was found that c-di-GMP levels regulate T4P expression, flagella motility and toxin synthesis (Purcell *et al.*, 2016). When examining one of the PDEs involved in c-di-GMP regulation, it was found that it was allosterically regulated by GTP and that its transcription was controlled by the nutrient-regulated transcriptional regulator CodY, linking c-di-GMP levels to nutrient availability (Purcell *et al.*, 2017). CodY is a global regulatory protein that regulates cellular activity in response to nutrient levels in the environment (Dineen *et al.*, 2010). In this way, biofilm formation is linked to nutrient availability through the action of CodY on c-di-GMP levels.

Another transcriptional regulator that plays a significant role in *C. difficile* biofilm formation is Spo0A. Spo0A is more commonly known as a sporulation regulatory element; however, depending on the phosphorylation state of Spo0A, it has been shown to influence biofilm formation. This was demonstrated when Spo0A mutants formed a significantly reduced biofilm *in vitro* (Dawson *et al.*, 2012, Dapa *et al.*, 2013). The Spo0A signalling pathway has been shown to play an important role in sporulation, cannibalism and biofilm formation, with the degree of phosphorylation determining the cell fate in *Bacillus subtilis* (Aguilar *et al.*, 2010). In *B. subtilis*, Spo0A is able to regulate the activity of the transcriptional regulator SinR through activation of the expression of its antagonist SinI (Newman *et al.*, 2013). SinR represses the expression of biofilm-related genes and therefore when Spo0A activates the expression of *sinI*, this results in the inhibition of SinR and subsequent expression of biofilm-related genes. Homologues of *sinR* and *sinI* have been found in *C. difficile* (Edwards *et al.*, 2014) and have been linked to sporulation, toxin production and motility (Girinathan *et al.*, 2018, Ciftci *et al.*, 2019). A SinR-like regulator in *C. difficile* (CD2214 and/or CD2215) control many genes associated with biofilm formation, with mutants in both causing an increase in biofilm formation (Poquet *et al.*, 2018). With sporulation and biofilm formation closely associated, the presence of sporulation in biofilms could have significant implications for disease persistence and dissemination. Semenyuk

et al. (2014) found that sporulation efficiency in *in vitro* biofilms formed from human clinical isolates had a sporulation efficiency of between 46 – 65 %, suggesting high levels of sporulation in these biofilms.

1.3.2 Characteristics of biofilms

1.3.2.1 Interactions within the biofilm

The GI tract is home to plethora of microorganisms who likely co-exist in a multispecies biofilm. Intra and interspecies interactions within multispecies biofilms are fundamental in shaping the overall structure, spatial organisation and regulation of gene expression of the different cells of the biofilm. Social phenotypes influence evolutionary fitness through cooperative and competitive interactions (Kim *et al.*, 2008, Liu *et al.*, 2016, Nadell *et al.*, 2016), which is fundamental in shaping the overall structure and function of the biofilm. Spatial organisation within biofilms can act to balance competitive and cooperative interactions leading to community stability (Kim *et al.*, 2008). This has distinct advantages over planktonic cells including protection against antimicrobial agents, host immune system, desiccation and protozoan predation (Burmølle *et al.*, 2014).

A key determinant in biofilm success and survival is the diversity of the species found therein. Population diversity increases the likelihood of survival when the biofilm is subjected to adverse conditions, with certain subpopulations demonstrating increased fitness when exposed to selected conditions. This may also be true in mono-species biofilms. Phenotypic heterogeneity in metabolism, physiology and gene expression create subpopulations with different biological roles within the biofilm, allowing rapid response to changes in the environment. Using FESEM micrographs, the presence of *C. difficile* vegetative cells were found growing in dense mats on an abiotic surface, interspersed with sporulating cells, spores and cell debris encased in a filamentous EPS matrix (Dawson *et al.*, 2012, Donelli *et al.*, 2012), with biofilm thickness increasing over time (Figure 1-7). Z-stack imaging and live/dead staining revealed multiple structured layers of cells composed largely of live cells (Đapa *et al.*, 2013). In a triple stage model of the human colon simulating CDI, dormant *C. difficile* spores and vegetative cells were found associated

with the multispecies biofilm throughout the experiment (Crowther *et al.*, 2014a), and Semenyuk *et al.* (2014) demonstrated the presence of two distinct exosporium morphotypes and toxin-producing vegetative cells during biofilm formation, further illustrating the heterogeneity found in *C. difficile* biofilms.

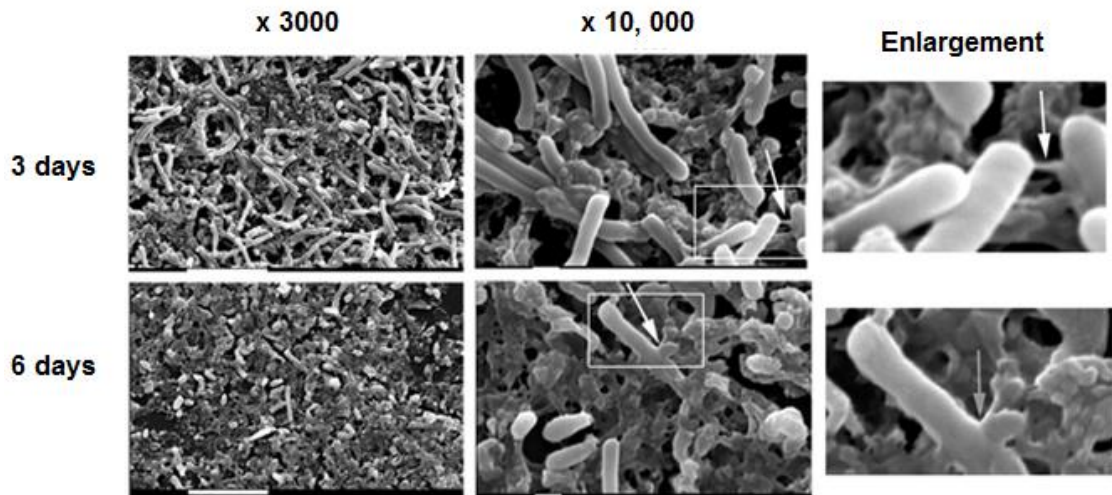


Figure 1-7 Scanning electron microscopy of *C. difficile* biofilms. *C. difficile* biofilms were visualised after 3 days incubation (top panels) and 6 days incubation (bottom panels) at x 3000 magnification (left panels) and x 10, 000 magnification (middle panels). The white boxes indicate areas enlarged (right panels) and the white arrows indicate connections between cells and assumed biofilm. Image from Dawson *et al.*, 2012.

Rapid diversity was seen in *Pseudomonas aeruginosa* biofilms with the development of heritable variants, suggesting genetic changes (Boles *et al.*, 2004). This diversity affected a number of cellular functions including motility, nutritional requirements, production of a secreted product and the generation of at least three different biofilm phenotypes. The presence of these diverse subpopulations enhanced the survival of the biofilm when exposed to environmental stresses. Similar results were seen in biofilms of *Serratia marcescens* (Koh *et al.*, 2007), *Pseudomonas fluorescens* and *Burkholderia cenocepacia* (Martin *et al.*, 2016). The latter study used spatially structured environments to demonstrate the evolution of microbial subpopulations from clonal ancestors with distinct ecotypes. The community was shaped by a range

of social and environmental interactions including antagonism (social exploitation), niche complementation and cooperation (cross-feeding). Planktonic cultures did not generate the variants seen in biofilm cultures (Martin *et al.*, 2016).

The diversity seen in the above experiments did not necessarily give a specific subpopulation increased fitness. It is more likely that the subpopulations specialisation enhances biofilm survival and sustainability under selected conditions and benefits the community as a whole. This self-generated diversity acts to safeguard the microbial community to ensure survival in adverse conditions (Figure 1-8).

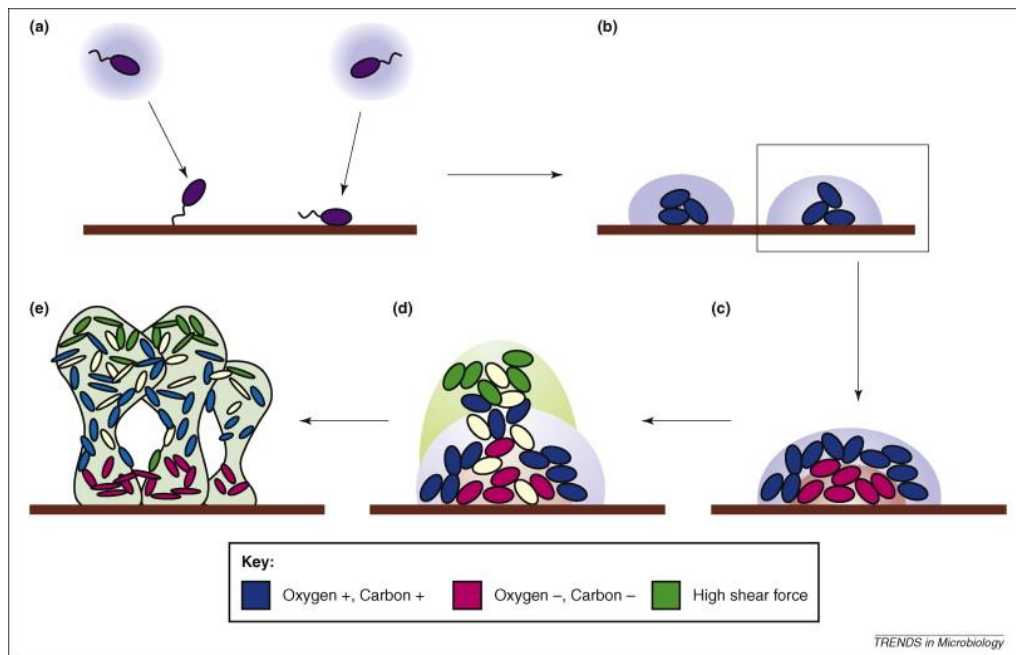


Figure 1-8 Theoretical simulation of the development of phenotypic heterogeneity within biofilms in response to environmental pressure.

This theoretical model is based on observations from predominantly Gram negative bacteria. It demonstrates the initial binding of cells to a surface in response to appropriate signals (a) followed by cell division to form isolated colonies (b). These colonies continue to expand and eventually merge, forming microcolonies (c). This generates different microenvironments and includes areas of oxygen and carbon limitation (pink cells). The cells in the pink zone adapt to this environment, generating phenotypic heterogeneity in the microcolony. (d) Further heterogeneity is seen as the biofilm continues to grow, including cells producing increased levels EPS (white) and exposure of cells to shear forces (green), leading to the establishment of a mature biofilm with distinct local adaptation and heterogeneity. Image from Monds and O'Toole, 2009.

1.3.2.2 Interspecies interactions

Physical interactions can be either direct through cell-to-cell interactions or indirect mediated by the growth or presence of another organism (Klayman *et al.*, 2009). An example of competitive direct interactions was demonstrated by Xie *et al.* (2000) when they reported that attachment of the oral pathogen

Porphyromonas gingivalis was specifically inhibited by the presence of the commensal *Streptococcus cristatus*. Contact-dependent downregulation of the *FimA* gene of *P. gingivalis* encoding components of fimbriae was mediated by the surface protein arginine deiminase (ArcA) of *S. cristatus* (Xie *et al.*, 2007). Klayman *et al.* (2009) demonstrated indirect interactions within biofilms between *Escherichia coli* and *P. aeruginosa*. They established that *E. coli* 0157 was unable to produce a biofilm when inoculated alone; however, was able to co-adhere in a co-inoculum with *P. aeruginosa*. They also noticed that *E. coli* inoculated after the establishment of a *P. aeruginosa* biofilm resulted in a 10 fold increase in *E. coli* adherence.

Co-metabolism and syntrophy are examples of cooperation within biofilms. It involves resource sharing and can be in the form of reliance on a by-product as a nutrient source. This can be seen in the relationship between the sulphate-reducing bacteria (SRB) *Desulfovibrio vulgaris* and other members of the biofilm community. SRBs can interact syntrophically with other bacteria in the biofilm in the absence of sulphate. Interactions with the hydrogen consuming methanogenic *Methanococcus maripaludis* are also beneficial when they consume the H₂ by-product of *D. vulgaris* that is potentially inhibitory at certain concentrations (Brileya *et al.*, 2014). This excretion and consumption of by-products may influence the physiochemical properties of the biofilm, generating new niches for further colonisation.

1.3.2.3 Quorum sensing

Quorum sensing (QS) is the regulation of gene expression mediated by the release of signalling molecules in response to cell density. This cell-to-cell communication facilitated by chemical messengers is able to co-ordinate the mechanism of biofilm formation and the social behaviour of mixed bacterial communities. It has been demonstrated to be pivotal in biofilm development, maturation and dispersal for both Gram positive bacteria (such as *Staphylococcus aureus* and *B. subtilis*) and Gram negative bacteria (such as *P. aeruginosa* and *P. fluorescens*) (Yarwood *et al.*, 2004, O'Loughlin *et al.*, 2013, Papenfort and Bassler, 2016, Verbeke *et al.*, 2017, Kalamara *et al.*, 2018) as well as being implicated in the regulation of virulence determinants (Percival *et al.*, 2011). The close proximity of cells within a biofilm provides ideal spatiochemical conditions to facilitate QS mediated genetic regulation. Bacterial

cells produce extracellular signalling molecules and at high cell densities they are able to accumulate and activate membrane receptors. This leads to the expression of genes involved in cooperative behaviour as well as a QS molecule feedforward loop (Rutherford and Bassler, 2012). QS signalling molecules can either be species specific or may cross species boundaries and consist of N-acyl-homoserine lactones (AHLs), autoinducing peptides (AIPs) and autoinducer-2 (AI-2). AHL systems are found primarily in Gram negative organisms (Gambello and Iglewski, 1991) and AIPs in Gram positive organisms (Li *et al.*, 2001, Percival *et al.*, 2011). Both Gram positive and negative organisms produce and sense AI-2 signals (Bassler *et al.*, 1994). The AI-2 signalling system is composed of three genes; *luxP* which encodes a periplasmic binding proteins, *luxQ* encodes a histidine kinase, and *luxS* which encodes an autoinducer synthase that produces the signal named AI-2. AI-2 is capable of operating across species boundaries and is therefore considered a universal signal and is associated with multispecies biofilms (Bassler *et al.*, 1997, Xavier and Bassler, 2003, Burmølle *et al.*, 2014). A *luxS* homologue was found in *C. difficile* that produces an active AI-2 molecule (Carter *et al.*, 2005), which was demonstrated to regulate virulence gene expression (Lee and Song, 2005). Using *luxS* mutants, biofilm formation was significantly impaired (Đapa *et al.*, 2013, Slater *et al.*, 2019). Interestingly, a *C. difficile luxS* mutant produced a larger biofilm in co-culture with the gut commensal *Bacteroides fragilis*, when compared to co-cultures with the *C. difficile* wild type, indicating that the mechanisms of AI-2 mediated biofilm formation in mixed species biofilms is not fully understood.

1.3.2.4 Biofilm tolerance to antimicrobial agents

One of the most medically important characteristics of a biofilm is its intrinsic tolerance to antimicrobial agents, making biofilm-associated infections difficult to treat and almost impossible to eradicate. Biofilm cells show between 10-1000-fold higher tolerance to antibiotics than planktonic counterparts (Ceri *et al.*, 1999). Tolerance of *C. difficile* biofilms to antimicrobials commonly used against CDI has been demonstrated; however, the mechanisms of this tolerance has not been fully explored. High concentrations of metronidazole (100 µg/mL) resulted in an approximately 10 fold reduction in sessile communities after 20 hours initial growth, whereas 1 µg/mL was effective at

reducing planktonic populations by 100-fold (Semenyuk *et al.*, 2014). A similar effect was seen when testing the efficacy of vancomycin against *C. difficile* biofilms, in which concentrations of 100 times the MIC failed to eliminate the sessile populations (Đapa *et al.*, 2013). This increased tolerance was negated when the biofilms were disrupted, suggesting that tolerance was conferred by the intact biofilm and not genetic changes in the cells. In a triple-stage model of the human colon simulating CDI, vancomycin was able to reduce planktonic populations to below the limit of detection whereas sessile populations were unaffected (Crowther *et al.*, 2014a). Evidence of lower vancomycin concentrations in the biofilm was seen (average 40.4 mg/L in the biofilms vs 54.7 mg/L in the vessel lumen) indicating reduced penetration into the biofilm and therefore the antimicrobial was unable to reach effective levels. Further, sub-inhibitory concentrations of metronidazole and vancomycin have also been shown to stimulate and promote biofilm formation of *C. difficile in vitro* (Đapa *et al.*, 2013, Vuotto *et al.*, 2015). This highlights that low concentrations of antimicrobials at the beginning and the end of treatment could potentially act as a stress signal to *C. difficile* displaying susceptibility to the antimicrobial, resulting in a stress response and stimulating increased biofilm formation. The antibiotics surtomycin and fidaxomicin were more effective at killing vegetative cells in established biofilms when compared to vancomycin and metronidazole, by disrupting the biofilm structure (James *et al.*, 2017).

This particular area of biofilms has been extensively studied and a number of mechanisms have emerged that are believed contribute to the resistance exhibited by biofilms. The presence of eDNA in the matrix of the biofilm serves as a genetic pool with high levels of horizontal gene transfer occurring within a community leading to the generation of new genetic combinations and increased horizontal transfer of resistance determinants (Molin and Tolker-Nielsen, 2003). This increased mutation frequency and the presence upregulated drug efflux pumps lead researchers to believe that the organisms themselves were displaying additional resistance mechanisms. Although this has been demonstrated to be true for certain bacteria (Tyerman *et al.*, 2013), the vast majority of bacteria, when removed from the biofilm, display similar resistance to the planktonic cells (Spoering and Lewis, 2001). This implied that

mechanisms other than traditional resistance determinants were responsible for the reduced susceptibility of biofilms to antimicrobials.

Further research has shown that several mechanisms can contribute to antimicrobial tolerance in biofilms. The EPS matrix can act as a physical barrier resulting in impaired or reduced penetration of antimicrobials into the biofilm (Flemming and Wingender, 2010). It was originally believed that the resistance conferred by the biofilm-mode of growth was due to the inability of antibiotics to penetrate the barrier created by the EPS matrix however, it was found that penetration of the biofilm varied between different types of antibiotic and therefore could not account for the degree of resistance displayed (Anderl *et al.*, 2000, Singh *et al.*, 2010). Shigeta *et al.* (1997) demonstrated that certain antimicrobial agents interacted chemically with the EPS matrix in addition to binding to anionic polysaccharides therein. This was confirmed by Walters *et al.* (2003) who showed that positively charged aminoglycosides bound to the negatively charged matrix and therefore retarded their penetration into the biofilm. Further work by Anderl *et al.* (2003) revealed an accumulation of secreted β -lactamase enzyme in surface layer which was able to deactivate β -lactam antibiotics before they were able to reach lower regions of the biofilm. As the nature of the EPS is dependent on the microbes present, the effect the matrix has on antimicrobials varies considerably and therefore the composition of the biofilm and the chemical properties of the antimicrobial need to be considered (Stewart, 2015). The metabolic state of microorganisms within the biofilm also influences tolerance to antimicrobials (Schiessl *et al.*, 2019). Nutrient limitation in inner regions of the biofilm causes bacterial cells to become less metabolically active resulting in slower growth, resembling the stationary phase of bacterial growth (Roberts and Stewart, 2004). Most antibiotics are only effective against actively dividing cells and therefore this stationary growth enables cells in the centre of clusters to survive antimicrobial exposure. The general stress response, initiated by the alternative σ -factor RpoS in response to cell density, results in physiological changes that act to protect the cell from various environmental stresses (Battesti *et al.*, 2011). These include the expression of osmoprotectants and catalase.

The highly complex architecture of biofilms leads to the generation of microenvironments within the biofilm displaying microscale gradients in pH,

oxygen concentration and nutrient and waste levels (Jensen *et al.*, 2017, Ren *et al.*, 2018). The different conditions in these microenvironments have been shown to interfere with the function of certain antibiotics and lead to their inactivation or reduced activity as demonstrated by Walters *et al.* (2003) when they noticed that oxygen limitation in lower levels antagonised antimicrobial action as well as the reduced efficiency of aminoglycosides in anaerobic conditions (Tack and Sabath, 1985). The distribution of bacteria in biofilms is not uniform and therefore the spatial distribution of cells and the size of clusters results in cells being exposed to different concentrations of antibiotic and in some regions the concentration achieved may not be high enough to eradicate the population. The presence of persister cells, a biofilm-specific phenotype, is induced in a subpopulation of cells that exhibits increased tolerance to antibiotics without undergoing genetic change (Lewis, 2008). These cells constitute < 1 % of the original population and persist despite continued exposure to antimicrobials. It is believed that the persister state results as a response to stress and nutrient limitation and is associated with the production of guanosine tetraphosphate (ppGpp) and the presence of toxin-antitoxin (TA) systems (Wood *et al.*, 2013) which cause the cells to become less metabolically active and enter a dormant state. This dormant, almost spore-like state suggests a pathway of differentiation with the potential to reseed the community after the death of susceptible populations (Wood *et al.*, 2013).

1.3.3 Methods used in biofilm culture and quantification

The increased interest in biofilm research has led to the development of various methodologies to cultivate, examine and quantify biofilms. Methods for studying biofilms are highly variable, and a lack of standardisation has resulted in difficulty reproducing data between laboratories. Here, the more common methods of biofilm formation and quantification will be briefly discussed.

1.3.3.1 Methods for culturing biofilms

1.3.3.1.1 Static biofilms

Static biofilm models include culture in wells, typically 96 or 24 per plate. These methods are high-throughput and relatively inexpensive, requiring little specialist equipment. Limitations include short duration of experiments due to nutrient limitation; poor reproducibility with a high degree of variability; biological environments not reflective of the gut; and end-point measurement only.

The Microwell plate – The microwell plate is the most commonly used method which was initially used to assess adhesion to plastic (Christensen *et al.*, 1985) and later used for the growth of biofilms by O'Toole and Kolter (1998b). Biofilms are grown in the wells of a microwell plate and by removing the planktonic phase; the sessile communities could be examined by measuring the attached biomass at various stages of biofilm development. They are most useful for screening biofilm formation capacity, especially for mutants defective in attachment (Valle *et al.*, 2003) and for the test of anti-microbial compounds (O'Toole and Kolter, 1998b). Individual wells could also be coated with different molecules to investigate biofilm formation to different supports (Cucarella *et al.*, 2002). Another limitation of this model is the sedimentation of cells that become embedded in the EPS resulting in a biomass not solely from the biofilm process.

The Calgary biofilm device overcomes the issue with sedimentation and consists of pegs attached to the lid of the microwell plate where the biofilm is formed when submerged into the substrate located in the wells. This allows for changing of the growth medium and therefore useful in MIC testing (Ceri *et al.*, 1999). Removal of the biofilm from the pegs is usually accomplished by sonication which can lead to incomplete population recovery (Müller *et al.*,

2011) with detached communities not necessarily reflective of the entire sessile community due to differences in adhesion and detachment properties (Grand *et al.*, 2011, Malhotra *et al.*, 2019).

The Biofilm ring test enables the study of early stages of biofilm formation (Chavant *et al.*, 2007) based on the ability of bacteria to immobilize paramagnetic microbeads in the presence of an applied magnetic field when forming a biofilm. This method reduces the variability seen in other static methods as no intervention, such as staining or fixation, is required. The method is more expensive and requires specific magnetic device and scanner.

1.3.3.1.2 Flow models

Unlike static models, flow models allow the continuous replenishment of nutrients and growth media, enabling experiments to run over longer periods of time and facilitate the study of biofilm development and maturation. Often requiring specialist knowledge and equipment, flow models are generally low-throughput with limited sampling opportunities and they tend to be expensive.

The Robbins and Modified Robbins device are used for screening surfaces supporting biofilm growth and in-line flow experiments. The Robbins device is comprised of numerous coupons mounted to screws that are inserted into the flow through threaded holes in a pipe or channel. It was initially used to monitor biofilm formation under different flow velocities in industrial drinking water systems (McCoy *et al.*, 1981) and later adapted for use in the laboratory (Nickel *et al.*, 1985). These models require specialist knowledge of the flow dynamics of the system for optimum results.

The Drip flow biofilm reactor consists of parallel chambers each containing a coupon where the biofilm forms under low shear stress (Goeres *et al.*, 2009). The growth medium or cell suspension is introduced through a gauge needle located in the lid of each chamber and therefore can be used to simultaneously test different disinfectant and antimicrobial strategies (Slade *et al.*, 2019) and to test biofilm formation under low shear stress. During operation, the reactor tilts at a specified angle from the horizontal, allowing fluid to pass over the length of the coupon. It is a compact design with easy operation (Agostinho *et al.*, 2011); however, biofilm heterogeneity on the coupons and limited number of samples are limitations in this system.

Rotary biofilm reactors allow for the formation of biofilms under constant shear forces with retrievable coupon inserts of various materials for analysis. They are composed of a stationary chamber housing a variable speed rotating mechanism housing the coupons for sampling (Coenye and Nelis, 2010). The rotation frequency can be set independently of the feed flow rate; enabling the dilution rate to be adjusted independently to shear forces. Contamination is frequent in these reactors and the system requires specialist equipment. The number of individual strains analysed simultaneously is limited and therefore offers low-throughput analysis of various strains.

The triple stage chemostat gut model, as discussed in section 1.1.8 and based on the design from Macfarlane *et al.* (1998) has been validated against the microbial and physiochemical properties of sudden death victims. It is a continuous model and is seeded with human faeces and the established environment mimics the human colon. It has been used extensively to model CDI and to assess the ability of a drug to induce or treat CDI with outcomes consistent with clinical findings (Baines *et al.*, 2005, Freeman *et al.*, 2005, Baines *et al.*, 2006, Freeman *et al.*, 2007, Chilton *et al.*, 2014a). The chamber reflecting the distal colon was modified to incorporate glass biofilm support structures inserted in the lid of the vessel, enabling emersion in the gut model contents and facilitating the formation of biofilms that can be periodically sampled (Crowther *et al.*, 2014b). This allows for the longitudinal monitoring of multispecies biofilms and their response to antimicrobial therapy and exposure to pathogens. Limitations of this model include the finite number of sampling rods and the requirement for specialist equipment. It is an expensive model to run and requires extensive manpower; therefore is low-throughput. The biofilm support structures were constructed of glass which is not reflective of the human gut. These models were used extensively in this thesis and will be described in more detail in Chapter 2.

Flow chambers allow the real time, non-destructive, in-line study of biofilm formation and development. Flow chambers can be either open or closed (Lewandowski *et al.*, 2004) with biofilms cultivated on coverslips in a chamber which allows for microscopic examination during biofilm development. The coverslips can also be coated with biological molecules to assess the effect on bacterial attachment (Landry *et al.*, 2006). The addition of fluorescent dyes and

proteins enable the visualisation of spatial organisation and community structure, as well as gene expression studies with confocal microscopy (Sternberg *et al.*, 1999, Haagensen *et al.*, 2007, Pamp *et al.*, 2009). These systems are low-throughput and require specialist equipment and do not allow direct access to the biofilm cells.

1.3.3.2 Methods to measure biofilms

Cell counting - The most common method used to quantify biofilms is to determine the colony forming units (CFU) using serial dilutions and plating the cells on appropriate agar. This method is inexpensive and does not require specialised equipment. Limitations of this method include incomplete homogenisation of the biofilm leading to variance, detached biofilm not representative of the whole biofilm, viable but nonculturable cells (VBNC) not detected, labour intensive and subject to counting errors and personal bias, and it is unable to provide information on dead cells and biofilm matrix components (Davey, 2011, Azeredo *et al.*, 2017). The use of flow cytometry coupled with fluorophores enables the rapid and accurate determination of viable, dead and VBNC (Berney *et al.*, 2007, Cerca *et al.*, 2011, Oliveira *et al.*, 2015); however, this method requires specialist equipment and experienced personnel, it's expensive, results may be influenced by the presence of organic matter in the sample (Frossard *et al.*, 2016) and the structure and spatial organisation of the biofilm cannot be studied.

Molecular – one of the more popular molecular based methods of bacterial detection and quantification is quantitative polymerase chain reaction (qPCR). qPCR provides rapid, high-throughput quantification of target and absolute DNA with high specificity and sensitivity (Hoffmann *et al.*, 2009). As qPCR is designed to detect DNA, results may be overestimated as it does not discriminate between live and dead cells or eDNA found in the biofilm matrix. The use of RNA persistence (Birch *et al.*, 2001) or intercalating fluorescent dyes, such as propidium monoazide and ethidium monoazide, (Nocker *et al.*, 2007, Nocker *et al.*, 2009, Alvarez *et al.*, 2013) together with qPCR, have been used to test for cell viability. Both methods come with additional limitations including the requirement for specialist knowledge in RNA isolation (Birch *et al.*, 2001) and the dependence on light-transparent matrix and membrane integrity for dyes (Nocker *et al.*, 2007, Nocker *et al.*, 2009, Sträuber and Müller, 2010).

Physical – the biomass of a biofilm can be quantified indirectly by measuring the wet or dry weight (Characklis *et al.*, 1982), the electrochemical impedance (Dominguez-Benetton *et al.*, 2012) or the acoustic impedance (Sim *et al.*, 2013, Anastasiadis *et al.*, 2014). Determining the weight of a biofilm is inexpensive without the need for specialist equipment; however, this method is time consuming and lacks accuracy. Both electrochemical and acoustic impedance are non-destructive methods allowing for real-time *in situ* measurement of biofilms; however, the heterogeneity of biofilms makes measurements and interpretations difficult.

Chemical – The wet or dry biomass of a biofilm can be measured by the adsorption followed by desorption of a dye, most commonly crystal violet (Christensen *et al.*, 1985). The dye is capable of staining both live and dead cells, as well as some matrix components (Merritt *et al.*, 2005). This method is high-throughput, inexpensive and versatile, allowing the simultaneous examination of different conditions and microbial species. Although commonly used, there is no standard protocol for this assay and therefore comparisons between studies are difficult (Stepanović *et al.*, 2007). It also lacks reproducibility and results are highly variable. The washing step of these assays often results in the loss of a portion of the biofilm, leading to underestimating the biomass as well as increasing the variability (Gómez-Suárez *et al.*, 2001). The metabolic activity of biofilms can also be quantified using colorimetric assays including the reduction of tetrazolium salts (Koban *et al.*, 2012, Sabaeifard *et al.*, 2014) and resazurin (Van den Driessche *et al.*, 2014).

Microscopy – Light microscopy is the most inexpensive and simple form of microscopy used in biofilm research. It can be used for biofilm detection and quantification of early stages of biofilm formation with a counting chamber (Lembke *et al.*, 2006). Samples are generally easy to prepare and require simple staining but do not allow for discrimination of components or structure of the biofilm. One of the main limitations of light microscopy is the limited magnification and resolution; however, this enables the imaging of larger parts of the biofilm and can be very useful in combination with higher magnification microscopes. Confocal laser scanning microscopy (CLSM) is capable of obtaining high-resolution images of biofilms at various depths, facilitating the 3-

D reconstruction of the biofilms and providing information on the biofilm architecture, spatial organisation, composition and function (Bridier *et al.*, 2010, Carvalho *et al.*, 2012, Neu and Lawrence, 2014). With the development of image capture and analysis software, it is now also possible to quantify the bacteria in a biofilm and differentiate between live/dead cells (Sommerfeld Ross *et al.*, 2014, Guilbaud *et al.*, 2015, González-Machado *et al.*, 2018). The main limitations of CLSM are the requirement for fluorophores and the limited number of available reporter molecules which restricts the amount of information obtainable. Scanning electron microscopy (SEM) is another high-resolution/high-magnification method which has the added advantage of a wide range of available magnifications allowing for the examination of large fields to get an overall impression of the biofilm down to single cell visualisation which includes surface details and EPS (Asahi *et al.*, 2015). One of the main limitations of SEM is the extensive and time-consuming destructive preparation of the sample that can cause shrinkage and can lead to damage of the structure of the biofilm (Alhede *et al.*, 2012). Both CLSM and SEM are expensive to perform and require specialist knowledge and equipment.

1.4 Rationale

The link between chronic infections and biofilms has been clearly established (Bjarnsholt, 2013, Jamal *et al.*, 2018), with GI tract mucosal populations gathering much interest in health and disease (Macfarlane and Dillon, 2007). rCDI displays the classic hallmarks of a biofilm-associated infection given its chronic nature and recalcitrance to antimicrobial therapy; however, biofilms have not yet been linked to the recurrence of CDI. Due to the relative inaccessibility of these populations *in vivo* and insufficient appropriate *in vitro* models, there is a paucity of information on the role of biofilms in rCDI. Here, we set out to define the biofilm niche that could potentially harbour *C. difficile* cells and facilitate rCDI, as well as to further characterise the interactions of *C. difficile* in a biofilm with selected commensal microflora.

1.5 Aims

This study aims to determine whether multispecies biofilms play a role in *C. difficile* recurrence and to characterise the interactions between *C. difficile* and commensal microorganisms found in biofilms.

1.5.1 Primary objectives

To determine if the Leeds triple-stage model of *C. difficile* infection can reflect the outcome of microbiome-based therapeutics used clinically;

to evaluate optimal dosing regimens for microbiome-based therapies currently in clinical trials using the triple-stage model of recurrent *C. difficile* infection;

to identify commensal microorganisms present in a multispecies biofilm and characterise their interactions with *C. difficile*;

to determine whether *C. difficile* within a biofilm can cause recurrent *C. difficile* infection.

Chapter 2 Materials and Methodology

2.1 Chemicals and Agars

All chemicals and growth media (pre-poured and powder) used were sourced from Sigma Aldrich, UK and Oxoid UK, respectively, unless stated otherwise.

2.2 *In vitro* gut model experiments

The *in vitro* gut model used in these experiments was based on Macfarlane *et al.* (1998) and has been validated against the physico-chemical and microbiological intestinal contents of sudden death victims. It has previously been used to profile the dynamics of microbiota and *C. difficile* population changes during CDI initiation, treatment and recurrence (Freeman *et al.*, 2003, Baines *et al.*, 2005, Chilton *et al.*, 2014b, Crowther *et al.*, 2015), with results reflecting those seen clinically. Data generated from different variations of the *in vitro* gut models was used in all chapters. Described here is a generic gut model experiment and associated tests. Each individual chapter details any deviation from this protocol and additional assays performed.

2.2.1 Ethical approval

Ethics for the investigation of pathogens and commensal bacteria using *in vitro* gut models was approved by the School of Medicine Research Ethics Committee (MREC 15-070). Human faeces is classified as tissue by the Human Tissue Act (HTA), therefore ethical approval was sought for the storage of donated faeces. The study received approval from East Midlands – Leicester South Research Ethics Committee (REC number: 16\EM\0263), IRAS project identification 206781, for the long term storage of donor faecal samples for the *in vitro* gut model experiments (appendix, A1).

2.2.2 Participant recruitment and specimen collection

Each gut model was initially started using a pooled faecal slurry made from the faeces from healthy donors. Potential participants were recruited from healthy members of the public and provided with an information sheet detailing the purpose of the study (appendix, A2). The information sheet provided instructions for sample collection and contact information of the primary

research scientists should any questions arise. By providing a sample, participants were consenting that the sample could be frozen, stored and used for the sole purpose of the gut model experiments and all donations were completely anonymous. 22 participants were recruited to provide faecal samples for a series of 9 gut models. Donors were required to be > 60 years old to reflect the age group at most risk of CDI, with no history of antimicrobial therapy in the preceding three months to ensure a healthy microbiota. Specimen kits included an AnaeroGen W-Zip Compact Generator system (Oxoid, Hampshire, UK) which maintained the sample in an anaerobic environment, for a maximum of 18 hours, before being transferred to an anaerobic cabinet (Whitley A95 anaerobic workstation, Don Whitley Scientific, UK).

2.2.3 Screening of faeces

To ensure the absence of *C. difficile* within the donor faecal material, all specimens were screened for the presence of GDH antigen (Goldenberg *et al.*, 2010, Sharp *et al.*, 2010) using the C.DIFF CHEK-60 enzyme immunoassay (DS2, DYNEX Magellon Biosciences, USA) and plated directly onto Brazier's CCEYL agar [cefoxitin (8 mg/L), cycloserine (250 mg/L), lysozyme (5 mg/L), supplemented with 2 % lysed horse blood] in triplicate and incubated anaerobically at 37°C for 48 hours. Any specimen testing positive for the presence of *C. difficile* was eliminated from the study.

2.2.4 Preparation of the faecal slurry

To provide increased consistency between a series of models, a stock of faecal slurry was prepared by pooling equal quantities of faeces from the 22 donors and diluting 1:3 in pre-reduced phosphate buffered saline (PBS) (MP Biomedicals, France) supplemented with 10 % (v/v) glycerol (Costello *et al.*, 2015), and the suspension emulsified in a stomacher (Borolabs, Aldermaston, UK). Large particulate matter was removed by filtration through a sterile muslin cloth (Bigger Trading Limited, Watford, UK). The slurry was separated into aliquots before being rapidly frozen using liquid nitrogen and stored at – 80°C (New Brunswick Scientific, Austria). When required, aliquots were defrosted at 4°C and further diluted with pre-reduced PBS to a 10 % (v/v) final

concentration. The preparation of the faecal slurry was performed under aerobic conditions.

2.2.5 Viability of frozen faeces

To ensure consistency between the different model sets, the same faecal slurry was used to inoculate the models and therefore the slurry was frozen and maintained at -80°C until required. Previous studies in our laboratory indicated that freezing a faecal slurry had a negligible effect on sampled bacterial populations (unpublished data, Buckley, AM, 2016). Prior to inoculating each model set, a sample of the defrosted slurry was enumerated on selected media as described in section 2.2.11. Statistical analysis using a Kruskal-Wallis with Pairwise Comparisons (IBM SPSS Statistics 23) were performed on total counts to determine if the fluctuations were significant. A p value of ≤ 0.05 was considered significant.

2.2.6 *C. difficile* strain

The *C. difficile* PCR ribotype 027 strain 210 (BI/NAP1/toxinotype III) used in this experiment was isolated during an outbreak of CDI at the Maine Medical Centre (Portland, ME, USA) and supplied courtesy of Dr Robert Owens (formally at Maine Medical Centre). This strain has been used in previous gut model experiments in our laboratory (Freeman *et al.*, 2003, Baines *et al.*, 2005, Freeman *et al.*, 2007, Chilton *et al.*, 2014a). Spore stocks were maintained at -80°C prior to subculture on Columbia blood agar (CBA) plates (E&O, UK) and incubated anaerobically for 48 hours at 37°C (Whitley A95 anaerobic workstation, Don Whitley Scientific, UK) in preparation for spore production.

2.2.7 Spore preparation and purification

The spore purification protocol was adapted from Lawley *et al.* (2009b). A single colony of *C. difficile* was inoculated into 150 mL of pre-reduced brain-heart infusion (BHI) broth and incubated anaerobically with agitation for 10 days at 37°C to ensure maximum spore production. The broth was divided equally three ways and centrifuged at 3270 g (Allegra X-12R centrifuge, Beckman Coulter) for 20 mins at 5°C and the supernatants discarded. Pellets were re-suspended in 1mL of sterile deionised water (SDW) and 3 mL of 100 % (v/v) ethanol (Fisher Scientific, Loughborough, UK) each and vortexed every 10

mins for one hour followed by centrifugation at 16,000g for 20 mins at 5°C. After discarding the supernatants, pellets were re-suspended in 10 mL PBS containing 1 % (v/v) sodium lauroyl sarcosinate (Sarkosyl) and incubated at 37°C for one hour aerobically for cell lysis and then centrifuged at 16,000g for 20 mins at 5°C and the supernatant discarded. Pellets were re-suspended in 10 mL PBS containing 0.125 M Tris buffer (pH 8) and 10 mg/mL lysozyme (Sigma) and incubated at 37°C with agitation overnight. Samples were layered onto 10 mL of 50 % sucrose solution and centrifuged at 3270 g for 20 mins at 5°C. After discarding the supernatants, the pellets were re-suspended in 10 mL PBS containing 200 mM ethylenediaminetetraacetic acid (EDTA), 300 ng/mL proteinase K and 1 % (v/v) Sarkosyl and incubated at 37°C for three hours and the sucrose centrifugation step repeated. The supernatants were discarded and the pellets re-suspended and washed twice in 10 mL SDW prior to pooling the samples and centrifuging at 3270 g for 20 mins at 5°C. Pellets were re-suspended in 2 mL of nutrient broth supplemented with 15 % (v/v) glycerol. Final spore preparations were enumerated (CBA, anaerobic incubation at 37°C) and diluted appropriately with SDW to a final concentration of approximately 1×10^7 CFU/mL for inoculation into the models.

2.2.8 The *in vitro* gut model set up

The model consists of three glass fermentation vessels (Soham Scientific, Cambridgeshire, UK) connected in a weir cascade formation, top fed with a complex growth medium through Saint-Gobain TYGON E-1000 tubing (Fisher) at a constant rate of 0.3 mL/min using a peristaltic pump (Masterflex L\ S, Cole-Parmer, UK) (Figure 2-1). Each vessel was inoculated with approximately 160 mL of the 10 % (w/v) faecal slurry and the gut model culture media flow started. An anaerobic atmosphere was maintained in all three vessels with nitrogen sparging (Parker Domnick Hunter, VWR, Leicestershire, UK) through a vented filter unit (Millex, USA), and the temperature maintained at 37°C using a circulating water bath (Grant LTD6G, Thermo Scientific, UK) round each vessel. The system was controlled to reflect the physiological conditions of the colon, with increasing pH and decreasing nutrient availability from the proximal (vessel one, 280 mL, pH 5.5 ± 0.2), through the medial (vessel two, 300 mL, pH 6.2 ± 0.2) to the distal colon (vessel three, 300 mL, pH 6.8 ± 0.2). All vessels were continuously agitated with a magnetic stirrer (VELP Scientifica, Italy) and

the pH maintained using pH controllers (Brighton Systems, Sussex, UK) with Chemotrode P200 pH probes (Hamilton, Birmingham, UK) linked to 1 M solutions of HCL and NaOH (Fisher Scientific, Loughborough, UK). Vessel three had been previously modified to incorporate between 16 - 18 glass rods to facilitate multispecies biofilm formation and sampling at designated time points (Crowther *et al.*, 2014b) without compromising the integrity of the system (Figure 2-2). Excessive foaming in the vessels was prevented by adding 0.5 mL of 10 % (w/v) polyethylene glycol (Sigma) when required. The gut models were set-up and maintained by the research technicians and research assistants within the Healthcare Associated Infection Research Group (HCAI), under the guidance of the principal investigator. Charmaine Normington assisted in the set-up and running of the models.

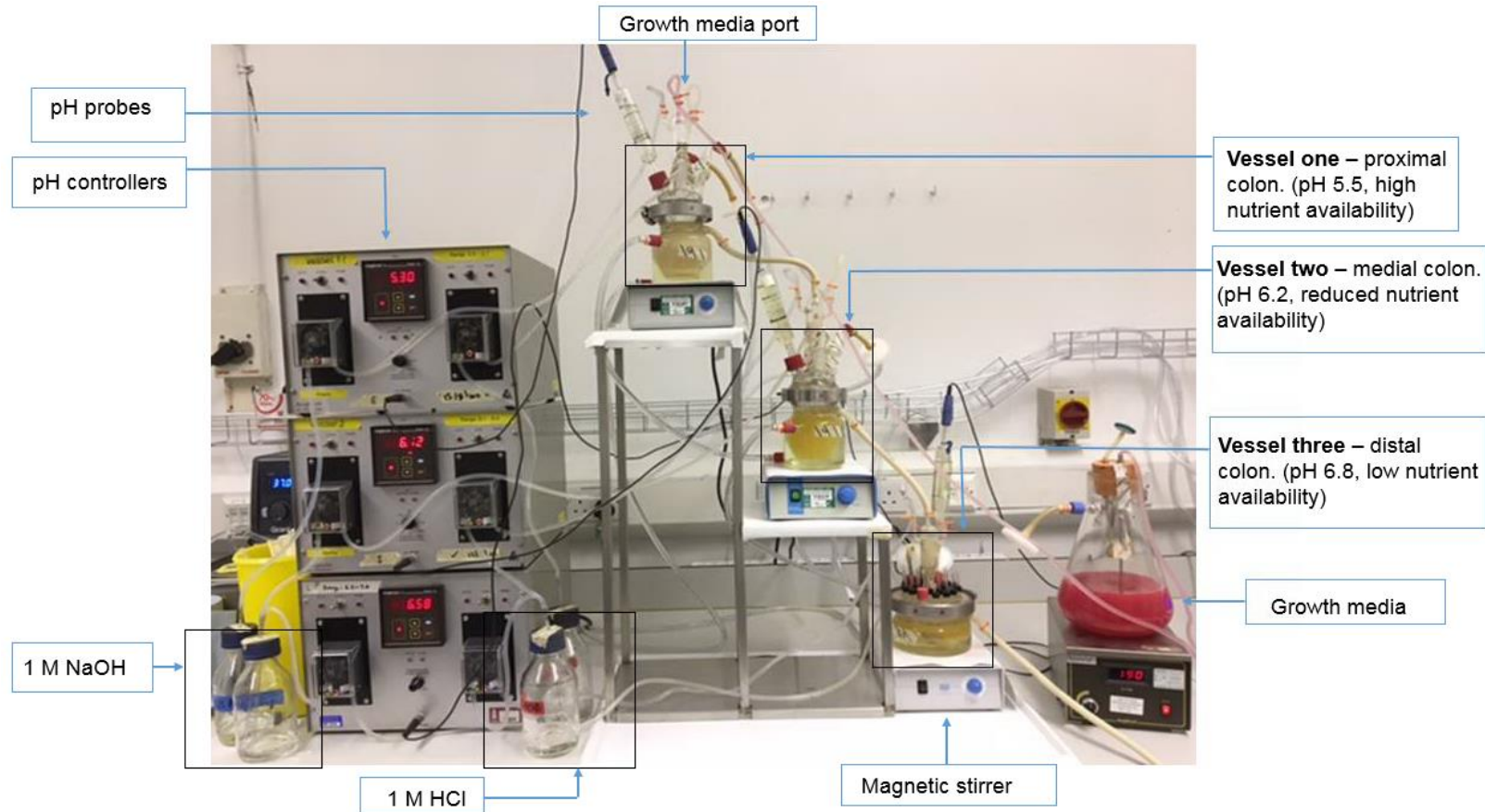


Figure 2-1 The Leeds *in vitro* gut model set-up. Vessels connected in a weir cascade, top fed by a complex growth medium and maintained to reflect physiological conditions of increased pH and decreased nutrient availability, from vessel one to three. The pH was controlled with pH probes in each vessel connected to a pH controller that automatically adjusted pH levels using 1 M NaOH and 1 M HCL solutions.

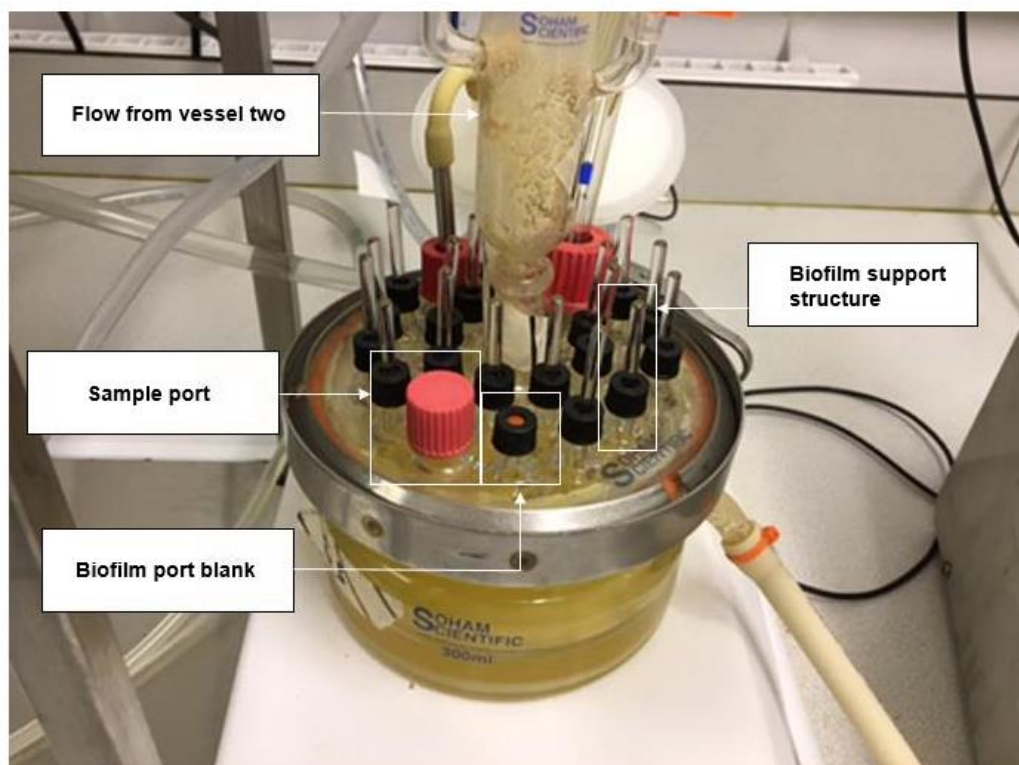


Figure 2-2 Biofilm vessel from the *in vitro* gut model. The third vessel of the gut model had a modified lid to accommodate biofilm support structures that facilitated the formation and sampling of a multispecies biofilm.

2.2.9 Preparation of Gut Model Growth Medium

The gut model was top fed into vessel one with a complex growth medium. The growth medium was prepared in 2 L volumes, the list of constituents and quantities are listed in Table 2-1. Growth medium was prepared in 2 L Büchner flasks with a gas venting port (vent filter unit, Millex, USA) and plugged with a bung containing media delivery ports. The reduction-oxidation (redox) indicator resazurin (Sigma; 0.005 g/L) and glucose (Sigma; 0.4 g/L) were filter sterilised into the medium through 0.22 µm syringe filters (Millipore Corporation, Billerica, MA, USA) after autoclaving (and once it had cooled to 50°C). Resazurin was used as an indicator of anaerobicity, with a pink colour indicating an anaerobic environment and a yellow colour indicating an anaerobic environment. The growth media had a magnetic bead inserted into the flask prior to autoclaving and was kept on a magnetic stirrer to prevent sedimentation.

Table 2-1 Composition of the *in vitro* gut model culture media.

Constituent	Amount (g/ L) (unless otherwise stated)	Supplier
Magnesium sulphate	0.01	Sigma
Calcium chloride	0.01	Sigma
Sodium chloride	0.1	Sigma
Di-potassium monohydrogen phosphate	0.04	Fisher
Potassium di-hydrogen phosphate	0.04	Fisher
Sodium hydrogen carbonate	2.0	Sigma
Tween-80	2.0 mL	Anatrace
Haemin	10.0 mL	Sigma
Cysteine HCL	0.5	Sigma
Bile salts	0.5	Sigma
Glucose (added after autoclaving)	0.4	Fisher
Arabinogalactan	1.0	ChemCruz
Pectin	2.0	Acros organics
Starch	3.0	Oxoid
Vitamin K	10 μ L	Sigma
Peptone water	2.0	Oxoid
Yeast extract	2.0	Oxoid

HCl – hydrochloric acid

2.2.10 Experimental design

The basic model timeline consisted of periods of bacterial population equilibrium, microbiota disruption, CDI and rCDI, with each state induced with the appropriate intervention (Figure 2-3). After inoculation with the faecal slurry, bacterial populations were left to stabilise and reach a steady state. This period lasted between 27-33 days. Once the microbial population stabilised, assessed by sampling selected populations every alternate day and monitoring for fluctuations (as described in 2.2.11), vessel one of the models were inoculated with a *C. difficile* spore preparation of approximately 1×10^7 CFU/mL (see section 2.2.7). The populations were monitored for a further week to ensure colonisation resistance was established, characterised by the inability of *C. difficile* populations to proliferate. Another dose of *C. difficile* spores were introduced to the models as above, to re-establish *C. difficile* spore levels. To create an environment susceptible to CDI, the microbial populations had to be disrupted. This induced microbial dysbiosis was achieved with clindamycin instillation in vessel one for 7 days, four times daily (33.9 mg/L). Clindamycin was selected as it is an antimicrobial agent strongly associated with the development of CDI (Tedesco *et al.*, 1974, Bartlett *et al.*, 1977) and has been used previously to induce CDI in the gut models (Freeman *et al.*, 2005, Freeman *et al.*, 2007). Simulated CDI was deemed to be present when evidence of *C. difficile* germination (active *C. difficile* vegetative proliferation when compared to spore counts) was seen, accompanied by a *C. difficile* toxin titre of ≥ 2 relative units (RU, as described by Freeman *et al.* (2003)).

During peak CDI, approximately two weeks after clindamycin treatment cessation, the system was dosed with vancomycin (125 mg/L 4 times daily, for 7 days, vessel one), to treat the infection. After vancomycin treatment, the models were either left without intervention or treated with a microbiome-based intervention. Populations were monitored closely for evidence of rCDI for approximately four weeks after vancomycin cessation. Recurrent simulated CDI was defined as for CDI using *C. difficile* germination and associated toxin levels.

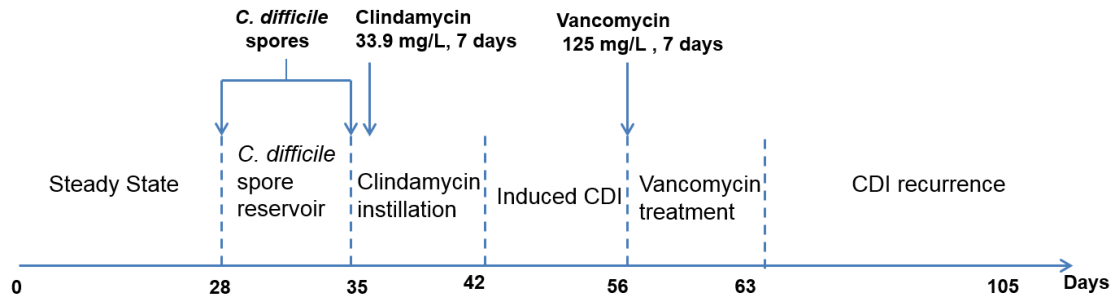


Figure 2-3 The general gut model timeline. A general timeline for gut model experiments showing approximate days for each stage. The steady state period allows time for the microbial populations to equilibrate and establish colonisation resistance. Colonisation resistance is confirmed with the failure of a *C. difficile* spore dose to germinate and cause infection within 7 days of inoculation. A second dose of *C. difficile* spores is added followed by clindamycin installation at 33.9 mg/L, four times daily, for 7 days. Clindamycin exposure disrupts the microbiota and creates an environment susceptible to CDI, resulting in induced CDI. CDI is then treated with vancomycin at 125 mg/L, four times daily, for 7 days, and the model is then monitored for rCDI.

2.2.11 Sampling planktonic populations

Planktonic fluid was sampled from each vessel of the gut model via an outlet port secured by a glass stopper. Culturable populations were enumerated from the planktonic phase in vessels two and three every other day during steady state and everyday thereafter. With the exception of *C. difficile* counts, culturable populations from vessel one were not enumerated as this vessel reflected an area of the colon less physiologically relevant in CDI. Planktonic fluid was transferred immediately to an anaerobic cabinet where it was serially diluted in pre-reduced peptone water and plated out in triplicate on pre-reduced (anaerobic populations) selective and non-selective agars (Table 2-2, constituents appendix A3). As populations were sampled daily, dilution changes could be monitored to ensure the correct dilution range was chosen for sampling. For spore counts, equal volumes of planktonic fluid and 96 % (v/v) ethanol were thoroughly mixed and allowed to incubate at room temperature for one hour before serially diluting and enumerating. Bacterial

populations were identified to the genus level on the basis of colony morphology and colony characteristics on selective media, with selected colonies undergoing matrix-assisted laser desorption/ionisation (MALDI TOF) analysis (Bruker Daltonik Biotyper) (described in 2.2.13) for confirmation of the identification. Results were represented as the mean \log_{10} CFU/mL planktonic fluid. Planktonic populations were sampled and enumerated by the research technicians and research assistants within the Healthcare Associated Infection Research Group (HCAI), under the guidance of the principal investigator.

2.2.12 Sampling biofilm populations

Biofilm populations were sampled and enumerated at designated time points (Figure 3-1 and Figure 4-1) due to the limited number of rods. Briefly, biofilm support structures with the multispecies biofilm attached (Figure 2-4), were removed from vessel 3 (Figure 2-2) and placed in 5ml pre-reduced PBS and thoroughly vortexed for 2 mins with 5mm sterile glass beads (Sigma), to enable homogenisation of the biofilm, prior to enumeration (Figure 2-5). Empty biofilm rod ports were sealed with sterile lid blanks. The biofilm pellet weight was determined by centrifugation (5 min, 16 000g) of the biofilm suspension in a pre-weighed Eppendorf, discarding the supernatant. The homogenised biofilm fluid was then serially diluted in pre-reduced peptone water and enumerated on pre-reduced selective and non-selective agars (Table 2-2). As biofilm populations were periodically sampled due to the limited number of rods available, dilutions were enumerated from neat to 10^{-7} in duplicate. Units were reported as the mean \log_{10} CFU/g of biofilm biomass. Excess biofilm suspension was retained for DNA extraction. Charmaine Normington was solely responsible for the sampling, enumeration and analysis of the biofilm.



Figure 2-4 Biofilm support structure with multispecies biofilm attached. A biofilm support structure, with multispecies biofilm attached, was removed from the lid of vessel 3 of the gut model for analysis.

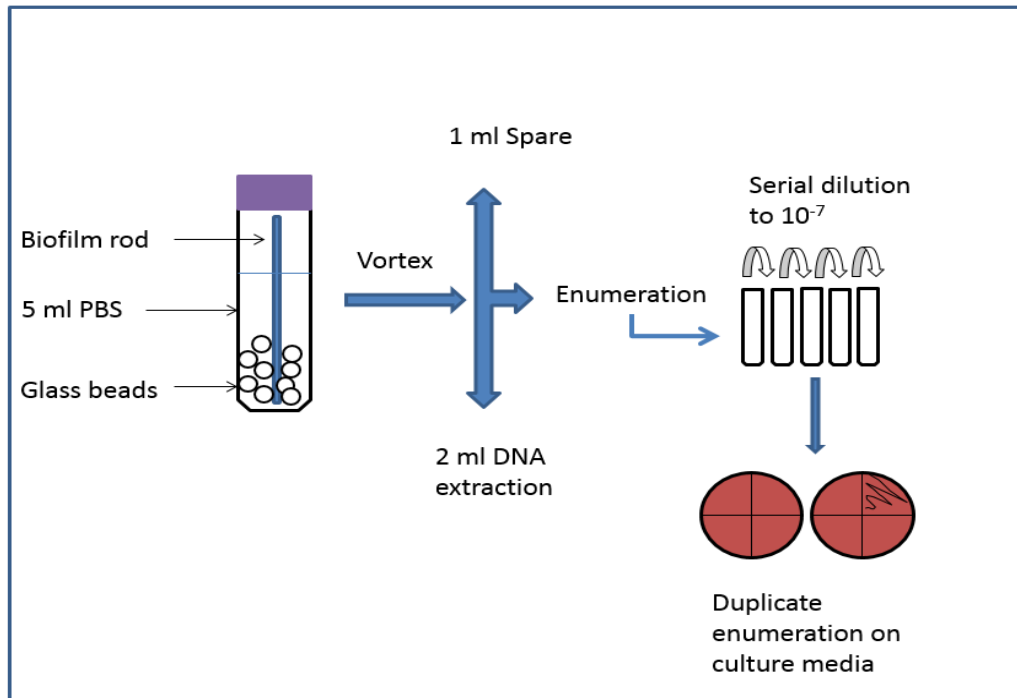


Figure 2-5 Biofilm sampling procedure. After the biofilm support structure was removed from the model, it was immediately transferred to 5 mL pre-reduced PBS along with sterilised glass beads and vortexed to homogenise the biofilm. The biofilm suspension was then separated for DNA extraction, microbial enumeration and storage. For enumeration, the biofilm suspension was serially diluted and plated onto appropriate agar media in duplicate.

2.2.13 Matrix-assisted laser desorption/ionisation (MALDI TOF) analysis

MALDI TOF analysis was used on selected colonies to identify microorganisms from the gut models to a species level for use in biofilm batch culture experiments in Chapter 5. Colonies were transferred to a reusable, polished, stainless steel MALDI target plate (96 positions, one colony per position) using a cocktail stick. 1 μ L of Matrix HCCA was added per target and air-dried. The target plate was run on a MALDI Biotyper (Bruker Daltonik Biotyper) by the Microbiology Department of Leeds General Infirmary and the mass spectrum was automatically compared against the MALDI Biotyper Reference Library (MBT Compass and MBT Explorer Software plus MBT Compass Library). The generated MALDI score is an indication of the reliability of the identification. A

score of > 2.3 indicates the identification of the genus and species are reliable; a score of 2.0 – 2.29 indicates the genus is reliable and the species is probable; a score of 1.7 – 1.99 indicates the genus is probable and a score < 1.7 indicates that the result is not reliable.

Table 2-2 Target microorganisms enumerated from the gut model experiments and appropriate culture media and growth conditions for their isolation.

Target organisms	Media and Supplements	Growth at 37 °C
<i>C. difficile</i> total viable counts	Brazier's CCEY agar with 2 % lysed horse blood, 5 mg/L lysozyme, 250 mg/L D-cycloserine, 8 mg/L cefoxitin, 2 mg/L moxifloxacin, 8 mg/L amphotericin B and 10 mg/L colisin	Anaerobic
<i>C. difficile</i> spores	1:1 ethanol (96 %) shock for one hour followed by enumeration on Brazier's CCEY agar with 2% lysed horse blood, 5 mg/L lysozyme, 250 mg/L D-cycloserine, 8 mg/L cefoxitin	Anaerobic
Total anaerobes and total <i>Clostridia spp.</i>	Pre-poured FAA with 5 % (v/v) horse blood	Anaerobic
<i>Lactobacillus spp.</i>	52.5 mg/L MRS broth and 20 mg/L agar technical with 0.5 g/L L-cysteine and 20 mg/L vancomycin	Anaerobic
<i>Bifidobacterium spp.</i>	42.5 mg/L Columbia agar and 5 mg/L agar technical with 5 mg/L glucose, 0.5 g/L L-cysteine and 5 ml propionic acid, adjusted to pH 5.	Anaerobic
<i>Bacteriodes spp.</i>	Bacteroides bile aesculin agar with 2 % (v/v) haemin and 0.002 % vitamin K1.	Anaerobic
<i>Enterococcus spp.</i>	Kanamycin aesculin azide agar with 10 mg/L nalidixic acid, 10 mg/L aztreonam, 20 mg/L kanamycin and 1 mg/L Lincomycin	Aerobic
Total facultative anaerobes	Pre-poured nutrient agar	Aerobic
Lactose-fermenting Enterobacteriaceae	Pre-poured MacConkey agar	Aerobic

CCEY – cefoxitin cycloserine egg yolk, FAA – Fastidious anaerobe agar, MRS – De Man, Rogosa, Sharpe

2.2.14 DNA extraction and taxonomic sequencing of the biofilm

DNA was extracted from the pellet remaining from centrifuging 2 mL of biofilm suspension (15 min, 16,000g) for 16S rRNA sequencing using a FastDNA Spin Kit for Soil (MP Biomedicals, Solon, USA) and following manufacturer's instructions. All extractions were done within 24 hours of harvesting the sample, with the pellet remaining at -20°C until extracted. Final DNA preparations were eluted in 70 μL volumes and stored at -80°C until shipping for offsite analysis. Purity and concentration of the DNA was determined using Ultraviolet spectrophotometry at 260-280 nm (Infinite F 200 Pro, Tecan). DNA extracts were shipped to Seres Therapeutics (Cambridge, USA) and 16S rRNA sequencing performed through proprietary pipelines. Briefly, 16S rRNA V4 sequences were PCR-amplified from 1 μL of DNA extract using the AccuPrime High Fidelity PCR kit (Invitrogen), with the primer pair 515F (5' AGCMGCCGCGGTAA 3') and 806R (5' GGACTACHVGGGTWTCTAAT 3') containing Illumina MiSeq adaptors and single-end barcodes. Amplicons were pooled in equal quantities, cleaned with AMPure beads (Beckman Coulter) and paired-end sequenced on the MiSeq platform following Nextera XT library preparation (Illumina).

Reads were demultiplexed with the `split_libraries_fastq.py` function in Qiime (version 1.9.1) (Caporaso *et al.*, 2010) and identical sequences were binned into amplicon sequence variants (ASVs) using the program DADA2 (version 1.4.0, parameters `EE=2`, `TruncL=c(200, 180)` and `q=10`) (Callahan *et al.*, 2016). The `assignTaxonomy` function in DADA2 was used to assign a taxonomic name to each unique ASV using the RDP Classifier with the SILVA 16S rRNA database (Silva nr v128) (Wang *et al.*, 2007, Quast *et al.*, 2013). Low abundance reads (≤ 10 reads) were removed from further analysis. Reads for each sample were assigned to the family taxonomic level and converted to percentage abundance. Results represent the mean abundance from at least 3 biofilm support structures from each model. Bacterial families represent all families whose values were ≥ 1 % abundance at a single sampling point throughout the model timeline. The Shannon Diversity Index was used as a measure of the microbiota diversity at selected time points throughout the models and was calculated using the mean OTUs to the family taxonomic level.

2.2.15 Bile acid analysis and quantification

One mL samples of planktonic fluid were removed from vessel three of the gut models each day and centrifuged at 16 000g for 10 min. The supernatant was then removed and stored at -80°C until shipping for offsite analysis (Seres T Therapeutics, USA). Samples were analysed for bile acid composition and quantification using ultra-performance liquid chromatography through Seres Therapeutics proprietary pipelines. Briefly, 100 μL of the planktonic fluid supernatant was extracted 1:1 (v/v) with liquid chromatography-mass spectrometry (LC-MS) grade acetonitrile and filtered through a 96 well 0.2 μm hydrophilic polypropylene (GHP) membrane filter. The extracted samples were transferred to LC-MS sampling tubes for analysis. The bile acids cholic acid (CA), deoxycholic acid (DCA) and oxidation bile acids (Oxo-BAs; 3-iso-deoxycholic acid, 3-oxo-chenodeoxycholic acid, 7-oxo-cholic acid, 12-oxo-deoxycholic acid) were separated on a Microslov bidentate C18 column using an Agilent 1260 high-performance liquid chromatography (HPLC) series coupled to a Bruker Compact quadrupole time-of-flight mass spectrometer (qTOF-MS) equipped with electrospray ionisation.

Liquid chromatography separation was achieved using a gradient of water and acetonitrile with 0.1 % (v/v) formic acid at 0.4 mL/min. The target bile acids fell between the mass range of 373.27 to 514.28 m/z. 5 μL of each of the samples and standards were injected into the system and target bile acids were identified using defined m/z and retention times compared with external standards. LC-MS grade pure bile acids were used to generate standard curves for quantification of the bile acids. Area under the curve was integrated using the Compass data analysis software (v4.4, Bruker). Data presented includes the concentration (nM/mg) of CA, DCA and the mean of the Oxo-BAs.

2.2.16 Cytotoxin assay

The Vero cell cytotoxin assay (Figure 2-6) was used to monitor levels of *C. difficile* toxin in the gut models and samples were taken during initial CDI and CDI recurrence. Samples of planktonic fluid were centrifuged at 16,000g for 10 min before the removal and storage of supernatant at 4°C until required. Vero cells (African Green Monkey Kidney Cells, ECACC 84113001) were passaged throughout the experiment and cultured in flat bottom tissue culture flasks

(Nunc, Rochester, USA) containing 20 mL of Dulbecco's Modified Eagles Medium (DMEM) (Sigma) supplemented with 10 % (v/v) newborn calf serum (Gibco, Paisley, UK), 1 % (v/v) L-glutamine (Sigma) and 1 % (v/v) antibiotic/antimycotic solution (Sigma) and incubated in 5 % CO₂ at 37°C (Sanyo, Watford, UK) for 48 hours until Vero cell monolayers were at least 80 % confluent upon examination under an inverted microscope (Olympus UK Ltd, Middlesex, UK). Vero cells were harvested by discarding the culture medium and gently washing with 1 mL of a 1:1 solution of trypsin-EDTA (sigma) and Hanks Balanced Salt Solution. A further 6 mL of this solution was added and incubated for 10 min at 37°C to detach the cells from the flask. The resulting suspension of cells was diluted 1 in 10 with fresh DMEM and used for either further passage or for setting up 96F microwell culture plates (Nunc, Rochester, USA).

Trays were incubated in 5 % CO₂ at 37°C for 48 hours and growth confluence examined microscopically before samples added. Samples were added to the tissue culture tray in triplicate at an initial 1 in 10 dilution, before being serially diluted to 10⁻⁶. *C. sordellii* antitoxin (Prolab Diagnostics, Bromborough, UK) was initially diluted 1 in 10 in PBS (inoculated into the tray 1:10 with a final concentration of 1 % v/v) and used to neutralise any cytotoxic effect caused by *C. difficile* toxins to ensure cell rounding was not caused by non-specific toxins found in the gut model fluid. A positive control using the supernatant of *C. difficile* 027 210 grown in BHI broth for 48 hours anaerobically at 37°C was used in each tray. Cell growth and appearance were assessed using inverted microscopy at 24 and 48 hours. Healthy, confluent Vero cells with < 50 % Vero cell rounding were deemed a negative result (Figure 2-7 a) whilst ≥ 50 % Vero cell rounding was deemed a positive result (Figure 2-7 b). Results were reported as relative units (RU), which are assigned based on the greatest dilution in which a positive result was seen. A positive result on the neat sample would return an RU of 1, on the 10⁻¹ dilution would return an RU of 2 etc. The cytotoxin assays were conducted by the research technicians and research assistants within the Healthcare Associated Infection Research Group (HCAI), under the guidance of the principal investigator.

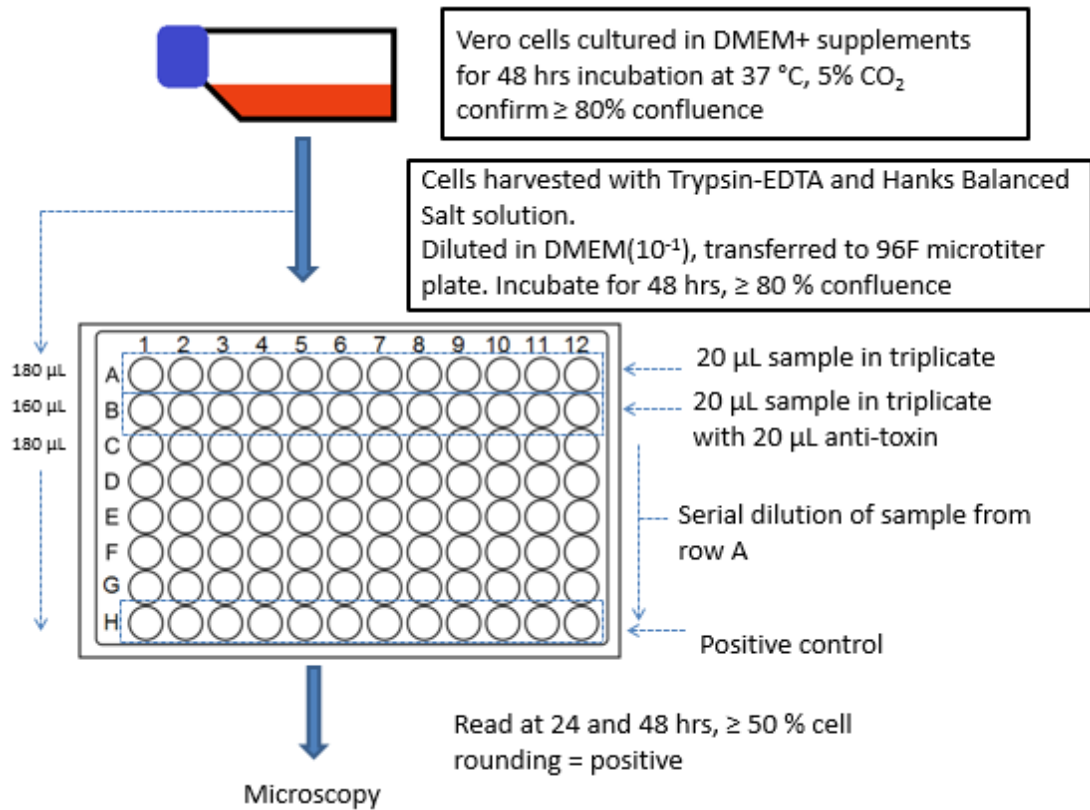


Figure 2-6 Graphical representation of the cytotoxin assay set up. Vero cells were cultured for 48 hours at 37°C and 5 % CO₂ before harvesting and transferring to 96 well trays and incubated for a further 48 hours, until ≥ 80 % cell confluence. Samples were added in triplicate to row A of the tray (1:10 v/v) and serially diluted (with the exception of row B). Row B, inoculated initially with 160 µL cell suspension, was inoculated with the sample (1:10 v/v) and *C. sordellii* anti-toxin (1:100 v/v) to act as a positive identifier for the action of *C. difficile* toxin. Vero cell growth and appearance were assessed with microscopy and ≥ 50 % cell rounding was deemed positive for *C. difficile* toxin. Positive controls of *C. difficile* supernatant and negative controls of PBS were included in each assay.

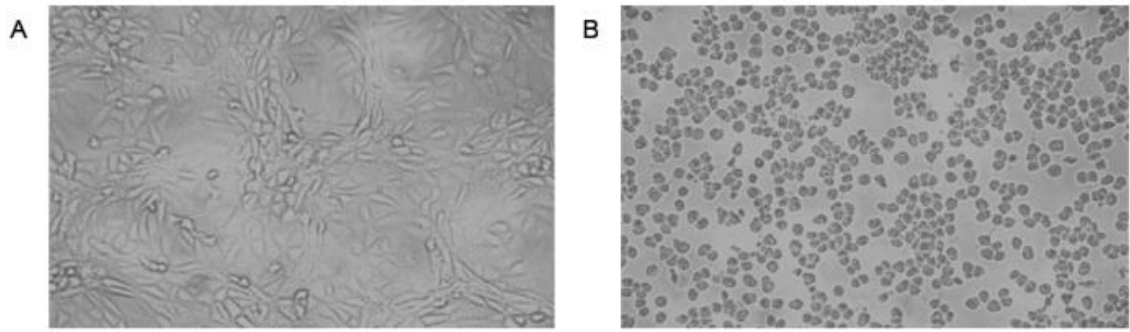


Figure 2-7 Image of Vero cell growth and appearance during the cytotoxicity assay. a) Toxin negative result demonstrating confluent growth of healthy Vero cells and b) *C. difficile* toxin positive result demonstrating $\geq 50\%$ cell rounding. Images at 400 x magnification.

2.2.17 Antimicrobial bioassays

An antimicrobial bioassay was used to monitor the antimicrobial concentrations achieved in the vessels during the experiment. Aliquots of gut model fluid (1 mL) were removed daily from each vessel and centrifuged (15 min, 16,000g), filter sterilised through 0.22 μm syringe filters (Millipore Corporation, Billerica, MA, USA) and the supernatants frozen at -20°C for retrospective analysis. Indicator organisms *Kocuria rhizophila* (ATCC 9341) and *Staphylococcus aureus* (ATCC 29213) were grown overnight in nutrient broth. 1 mL of a 0.5 McFarland standard from each organism were inoculated into 100 mL bottles of sterile molten (50°C) Wilkins-Chalgren agar and Mueller-Hinton agar, respectively. *K. rhizophila* was used to determine clindamycin concentrations and *S. aureus* was used to determine vancomycin concentrations. Agars were gently mixed and poured into sterile bioassay plates (245 mm^2 , Nunc) and allowed to set at room temperature for one hour before drying at 37°C for 20 mins. 25 wells (9 mm diameter) were cut from the agar using a sterile number 5 cork borer and inoculated with a calibration series ranging from 4 to 256 mg/L for clindamycin and 8 to 512 mg/L for vancomycin. 20 μL of each sample were added to the wells, with each plate run in triplicate and incubated at 37°C for 24 hours. Growth inhibition zone diameters were measured using callipers accurate to 0.1 mm. Calibration curves were determined from the squared zone diameters (red arrow, Figure 2-8) from the doubling dilution calibration series and used to determine the concentrations of the unknown samples (Figure

2-8). The antimicrobial bioassays were conducted by the research technicians and research assistants within the Healthcare Associated Infection Research Group (HCAI), under the guidance of the principal investigator.

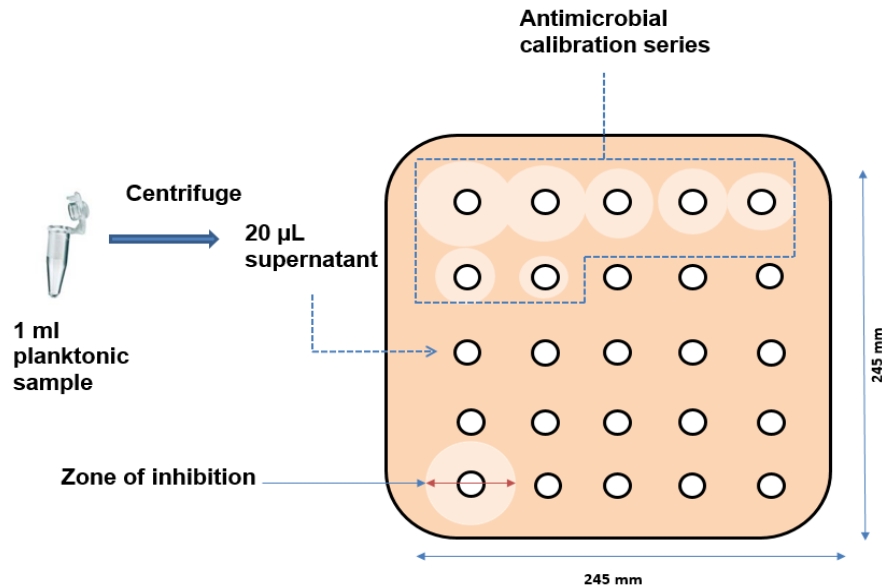


Figure 2-8 Antimicrobial bioassay plate. An antimicrobial bioassay was used to monitor antimicrobial concentrations achieved in each of the vessels of the gut model. Agar (either Wilkins-Chalgren agar or Mueller-Hinton agar) inoculated with the appropriate indicator organism (either *K. rhizophila* or *S. aureus*) were poured into a bioassay plate (245mm x 245mm) and 9 mm diameter holes were bored an equal intervals. On each plate, a calibration series of the target antimicrobial was added (top) and 20 µL of each sample was added to the remaining holes. Bioassay plates were incubated at 37°C for 24 hours and the zone of inhibition read and compared to the calibration curve generated with the calibration series. Each bioassay plate was run in triplicate.

Chapter 3 Resolution of simulated recurrent CDI using FMT; delineating the sessile and planktonic populations

3.1 Background

The clinical success of FMT therapy against rCDI demonstrates the importance of restoring the gut microbiota to a pre-antibiotic state. FMT-based microbiota restorative therapy is based on introducing the healthy microbiota of a donor to a patient with intestinal dysbiosis. A recent systematic review and meta-analysis of the efficacy of FMT therapy found an overall clinical cure rate of 76.1 % (Tariq *et al.*, 2018). This study revealed a significant difference in efficacy between randomised, controlled studies and open-label studies (WPR; 67.7 % and 82.7 %, respectively). The efficacy of FMT therapy also has implications for other infectious intestinal disorders, including the reduction of antimicrobial resistance genes (Jouhten *et al.*, 2016, Millan *et al.*, 2016, Huttner *et al.*, 2019). The indigenous microbiota of the intestinal tract is a diverse community displaying dynamic interactions with the host and other microorganisms. It is increasingly recognised as a regulator of the host immune and metabolic homeostasis (Bien *et al.*, 2013).

The microbiota of patients with rCDI is characterised by reduced community diversity and subsequent reduced community structure and function, characterised by a reduction in the phyla of Bacteroidetes and Firmicutes, with an increase in Proteobacteria (Chang *et al.*, 2008, Khoruts *et al.*, 2010). Antibiotic therapy has also been shown to cause metabolic changes in the gut, such as faecal bile acid metabolism. Broad spectrum antibiotics significantly diminish bacterial populations responsible for secondary bile acid metabolism, including the families *Lachnospiraceae* and *Ruminococcaceae* (Theriot *et al.*, 2014). Secondary bile acids are known to inhibit *C. difficile* spore germination (Weingarden *et al.*, 2014). This leads to the accumulation of primary bile acids such as taurocholate and cholate, both being potent *C. difficile* germinants (Sorg and Sonenshein, 2008).

The exact mechanisms underlying the success of FMT are not fully understood; however, bacterial diversity and richness of patient faeces was found to have increased after FMT instillation, with a community profile similar to that of the

donor (van Nood *et al.*, 2013, Youngster *et al.*, 2014, Kelly *et al.*, 2016, Kumar *et al.*, 2017). FMT therapy has been shown to normalise the metabolic profile demonstrating that FMT not only restores the structure and composition of the microbiota, but also influences its function (Mullish *et al.*, 2019). Due to non-standardised procedures for FMT preparation and installation, together with increased safety concerns, the identification of specific microbial taxa and mechanisms for FMT-mediated rCDI resolution is essential to enable a more targeted approach to microbiome restoration therapies.

3.1.1 Rationale

There is currently a lack of *in vitro* models that can predict the outcome of microbiome-based therapies. Additionally, most studies investigating microbial populations implicated in the efficacy of FMT therapy only consider luminal populations derived from faecal matter. Here we used our gut model to simulate rCDI which we adapted to mimic nasojejunal FMT therapy. Using this model we delineated the microbial planktonic and sessile dynamics during simulated CDI and FMT treatment to gain an understanding of the mechanisms of FMT in these two distinct communities.

3.2 Methodology

3.2.1 Experimental design

In this study, two *in vitro* gut models used to simulate rCDI were run in parallel, with one model adapted to facilitate a simulated FMT. The FMT model was later repeated for reproducibility and followed the same methodology, therefore will not be discussed here (results presented in appendix, A4). The initial set up of the gut models was as described in section 2.2.8. This experiment simulated a naso-jejunal FMT, and followed the experimental procedure used at Leeds General Infirmary (personal communication with Dr Jane Freeman, Clinical Scientist, LGI NHS Trust).

The models followed the timeline detailed in Figure 3-1 and according to 2.2.10, with deviations and exact time points detailed here. Briefly, both models were initially inoculated with a prepared faecal slurry (2.2.4) and populations left for 33 days in the steady state period. This period allowed the microbial populations time to stabilise and equilibrate. Models were sampled every other day to ensure populations recoveries were consistent. Both models were then challenged with a *C. difficile* spore dose (produced as described in section 2.2.7) and from this point forward, planktonic populations were sampled daily according to section 2.2.11. As vessel three is more clinically reflective of CDI, results represented here are solely from this vessel. The models were left for a week to ensure the model had reached a point of colonisation resistance. This was demonstrated by the inability of the inoculated *C. difficile* spores to germinate during this phase. A second dose of *C. difficile* spores were added to replenish the *C. difficile* reservoir prior to clindamycin instillation.

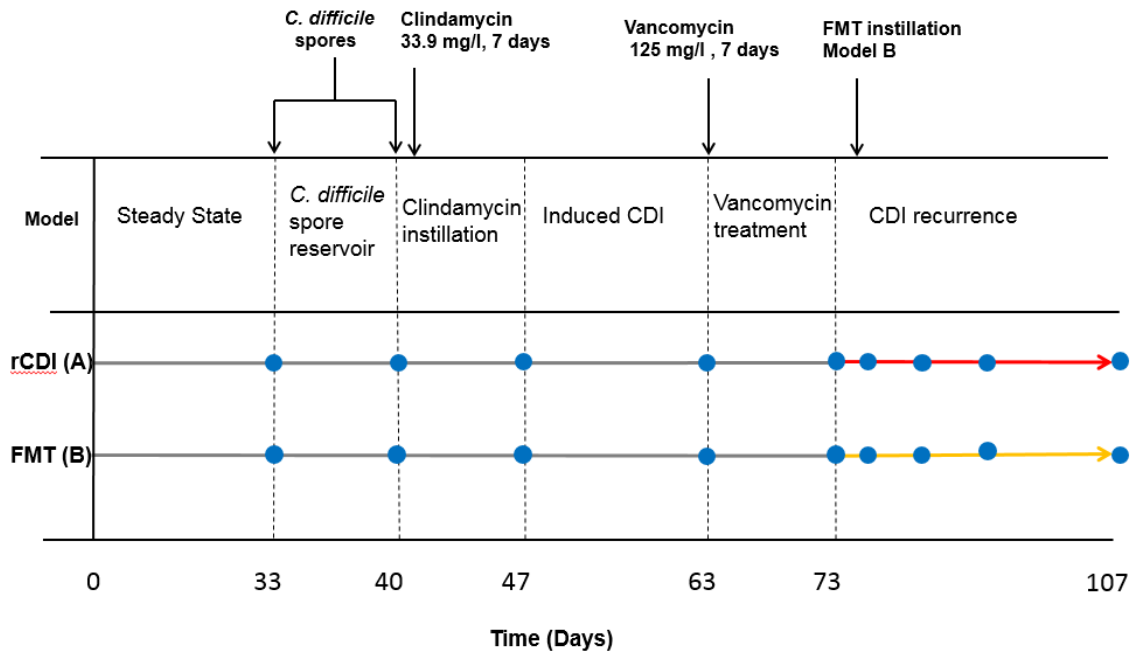


Figure 3-1 The *in vitro* gut model timeline for the rCDI model (A) and the FMT model (B). The different stages of the model are indicated at the corresponding day in the timeline. Both models A and B followed the same progression (grey lines) up to the end of vancomycin treatment. After cessation of vancomycin, model A was left without further intervention (red line) and model B received a simulated FMT 3 days post vancomycin cessation (yellow line). Biofilm sampling time points are indicated by a blue circle.

Clindamycin was used to disrupt the microbial populations and create an environment susceptible to CDI. Active CDI was deemed present when there was evidence of *C. difficile* spore germination accompanied with *C. difficile* outgrowth and toxin production. *C. difficile* toxin levels were monitored daily using the Vero cell cytotoxin assay described in section 2.2.16. Once peak toxin levels were detected, both models were dosed with vancomycin to treat the simulated CDI. Upon cessation of vancomycin, one model was left without further intervention for the duration of the experiment to model rCDI (model A), whilst model B received a simulated FMT 3 days post vancomycin cessation, on day 75 of the model.

3.2.2 Preparation of the FMT faecal slurry

The FMT simulated in this study used a faecal slurry from fresh stool sourced from a healthy 30 year old donor. Donor recruitment and specimen collection protocol was as described in section 2.2.2 and 2.2.3 with the exception of the age of the participant. Additionally, the donor was a co-inhabiting relative of one of the donors that contributed to the original faecal slurry used to seed the models. The use of a relative's or an intimate contact's faecal matter is generally preferred clinically as the microbiota is believed to be similar to that of the recipient prior to dysbiosis as is the likelihood of sharing infectious risk factors (Bakken *et al.*, 2011). The donor specimen was screened (described in section 2.2.3) and the FMT faecal slurry was prepared by homogenising the faecal matter with pre-reduced saline (10 % w/v) in a stomacher before being filtered to remove large particulate matter. The FMT slurry was prepared immediately prior to FMT instillation.

3.2.3 Administration of the simulated FMT

The 3 day period between vancomycin cessation and FMT instillation was to allow vancomycin levels to drop in vessel one to a level where it would not compromise the viability of the FMT. Preparation of the FMT slurry was described in section 3.2.2. 50 mL of the FMT slurry was top-fed into vessel one of model B to simulate a nasojejunal FMT through a sterile glass tube reaching the bottom of the vessel to prevent volume displacement (Figure 3-2). A peristaltic pump was used to deliver the slurry over a period of 1 hour (50 mL/hr). 30 mL of pre-reduced saline was used to flush the line into the model after the FMT. After FMT instillation, the model was left for a further 30 days and monitored for evidence of rCDI. In addition to routine planktonic sampling, an aliquot of planktonic supernatant was stored each day for offsite bile acid analysis (2.2.15). Concentrations of clindamycin and vancomycin in the planktonic phase were retrospectively analysed using antimicrobial bioassays (2.2.17). To monitor sessile populations in the models, the biofilm was periodically sampled and enumerated as described in 2.2.12 (sampling schedule Table 3-1 and blue circles in Figure 3-1) with the addition of oxytetracycline-glucose-yeast extract agar (OGYEA) media for the isolation of

fungi. DNA was extracted from biofilm samples and sent for 3rd party taxonomic analysis (2.2.14).

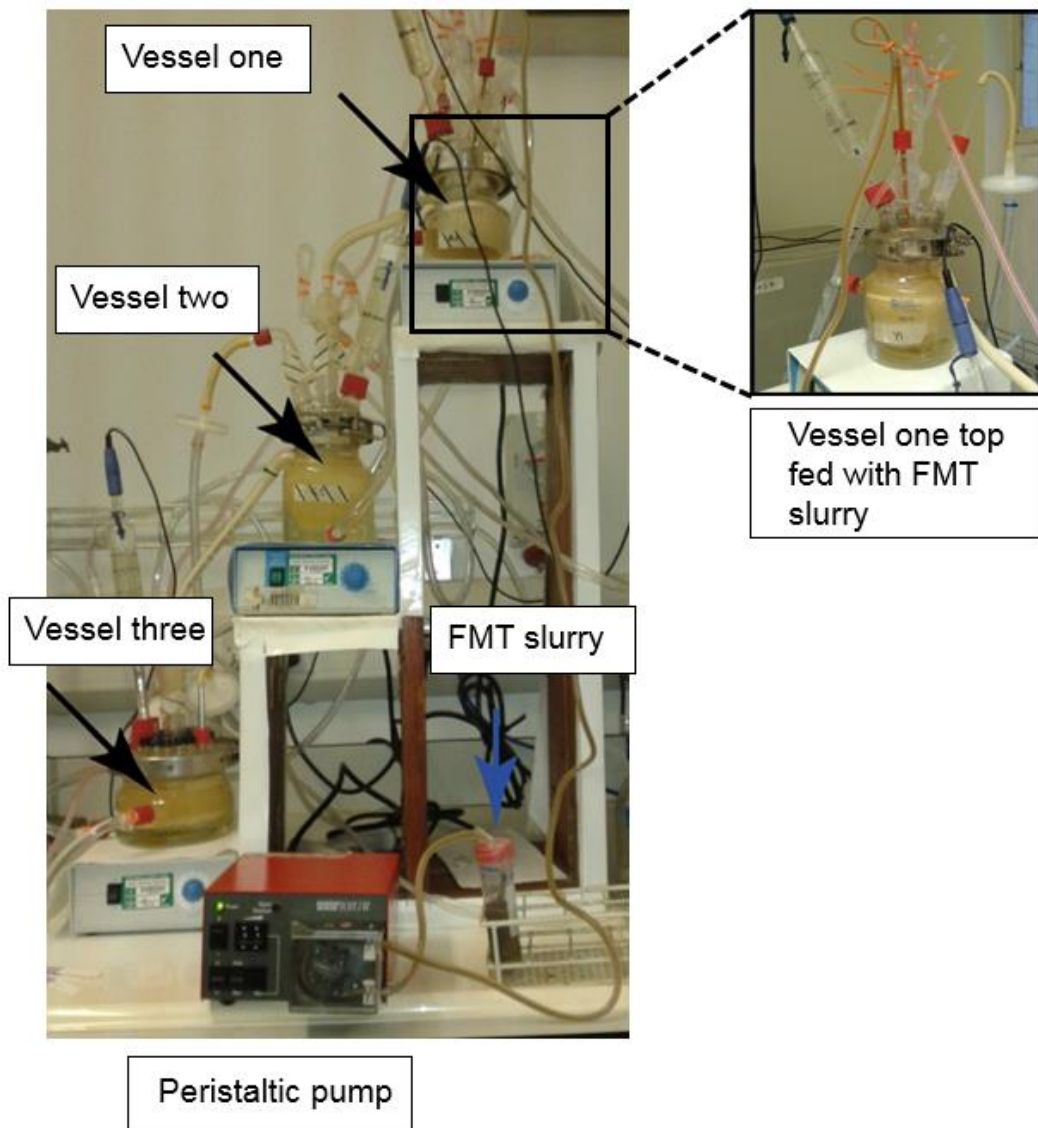


Figure 3-2 Simulated faecal microbiota transplantation (FMT) instillation into the triple stage gut model. 50 mL of the faecal microbiota slurry (blue arrow) was top fed into vessel one (enlarged) through a sterile glass tube using a peristaltic pump over a period of 1 hour (flow rate of 0.83 mL/min), 3 days after vancomycin cessation. The line was flushed with 30 mL of pre-reduced saline into the model after FMT instillation. The model was then left without further intervention for a further 30 days and monitored for evidence of recurrent CDI.

Table 3-1 Biofilm sampling schedule.

Model stage	Day	Number of rods per model
Steady state	33	1
Pre-clindamycin	40	1
Post-clindamycin	47	1
Pre-vancomycin	63	2
Post-vancomycin/ pre-FMT	73	3
rCDI/ FMT instillation (+ 2 days)	78	3
rCDI/ recovery	80	3
rCDI/ recovery	85	1
End of experiment	105	2

3.3 Results

3.3.1 Viability of frozen faecal slurry

To improve consistency between gut model runs, a faecal slurry was frozen and used to seed each gut model (procedure described in section 2.2.4). For each aliquot defrosted, selected bacterial populations were enumerated to determine if there was any loss of viability over time, using selective agars (Table 2-2). The slurry was frozen for a maximum of 81 weeks before use in the last model set (Chapter 4). Total viable counts (mean \log_{10} CFU/mL) from three technical replicates from each aliquot and the \log_{10} difference in range is listed in Table 3-2. The total facultative anaerobes, lactose fermenting (LF) Enterobacteriaceae, *Enterococcus* spp., *Clostridium* spp., *Lactobacillus* spp., and total spore populations remained fairly stable with a non-significant ($p \geq 0.05$) $\leq 0.6 \log_{10}$ CFU/mL difference in counts throughout the 81 week freezing period. There was a significant difference between total counts for *Bacteroides fragilis* gp., (difference of $0.8 \log_{10}$ CFU/mL from 48 hours vs 81 weeks, $p = 0.026$) and *Bifidobacterium* spp., (difference of $0.9 \log_{10}$ CFU/mL from 41 weeks vs 81 weeks, $p = 0.017$). The largest fluctuations in counts were found in the total anaerobes with a decrease of $1.3 \log_{10}$ CFU/mL from 48 hours and 13 weeks vs 81 weeks ($p = 0.033$).

Table 3-2 Comparison of the total viable counts of bacteria in the defrosted faecal emulsion used to seed the gut models

Bacterial population	Time concentrated faecal slurry frozen					Range (log ₁₀ difference)
	48 hours	13 weeks	29 weeks	41 weeks	81 weeks	
Facultative anaerobes	7.3	7.3	6.9	7.2	7.0	6.9 - 7.3 (0.4)
LF Enterobacteriaceae ^e	7.3	7.2	6.9	6.9	6.8	6.8 - 7.3 (0.5)
<i>Enterococcus</i> spp.	5.3	5.4	5.4	5.4	5.2	5.2 - 5.4 (0.2)
Total anaerobes	9.3*	9.3*	9.0	9.0	8.0*	8.0 - 9.3 (1.3)
<i>Clostridium</i> spp.	6.8	6.2	6.3	6.4	6.2	6.2 - 6.8 (0.6)
<i>Bacteroides fragilis</i> gp.	5.6*	6.4	6.1	6.0	6.4*	5.6 - 6.4 (0.8)
<i>Bifidobacterium</i> spp.	6.4	5.9	6.0	5.7*	6.6*	5.7 - 6.6 (0.9)
<i>Lactobacillus</i> spp.	5.4	5.4	5.4	5.4	5.2	5.2 - 5.4 (0.2)
Total spores	6.3	6.0	6.4	6.1	6.0	6.0 - 6.4 (0.4)

^a LF, Lactose fermenting. Values represent the mean log₁₀ CFU/mL from 3 technical replicates. Statistical analysis done using a Kruskal-Wallis Pairwise comparison where $p \geq 0.05$ was considered significant. * significantly different ($p \leq 0.03$).

3.3.2 Planktonic population kinetics

Each phase of the gut model and subsequent planktonic and biofilm population changes have been described in detail in this chapter as this is the first time the models are being outlined. In later chapters, trends will be discussed to avoid repetition.

3.3.2.1 Planktonic population dynamics of commensal bacteria during steady state and spore reservoir phase.

After inoculation with the faecal slurry, the models were left without intervention for 32 days during the steady state phase. This allowed the microbial populations to stabilize and establish colonisation resistance in the model. At the end of steady state, total anaerobes were approximately 9 log₁₀ CFU/mL, *Clostridia* spp. were 6.5 - 7 log₁₀ CFU/mL, *Bacteroides fragilis* gp. were approximately 8 log₁₀ CFU/mL, *Bifidobacterium* spp. were approximately 8 log₁₀ CFU/mL and total spores were approximately 5 - 5.5 log₁₀ CFU/mL (steady

state phase represented by the blue arrow Figure 3-3). In model A, the facultative anaerobic populations stabilized faster than model B, with model B experiencing an initial decrease in LF Enterobacteriaceae during the first week. By the end of steady state, the total facultative anaerobic populations were predominantly comprised of LF Enterobacteriaceae at approximately 8 – 9 log₁₀ CFU/mL and levels of *Enterococcus* spp. and *Lactobacillus* spp. reaching 6 – 7 log₁₀ CFU/mL and 7 log₁₀ CFU/mL, respectively (steady state phase represented by the blue arrow, Figure 3-4).

To ensure colonisation resistance was established in the models, a dose of *C. difficile* spores were added to vessel one of each model at the start of the *C. difficile* reservoir phase. Colonisation resistance was deemed to be established with the failure of *C. difficile* spores to germinate and produce toxins. This phase lasted one week in which population levels remained consistent (orange arrow, Figure 3-3 and Figure 3-4). After the initial inoculation with *C. difficile* spores, counts were approximately 5 log₁₀ CFU/mL in each vessel, with *C. difficile* recoveries reducing over the week. As the *C. difficile* spores added to the model failed to colonise, the *C. difficile* spore reservoir was replenished with another dose of spores into vessel one immediately prior to clindamycin instillation.

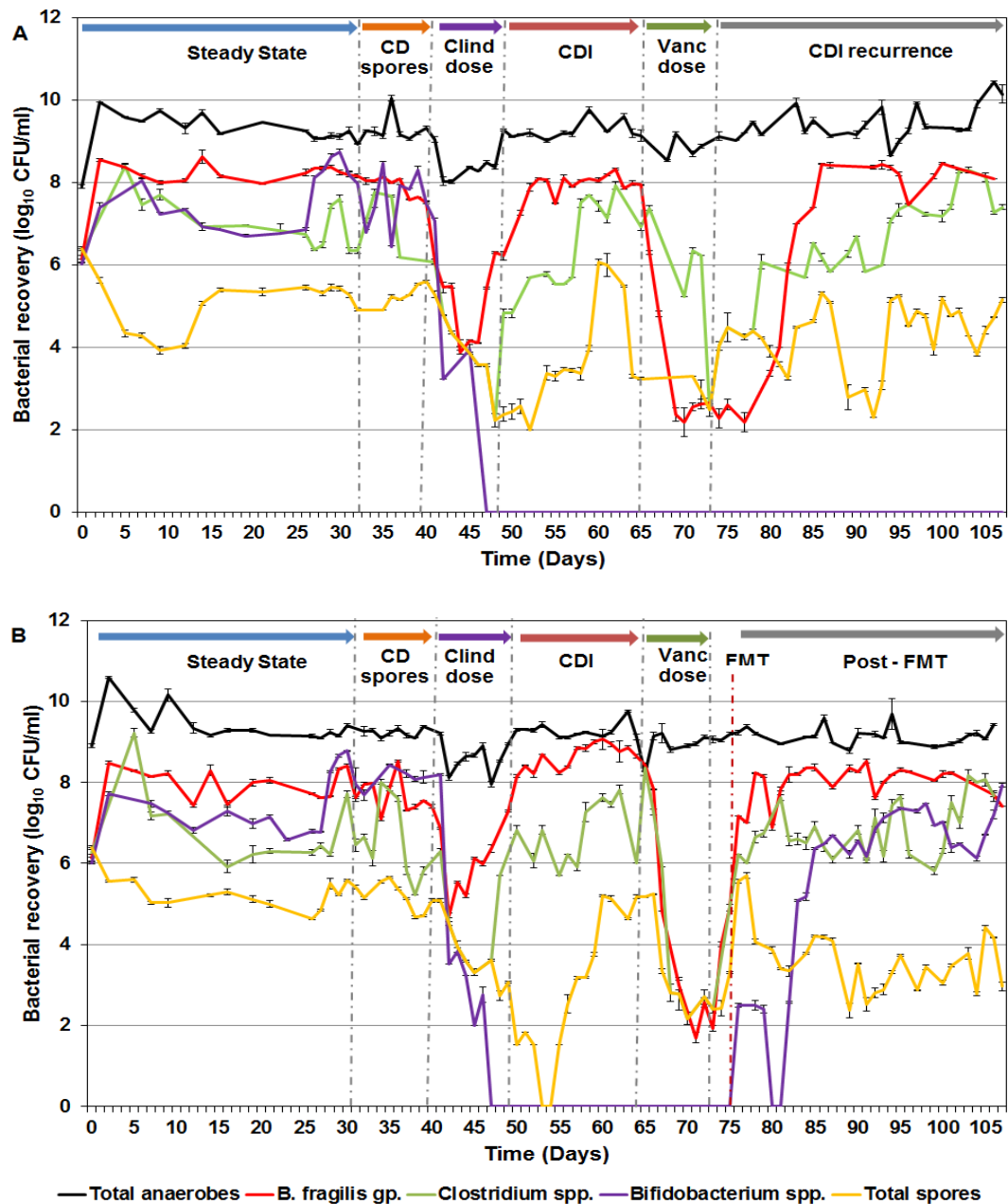


Figure 3-3 Enumeration of planktonic anaerobes in (a) the *C. difficile* recurrence model (model A) and (b) the simulated FMT model (model B). Bacterial enumeration of total anaerobes (black), *B. fragilis* gp. (red), *Clostridium* spp. (green), *Bifidobacterium* spp. (purple), and spores (yellow). Data demonstrates the disruption to the microflora during clindamycin and vancomycin therapy, and its rapid recovery after FMT in model B. Data shown are the mean log₁₀ CFU/mL ± standard error from three technical replicates per day of the model timeline of a single biological replicate. Different model stages are separated by vertical broken lines (grey; FMT instillation red – model B only). Clind – clindamycin, Vanc – vancomycin, FMT – faecal microbiota transplantation, CDI – *C. difficile* infection.

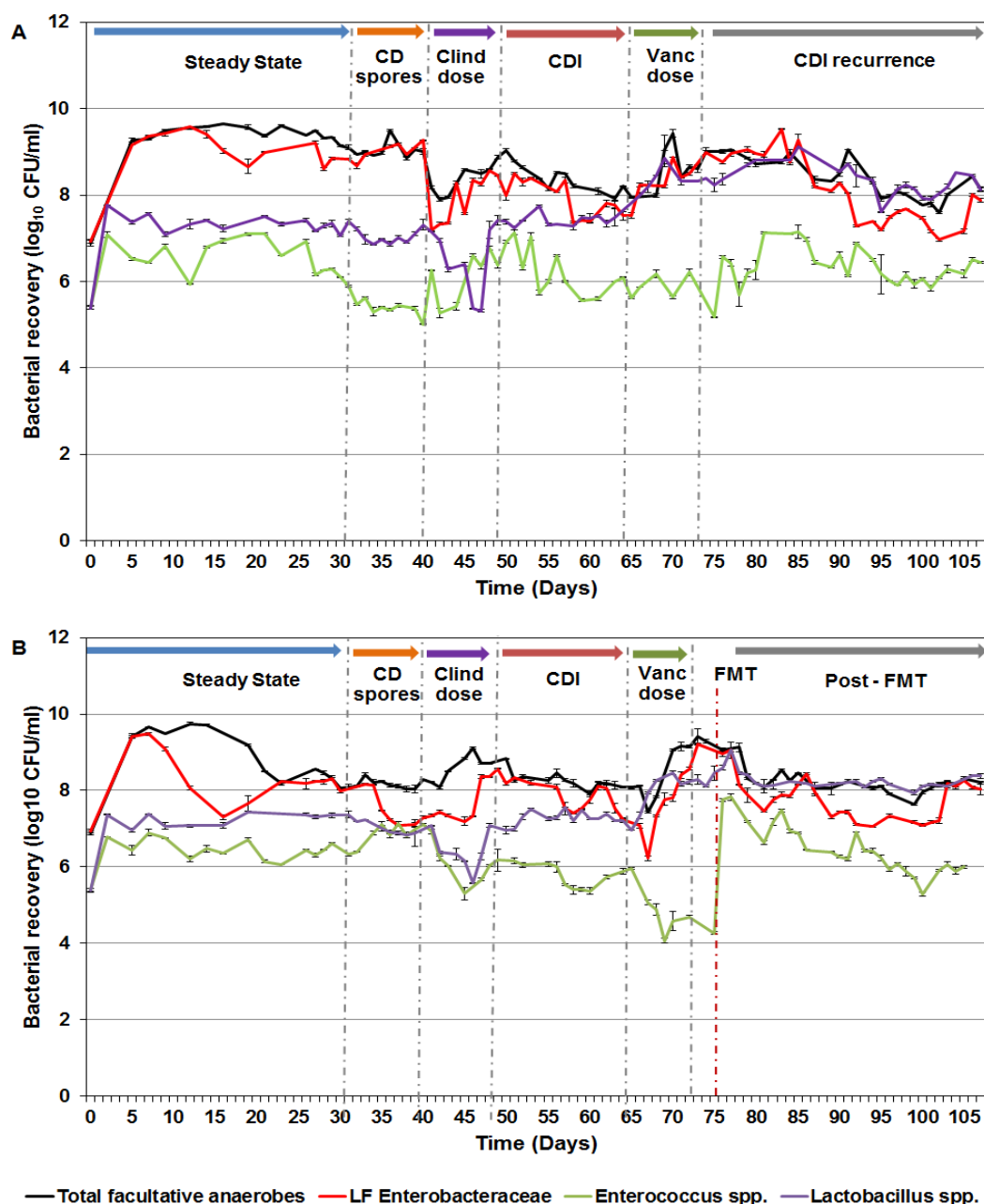


Figure 3-4 Enumeration of planktonic facultative anaerobes in (a) the *C. difficile* recurrence model (model A) and (b) the simulated FMT model (model B). Bacterial enumeration of total facultative anaerobes (black), lactose fermenting (LF) Enterobacteriaceae (red), *Enterococcus* spp. (green), and *Lactobacillus* spp. (purple). Data demonstrates an increase of facultative anaerobes during clindamycin and vancomycin therapy. Data shown are the mean log₁₀ CFU/mL ± standard error from three technical replicates per day of the model timeline of a single biological replicate. Different model stages are separated by vertical broken lines (grey; FMT instillation red – model B only). Clind – clindamycin, Vanc – vancomycin, FMT – faecal microbiota transplantation, CDI – *C. difficile* infection.

3.3.2.2 Clindamycin-induced dysbiosis resulted in simulated CDI.

As CDI is associated with disruption of the microbiota, clindamycin was used to perturb the populations and create a microbial niche conducive to *C. difficile* colonisation and outgrowth. Both models were dosed with clindamycin in vessel one 4 times daily, for 7 days (purple arrow, Figure 3-3 and Figure 3-4). Gut model fluid was removed from each vessel on a daily basis throughout clindamycin exposure and for a further seven days post clindamycin cessation to monitor antimicrobial concentrations in each vessel. Peak clindamycin levels for model A were found in vessel one on day 5 of dosing at 105.5 mg/L and on day 6 for vessels two and three at 120.3 mg/L and 104.5 mg/L, respectively. In model B, peak clindamycin concentrations of 165.2 mg/L, 117.3 mg/L and 94.8 mg/L were found on day 7 in vessel one, two and three, respectively (Table 3-3). A number of factors could contribute to the discrepancy of clindamycin peak levels between dosing days, models and vessels. Flow rate between vessels most likely had the highest influence of antibiotic levels. Biofilm accumulation in the piping connecting vessels as well as the flow of nitrogen into the vessels could both affect flow through the model. Despite these differences, both models were able to induce CDI at the same time point, reaching the similar levels of *C. difficile* toxin titre.

Clindamycin instillation resulted in dramatic changes to the microbial populations. The populations affected to the highest degree in both models were the *Bacteroides fragilis* gp., *Clostridium* spp., and *Bifidobacterium* spp.. *Bacteroides fragilis* gp. populations declined rapidly immediately after clindamycin instillation by approximately 3 – 3.5 log₁₀ CFU/mL, and recovered to pre-dosing levels 4 days after clindamycin cessation. *Clostridium* spp. declined by approximately 3 – 4 log₁₀ CFU/mL by mid-clindamycin dosing, with populations recovering from between 4 to 5 days post clindamycin cessation. The most dramatic effect was seen in *Bifidobacterium* spp. populations that reduced from approximately 8.2 log₁₀ CFU/mL to below the limit of detection, and did not recover in this phase of the models. Total spore recoveries declined gradually during clindamycin exposure and continued to decline after clindamycin cessation from approximately 5 log₁₀ CFU/mL to approximately 1.5 log₁₀ CFU/mL. Recovery of spore populations was gradual, with pre-dosing levels achieved 2 weeks after clindamycin cessation, with a spike in

populations to approximately $6 \log_{10}$ CFU/mL at this point (purple and red arrows, Figure 3-3). The facultative anaerobic populations were not affected to the same degree, with only marginal disruption to populations that recovered rapidly (purple arrow, Figure 3-4).

C. difficile populations began to show signs of germination approximately 9 - 10 days post clindamycin cessation (Figure 3-5). Peak *C. difficile* was recovered approximately 2 week post-clindamycin in both models, with total counts of $5.5 - 6 \log_{10}$ CFU/mL and spore counts of approximately $2 - 3 \log_{10}$ CFU/mL, indicating germination of *C. difficile* spores in both models. Germination was accompanied by the detection of *C. difficile* toxin, reaching peak levels of 3 RU and 2 RU approximately 2 weeks after clindamycin cessation for models A and B, respectively (black broken line, Figure 3-5). In both models, peak toxin titres were achieved in vessel 3 and persisted longer than in vessel two. No evidence of germination or toxin production was seen in vessel one (results not shown).

Table 3-3 Peak clindamycin and vancomycin concentrations (mg/L) and corresponding treatment day in model A and model B.

		Model A		Model B	
Antibiotic	Model vessel	Treatment day	Peak concentration of antibiotic (mg/L)	Treatment day	Peak concentration of antibiotic (mg/L)
Clindamycin	One	5	105.5	7	165.2
	Two	6	120.3	7	117.3
	Three	6	104.5	7	94.8
Vancomycin	One	4	138.7	5	153.7
	Two	6	134.7	6	174.9
	Three	7	135.1	6	154.9

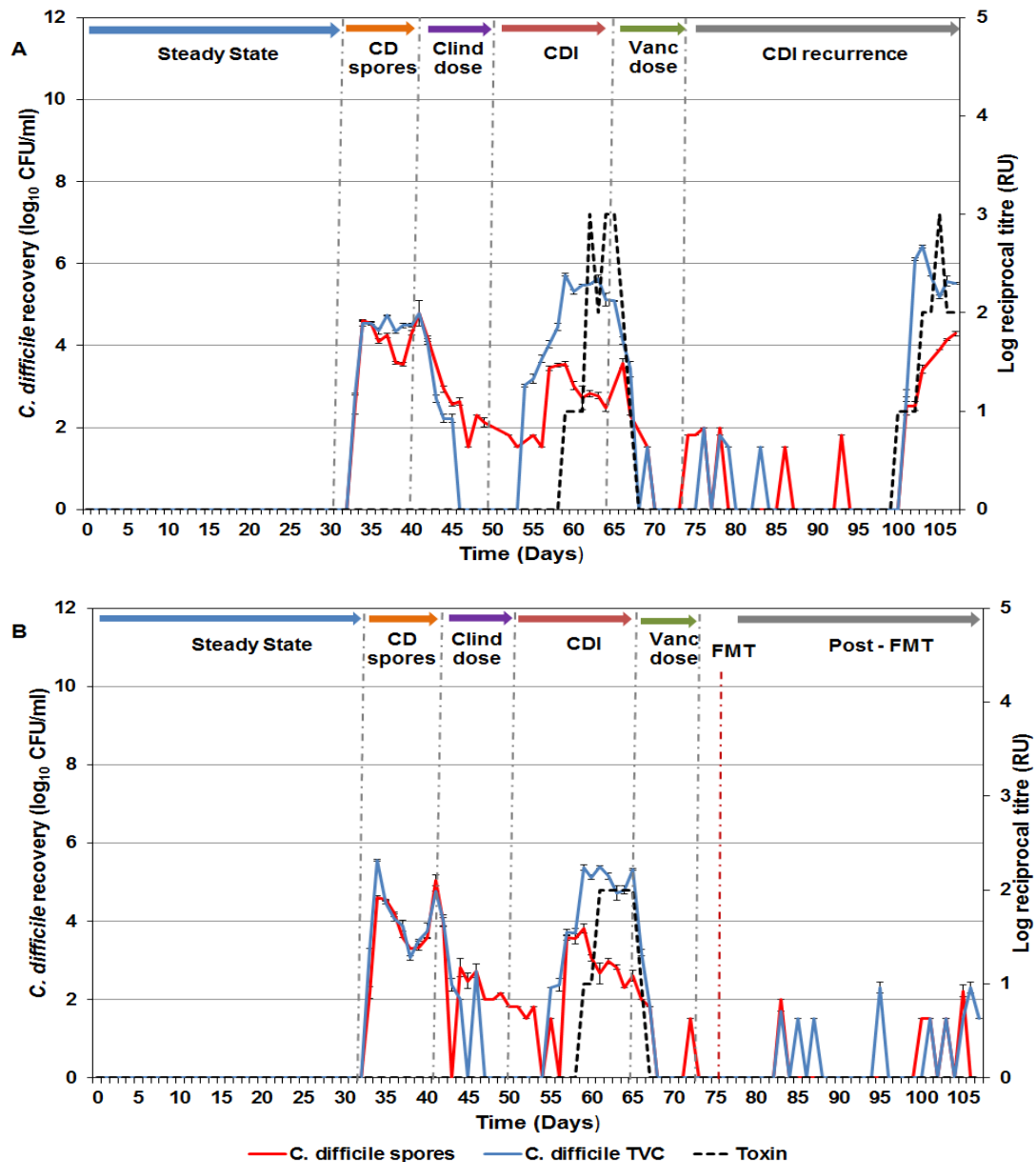


Figure 3-5 Enumeration of planktonic *C. difficile* total and spore counts in (a) the *C. difficile* recurrence model (model A) and (b) the simulated FMT model (model B). Enumerations of *C. difficile* spores (red) and total viable counts (blue) are represented for both models in mean \log_{10} CFU/mL \pm standard error (left axis). *C. difficile* toxin (black broken line) is represented as log reciprocal units (RU, right axis). Evidence of *C. difficile* recurrence is seen in model A but prevented after FMT in model B. Data shown are from three technical replicates per day of the model timeline of a single biological replicate. Different model stages are separated by vertical broken lines (grey; FMT instillation red – model B only). Clind – clindamycin, Vanc – vancomycin, FMT – faecal microbiota transplantation, CDI – *C. difficile* infection.

3.3.2.3 Planktonic microbial population dynamics during vancomycin treatment.

Most of the populations enumerated recovered to pre-clindamycin levels with the exception of *Bifidobacterium* spp. which remained below the limit of detection in both models when entering the vancomycin treatment phase. Vancomycin was introduced to both models in vessel one, 4 times daily for 7 days. Vancomycin was chosen as it is used clinically to treat CDI and has been used in our models previously to successfully model rCDI at the concentrations stated (Chilton *et al.*, 2014b, Crowther *et al.*, 2014a). Peak vancomycin levels in model A reached 138.7 mg/L (day 4 of treatment), 134.7 mg/L (day 6 of treatment) and 135.1 mg/L (day 7 of treatment) for vessel one, two and three, respectively. Peak vancomycin levels in model B reached 153.7 mg/L (day 5 of treatment), 174.9 mg/L (day 6 of treatment) and 154.9 mg/L (day 6 of treatment) for vessel one, two and three, respectively (Table 3-3). The population changes during vancomycin treatment were similar in both models, with the most dramatic changes occurring in *Clostridium* spp., and *Bacteroides fragilis* gp. with approximately 5 log₁₀ CFU/mL and approximately 6 log₁₀ CFU/mL reductions in counts, respectively (green arrow, Figure 3-3 and Figure 3-4). *C. difficile* TVC and spore counts rapidly declined, falling below the limit of detection in both models 3 days after vancomycin commencement (Figure 3-5). Most of the other populations enumerated remained unaffected or experienced minor, transient differences in population counts.

3.3.2.4 Differences in planktonic populations between model A and model B after FMT instillation

After vancomycin treatment, model A was left without further intervention whereas model B underwent a simulated FMT 3 days after vancomycin cessation. At the time of FMT intervention, vancomycin levels in model B were 17.5 mg/L, 26.5 mg/L and 30.94 mg/L in vessel one, two and three, respectively. Vancomycin levels were below the limit of detection one day after FMT instillation. In model A, *Clostridium* spp. and *Bacteroides fragilis* gp. populations gradually recovered 7 and 10 days post-vancomycin, respectively. *Bifidobacterium* spp. remained undetectable for the duration of model A Figure 3-3 a). *C. difficile* was detected 28 days after vancomycin cessation, with evidence of germination seen with an approximately 2 log₁₀ CFU/mL

divergence in spore and total counts, with peak TVCs of $6.4 \log_{10}$ CFU/mL. This was accompanied by the detection of *C. difficile* toxin, reaching peak titres of 3 RU 33 days post-vancomycin (Figure 3-5 a), indicating the recurrence of CDI in this model.

A considerable difference in recovery rate of commensal populations was evident immediately after FMT instillation in model B, with next day sampling revealing the complete recovery of *Clostridium* spp. and *Bacteroides fragilis* gp. to pre-vancomycin levels. Evidence of *Bifidobacterium* spp. recovery was seen immediately after FMT instillation (Figure 3-3 b). *C. difficile* was detected sporadically at very low levels, with no evidence of germination or toxin production (Figure 3-5 b), indicating that the FMT instillation successfully prevented rCDI in this model.

3.3.3 Biofilm population kinetics

3.3.3.1 Biofilm population dynamics during steady state and spore reservoir phase.

Multispecies biofilms consistently formed on the walls of the vessels and the glass sampling rods (Figure 3-6). Vessel one appeared to have accumulated the most biofilm on the vessel walls, however sampling was not performed from this vessel due to the relevance of the third vessel in *C. difficile* infection. As the number of glass rods in each model was limited, earlier biofilm samples spanning steady state, spore reservoir and early CDI were extensively studied in earlier models (two models detailing early planktonic and biofilm sampling presented in appendix A5), with results comparable to models A and B Figure 3-7 and Figure 3-8). These data suggested stable biofilm populations established in the steady state period that were not influenced by the addition of *C. difficile* spores. *C. difficile* spores rapidly became associated with the biofilm at level of approximately $4 - 5 \log_{10}$ CFU/g (Figure 3-9). Total facultative anaerobes were the predominant populations recovered from the biofilm. In planktonic populations, the LF Enterobacteriaceae counts closely match the total facultative anaerobic populations; however, there was an approximately $2 \log_{10}$ CFU/g difference in these counts in biofilm populations, indicating a difference in composition of the total facultative anaerobic populations between the planktonic and biofilm populations.

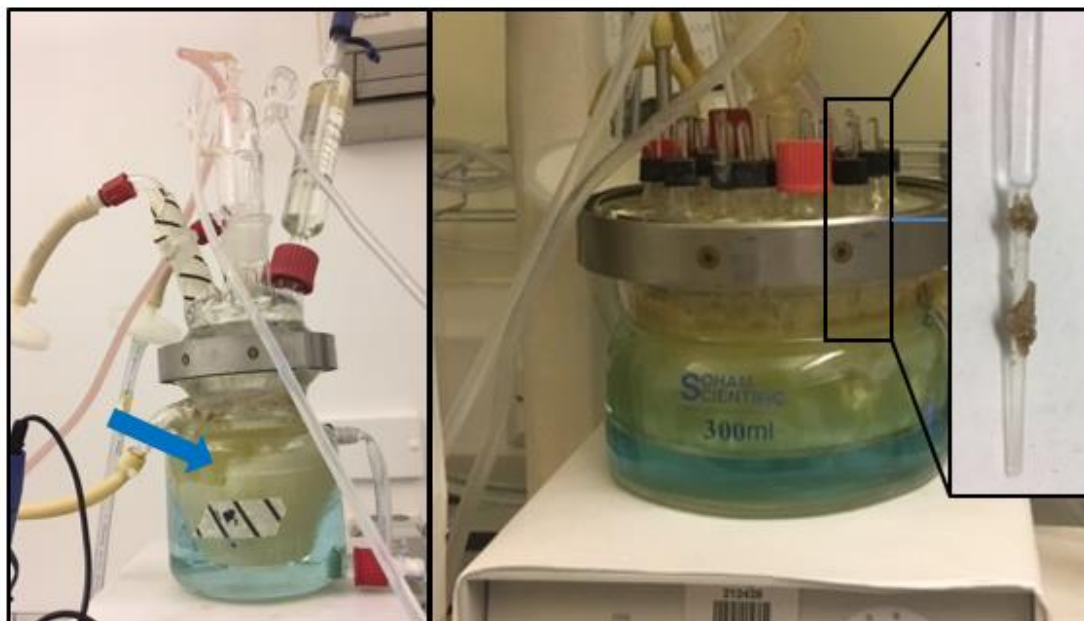


Figure 3-6 Biofilm formation in the gut model. The presence of biofilm formation can be seen on the vessel walls of the gut model (blue arrow) and on the biofilm support structures inserted in the lid vessel three of the gut model (insert).

3.3.3.2 Biofilm populations are more resilient to clindamycin treatment than planktonic populations.

As in steady state and the spore reservoir phase, the biofilm populations were predominantly sampled during clindamycin instillation and CDI induction in previous model runs (appendix, A5) with results comparable to models A and B (Figure 3-7 and Figure 3-8). Biofilm populations were not affected to the same degree as the planktonic phase during clindamycin instillation, demonstrating the resilience of biofilms to antimicrobial stress. A approximately 1 – 2 log₁₀ CFU/g reduction in counts was seen in *Bacteroides fragilis* gp. after clindamycin instillation, with populations recovering during peak CDI. *Bifidobacterium* spp. population initially dropped by approximately 3 log₁₀ CFU/g after clindamycin dosing, with populations continuing to decline to below the limit of detection during CDI. Total facultative anaerobic populations increased during clindamycin dosing by approximately 2 log₁₀ CFU/g before dropping back down to steady state levels during peak CDI. Different trends were seen in the total anaerobic populations and *Clostridium* spp., between the

two models. Total anaerobes in model A increased by approximately $1 \log_{10}$ CFU/g during clindamycin instillation followed by a fall in populations approximately $2 \log_{10}$ CFU/g; whereas in model B an initial decrease of approximately $2 \log_{10}$ CFU/g was seen after clindamycin dosing, followed by an increase in populations of approximately $1.5 \log_{10}$ CFU/g during CDI. *Clostridium* spp. populations in model A gradually increased from the spore reservoir phase, through clindamycin treatment and into CDI; whereas in model B there was a transient decrease in the populations during clindamycin instillation that recovered rapidly during CDI. *C. difficile* was isolated from the multispecies biofilm at approximately $4 - 5 \log_{10}$ CFU/g throughout clindamycin dosing and CDI induction (Figure 3-9).

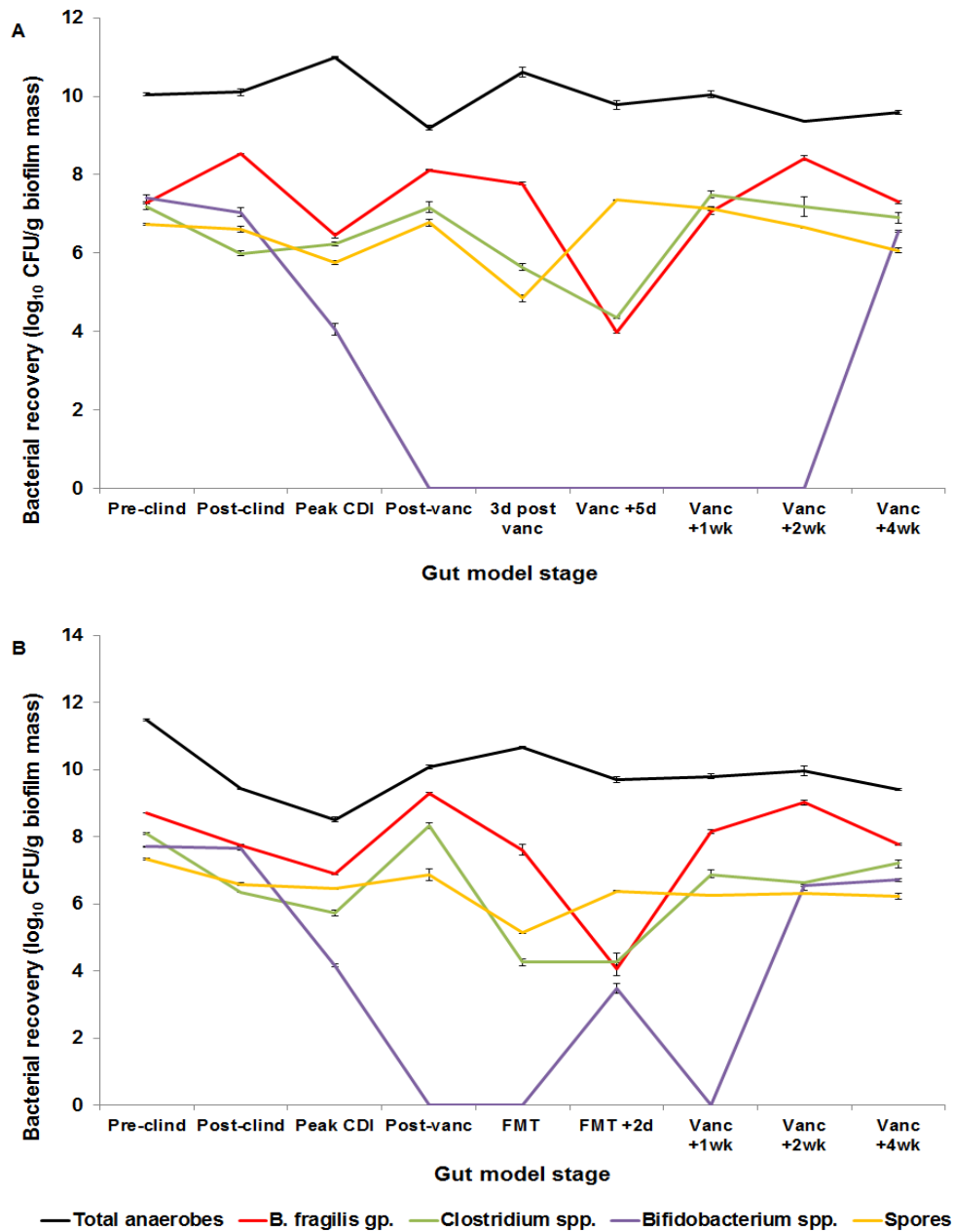


Figure 3-7 Enumeration of biofilm anaerobes in (a) the *C. difficile* recurrence model (model A) and (b) the simulated FMT model (model B). Bacterial enumeration of total anaerobes (black), *B. fragilis* gp. (red), *Clostridium* spp. (green), *Bifidobacterium* spp. (purple), and spores (yellow) from the biofilm recovered from biofilm support structures of the gut models. Data demonstrates the disruption to the biofilm populations during clindamycin and vancomycin therapy. Data shown are the mean log₁₀ CFU/g biofilm mass ± standard error from three technical replicates of a single biological replicate. Clind – clindamycin, Vanc – vancomycin, FMT – faecal microbiota transplantation, CDI – *C. difficile* infection, d – days, wk – weeks.

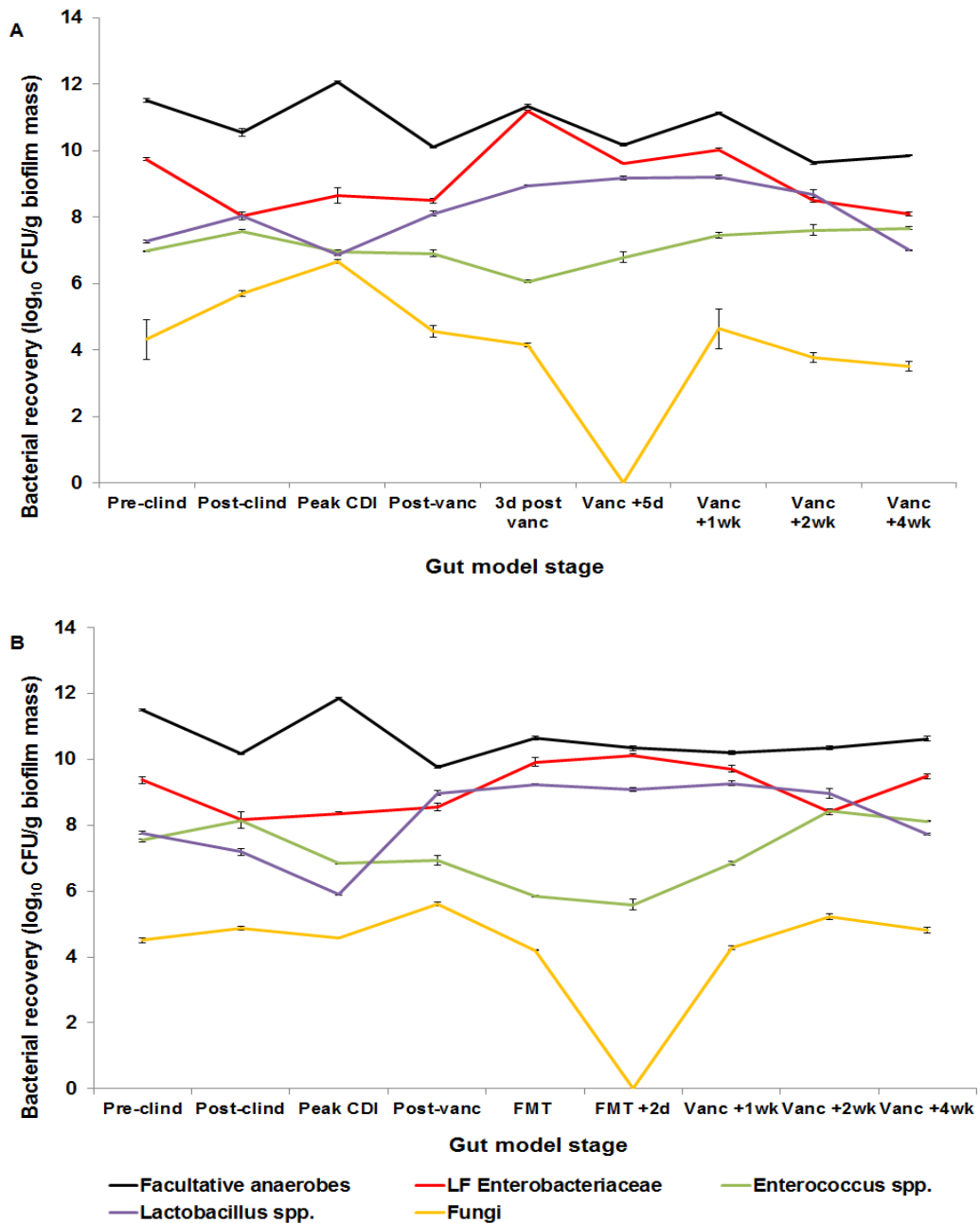


Figure 3-8 Enumeration of biofilm facultative anaerobes in (a) the *C. difficile* recurrence model (model A) and (b) the simulated FMT model (model B). Bacterial enumeration of total facultative anaerobes (black), lactose fermenting (LF) Enterobacteriaceae (red), *Enterococcus* spp. (green), *Lactobacillus* spp. (purple), and fungi (yellow) from the biofilm recovered from biofilm support structures of the gut models. The facultative anaerobic populations of the biofilm remained stable through antimicrobial therapy. Data shown are the mean log₁₀ CFU/g biofilm mass ± standard error from three technical replicates of a single biological replicate. Clind – clindamycin, Vanc – vancomycin, FMT – faecal microbiota transplantation, CDI – *C. difficile* infection, d – days, wk – weeks.

3.3.3.3 Vancomycin treatment induced pleiotropic changes in biofilm populations in Model A.

Total obligate anaerobic populations remained stable throughout vancomycin treatment, with levels between 9 – 10.5 log₁₀ CFU/g. *Clostridia* spp. populations reduced by approximately 3 log₁₀ CFU/g during vancomycin treatment, recovering approximately 7 days post-vancomycin cessation to steady state levels. *B. fragilis* populations gradually dropped during vancomycin treatment, reducing by approximately 4 log₁₀ CFU/g, 5 days post treatment cessation. Recovery of this population began 7 days after the end of treatment with counts between 7 - 8 log₁₀ CFU/g for the remainder of the experiment. *Bifidobacterium* spp. levels dropped below the limit of detection after clindamycin treatment and remained so until the last biofilm sample 33 days after the last vancomycin dose with levels similar to that seen in steady state. Total spore counts dropped by 2 log₁₀ CFU/g by the end of vancomycin treatment, recovering 5 days later and maintaining populations between 6 – 7.5 log₁₀ CFU/g (Figure 3-7a).

Total facultative anaerobic populations and LF Enterobacteriaceae experienced an increase in counts during vancomycin treatment of 1 and 2.5 log₁₀ CFU/g, respectively. *Lactobacillus* spp. populations increased by approximately 1 log₁₀ CFU/g and *Enterococcus* spp. decreased by approximately 1 log₁₀ CFU/g during vancomycin treatment, with both populations recovering to pre-vancomycin levels 12 days after treatment ended. Fungal populations in the biofilm during steady state reached levels of approximately 5.5 log₁₀ CFU/g. Levels dropped to 4.5 log₁₀ CFU/g during clindamycin treatment and continued to decline to below the limit of detection after vancomycin treatment, recovering 2 weeks after vancomycin cessation (Figure 3-8 a). *C. difficile* levels remained between 3.5 – 4.3 log₁₀ CFU/g for the duration of the experiment, with *C. difficile* predominantly in spore form (Figure 3-9).

3.3.3.4 FMT fails to eradicate *C. difficile* from the biofilm.

Clostridia spp. populations reduced from approximately 8 to 4 log₁₀ CFU/g during vancomycin treatment with levels increasing to approximately 7 log₁₀ CFU/g 4 days after FMT instillation. *B. fragilis* gp. counts decreased throughout vancomycin dosing reaching 4 log₁₀ CFU/g before levels increased to 8 log₁₀ CFU/g 4 days after FMT instillation. *Bifidobacterium* spp. failed to recover after

clindamycin treatment and therefore levels were undetectable during vancomycin treatment. *Bifidobacterium* spp. was detected 7 days after FMT instillation and levels remained stable for the duration of the experiment. Total spores decreased by approximately 2 log₁₀ CFU/g during vancomycin treatment and reached steady state levels 2 days post FMT instillation (Figure 3-7b).

Total facultative anaerobic populations and LF *Enterobacteriaceae* spp. increased by approximately 1 log₁₀ CFU/g during vancomycin before stabilising at approximately 10 log₁₀ CFU/g for the duration of the experiment.

Enterococcus spp. dropped by 1 log₁₀ CFU/g after vancomycin treatment followed by a gradual increase in populations to steady state levels 4 days after FMT, further increasing by 1.5 log₁₀ CFU/g at the end of the experiment. Total fungal populations increased slightly after clindamycin treatment from approximately 4.5 – 5.5 log₁₀ CFU/g before counts dropped during vancomycin treatment to 4 log₁₀ CFU/g. After FMT instillation, fungal populations stabilised at approximately 5 log₁₀ CFU/g. *Lactobacillus* spp. were stable throughout vancomycin treatment and FMT instillation (Figure 3-8 b). *C. difficile* counts decreased marginally after FMT instillation; however, *C. difficile* was not eliminated from the biofilm and remained associated with sessile communities for the remainder of the experiment at levels of approximately 3.5 - 4 log₁₀ CFU/g, predominantly in spore form (Figure 3-9).

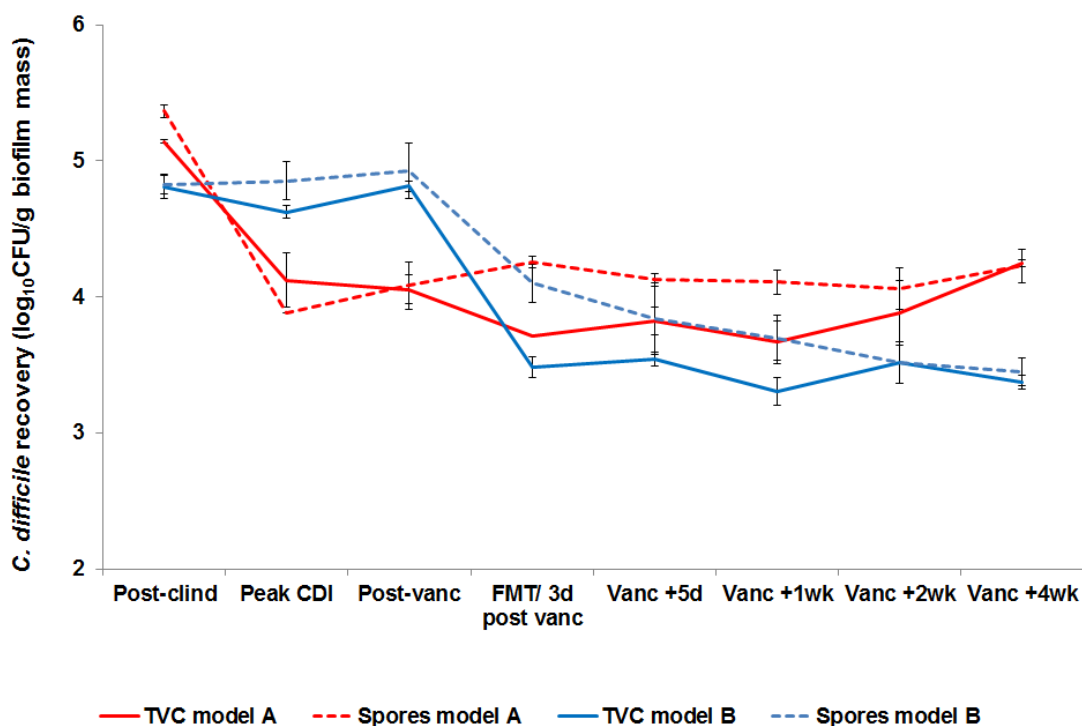


Figure 3-9 Enumeration of *C. difficile* total and spore counts recovered from the biofilm in models A and B. Bacterial enumeration of the total viable counts (TVC - solid line) and spore counts (broken line) of *C. difficile* for the recurrence model (model A - red) and the faecal microbiota transplant model (model B – blue) from biofilm recovered from biofilm support structures in the respective models. Data demonstrates the persistence of *C. difficile* cells in the biofilm through antimicrobial and faecal microbiota transplant therapy. Data shown are the mean log₁₀ CFU/g biofilm mass ± standard error from three technical replicates of a single biological replicate, at various stages throughout the model timeline. Clind – clindamycin, Vanc – vancomycin, FMT – faecal microbiota transplantation, CDI – *C. difficile* infection, d – days, wk – weeks, TVC – total viable counts.

3.3.3.5 Taxonomic analysis of biofilm populations

DNA was extracted from biofilm pellets after centrifugation and the A260/A280 ratio was used as an indication of DNA purity. All DNA extracts had ratios of between 1.8 – 2.0, indicating acceptable DNA purity, and extracts were then shipped for offsite taxonomic analysis using 16S rRNA Illumina sequencing and analysis (section 2.2.14). Reads were aligned to a curated database consisting of the full-length 16S region. Operational taxonomic units (OTU) with fewer than 10 reads in a given sample were discarded. The OTU data was organised at the family level, with the 14 most prevalent families considered.

In both models, treatment with clindamycin and vancomycin were associated with an increase in Enterobacteriaceae populations and a decrease in Eubacteriaceae and Bifidobacteriaceae. Vancomycin treatment had a larger effect on microbial communities, with additional decreases in Bacteroidaceae, Lachnospiraceae, Ruminococcaceae and Comamonadaceae; and increases in Synergistaceae, Lactobacillaceae and Desulfovibrionaceae. In model A, Enterobacteriaceae and Synergistaceae populations continued to increase to 38.9 % and 19.5 % abundance, respectively. Eubacteriaceae, Lachnospiraceae and Bifidobacteriaceae remained low, recovering 4 weeks post-vancomycin treatment. Bacteroidaceae, Ruminococcaceae and Comamonadaceae failed to recover to pre-antibiotic levels by the end of sampling (Figure 3-10 a). These population changes were associated with rCDI in the planktonic phase.

In contrast, model B post-FMT analysis revealed a decrease in Enterobacteriaceae, Synergistaceae and Desulfovibrionaceae populations to 1.16 %, 8.2 % and 1.2 % respectively. This was accompanied with the rapid recovery of Bacteroidaceae, Eubacteriaceae, Lachnospiraceae, Bifidobacteriaceae and Ruminococcaceae (Figure 3-10 b). Analysis of the microbiota diversity, using the Shannon diversity index, showed an increase in diversity of samples post-FMT in model B, increasing from 1.72 ± 0.51 to 2.03 ± 0.52 at one week post-FMT and continued to increase, ending the experiment on 2.33 ± 0.21 . Model A by comparison, had a diversity index of 1.79 ± 0.52 one week post vancomycin cessation, dropping to 1.76 ± 0.28 the following week and by the end of the experiment, increased to 2.0 ± 0.26 (Figure 3-11).

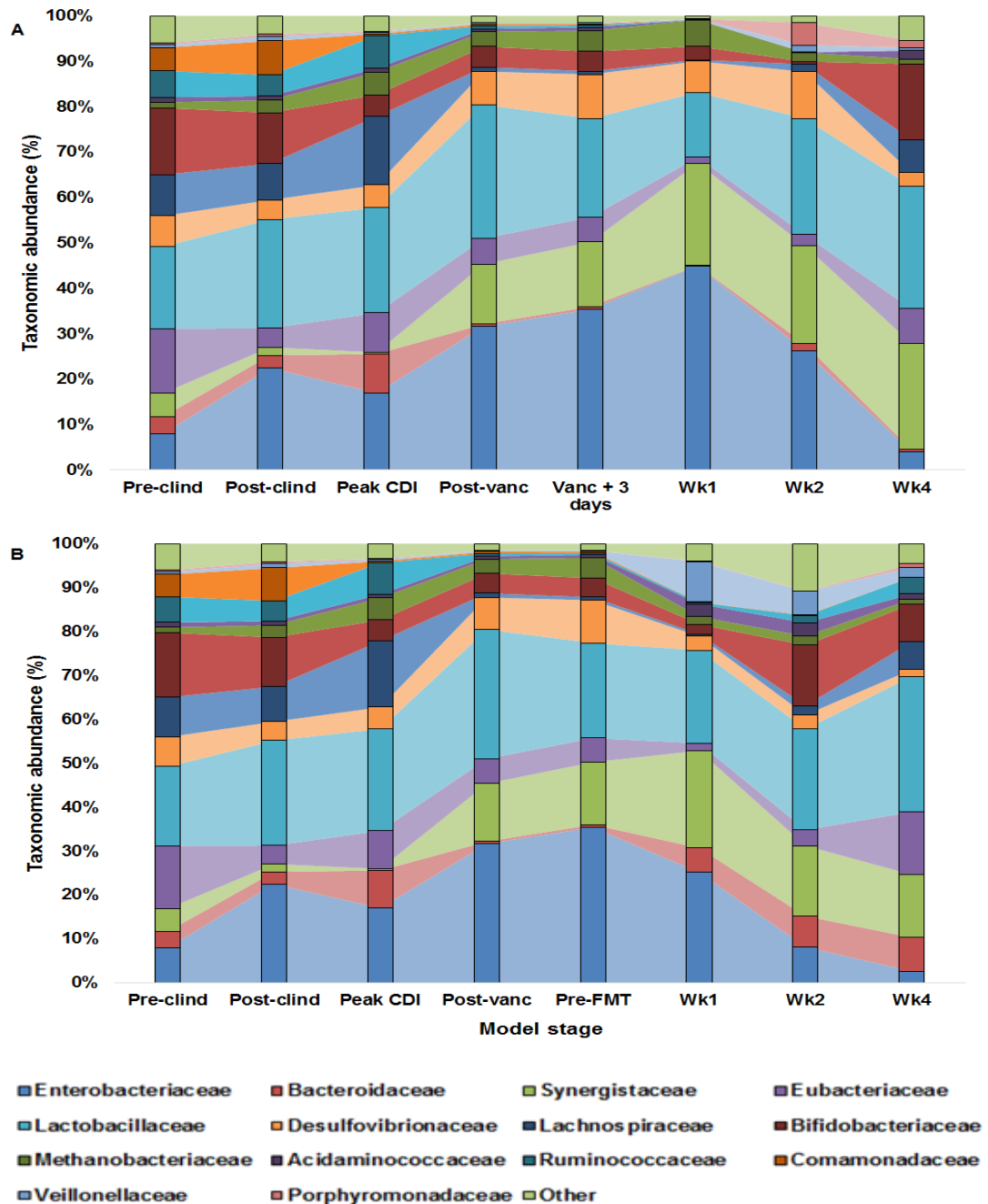


Figure 3-10 Changes in bacterial taxonomic abundance of the biofilm microbial community at selected time points in the recurrence model (A) and the simulated FMT model (B). Taxonomic abundance (percentage) of the top 14 bacterial families recovered from biofilm support structures in the triple stage gut models. Graphs constructed using the mean (of least 3 support structures) percent abundance of bacterial OTUs assigned to a family taxonomic level, for one biological replicate for the recurrence model and two biological replicates for the FMT model. Clind – clindamycin, Vanc – vancomycin, FMT – faecal microbiota transplantation, CDI – *C. difficile* infection, wk - week.

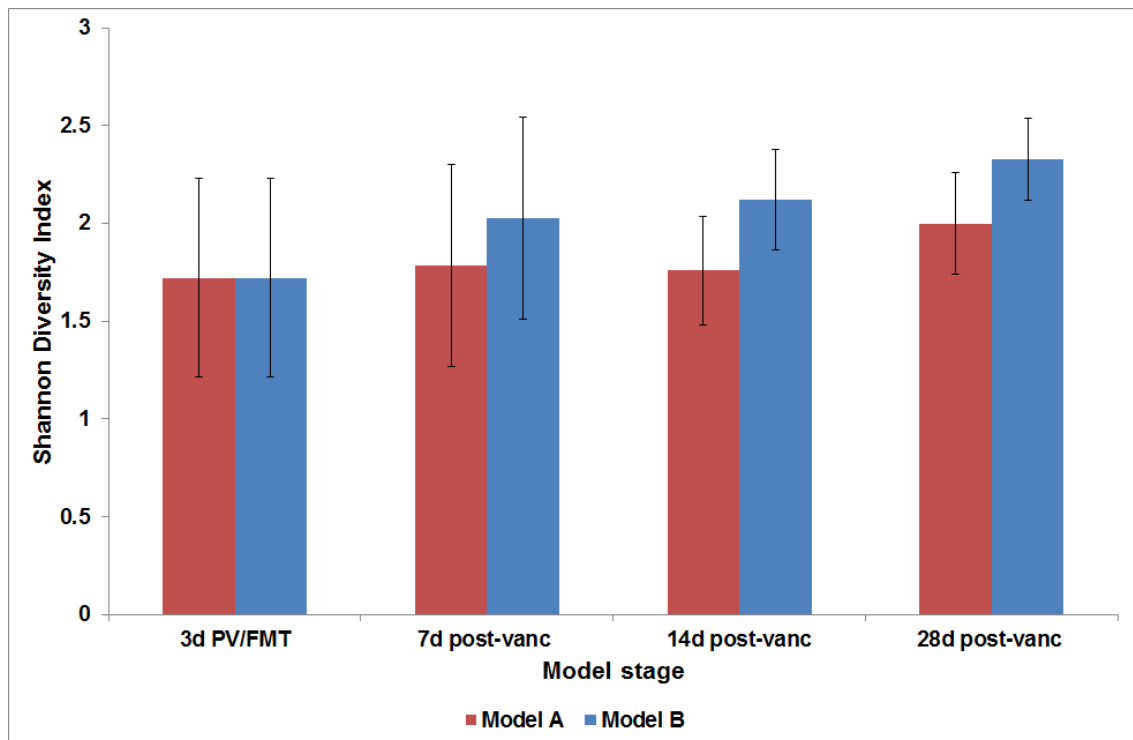


Figure 3-11 Shannon Diversity Index of biofilm samples from model A and model B. The Shannon (alpha) diversity of the biofilm populations was measured after vancomycin treatment for model A (red) and model B (blue). There was an increase in bacterial diversity in model B from 7 days post vancomycin cessation when compared to model A, which lasted to the end of the experiment. The Shannon Diversity Index was calculated using bacterial OTUs assigned to a family taxonomic level using mean data from at least 3 support structures for each time point, for one biological replicate for the recurrence model and two biological replicates for the FMT model. Error bars indicate standard deviation. FMT – faecal microbiota transplant, vanc – vancomycin, d – days.

3.3.3.6 Changes in bile acid levels during rCDI and FMT

Bile acid metabolism has been demonstrated to play an important role in CDI and therefore we wanted to monitor the changes to the bile acid profile during rCDI and FMT treatment. The levels of the primary bile acid, cholic acid (CA), and the secondary bile acids deoxycholic acid (DCA) and oxo-bile acids (oxo-BAs) were analysed at different time points throughout the models. CA and DCA were components of our gut model growth media and were continuously fed to the model. Bile acid levels stabilised during steady state, with similar levels seen in both models. Antimicrobial therapy resulted in an increase in CA levels, accompanied by a decrease in DCA levels, indicating a decrease in microbiome mediated 7 α - dehydroxylation bile acid metabolism using CA with antimicrobial treatment. CA levels decrease while DCA and OXO-Bas increase as the microbiota diversity increased. In model A, high levels of CA were seen for an extended period of time after vancomycin treatment. This was accompanied by relatively high levels of DCA and low levels of oxo-BAs. As DCA was continuously added to the model in the growth media, increased levels could indicate the accumulation of DCA from the input rather than CA metabolism. The potential accumulation of DCA and low oxo-BA levels could indicate a decrease in downstream bile acid metabolism by the microbiome (Figure 3-12 a). In model B, there was a rapid decrease in CA levels post-FMT. This was accompanied by an increase in DCA and oxo-BA levels, indicating downstream secondary bile acid metabolism as the microbiome diversity was restored from FMT instillation (Figure 3-12 b).

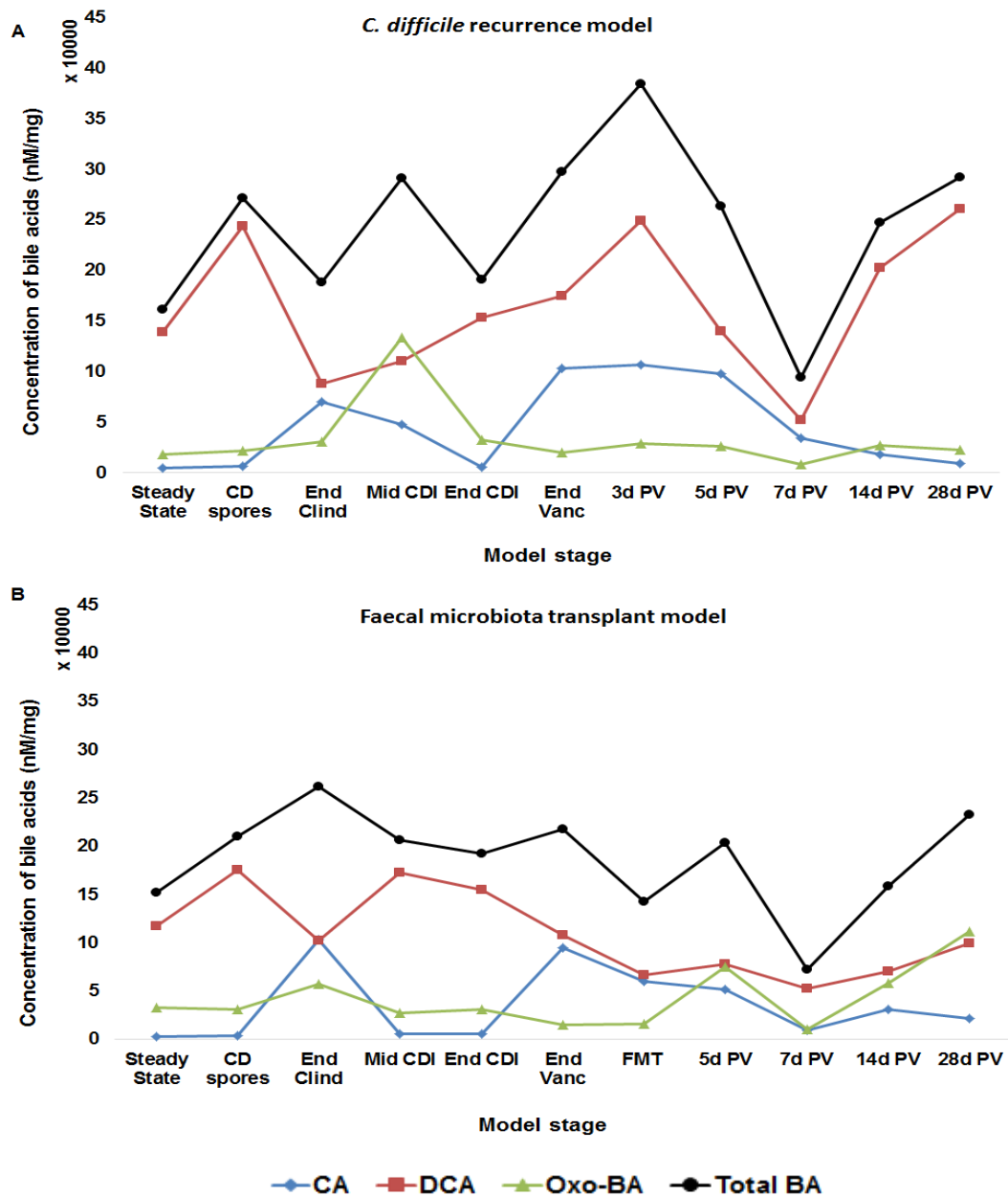


Figure 3-12 Bile acid analysis of the *C. difficile* recurrence model (A) and the faecal microbiota transplant model (B). The concentration of cholic acid (CA; blue, diamond), deoxycholic acid (DCA; red, square) and oxo-bile acids (oxo-BAs; green, triangle) were measured in nM/mg at selected time points during the model timeline. Total bile acids (black, circle) represent the sum of CA, DCA and Oxo-BAs. Data demonstrates increased CA levels during clindamycin and vancomycin instillation, with prolonged elevated CA levels in model A coinciding with CDI recurrence. Data are single samples from one biological replicate. CD – *C. difficile*, Clind – clindamycin, Vanc – vancomycin, d – days, PV – post-vancomycin.

3.4 Discussion

With the clinical success of FMTs in preventing rCDI, microbiota restoration has become a key area of interest. Currently, there is no standard protocol for either FMT preparation or FMT administration, and with increasing safety concerns regarding the unknown long term effects of FMT therapy (DeFilipp *et al.*, 2019), there has been increased interest in determining the mechanisms of FMT efficacy and the drive to develop more defined, regulated microbiome based therapeutics. To date, there are insufficient *in vitro* models to test microbiome based therapeutics. Here we sought to modify our current *in vitro* gut model to simulate FMT treatment of rCDI to determine whether the model could be used to accurately predict the outcome of microbiome based therapies used to prevent rCDI. The University of Leeds *in vitro* gut models have been used previously to determine the propensity of antimicrobials to induce simulated CDI, as well as the efficacy of antimicrobials against primary and rCDI (Freeman *et al.*, 2003, Freeman *et al.*, 2007, Chilton *et al.*, 2014b). The gut models have been demonstrated to be clinically reflective in both microbial contents and study outcome (Freeman *et al.*, 2003, Baines *et al.*, 2005). This model also has the advantage of facilitating the development and longitudinal sampling of biofilm populations (Crowther *et al.*, 2014a, Crowther *et al.*, 2014b), which is an area severely lacking in CDI research. Two gut models were run in parallel, one simulating rCDI and the other simulating an FMT, allowing a direct comparison between the two using culture of the planktonic and sessile populations, bile acid profiling and taxonomic analysis of sessile communities.

During the initial stages of the models, the indigenous intestinal microbiota were left to equilibrate, modelling the environment of a healthy gut. This was confirmed when *C. difficile* spores were added and populations monitored for one week. There was no evidence of *C. difficile* germination or outgrowth during this period, indicating colonisation resistance was established in the models. This is critical in the validation of the model as it ensures that the model is reflective of a healthy microbiota by inhibiting pathogen invasion and that the resulting CDI was as a result of antibiotic-induced dysbiosis of the gut microflora, a step which has not been demonstrated in previous simulated FMT models (McDonald *et al.*, 2018a). Biofilm composition during this period

revealed an abundance of populations, dominated by the phyla Firmicutes, Bacteroidetes and Proteobacteria, consistent with *in vivo* findings (Hold *et al.*, 2002, Lyra *et al.*, 2012). As CDI is dysbiosis-mediated, clindamycin was used to perturb the microbiota, generating an environment susceptible to *C. difficile* outgrowth. This disruption was characterised by a reduction in *B. fragilis*, *Bifidobacterium* spp. and *Clostridia* spp. with an increase in facultative anaerobic populations. Biofilm response to antibiotic instillation was delayed and not as dramatic as those seen in planktonic populations, demonstrating the resilience of biofilms in hostile environments. Taxonomy of biofilm populations reflected findings of increased recoveries of Enterobacteriaceae following antibiotic treatment, confirming dysbiosis in the sessile communities, in line with *in vivo* observations (Morgan *et al.*, 2012, Shin *et al.*, 2015). Planktonic levels of the primary bile acid CA increased during clindamycin instillation, accompanied by a decrease in DCA levels, indicating the potential loss of microbiome mediated 7 α – dehydroxylation secondary bile acid synthesis. Active CDI was confirmed with evidence of *C. difficile* spore germination and vegetative outgrowth, accompanied by toxin production, approximately 9 days post-clindamycin cessation. Recovery of the microbiota to pre-clindamycin levels coincided with a decrease in CA and increase of DCA levels.

Vancomycin treatment of CDI in our models successfully reduced planktonic *C. difficile* populations to below the limit of detection, accompanied with the loss of toxin detection. Vancomycin instillation had a dramatic effect on microbial populations, with reductions in *B. fragilis* gp., *Clostridium* spp., and the continued suppression of *Bifidobacterium* spp., together with increased abundance of Enterobacteriaceae. Once again, sessile communities displayed a similar trend to those seen in planktonic populations; however, these were not as susceptible to antimicrobial therapy and populations changes more gradual. Consistent with clindamycin instillation, vancomycin dosing resulted in an increase in CA levels, with decreased DCA and oxo-BAs. Planktonic enumeration of *Clostridium* spp., and *B. fragilis* gp., from Model A, indicated population recovery 7 and 10 days after vancomycin cessation, respectively. *Bifidobacterium* spp., failed to recover in planktonic populations, with sessile recovery seen in the last sample of the model. The ability of *Bifidobacterium longum* and *Bifidobacterium breve* to reduce the growth of *C. difficile in vitro*

has led to the potential use of these organisms as pro and prebiotics (Valdes-Varela *et al.*, 2016) and therefore the reduction and/or absence of these populations during initial and rCDI could be significant.

Evidence of rCDI was seen 28 post-vancomycin treatment in Model A, consistent with findings from previous models (Chilton *et al.*, 2014b, Crowther *et al.*, 2014a). Bile acid profiling demonstrated a prolonged exposure to high levels of CA. Primary bile acids, such as CA, are associated with *C. difficile* spore germination (Sorg and Sonenshein, 2008) and therefore this increased exposure to the biofilm-associated *C. difficile* spores could potentially contribute to the development of rCDI in this model. High levels of DCA during this period indicates an accumulation of DCA in the model from the media input, most likely due to a reduction in the downstream metabolism of bile acids. Reduced levels of oxo-BAs seem to confirm this theory. Biofilm 16S rRNA sequencing demonstrated increased Enterobacteriaceae after vancomycin treatment, accompanied by reduced levels bacterial families predominantly responsible for bile-acid metabolism, namely Bacteroidaceae, Bifidobacteriaceae and Ruminococcaceae (Song *et al.*, 2019, Vital *et al.*, 2019).

In model B, 3 days after vancomycin cessation, a simulated FMT was performed. Almost immediately following simulated FMT instillation, planktonic *Clostridia spp.* and *B. fragilis* gp recovered to pre-treatment levels, accompanied by the more gradual recovery of *Bifidobacterium spp.*. It took on average 10 days for populations to fully stabilise after the FMT dose, indicating a potential time frame for microbial engraftment, raising the possibility of rCDI risk within early phases after FMT, which could explain the need for multiple FMT instillations in the clinical setting (Lee *et al.*, 2016). FMT instillation had a notable effect on biofilm communities, with the reduction in Enterobacteriaceae and the rapid recovery of Bacteroidaceae and Bifidobacteriaceae. Bile acid analysis indicated a rapid reduction in CA levels following FMT treatment. Oxo-BA levels also increased, indicating increased microbial secondary bile acid metabolism which coincided with the restoration of these bile-acid metabolising families. This rapid restoration of the microbiota successfully prevented rCDI in this model, for the duration of the experiment. These results are consistent with findings from McDonald *et al.* (2018a) that demonstrate that FMT restores

microbial populations responsible for performing key metabolic functions that prevent CDI.

The dynamics of the sessile communities during antibiotic treatment, CDI, rCDI and FMT instillation have not been well studied due to the inaccessibility of the mucosal populations. In our models, modifications to the vessel reflecting the distal colon with glass rods enabled the longitudinal sampling of mature, multispecies biofilms without compromising the integrity of the system (Crowther *et al.*, 2014b). Results from the sessile communities confirmed the tolerance of biofilms to antibiotic treatment (Stewart, 2002) as the populations showed high resilience to both clindamycin and vancomycin treatment. Our results show that *C. difficile* spores became intimately associated with the healthy biofilm early on. This could have major implications for clinical prescribing practises, as well as raising questions on under reported asymptomatic carriage rates of *C. difficile*. The levels of *C. difficile* spores remained steady between 3 to 5 log₁₀ CFU/g throughout the experiment and were not affected by vancomycin treatment or eliminated by the FMT instillation. This was in contrast to the planktonic phase where *C. difficile* viable and spore counts dropped below the limit of detection, with only transient *C. difficile* detection. We hypothesise that the biofilm acts as a reservoir for *C. difficile* spores, with spores detaching from the biofilm to periodically seed the planktonic phase. When the spores encounter an environment susceptible to *C. difficile* outgrowth, as seen in model A, the spores are able seed the planktonic phase and lead to vegetative cell proliferation. If the environment is not favourable, as seen in model B after FMT-mediated microbiota restoration, the spores fail to germinate; however, the spores are still detectable in the biofilm. This suggests that patients who have undergone FMT therapy potentially remain at risk of CDI with future antibiotic exposure. It also highlights the need to develop therapies with greater activity against sessile communities to reduce the risk of future CDI and/or eradicate *C. difficile* from the biofilm. Lower recurrence rates of CDI are seen with fidaxomicin treatment when compared to vancomycin (Cornely *et al.*, 2012a), in which the higher activity against biofilms as well as the persistence of fidaxomicin on spores could be a factor (James *et al.*, 2017).

The success of FMT infusions has previously been rationalised as the re-establishment of colonisation resistance by introducing commensal microorganisms to restore the function and structure of the community (Khoruts and Sadowsky, 2016). A number of specific metabolic pathways have been shown to influence CDI and therefore determining the shifts in populations that are responsible for these pathways could expand our understanding of the functional profile of the microbiome. It is believed that the reduction in members of the indigenous bacterial community that are responsible for converting primary bile acids into secondary bile acids reduces the resistance to *C. difficile* colonisation and increases the risk for CDI (Winston and Theriot, 2016). The presence of secondary bile acids are essentially absent in patients with multiply recurrent CDI (Weingarden *et al.*, 2014). Treatment with *Clostridium scindens*, a bile acid 7 α -dehydroxylating bacterium, enhanced resistance to CDI in a mouse model in a secondary bile acid mediated manner (Buffie *et al.*, 2015). A correlation analysis looking at the burden of *C. difficile* relative to other species revealed a negative association with *C. scindens* (Daquigan *et al.*, 2017). Indeed, the restoration of the bile acid profile through the modulation of the microbiota has been demonstrated to play a key role in the effectiveness of FMT therapy (Mullish *et al.*, 2019).

Bacteroides thetaiotaomicron has been shown to act symbiotically with *C. difficile* and aids in its expansion by producing fermentation end-products succinate and sialic acid which *C. difficile* is able to exploit and metabolise to butyrate (Ng *et al.*, 2013, Ferreyra *et al.*, 2014). Levels of succinate are transiently elevated after antibiotic therapy, which *C. difficile* is able to utilize in order to proliferate (Ferreyra *et al.*, 2014). Genes relating to the succinate-butyrate pathway are present in the *C. difficile* spore proteome, indicating that these pathways are utilised soon after germination (Lawley *et al.*, 2009b). An understanding of the spatial organisation in the indigenous communities would also prove valuable in understanding functional aspects of the microbiota, as indicated by an increased prevalence of *Clostridium* spp. closely associated with the intestinal mucosa, with a role in colonocyte maintenance in mice (Lopetuso *et al.*, 2013). A study by Ott *et al.* (2017) examined the efficacy of sterile faecal filtrate transfers (FFT) to treat rCDI. Although only a small study involving five patients with multiply recurrent CDI, clinical cure was achieved in

100 % of cases. This raises the question of whether the underlying mechanisms of FMT involve microbial components, metabolites and bacteriophages rather than the live micro-organisms themselves. This highlights the need to study the structural and functional profile of the microbial community.

In this study, we successfully simulated a FMT using a clinically reflective gut model that facilitates the longitudinal analysis of planktonic and sessile populations, as well as the metabolic profiling of the communities. The ability of this model to clinically predict the outcome of a FMT could prove an invaluable tool in developing more targeted microbiome therapies. We also found that despite vancomycin reducing planktonic *C. difficile* populations below the limit of detection, *C. difficile* remained associated with the biofilm, potentially providing a reservoir for future infections. FMT treatment successfully prevented rCDI; however, the combined vancomycin and FMT treatment failed to eradicate *C. difficile* spores from the biofilm, demonstrating the potential of biofilms in the aetiology of rCDI.

Chapter 4 Increased dosing of targeted microbiome therapeutic SER-109 prevents rCDI in an *in vitro* model of the human gut.

4.1 Background

The success of FMT therapy has demonstrated the effectiveness of microbiome restoration in preventing rCDI (Kassam *et al.*, 2013, Cammarota *et al.*, 2014, Tariq *et al.*, 2018); however, safety concerns regarding long term implications, transmissible infections, non-standardised procedures, and patient reluctance has led to the development of more targeted microbiome therapies (DeFilipp *et al.*, 2019). The concept of microbiome restoration with a defined microbial consortium was initially proposed by Tvede and Rask-Madsen in 1989, when they used a mix of ten bacterial strains to successfully treat rCDI in six patients (Tvede and Rask-Madsen, 1989). Lawley *et al.* (2012) used a mouse model of CDI to successfully model the restoration of the mouse microbiota using a combination of six phylogenetically diverse intestinal bacteria. They were able to demonstrate that this targeted therapy could trigger major shifts in the microbial community structure and function, effectively displacing *C. difficile* and resolving disease. The Human Microbiome Project and the Metagenomics Project of the Human Intestinal Tract have provided new insights into the human microbiome and increased the understanding of the microbiota in health and disease. These projects have demonstrated that there is great diversity in the microbiome of healthy individuals (Lloyd-Price *et al.*, 2017) and as such dysbiosis is linked with functional changes in the microbiome.

Seres Therapeutics, a clinical biopharmaceutical company, specialises in the development of microbiome therapies. Using computational models to identify and characterise functional differences between healthy and dysbiotic microbiomes, Seres has developed investigational Ecobiotic® drugs targeted to restore the underlying ecology and function of a healthy microbiome. One of these products, SER-109, is a collection of bacterial spores purified from healthy human faeces, and is an investigational oral microbiome therapeutic for the prevention of rCDI. SER-109 is believed to prevent rCDI by replenishing

helpful bacteria in the gut. Initial Phase 1 clinical results were promising, with 86.7 % of patients meeting the primary efficacy end point, and 96.7 % of patients achieving clinical cure (Khanna *et al.*, 2016). In contrast, in the Phase 2 clinical trial, the relative risk of CDI recurrence for placebo compared with SER-109 recipients was not statistically significant. An in depth post-trial analysis indicated that suboptimal dosing and patient selection/CDI diagnosis issues could have impacted the measured clinical efficacy of this drug. It was found that Phase 1 subjects receiving a higher dose of SER-109 had significantly higher species richness in spore-forming bacteria when compared with subjects receiving a low dose, indicating the dose used in Phase 2 trials was insufficient. Here, we aim to determine whether increased doses of SER-109 are more efficacious in rCDI.

4.1.1 Rationale

After demonstrating the efficacy of an undefined microbial therapy (FMT) in our gut model, we evaluated the efficacy of different doses of SER-109 in our system. We used taxonomic analysis, bile acid analysis and identified microbial-microbial signalling mechanisms to understand the mechanism of action behind both SER-109 therapy failure and success to inform further clinical trials.

4.2 Methodology

4.2.1 Experimental design

In this study, two gut models used to simulate rCDI were run in parallel. One model was used to determine the efficacy of a single SER-109 dose and the other to determine the efficacy of a single SER-109 dose given over 3 consecutive days. The experiment was repeated to ensure reproducibility. Results are an average of the two models for each dose combined. The model timelines are depicted in Figure 4-1. As timescales ran slightly differently for each model run, days are approximate. The initial set up of the gut models was as described in section 2.2.8 and followed the experimental design in section 2.2.10. Briefly, during steady state, model planktonic populations were sampled every other day until challenge with *C. difficile* spores (spore preparation detailed in section 2.2.7) where populations were sampled daily thereafter (section 2.2.11). Results presented were from vessel 3 only. Once colonisation resistance was confirmed by the lack of *C. difficile* spore germination, another *C. difficile* spore dose was added before dosing the model with clindamycin. Active CDI was deemed present with evidence of *C. difficile* spore germination, vegetative cell proliferation and peak toxin levels detected; models were then dosed with vancomycin. Three days after vancomycin cessation, the models were dosed with SER-109, a single dose in one model, and 3 doses in the other (1 dose per day for 3 days). Preparation of the SER-109 spores is detailed in 4.2.2. Models were then left without further intervention for 30 days and monitored for evidence of rCDI. Planktonic samples were taken daily, centrifuged at 16 000g and the supernatant kept for third party bile acid analysis, cytotoxin testing and antimicrobial bioassays (sections 2.2.15, 2.2.16 and 2.2.17, respectively). Biofilms were sampled at designated time points (blue dots, Figure 4-1 and Table 4-1) according to section 2.2.12. Most of the biofilm rods were kept for sampling in the later stages of the model to study the effects of SER-109 dosing in sessile communities. DNA was extracted from biofilm samples and sent for third party 16S rRNA analysis (section 2.2.14). Biofilm sample supernatants were retained at -20°C for investigations into AI-2 mediated quorum sensing in biofilms.

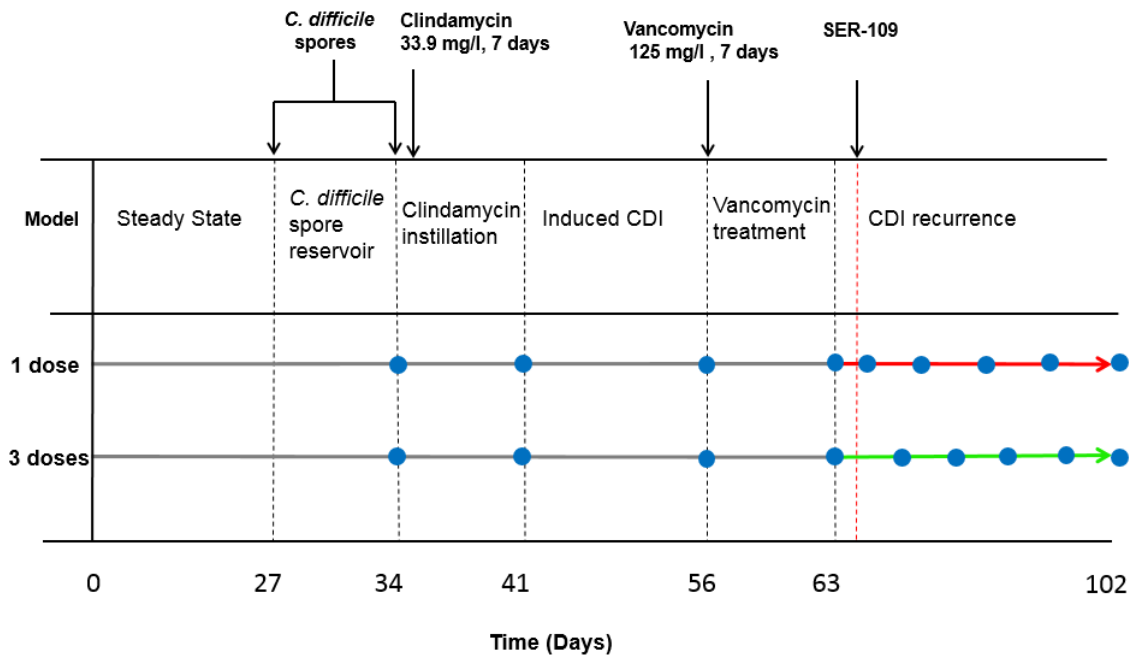


Figure 4-1 The *in vitro* gut model timeline for SER-109 dosing regimens.

The different stages of the model are indicated at the corresponding day in the timeline. Both models followed the same pregression (grey lines) up to the end of vancomycin treatment. SER-109 was added to the models 3 days after vancomycin cessation (red broken line). One model received 1 SER-109 dose (red arrow) and the other model received 1 dose of SER-109 daily, for 3 days (green arrow). Biofilm sampling time points are indicated by a blue circle.

Table 4-1 Biofilm sampling schedule of the SER-109 single and triple dose models.

Model stage	Day (approximate)		Number of rods per model
	1 dose	3 doses	
Pre-clindamycin	35	35	1
Post-clindamycin	42	42	1
Pre-vancomycin	57	57	1
Post-vancomycin	64	64	2
SER-109	67	67	2
End SER-109 + 7 days	74	77	2
End SER-109 + 14 days	81	84	3
End SER-109 + 21 days	88	91	3
End of experiment	95	98	3

4.2.2 Preparation of SER-109 spores.

SER-109 spores were prepared as instructed by Seres Therapeutics. Briefly, two aliquots of SER-109 (30 mL each) were received from Seres Therapeutics and stored at -80°C until ready to use. SER-109 aliquots were defrosted at room temperature, centrifuged to pellet the bacterial spores and the supernatant discarded. The spore pellet was washed with sterile PBS supplemented with 12 % glycerol before being aliquoted into 10 mL volumes and frozen at -80°C. When a dose was required, an aliquot was defrosted at room temperature and 10 mL added to the base of vessel one of each model.

4.2.3 Detection of quorum sensing Autoinducer-2 in biofilms

The presence of the quorum sensing molecule, autoinducer-2 (AI-2), was measured in biofilm supernatants from one set of models. Once the biofilm rod had been processed (2.2.12) and samples taken for DNA extraction (2.2.13), the biofilm supernatant was removed from the biofilm pellet and filter sterilised before being frozen at – 20°C until required for AI-2 detection. Aliquots were defrosted at room temperature prior to use.

4.2.3.1 Bacterial strains and growth conditions

The AI-2 bioassay was used to detect and quantify the presence of autoinducer-2 signalling molecules in biofilm samples. *Vibrio campbellii* strains BB-170 (ATCC BAA-1117) and BB-152 (ATCC BAA-1119), previously designated *Vibrio harveyi* (Bassler *et al.*, 1993, Thompson *et al.*, 2007) were grown on nutrient agar plates at 30°C aerobically. *V. campbellii* BB-152 was grown in Luria-Bertani (LB) broth (Lennox) overnight with agitation, followed by centrifugation at 16 000g for 15 min and filter sterilisation. The supernatant was maintained at -20°C for use as a positive control. Autoinducer bioassay (AB) medium was used for analysis during the AI-2 assay and was prepared according to Bassler *et al.* (1994). Briefly, medium was prepared in 1L volumes and contained 0.3M sodium chloride, 0.05 M magnesium sulphate and 0.2 % vitamin-free casamino acids, adjusted to pH 7.5 before sterilisation. After cooling, 10 mL of 1M potassium phosphate, 10 mL of 0.1M L-arginine, 20 mL glycerol, 1 mL of 10 µg/mL riboflavin and 1 mL of 1 mg/mL thiamine were added.

4.2.3.2 AI-2 assay

V. campbellii strain BB-170 *luxN::Tn5kan* AI-1 sensor negative AI-2 sensor positive reporter strain (Bassler *et al.*, 1993) was grown aerobically at 30°C on nutrient agar for 24 hours. The AI-2 assay was performed according to Lombardia *et al.* (2006) with the following variations. The overnight culture was scraped off the plate and resuspended in fresh AB medium and adjusted to an OD₆₀₀ of 0.5 and then further diluted 1:100 in AB medium. Filter sterilised sample cell-free supernatants, previously obtained and stored at -20°C from the gut models, were defrosted and added in triplicate to a white 96 microwell plate (93F Nunclon Delta), along with the reporter strain suspension to a final volume of 10 % (v/v). *V. campbellii* BB-152 was used as a positive control, with results recorded at the point of maximum bioluminescence from this positive control. PBS was used as a negative control and to determine the baseline bioluminescence. The cultures were shaken at 30°C in a thermoshaker (Grant-bio) and bioluminescence (Infinite Pro, Tecan) measured every hour, for 8 hours. Results were reported as relative light units (RLU) per gram of biofilm mass normalised using the value of bioluminescence from the negative control.

4.3 Results

4.3.1 Multiple changes to planktonic populations after antibiotic treatment.

Antibiotic treatment with both clindamycin and vancomycin resulted in considerable changes to the planktonic populations (Figure 4-2 and Figure 4-3). Peak levels of clindamycin and vancomycin were 68.8 mg/L and 234.9 mg/L in vessel one, respectively. Clindamycin instillation resulted in the successful induction of CDI, with a divergence of 2.2 – 3.5 log₁₀ CFU/mL between TVCs and spore counts, accompanied with peak *C. difficile* cytotoxin levels reaching between 2 – 3 RU. Reductions *B. fragilis* gp., *Clostridium* spp., *Bifidobacterium* spp., and total spores were seen with both antibiotics, consistent with findings from models in Chapter 3, with vancomycin causing the most dramatic effect (Figure 4-2). Additionally, *Enterococcus* spp. counts reduced after vancomycin treatment (Figure 4-3). In contrast to our previous models, *Bifidobacterium* spp., began to recover immediately before vancomycin dosing; however, these populations dropped to below the limit of detection soon after vancomycin commencement. *Lactobacillus* populations increased during vancomycin treatment and remained high for the duration of the experiment, most likely due to the innate resistance of this species to vancomycin. *C. difficile* levels and consequently toxin levels decreased to below the limit of detection during vancomycin instillation.

4.3.2 Only three doses of SER-109 successfully prevented rCDI.

All models followed the same timeline up to the end of vancomycin treatment. Three days after vancomycin cessation, the models were dosed with either a single dose of a SER-109 spore preparation or with a single dose for three consecutive days (vancomycin levels in vessel one of 4.97 to 5.86 mg/L at the time of dosing, respectively). In models with a single SER-109 dose, total spores and *Clostridium* spp., populations increased modestly, with populations fluctuating between 3.5 - 5 log₁₀ CFU/mL and 3 - 4.5 log₁₀ CFU/mL, respectively, and *B. fragilis* gp., populations increasing to approximately 7 log₁₀ CFU/mL 10 days post-SER-109 dosing. *Bifidobacterium* spp., failed to recover for the duration of the experiment (Figure 4-2 a). 10 days after vancomycin

cessation, evidence of *C. difficile* spore germination was seen, with a difference in TVC and spore populations of 3 log₁₀ CFU/mL, accompanied with the detection of *C. difficile* cytotoxin at 3 RU, confirming a relapse in CDI with a single dose of SER-109 (Figure 4-4 a). In models with SER-109 dosed on three consecutive days, *B. fragilis* gp., populations increased to pre-antibiotic levels of between 7 – 8 log₁₀ CFU/mL 4 days after the last SER-109 dose. *Clostridium* spp. and total spore populations increased 2 days after the last dose, with levels of *Clostridium* spp. exceeding those seen in the single SER-109 dose model by 1 log₁₀ CFU/mL. Spore populations in this model decreased by approximately 2 log₁₀ CFU/mL 3 days after the last SER-109 dose, recovering soon after. This was in line with increased *Clostridium* spp. recoveries and could potentially indicate increased germination in this model. *Bifidobacterium* spp., populations did not recover for the duration of these models (Figure 4-2 b). *C. difficile* levels dropped below the limit of detection during vancomycin treatment, and although sporadic detection, *C. difficile* failed to colonise the planktonic phase and rCDI was prevented (Figure 4-4 b).

4.3.3 Increased exposure to cholic acid corresponds with rCDI

As in our previous rCDI and FMT models, levels of bile acids CA, DCA and oxo-BA were analysed at different time points in the planktonic phase. During steady state, low levels of CA were seen, accompanied by increased DCA levels. Exposure to clindamycin resulted in an increase in the pro-germinant CA and the decrease in DCA levels, indicating a decrease in microbiome mediated 7 α - dehydroxylation bile acid metabolism. In line with microbiome recovery, the CA levels reduced and the DCA levels increased accordingly until vancomycin dosing where a similar trend was seen. In the single dose model (Figure 4-5 a), higher levels of CA were seen for a prolonged period of time when compared with levels in the triple dosed model (Figure 4-5 b), and this correlated with rCDI. In the triple dosed model, CA levels reduced rapidly with an increase in DCA and oxo-BA levels, and this correlated with the absence of rCDI in this model.

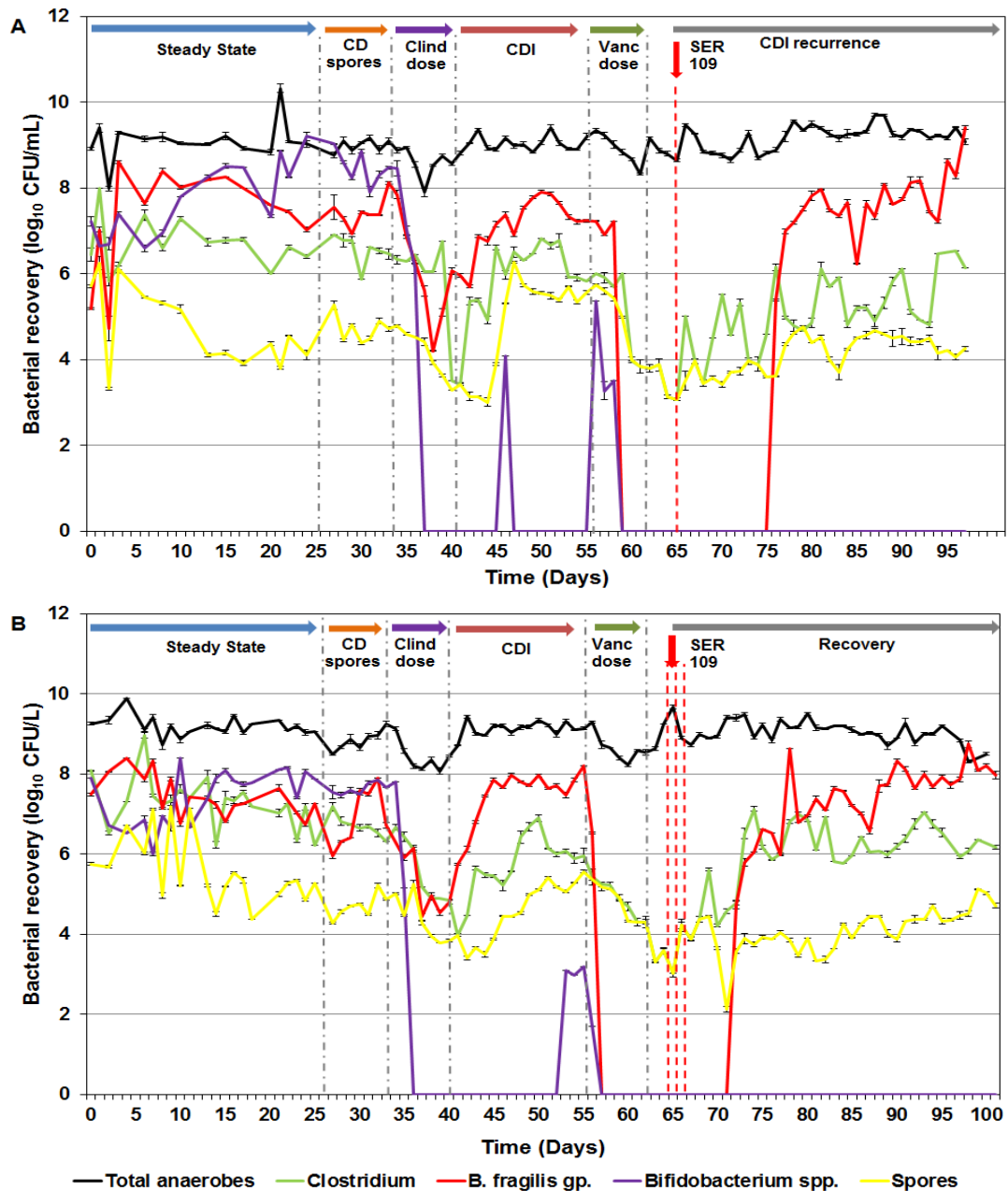


Figure 4-2 Enumeration of planktonic anaerobes in (a) the single SER-109 dose model and (b) the triple SER-109 dose model. Bacterial enumeration of total anaerobes (black), *B. fragilis* gp. (red), *Clostridium* spp. (green), *Bifidobacterium* spp. (purple), and spores (yellow). Data demonstrates the disruption to the microflora during clindamycin and vancomycin therapy and a more rapid recovery in the triple SER-109 dosed model. Data shown are the mean \log_{10} CFU/mL \pm standard error from three technical replicates per day of the model timeline of two biological replicates. Different model stages are separated by vertical broken lines (grey; SER-109 instillation - red). Clind – clindamycin, Vanc – vancomycin, FMT – faecal microbiota transplantation, CDI – *C. difficile* infection.

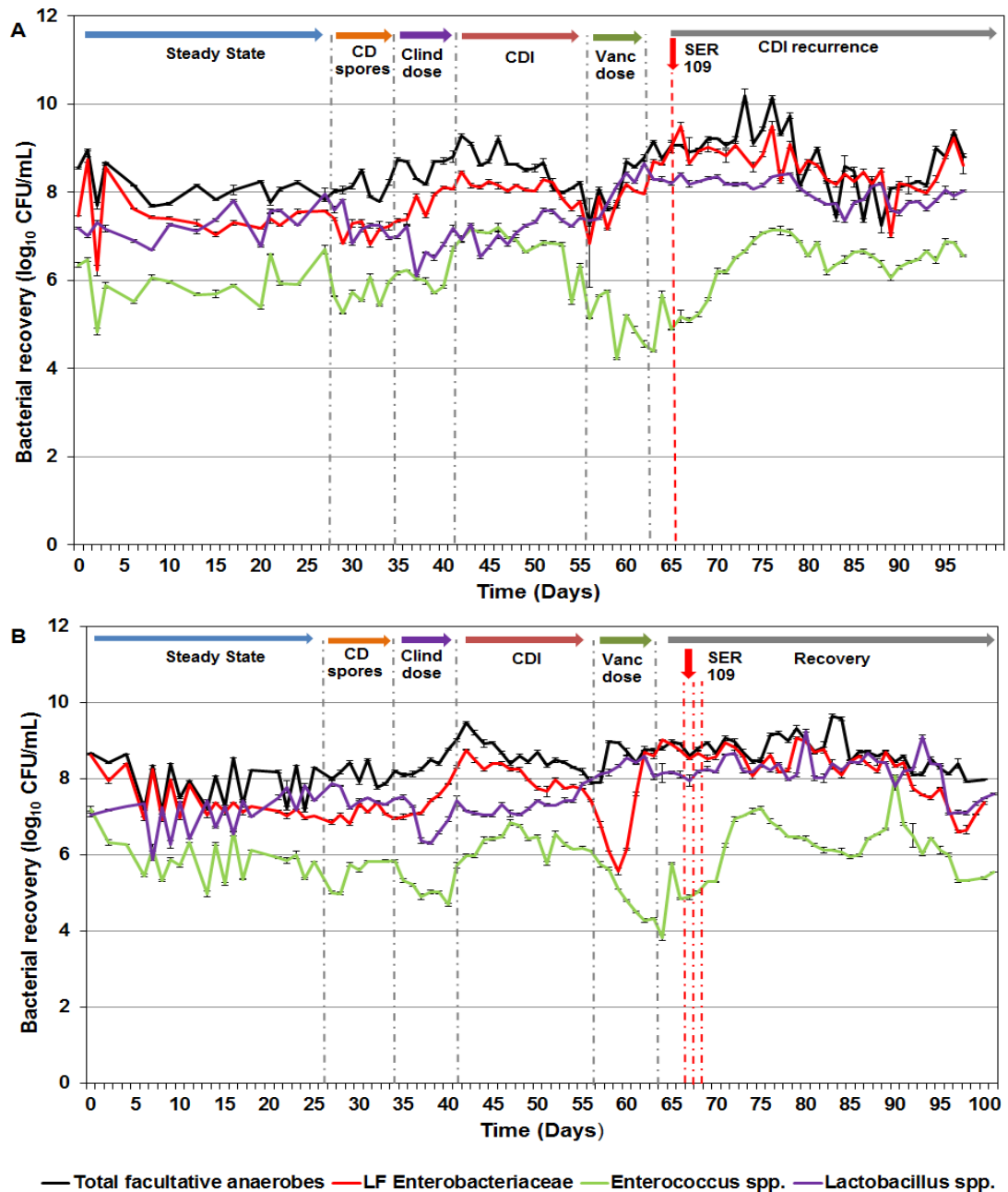


Figure 4-3 Enumeration of planktonic facultative anaerobes in (a) the single SER-109 dose model and (b) the triple SER-109 dose model. Bacterial enumeration of total facultative anaerobes (black), lactose fermenting (LF) Enterobacteriaceae (red), *Enterococcus* spp. (green), and *Lactobacillus* spp. (purple). Data demonstrates an increase in facultative anaerobes following clindamycin and vancomycin therapy. Data shown are the mean \log_{10} CFU/mL \pm standard error from three technical replicates per day of the model timeline of two biological replicates. Different model stages are separated by vertical broken lines (grey; SER-109 instillation - red). Clind – clindamycin, Vanc – vancomycin, FMT – faecal microbiota transplantation, CDI – *C. difficile* infection.

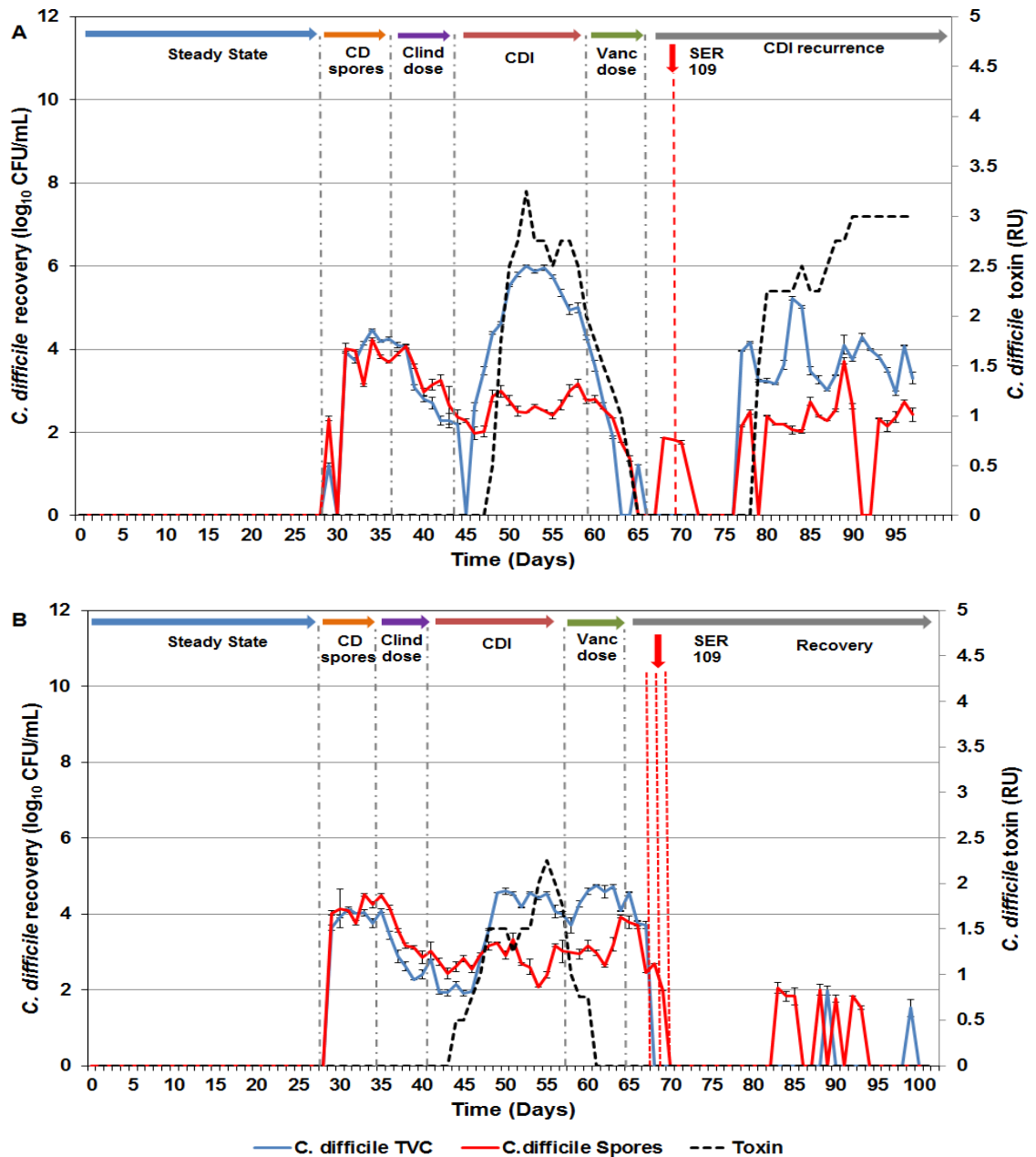


Figure 4-4 Enumeration of planktonic *C. difficile* total and spore counts in (a) the single SER-109 dose model and (b) the triple SER-109 dose model. Enumerations of *C. difficile* spores (red) and total viable counts (blue) are represented for both models in mean log₁₀ CFU/mL ± standard error (left axis). *C. difficile* toxin (black broken line) is represented as log reciprocal units (RU, right axis). Evidence of *C. difficile* recurrence was seen in the single SER-109 dose model but absent in the triple SER-109 dosed model. Data shown are from three technical replicates per day of the model timeline from two biological replicates. Different model stages are separated by vertical broken lines (grey; SER-109 instillation - red). Clind – clindamycin, Vanc – vancomycin, FMT – faecal microbiota transplantation, CDI – *C. difficile* infection.

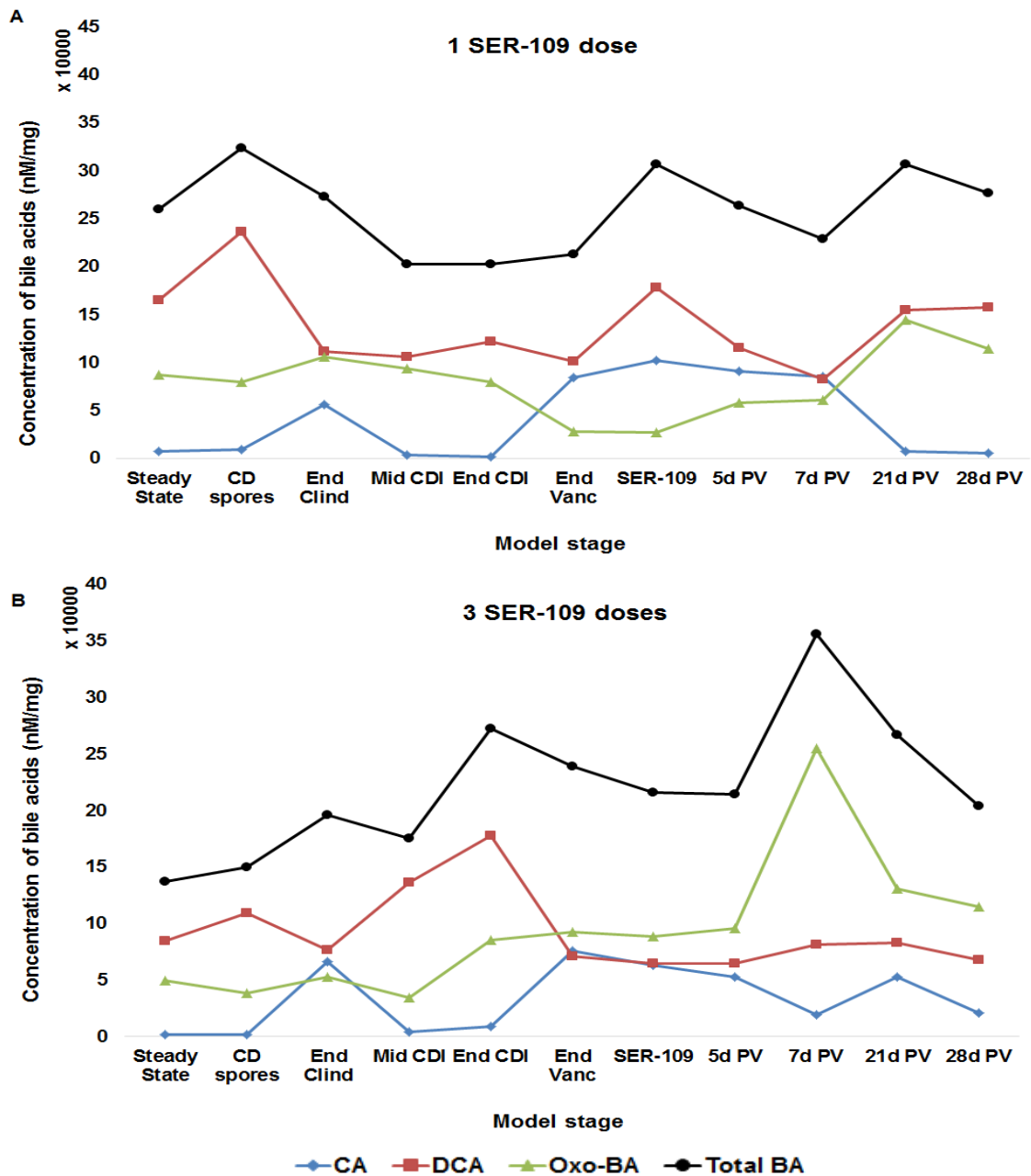


Figure 4-5 Bile acid analysis of the (a) 1 SER-109 dose model and (b) 3 SER-109 doses model. The concentration of cholic acid (CA; blue, diamond), deoxycholic acid (DCA; red, square) and oxo-bile acids (oxo-BAs; green, triangle) were measured in nM/mg at selected time points during the model timeline. Total bile acids (black, circle) represent the sum of CA, DCA and Oxo-Bas. Prolonged elevated levels of CA were seen after a single sER-109 dose; whereas, increased oxo-BAs were seen after a triple SER-109 dose. Data are single samples from one biological replicate. CD – *C. difficile*, Clind – clindamycin, Vanc – vancomycin, d – days, PV – post-vancomycin

4.3.4 Biofilm population diversity increased after multiple SER-109 doses

Clindamycin dosing resulted in decreases of 2 – 3 log₁₀ CFU/g in *Clostridium* spp. and a decrease of approximately 8 log₁₀ CFU/g in *Bifidobacterium* spp., dropping below the limit of detection (Figure 4-6). This was accompanied with approximately 1 log₁₀ CFU/g increases in total facultative anaerobes, LF Enterobacteriaceae and *Lactobacillus* spp. (Figure 4-7). In contrast to previous models, there was an increase of approximately 1 log₁₀ CFU/g in the *B. fragilis* gp. *C. difficile* was recovered from the biofilm at 5 – 6 log₁₀ CFU/g and was unaffected by clindamycin dosing (Figure 4-8). During CDI, total facultative anaerobes dropped back to pre-clindamycin levels and spores, *Clostridium* spp. and *Bifidobacterium* spp. numbers increased by approximately 0.5 – 1 log₁₀ CFU/g, 1 – 2 log₁₀ CFU/g and 2 – 4 log₁₀ CFU/g, respectively.

Vancomycin instillation had a more dramatic effect on the sessile populations, with *Clostridium* spp. reducing by 1 – 2 log₁₀ CFU/g and *B. fragilis* gp. and *Bifidobacterium* spp. dropping below the limit of detection (Figure 4-6).

A week after SER-109 dosing in the single dose model, *B. fragilis* gp. was isolated at 4.1 log₁₀ CFU/g and enterococci increased from 6.4 – 8.1 log₁₀ CFU/g. *Bifidobacterium* spp. began recovering 14 days after the SER-109 dose and maintained levels of between 3.8 – 4 log₁₀ CFU/g for the duration of the experiment. *B. fragilis* gp. increased 8.3 log₁₀ CFU/g and maintained similar levels for the duration of the model run (Figure 4-6 a and Figure 4-7 b). In the triple SER-109 dosed model, *B. fragilis* gp. was isolated at 7 log₁₀ CFU/g 7 days after the last dose, which was approximately 3 log₁₀ CFU/g higher than the single dose model. *Enterococcus* spp. increased from 6 – 7.6 log₁₀ CFU/g and this level remained stable for the duration of the experiment.

Bifidobacterium spp. failed to recover in this model and remained below the limit of detection for the duration of experiment (Figure 4-6 b and Figure 4-7 b). Throughout both models, *C. difficile* was consistently isolated at approximately 4 log₁₀ CFU/g (Figure 4-8).

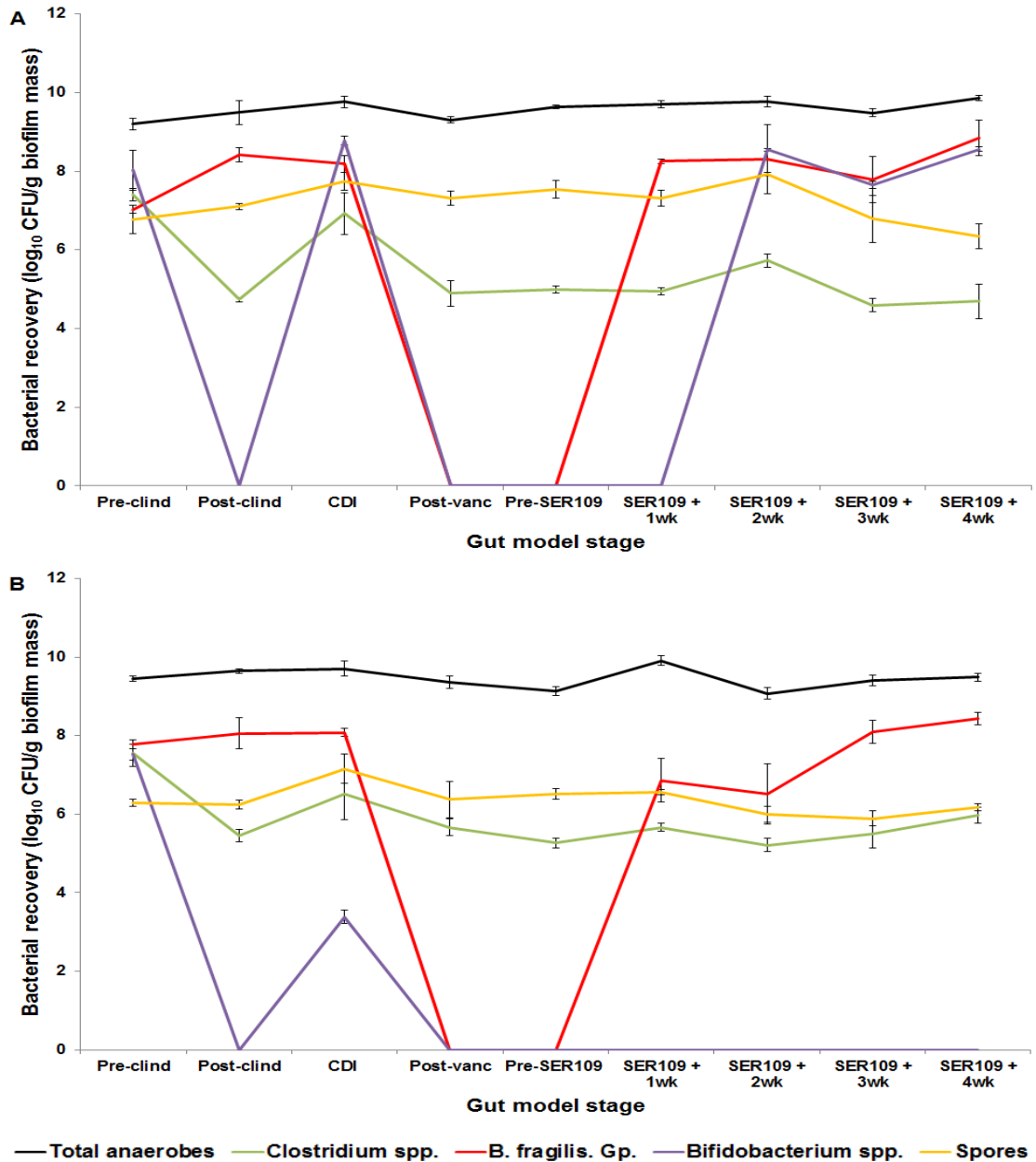


Figure 4-6 Enumeration of biofilm anaerobes in (a) the single dose SER-109 model and (b) the triple dosed SER-109 model. Bacterial enumeration of total anaerobes (black), *B. fragilis* gp. (red), *Clostridium* spp. (green), *Bifidobacterium* spp. (purple), and spores (yellow) from the biofilm recovered from the biofilm support structures of the gut models. Data demonstrates the disruption to the biofilm populations during clindamycin and vancomycin therapy. Data shown are the mean \log_{10} CFU/g biofilm mass \pm standard error from three technical replicates of two biological replicates. Clind – clindamycin, Vanc – vancomycin, FMT – faecal microbiota transplantation, CDI – *C. difficile* infection, wk – weeks

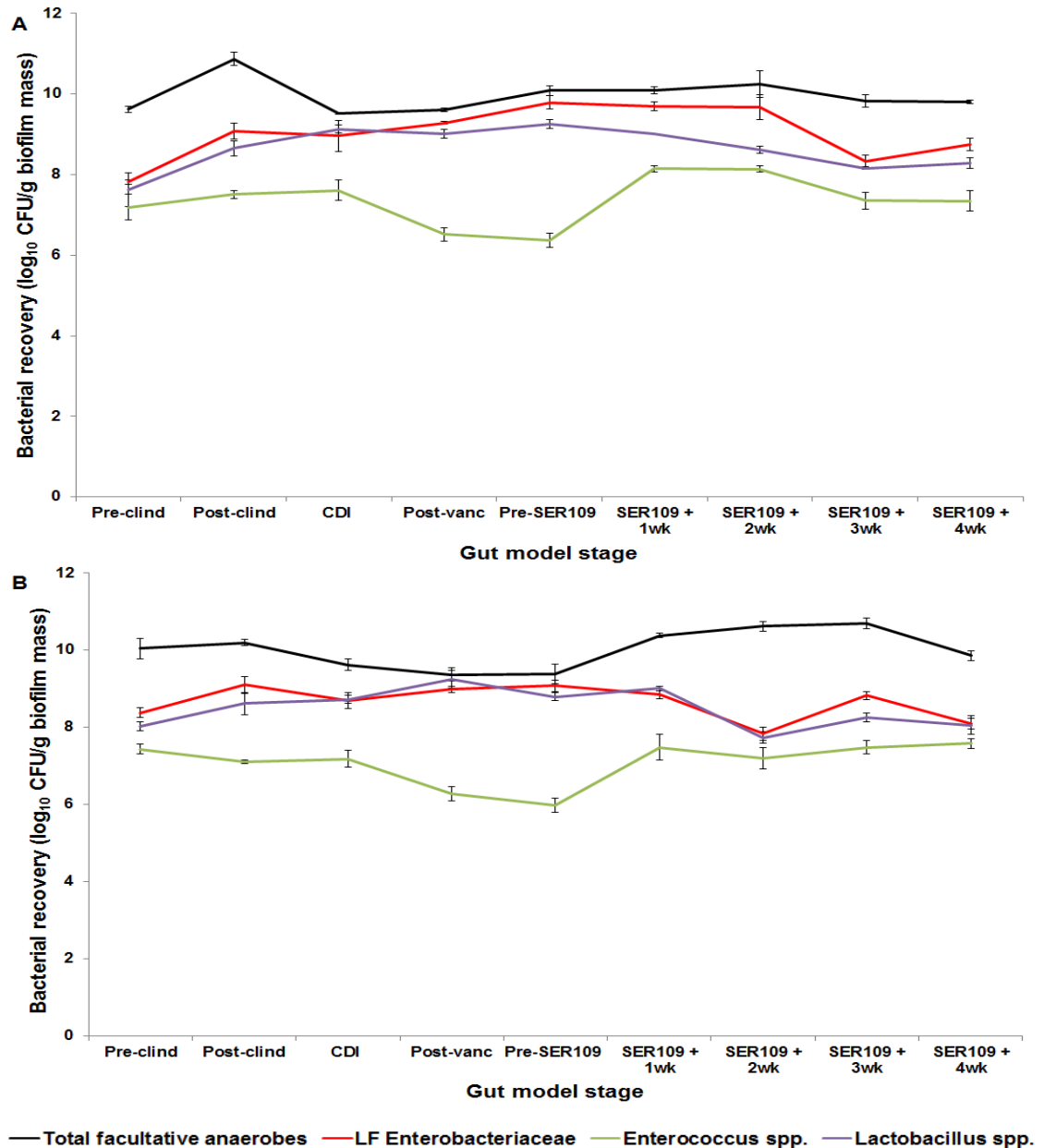


Figure 4-7 Enumeration of biofilm facultative anaerobes in (a) the single dose SER-109 model (b) the triple dosed SER-109 model. Bacterial enumeration of total facultative anaerobes (black), lactose fermenting (LF) Enterobacteriaceae (red), *Enterococcus* spp. (green), *Lactobacillus* spp. (purple), and fungi (yellow) from the biofilm recovered from biofilm support structures of the gut models. The facultative anaerobic populations of the biofilm remained stable through antimicrobial therapy. Data shown are the mean \log_{10} CFU/g biofilm mass \pm standard error from three technical replicates of two biological replicates. Clind – clindamycin, Vanc – vancomycin, FMT – faecal microbiota transplantation, CDI – *C. difficile* infection, wk – weeks.

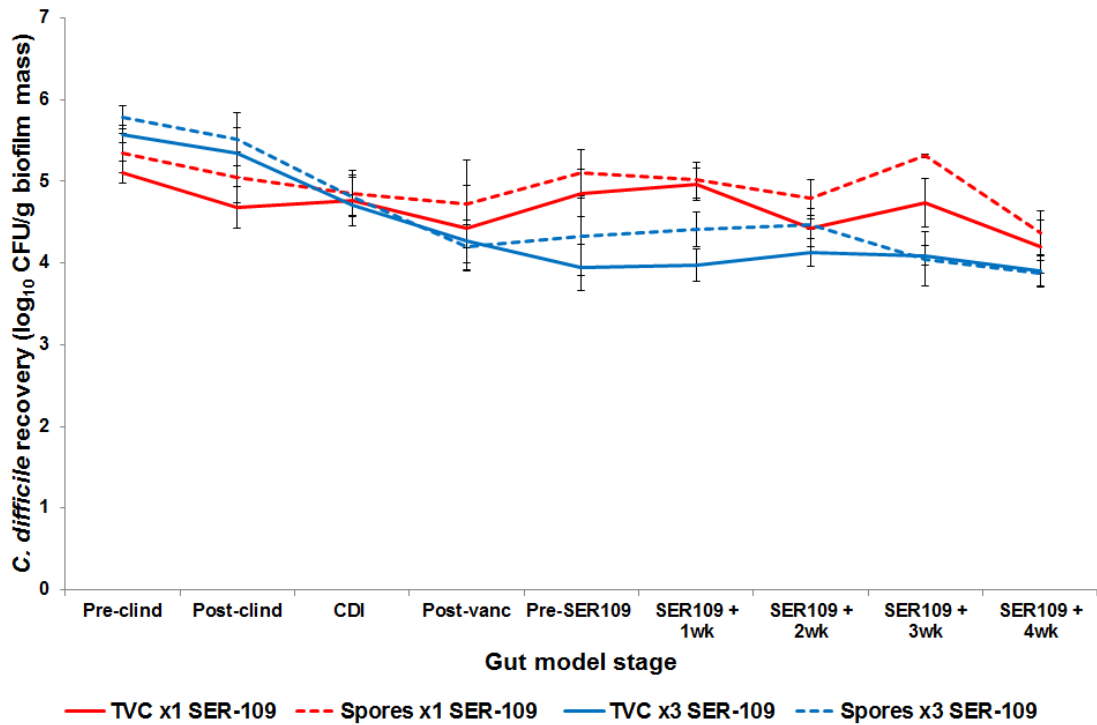


Figure 4-8 Enumeration of *C. difficile* total and spore counts recovered from the biofilm in the SER-109 gut models. Bacterial enumeration of the total viable counts (TVC - solid line) and spore counts (broken line) of *C. difficile* for the single SER-109 dosed model (red) and the triple dosed SER-109 model (blue) from biofilm recovered from biofilm support structures. Data demonstrates the persistence of *C. difficile* cells in the biofilm through antimicrobial and SER-109 therapy. Data shown are the mean log₁₀ CFU/g biofilm mass \pm standard error from three technical replicates of two biological replicates, at various stages throughout the model timeline. Clind – clindamycin, Vanc – vancomycin, TVC – total viable counts, CDI – *C. difficile* infection, wk – weeks.

Taxonomic analysis of the biofilm populations revealed an abundance of Enterobacteriaceae of 26.8 % before SER-109 dosing which reduced 7 days after dosing to 21.1 % and 7.1 % in the single dose model and the triple dose model, respectively. After 28 days however, Enterobacteriaceae comprised 20.6 % abundance in the single dose model and 8.7 % in the triple dose model. Bacteroidaceae increased from 0.5 % to 1.5 % in the single dose model and 10 % in the triple dose model after 28 days. Lactobacillaceae decreased from pre-dose levels of 16.4 % to 6.3 % and 2.5 % in the single and triple dosed model, respectively. Bifidobacteriaceae at pre-dose levels of 3.3 % increased to 6.7 % after 7 days and 25.9 % after 28 days in the single dose model. This population did not increase in abundance in the triple dose model. Methanobacteriaceae abundance remained steady in the single dose model, but increased from 3.4 % to 13.4 % in the triple dosed model. The family Porphyromonadaceae increased from 0.02 % pre-dose to 6.1 % at 28 days in the triple dose model. This population remained at 0.1 % in the single dose model (Figure 4-9). Overall at 28 day post-dosing, the triple dosed model displayed a greater variation in different bacterial families, indicating increased diversity in population abundance. The predominant phyla abundance of the single dose model was 28.8 % Proteobacteria, 30.8 % Firmicutes and 25.9 % Actinobacteria whereas the triple dose model was comprised of 11.7 % Proteobacteria, 33.6 % Firmicutes and 16.1 % Bacteroidales. Analysis of the microbiota diversity, using the Shannon diversity index, showed the greatest increase in diversity from the triple dosed SER-109 model. Pre-SER-109, the diversity index was 1.72 ± 0.51 which increased to 2.31 ± 0.26 and 2.49 ± 0.42 , for weeks three and four, respectively. In the single dose SER-109 model, an initial increase in diversity from 1.55 ± 0.10 to 1.84 ± 0.14 was seen at two weeks post-SER-109, increasing to 1.89 ± 0.36 at the end of the experiment. The reduced diversity in the single dose model, when compared to the triple dose model, was associated with the recurrence of CDI (Figure 4-10).

4.3.5 Evidence of AI-2 mediated quorum sensing in biofilms

The presence of the quorum sensing AI-2 was determined using the reporter organism *V. campbellii* in the AI-2 bioluminescence assay. The increase in bioluminescence of *V. campbellii* was proportional to the amount of AI-2 present and therefore could be quantified in biofilm samples at selected times.

Biofilms from both models were positive for AI-2 production. Clindamycin exposure resulted in a dramatic decrease of approximately 2 log₁₀ RLU in AI-2 detection during disruption to the biofilm. In line with post-antibiotic recovery of the biofilm, increased AI-2 was seen with levels similar to pre-antibiotic exposure. A similar trend was seen after vancomycin dosing; however, the AI-2 detection did not reduce to the same degree as seen in clindamycin. AI-2 levels increased at SER-109 dosing in both models and remained stable for the duration of the experiment with the exception of a transient 1.5 and 1 log₁₀ RLU drop in AI-2 levels (single SER-109 dose and triple SER-109 dose, respectively) two weeks post SER-109 dosing (Figure 4-11).

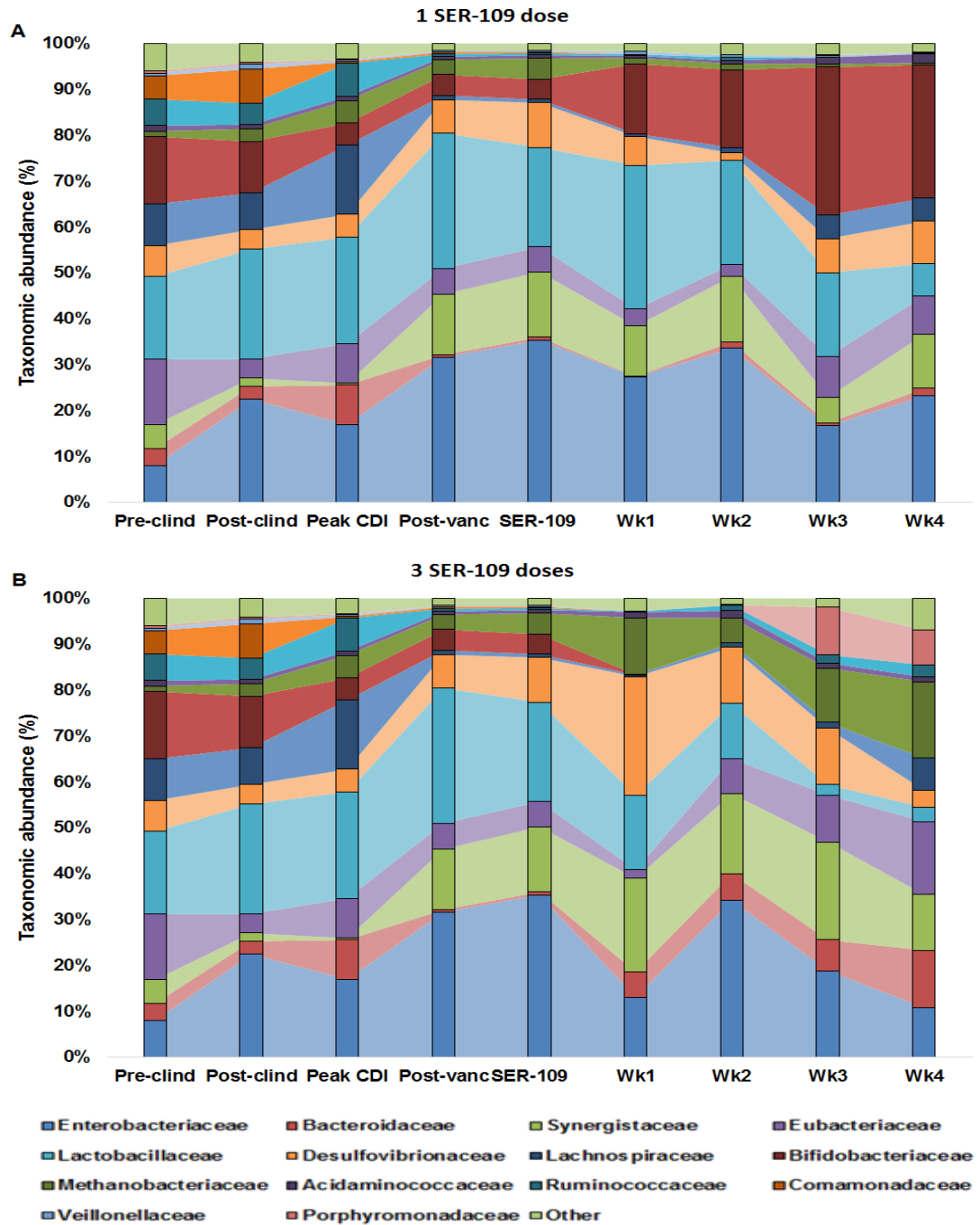


Figure 4-9 Changes in bacterial taxonomic abundance of the biofilm microbial community at selected time points in the (a) single dose SER-109 model and (b) the triple dosed SER-109 model. Taxonomic abundance (percentage) of the top 14 bacterial families recovered from biofilm support structures in the triple stage gut models. Graphs constructed using the mean (of least 3 support structures) percent abundance of bacterial OTUs assigned to a family taxonomic level for two biological replicates. Clind – clindamycin, Vanc – vancomycin, CDI – *C. difficile* infection, wk - week.

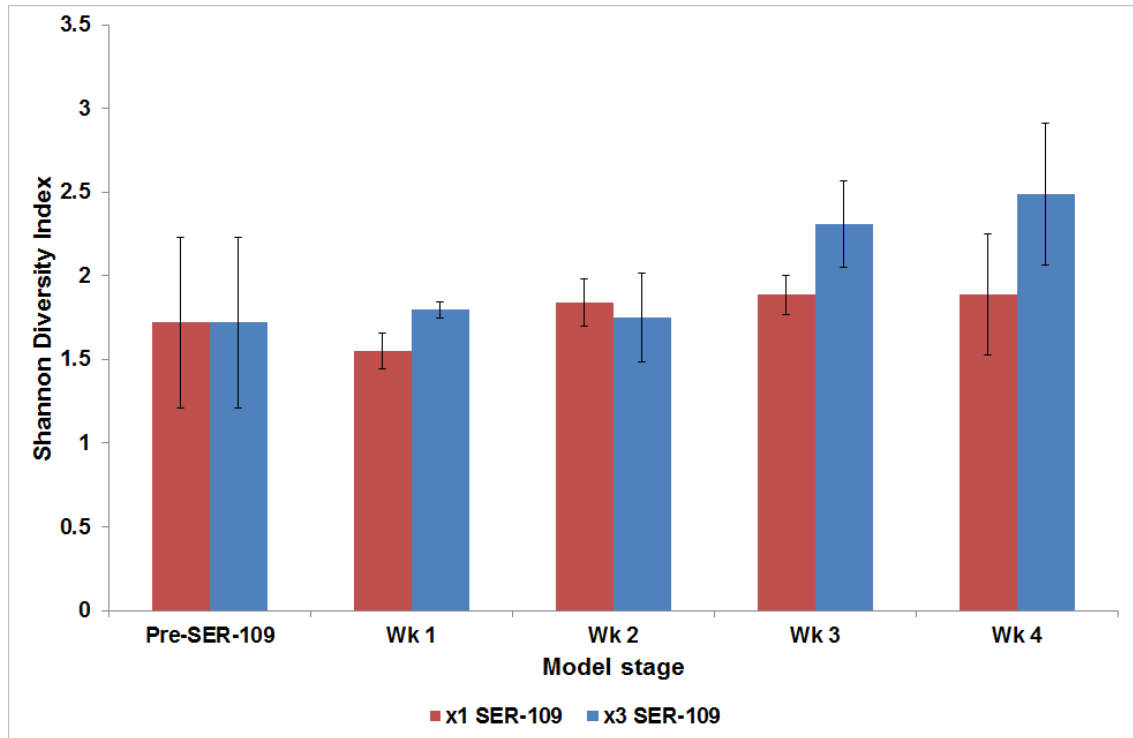


Figure 4-10 Shannon Diversity Index of biofilm samples from the SER-109 triple stage gut models. The Shannon (alpha) diversity of the biofilm populations was measured immediately before SER-109 dosing (x1 dose, red; x3 doses, blue) and weekly thereafter, for four weeks. The model that received three consecutive SER-109 demonstrated increased microbial diversity in the last two weeks of the experiment. The Shannon Diversity Index was calculated using bacterial OTUs assigned to a family taxonomic level using mean data from at least 3 support structures for each time point, for two biological replicates. Error bars indicate standard deviation., vanc – vancomycin, wk - week.

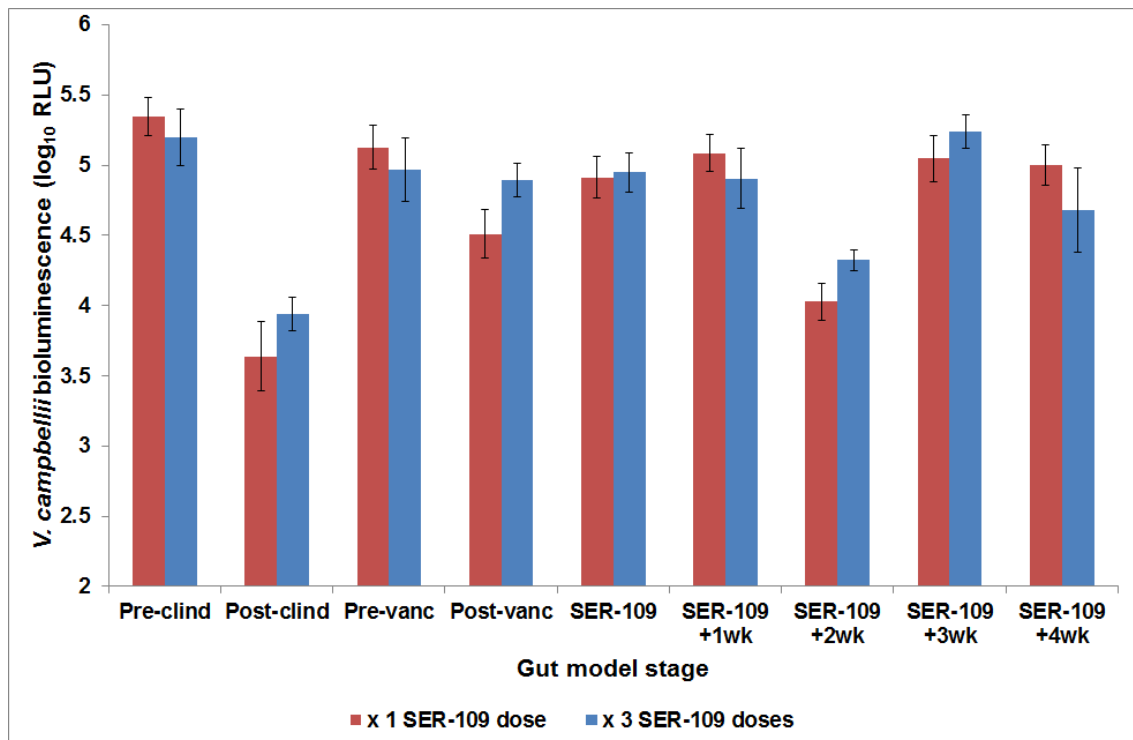


Figure 4-11 *Vibrio campbellii* bioluminescence in response to the presence of Autoinducer-2 molecules in biofilms isolated from gut models dosed with SER-109. *V. campbellii* bioluminescence was measured using the Autoinducer-2 assay in response to the presence of AI-2 quorum sensing molecules (represented as log₁₀ relative light units – RLU ± standard error) in the biofilms from gut models receiving a single dose of SER-109 (red) and a triple dose of SER-109 (blue). A drop in bioluminescence was detected after clindamycin instillation which coincided with disruption to the biofilm, and again two weeks after SER-109 instillation. Data represents three technical replicates from one biological replicate.

4.4 Discussion

The models used in this experiment were designed to determine the efficacy of different SER-109 dosing regimens to prevent simulated rCDI. Pleiotropic changes to the microbiota during clindamycin treatment induced CDI and vancomycin treatment caused further disruption to the microbiota, similar to findings in the previous models. Clindamycin instillation was characterised by reductions in *Clostridium* spp., *Bifidobacterium* spp., and *B. fragilis* gp., which created a niche for *C. difficile* colonisation leading to active CDI with vegetative cell outgrowth and subsequent toxin production. It should be noted that the extent of clindamycin-induced CDI differed between the two treatment models, with total *C. difficile* counts reaching approximately $6 \log_{10}$ CFU/mL the single SER-109 dose model; whereas in the triple dose model, these levels peaked at $4.5 \log_{10}$ CFU/mL. This was reflected in a higher toxin titre of 3.5 RU in the single dose model and 2 RU in the triple dose model. It is unknown whether this had any impact on the outcome of the study.

Although vancomycin instillation resulted in the reduction of planktonic *C. difficile* levels, further and more exaggerated dysbiosis to the microbiota was seen, including increases in facultative anaerobic populations and LF Enterobacteriaceae. Bile acid analysis indicated an increase in the primary bile acid CA during antibiotic treatment, accompanied by a reduction in the secondary bile acid DCA, indicating a reduction of secondary bile acid metabolism using CA as a substrate during antibiotic instillation, consistent with antibiotic-induced metabolic shifts in mouse models (Theriot *et al.*, 2014). CA has been shown to be a pro-germinant to *C. difficile* spores whilst the presence of DCA was inhibitory to *C. difficile* vegetative growth (Sorg and Sonenshein, 2008). The CA/DCA balance was restored in line with recovery of the microbiome. Sessile populations were not affected by antibiotic instillation to the same degree and any antibiotic-mediated effect was delayed in comparison with planktonic populations. The presence of biofilm-associated *C. difficile* cells were unaffected by antibiotic instillation, potentially providing a reservoir for disease recurrence should they encounter a susceptible environment.

During Phase 1 clinical trials, the use of the microbiome therapeutic SER-109 has previously been shown to be effective at preventing rCDI (Khanna *et al.*,

2016), with 86.7 % of patients meeting the primary efficacy end point and 96.7 % achieving clinical resolution. This clinical success was not repeated in Phase 2 trials, with the study not achieving the end point of reducing the relative risk of recurrence for up to 8 weeks when compared with placebo (Ratner, 2016). During an in-depth Phase 2 trial analysis, it was determined that misdiagnosis of CDI, caused by using stand-alone PCR testing, and suboptimal dosing of SER-109 when compared to Phase 1 trials could explain these findings (Press release, Seres Therapeutics, 2017).

In this experiment, we tested the efficacy of two different dosing regimens of SER-109 to prevent rCDI. In our models, treatment with the two different doses of SER-109 was associated with distinct changes to the microbial population recoveries. A single dose of SER-109 was associated with unstable, fluctuating *Clostridium* spp. recoveries and the recovery of *B. fragilis* gp. approximately 10 days after dosing. In the triple dose models, *Clostridium* spp. recovered rapidly, with populations stabilising approximately 1 log₁₀ CFU/ml higher than the single dose models. *B. fragilis* gp. also recovered roughly 4 days earlier in the triple dose models. A drop in spore populations in the triple dose model, accompanied by the subsequent increase in *Clostridium* spp. could potentially indicate enhanced germination with increased dosing of SER-109.

Bile acid analysis indicated an increased and prolonged exposure to the primary bile acid CA in the single dose models, accompanied with a decrease in the secondary bile acid DCA and oxo-BA. This suggests a drop in microbiome mediated bile acid metabolism in these models. These results reflected findings in our previous model of rCDI and correlated with the relapse of CDI. In the triple SER-109 dosed models, CA levels rapidly declined after SER-109 dosing, with increases in DCA and oxo-BA levels. These results reflect findings in our FMT model, with both sets of models successfully preventing rCDI. As CA is a pro-germinant for *C. difficile* spores (Sorg and Sonenshein, 2008), it was not surprising that increased levels were associated with rCDI. Indeed, it was found that after FMT therapy, bile acid profiles closely resembled that of donors, indicating the efficacy of FMT was closely related to bile acid metabolism (Weingarden *et al.*, 2014). Our results demonstrate a similar trend in bile acid profiles comparing the triple dose SER-109 and the FMT models, indicating a similar restoration of bile acid metabolism. These

results are consistent with findings of targeted reconstruction of the microbiome leading to increased resistance to rCDI in mouse models in a secondary bile acid dependent manner (Buffie *et al.*, 2015). These results contributed to the progression to Phase 3 clinical trials despite the setback from the Phase 2 trial results (ClinicalTrials.gov Identifier: NCT03183128).

Enumeration of the sessile communities demonstrated only minor changes after SER-109 dosing. One of the main differences between the two model sets was the recovery of *B. fragilis* gp. which recovered more rapidly, and to a higher degree in the triple versus single dose model. 16S rRNA sequencing of these populations revealed an increased abundance of Enterobacteriaceae after antibiotic treatment. A single dose of SER-109 transiently reduced levels of Enterobacteriaceae; however, at the end of the experiment, these levels increased again to levels seen with antibiotic treatment, and reflected those seen in a dysbiotic microbiome (Shin *et al.*, 2015). With a triple dose of SER-109, levels of Enterobacteriaceae abundance decreased from post-antibiotic abundance of 26.8 % to 8.7 %. This was accompanied by the general increase in relative abundances of the top 13 bacterial families, indicating a greater diversity in sessile populations at the end of the experiment with multiple doses of SER-109. The difference in the sessile bacterial abundances 28 days after SER-109 treatment in the triple dosed models indicates increased diversification of the commensal bacteria. Increases in family abundance was not limited to sporulating bacteria that potentially originated in the SER-109 spore preparation, indicating both engraftment and possible augmentation of commensals present, mediated by the increased SER-109 dose, consistent with Khanna *et al.* (2016). Despite the triple dose of SER-109 successfully preventing rCDI, both SER-109 dosing regimens failed to displace *C. difficile* cells from the biofilm. This was consistent with findings with the vancomycin-only treatment arm and the FMT models. This population of *C. difficile* cells that remain associated with the biofilm, despite vancomycin treatment and microbiome restoration therapies, raises the possibility of risk of rCDI with future antibiotic therapy. Transient *C. difficile* detection in the planktonic phase leads to speculation that they arise from the biofilm and that the biofilm acts as a *C. difficile* reservoir, seeding the planktonic phase with *C. difficile* cells. Potentially,

if the environment is susceptible as in the case of the vancomycin-only treatment arm and the single dose SER-109, relapse may occur.

I have previously demonstrated the potential role of biofilms in rCDI using *in vitro* models. Given the potential of biofilms in rCDI, I set out to further examine interactions of *C. difficile* with other commensals in the biofilm by determining if AI-2 quorum sensing could be demonstrated in the multispecies biofilms within the gut models. AI-2 mediated quorum sensing represents a key mechanism that regulates social activities in mixed microbial populations (Li and Tian, 2012). Detected in a diverse range of both Gram positive and Gram negative species, it represents a means to allow inter-species communication and social interactions (Bassler *et al.*, 1993, Bassler *et al.*, 1994, Bassler *et al.*, 1997). Using the *V. campbellii* reporter bioluminescence assay, I was able to demonstrate the presence of the AI-2 signalling molecules within the biofilm at various time points of the models. I was also able to show that the levels of AI-2 detected altered during antibiotic treatment, with levels decreasing in line with reductions in bacterial numbers in the biofilm due to antibiotic therapy. During microbiome restoration, detection of AI-2 molecules increased with the reconstruction of the multispecies biofilm, demonstrating social interaction and community dynamics in biofilms in this *in vitro* model. The AI-2 signalling system has been found in *C. difficile* (Carter *et al.*, 2005) and mutation experiments of the *luxS* gene in *C. difficile* revealed a disruption to biofilm formation in *C. difficile* and altered interactions with other commensals (Đapa *et al.*, 2013, Slater *et al.*, 2019), suggesting this could be an important signalling system in *C. difficile* biofilm dynamics.

One of the greatest defense mechanisms against pathogen establishment is through colonisation resistance mediated by a healthy microbiome. This colonisation resistance is established by multiple members of the microbiota interacting to produce a healthy functional and structural profile. Antibiotic-induced alterations of the microbiome creates an environment susceptible to CDI. FMT therapy has successfully been used to prevent multiply recurrent CDI and has paved the path to understanding colonisation resistance and developing more targeted microbiome restoration therapies (Lawley *et al.*, 2012, Schubert *et al.*, 2015). *C. difficile* has also been shown to exacerbate intestinal dysbiosis and maintain this environment during CDI (Horvat *et al.*,

2017). Here, we were able to successfully prevent rCDI in an *in vitro* model using an increased dosing strategy of the targeted SER-109 faecal spore preparation. SER-109 administered on 3 consecutive days was able to effectively disrupt the microbiota dysbiosis and facilitated the restoration of the microbiota through both engraftment and augmentation of the commensal flora.

Chapter 5 Influence of intestinal microorganisms on *C. difficile* biofilm formation

5.1 Background

It is commonly accepted that biofilms may constitute the predominant mode of bacterial growth in the environment and in the human body (Costerton *et al.*, 1995). Biofilms are rarely composed of mono-culture species, being typically composed of numerous species of microorganisms that form complex and diverse communities. The composition and structure of a biofilm varies depending on the microorganisms present and the environment in which the biofilm formed. Different bacterial species interact extensively with each other and the attachment surface, and these interactions influence the structure and functional dynamics of the subsequent multispecies biofilms. To understand the complex interactions seen in a multispecies biofilm, it is critical to identify the different species present and the influence they have on the biofilm community.

Competition is one of the most common interactions seen in a biofilm due to limited space and nutrient availability. Many microorganisms have developed ways to inhibit the growth of competing microorganisms as was demonstrated by the suppression of *Streptococcus mutans* growth by *Streptococcus oligofermentans* through the production of hydrogen peroxide via lactate oxidase activity (Tong *et al.*, 2008). The production of *p*-cresol by *C. difficile* was found to inhibit hypha formation in *C. albicans* affecting both biofilm formation and virulence of the yeast (van Leeuwen *et al.*, 2016) and also gave *C. difficile* a competitive advantage over Gram negative bacteria in a mouse model (Passmore *et al.*, 2018). Interactions can also be co-operative, with different microorganisms benefiting from excreted metabolic by-products or facilitating the expression of genes beneficial to growth in that environment, such as *Actinomyces naeslundii* stabilising *Streptococcus gordonii* expression of genes involved in arginine biosynthesis in co-aggregates (Jakubovics *et al.*, 2008). This has also been seen in the gut with *Bacteroides ovatus* and

Bacteroides vulgatus. *B. ovatus* is capable of expressing extracellular inulin glycoside hydrolases, which are not required for its own growth on inulin. The metabolic products but were required to promote *B. vulgatus* growth, which lacks these enzymes and hence the ability to utilize inulin. Growth of *B. ovatus* in proximity to *B. vulgatus* is enhanced, and therefore benefits reciprocally through an unknown mechanism (Rakoff-Nahoum *et al.*, 2016). These interactions also have the ability to influence the function of the community such as the increased resistance to vancomycin displayed in polymicrobial biofilms with *Staphylococcus aureus* and *Candida albicans* in serum (Harriott and Noverr, 2010).

5.1.1 Rationale

Biofilms have been associated with the persistence and recurrence of infections, and due to the chronic nature of biofilm-associated infections, they have been implicated in relapsing *C. difficile* infection. The ability of *C. difficile* to become incorporated into intestinal sessile communities was demonstrated using the *in vitro* gut model adapted to facilitate biofilm formation (Crowther *et al.*, 2014a, Crowther *et al.*, 2014b). Little is known about the relationship between sessile species of the intestinal tract and *C. difficile* colonisation and persistence. Here, I sought to better understand the role of the individual species within biofilms in CDI. A range of microorganisms present in the biofilm during simulated CDI in the *in vitro* gut model were isolated and identified to the species level and combined with *C. difficile* in biofilm co-culture batch experiments to identify the effect of these different species on *C. difficile* biofilm formation.

5.2 Methods

5.2.1 Bacterial Strains and growth conditions

All strains used in this study are listed in Table 5-2. The *C. difficile* PCR ribotype 027 strain R20291 was isolated during a CDI outbreak at the Stoke Mandeville Hospital (Aylesbury, UK) in 2006 and was supplied courtesy of Dr Anthony Buckley (University of Leeds) and was used in all co-culture experiments. The *C. difficile* PCR ribotype 027 strain 210 (BI/NAP1/toxinotype III) was isolated during an outbreak of CDI at the Maine Medical Centre (Portland, ME, USA) and supplied courtesy of Dr Robert Owens (formally at Maine Medical Centre) and was used to compare biofilm growth against strain R20291. Other microorganisms used in co-culture experiments were isolated from a series of *in vitro* CDI and rCDI gut model experiments conducted in this study, detailed in chapters 3 and 4, with the exception of *Fingoldia magna* and *Fusobacterium polymorphum* that were sourced from the National Collection of Type Cultures (NCTC). Overnight liquid cultures were grown in pre-reduced BHIS (Brain heart infusion medium supplemented with 5 mg/mL yeast extract) at 37°C with agitation in T25 constant airflow tissue culture flasks (Nunc EasYFlask, T25).

5.2.2 Microbial isolation from the *in vitro* gut models

A series of *in vitro* gut models simulating CDI and rCDI were run in separate experiments (Chapters 3 and 4). Outcomes from these models have been demonstrated to reflect clinical outcomes and have been used extensively to assess therapeutic interventions in CDI (Macfarlane *et al.*, 1998, Freeman *et al.*, 2003, Baines *et al.*, 2005). These models were seeded with human microbiota and the isolated microbial species are routinely found in the human intestine. The isolates from the gut models were recovered from sessile populations adherent to biofilm support structures located in the final vessel of the models. Colonies were selected from enumeration plates (chapters 3 and 4) at various time points during the model timeline (Table 2-2). Additional agar types were trialled in order to isolate a wider range of microorganisms from sessile communities (Table 5-1). Different colony morphologies were selected for isolation and identification from selective and non-selective agars used in the microbial enumeration in the gut model experiments to generate an isolate

culture bank of biofilm-associated microorganisms for use in co-culture experiments. After sub-culturing colonies on CBA to ensure purity, microorganisms were identified by MALDI-TOF mass spectrometry analysis (section 2.2.13) to a species level and stored at -80°C in 12 % (v/v) glycerol. Isolates were sub-cultured from frozen stocks onto CBA and incubated either aerobically or anaerobically at 37°C (see Table 5-2 for culture conditions).

Table 5-1 Additional agars used to expand recoveries of sessile populations in the gut models.

Target genus	Agar	Source
<i>Vibrio spp.</i>	Thiosulphate Citrate Bile Salts Sucrose Agar	E & O
<i>Bacillus spp.</i>	Bacillus Cereus (MYP) Agar	E & O
<i>Staphylococcus ssp.</i> and <i>Streptococcus spp.</i>	Columbia Agar Base with 5% horse blood supplemented with colistin sulphate(10 mg/L) and nalidixic acid (15 mg/L)	E & O
<i>Neisseria spp.</i>	Gonococci selective agar supplemented with vancomycin (3 mg/L), colistin sulphate (7.25 mg/L), nystatin (12.5 IU/L), trimethoprim (5 mg/L).	E & O
<i>Actinomyces spp.</i>	Actinomyces Agar	E & O
<i>Fungi and yeasts</i>	Sabouraud Dextrose agar	E & O

MYP – Mannitol egg yolk polymyxin agar.

Table 5-2 Microbial strains used in co- and poly culture experiments, including source, culture conditions and MALDI-TOF analysis score.

Micro-organism	Source	Culture conditions (37°C)	Culture agar media	MALDI -TOF Score
<i>C. difficile</i> R20291	Stoke Mandeville Hospital (Aylesbury)	Anaerobic	Brazier's CCEYL/MXF	NA
<i>C. difficile</i> 027 210	Maine Medical Centre (Portland)	Anaerobic	Brazier's CCEY	NA
<i>Candida albicans</i>	<i>in vitro</i> gut model	Aerobic	OGYE	2.152
<i>Candida parapsilosis</i>	<i>in vitro</i> gut model	Aerobic	OGYE	2.002
<i>Enterococcus gallinarum</i>	<i>in vitro</i> gut model	Aerobic	KAA	2.216
<i>Staphylococcus aureus</i>	<i>in vitro</i> gut model	Aerobic	CBA	2.132
<i>Staphylococcus warneri</i>	<i>in vitro</i> gut model	Aerobic	CBA	2.243
<i>Klebsiella pneumoniae</i>	<i>in vitro</i> gut model	Aerobic	CBA	2.364
<i>Morganella morganii</i>	<i>in vitro</i> gut model	Aerobic	CBA	2.342
<i>Lactobacillus rhamnosus</i>	<i>in vitro</i> gut model	Anaerobic	MRS	2.298
<i>Bifidobacterium longum</i>	<i>in vitro</i> gut model	Anaerobic	BM	2.12
<i>Bacteroides thetaiotaomicron</i>	<i>in vitro</i> gut model	Anaerobic	BBE	2.224
<i>Clostridium butyricum</i>	<i>in vitro</i> gut model	Anaerobic	FAA	2.181
<i>Clostridium celecrescens</i>	<i>in vitro</i> gut model	Anaerobic	FAA	2.063
<i>Clostridium clostridioforme</i>	<i>in vitro</i> gut model	Anaerobic	FAA	2.328
<i>Clostridium symbiosum</i>	<i>in vitro</i> gut model	Anaerobic	FAA	2.09
<i>Clostridium paraputrificum</i>	<i>in vitro</i> gut model	Anaerobic	FAA	2.335
<i>Fingoldia magna</i>	NCTC 11804	Anaerobic	FAA	NA
<i>Fusobacterium polymorphum</i>	NCTC 10562	Anaerobic	FAA	NA

CCEY – cycloserine/cefoxitin egg yolk, MXF – moxifloxacin, OGYE – oxytetracycline glucose yeast extract, KAA - Kanamycin aesculin azide agar, CBA- Columbia blood agar, MRS – De Man, Rogosa, Sharpe agar, BM – Bifidobacterium medium, BBE - Bacteroides bile aesculin agar, FAA – fastidious anaerobe agar

5.2.3 Biofilm assay

The biofilm assay, modified from Dawson *et al.* (2012) was used to evaluate the ability of different microorganisms to form a biofilm *in vitro*, and to assess the influence of these species on *C. difficile* biofilm formation. Biofilms were quantified using the Crystal Violet (CV) assay and selected co-cultures were additionally evaluated using total viable counts (TVCs). Briefly, isolates were inoculated in pre-reduced BHI and grown with agitation for 18-24 hours at 37°C either anaerobically or aerobically, depending on the species (Table 5-2). Sterilised circular glass coverslips (Appleton Woods, UK) were placed in each well of a sterile 24 well plate (Nunc, UK) together with fresh BHISC media (BHIS media supplemented with 0.05 % (w/v) L-cysteine) and pre-reduced overnight. The amount of BHISC added to the wells depended on how many microorganisms were to be inoculated into the wells. 1.8 mL was added for mono-cultures, 1.6 mL for co-cultures and co-inoculation biofilms of *C. difficile* with cell-free supernatants (CFS), and 1.4 mL for polycultures (three microorganisms cultured together). The overnight broth culture for each microorganism was adjusted to an OD₆₀₀ of 0.5 ± 0.03 (Genesys 20 spectrophotometer, Thermo Scientific) in an attempt to normalise the culture. It is acknowledged that individual growth rate and cell size may impact the outcome of this intervention; however, results from this assay were only used as a preliminary screen to identify potential microorganisms of interest and therefore was sufficient for the scope of this study. 200 µL of the overnight, adjusted broth were inoculated into their respective wells. A glass coverslip with uninoculated culture medium was used as a negative control in all experiments. Trays were placed in a humidified container to prevent evaporation and incubated for 3 days anaerobically at 37°C where the biofilms were either analysed for biofilm biomass in the CV assay or TVCs (Figure 5-1). Results shown are the median values and interquartile range from at least three technical and three biological replicates.

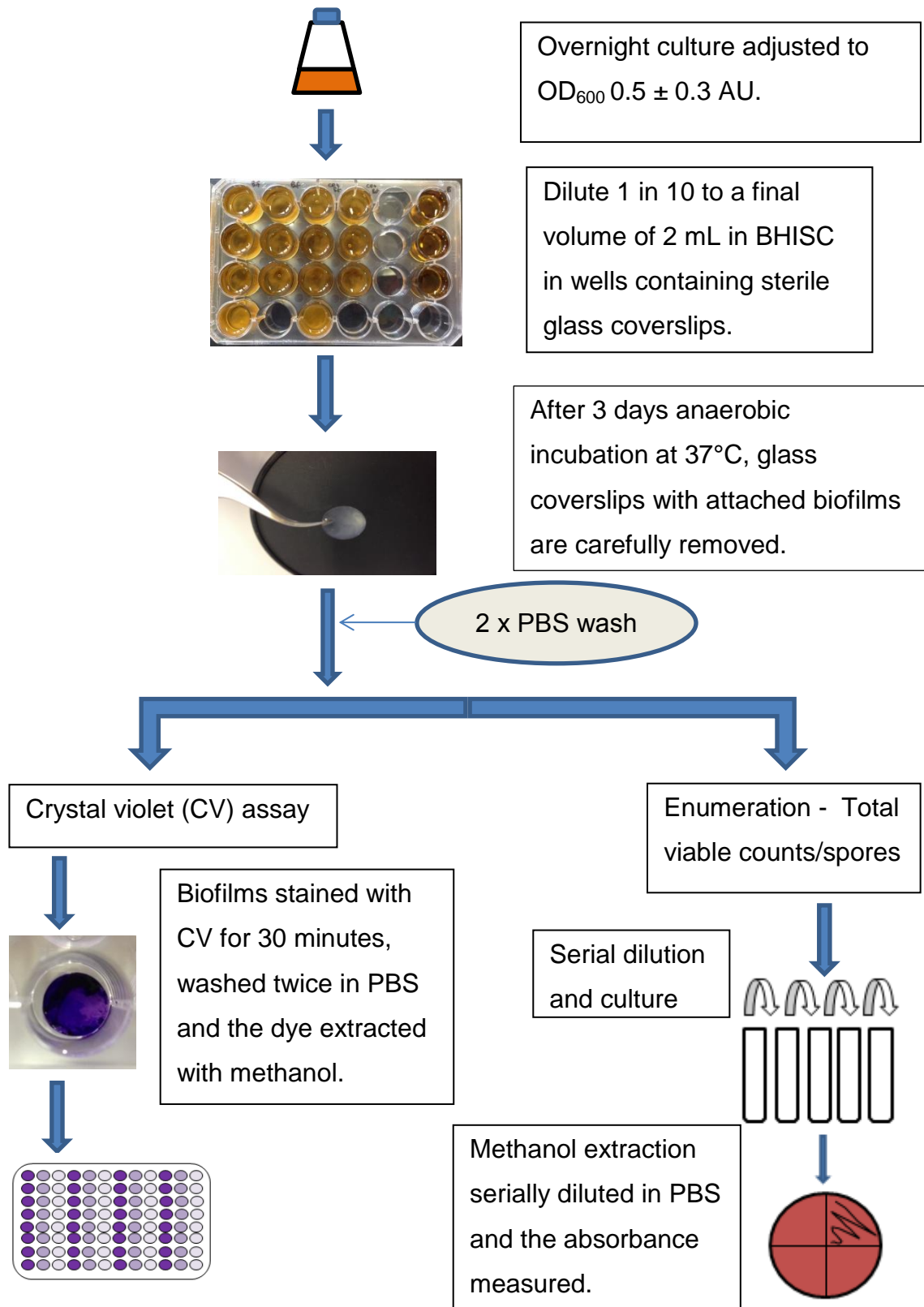


Figure 5-1 The biofilm batch culture assay set up and analysis. After inoculation with an overnight culture, biofilms are grown for three days before being analysed with either the crystal violet assay or enumerated for total and/or spore counts. AU – absorbance units, PBS – phosphate buffered saline, CV – crystal violet, TVC – total viable counts.

5.2.4 Semi-quantitative Crystal Violet (CV) assay for total biofilm biomass

Each biofilm assay was incubated for 3 days anaerobically and the biomass of each biofilm was semi-quantitatively analysed using the CV assay. The CV assay has been used extensively as a means to semi-quantitatively measure total biofilm biomass as the dye is capable of staining both live and dead cells, as well as certain components of the biofilm EPS (Merritt *et al.*, 2005, Skogman *et al.*, 2012, Stiefel *et al.*, 2016, Azeredo *et al.*, 2017). The microorganisms used in this assay can be found in Table 5-2. The glass coverslips containing the biofilms were carefully removed from wells using sterilised forceps, washed by dipping twice in PBS, and placed in a well containing 1 mL of a 1 % (w/v) CV solution, followed by incubation at room temperature for 30 minutes. Coverslips were again carefully removed, washed twice by dipping in PBS and incubated at room temperature for 30 minutes in 500 μ L of 100 % methanol (BDH Laboratory Supplies, Poole, UK) to extract the CV. The extracted CV/methanol solution was transferred to a 96 well plate in duplicate and serially diluted in PBS. The presence of cells and biofilm matrix in the extract may impact the colorimetric measurement and therefore this assay was only used as a screen to identify potentially antagonistic and co-operative interactions. The optical density was then measured at 595 nm (Infinite P 200 Pro, Tecan). A negative control well containing an uninoculated glass coverslip was used to normalise the results against the methanol, PBS and CV carryover.

5.2.5 Total viable and spore counts

Total viable counts were used to evaluate the total number of viable cells present in selected mono-, co- and poly culture biofilms. Coverslips with biofilms attached were carefully removed from the wells, washed twice in PBS and placed in wells with 500 μ L of pre-reduced PBS. Biofilms were then disrupted by vigorous pipetting. To determine the proportion of spores making up the TVCs in *C. difficile* mono-culture biofilms, 250 μ L of this suspension was then incubated for one hour at room temperature in a 1:1 ratio with 100 % (v/v) ethanol. The biofilm suspension was serially diluted in pre-reduced PBS and plated onto appropriate agars in triplicate (Table 2-2 and Table 5-2) and enumerated after 48 hours incubation. In co-cultures with *L. rhamnosus*, *C.*

difficile was cultured on CCEYL MXF medium (medium formulation found in Table 2-2) to reduce the *Lactobacilli* overgrowth on the CCEYL plates. Results were reported as median log₁₀ CFU/mL.

5.2.6 Effect of culture media pH on *C. difficile* biofilm formation

To find the optimum pH for *C. difficile* R20291 biofilm formation, the ability of *C. difficile* to form a biofilm in a pH range typically found as you traverse the colon was assessed. As such, pH 5 was selected to roughly reflect conditions seen in the proximal colon and pH 7 to reflect conditions encountered in the distal colon. Due to the presence of pH gradients within a biofilm, the effect of a highly alkaline environment of pH 9 was also tested. Biofilms were grown in BHISC medium with the pH adjusted to pH 5, pH 7 and pH 9 using 1M NaOH and 1M HCl, according to section 5.2.3 and analysed using the CV assay (section 5.2.4) and enumeration of total and spore counts 5.2.5).

5.2.7 Co- and poly culture biofilm assay

The ability of different microorganisms' isolated from the gut model to form an *in vitro* co-culture biofilms with *C. difficile* was investigated (Table 5-2). Each microbial strain, including *C. difficile*, was individually grown overnight as described in section 5.2.15.2.3. Overnight cultures were adjusted to an OD₆₀₀ of 0.5 ± 0.3 with BHISC before being diluted 1 in 10 with pre-reduced BHISC to a final total volume of 2 mL in a 24 well plate, as stated in section 5.2.3. Each assay consisted of a mono-culture biofilm for each microorganism investigated in addition to being cultured with *C. difficile* in a co-culture. Selected microorganisms were then cultured in a polyculture that consisted of two test microorganisms cultured together with *C. difficile* (Figure 5-2). Combinations of microorganisms used in poly-culture experiments can be found in Table 5-3. *L. rhamnosus*, *B. longum*, *B. thetaiotaomicron* and *C. butyricum* were selected as each of these microorganisms have been suggested as potential probiotics (Takahashi *et al.*, 2004, Lebeer *et al.*, 2008, Chang *et al.*, 2019, Martín *et al.*, 2019, Wang *et al.*, 2020). *M. morganii* was chosen to co-culture alongside *C. butyricum* as they were observed to grow in close proximity on enumeration plates from the gut models and *M. morganii* was often found growing over *C. butyricum* colonies. *S. aureus* and *C. albicans* were selected to investigate poly-culture growth with *C. difficile* as *C. albicans* has been demonstrated to

enhance *S. aureus* adhesion and biofilm formation (Kean *et al.*, 2017). Results from the *C. difficile* monoculture biofilm were compared with the results in the co-and/or poly-culture biofilms.

Table 5-3 Microbial combinations for poly-culture biofilms.

Co-culture	Co-culture	Poly-culture
<i>C. difficile</i> and <i>L. rhamnosus</i>	<i>C. difficile</i> and <i>C. albicans</i>	<i>C. difficile</i> , <i>L. rhamnosus</i> and <i>C. albicans</i>
<i>C. difficile</i> and <i>B. longum</i>	<i>C. difficile</i> and <i>B. thetaiotaomicron</i>	<i>C. difficile</i> , <i>B. longum</i> and <i>B. thetaiotaomicron</i>
<i>C. difficile</i> and <i>S. aureus</i>	<i>C. difficile</i> and <i>C. albicans</i>	<i>C. difficile</i> , <i>S. aureus</i> and <i>C. albicans</i>
<i>C. difficile</i> and <i>C. butyricum</i>	<i>C. difficile</i> and <i>M. morgani</i>	<i>C. difficile</i> , <i>C. butyricum</i> and <i>M. morgani</i>

5.2.8 Co-culture biofilms with cell free supernatants

Microbial metabolites or secreted factors have been implicated in the ability of certain species to reduce the toxicity of *C. difficile* cell-free supernatants (CFS) (Valdés-Varela *et al.*, 2016). However, some effects require viable cells to be present (Woo *et al.*, 2011). To determine whether these interactions extend to biofilm formation and whether the effect seen in co-culture biofilms was due to interaction with viable cells or metabolic products, the ability of *C. difficile* to form a biofilm in the presence of CFS from selected microorganisms was investigated. Bacterial strains *L. rhamnosus* and *B. longum* were selected for this experiment due to the observe decrease or increase in biofilm formation in co-culture with *C. difficile*. In these experiments, *C. difficile* was co-inoculated (1:1) with the CFS from overnight cultures of the above microorganisms and results compared to those obtained in co-cultures with viable cells and *C. difficile* mono-culture biofilms (Figure 5-2). The CFS was obtained by centrifuging overnight cultures of target microorganisms (after normalisation to OD₆₀₀ of 0.5 ± 0.03) at 16 000g for 10 mins followed by filter sterilising. The

production of organic acids from *Lactobacilli* and *Bifidobacterium* have been implicated as a potential inhibitory mechanism to *C. difficile* growth, therefore for our experiments with *L. rhamnosus* and *B. longum*, an additional CFS experiment was conducted whereby the CFS was neutralised to pH 6.8 to equal that of the culture medium BHIS with 1M NaOH. 200 μ L of *C. difficile* overnight culture and 200 μ L of the CFS from the selected microorganism was then co-inoculated into 1.6 mL of BHISC in the wells, as in section 5.2.7.

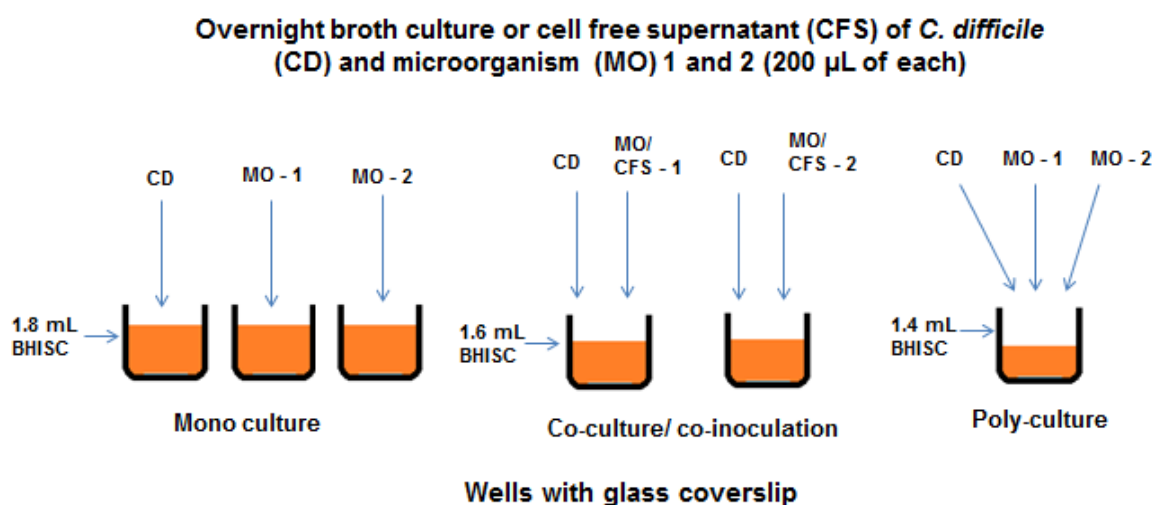


Figure 5-2 Inoculation of the biofilm batch culture experiments for co- and poly-culture assays. To investigate the nature of the interactions of *C. difficile* in co- and poly-culture with selected microorganisms (1 and 2), biofilm batch culture assays were used. For each microorganism, a mono culture biofilm was grown comprising of 1.8 mL culture medium and 200 μ L of overnight broth culture. Co-culture experiments consisted of 1.6 mL culture media and 200 μ L of *C. difficile* and 200 μ L of the microorganism or cell free supernatant (CFS). Poly-culture experiments consisted of 1.4 mL culture medium and 200 μ L of *C. difficile* and 200 μ L of each of the two target microorganisms or CFS. The biofilms were then left to grow for three days before analysis. CD- *C. difficile*, MO – microorganism, CFS - cell free supernatant.

5.2.9 *C. difficile* cytotoxin testing

In selected biofilms, the amount of *C. difficile* cytotoxin was quantified using the Vero cell cytotoxin assay as described in section 2.2.16. Briefly, the biofilm was resuspended by vigorous pipetting in 500 μ L PBS, as for TVC counts. This biofilm suspension was then centrifuged at 16 000g for 10 minutes and filter sterilised. The biofilm suspension was serially diluted in pre-prepared Vero cell culture trays and left for 48 hours incubation. All biofilms were assayed in duplicate and results reported as relative units (RU).

5.2.10 Scanning Electron Microscopy – sample preparation and biofilm imaging

Biofilms were grown on glass coverslips as per section 5.2.3, harvested after 3 days and rinsed twice in PBS. Biofilms were fixed in 2.5 % (v/v) glutaraldehyde in 0.1 M phosphate buffer overnight and washed twice in 0.1 M phosphate buffer for 30 min each. Biofilms were post fixed in 1 % osmium tetroxide (w/v) in phosphate buffer for 2 hours and washed twice for 20 mins in phosphate buffer. Biofilms were dehydrated using an ascending acetone series (20 %, 40 %, 60 %, 80 %, 100 %, (v/v)) for 30 mins each change, washing twice with phosphate buffer after each change. Biofilms were then critical point dried in a critical point drying apparatus (Polaron E3000, Quorum Technologies) using liquid CO₂ as the transition fluid. The biofilm samples were mounted on 13mm diameter pin stubs with double sided adhesive tape and coated with platinum to a thickness of 5 nm using a high resolution sputter coating unit (Cressington 208HR). Biofilms were observed and imaged using an Hitachi SU8230 ultra high resolution field emission scanning electron microscope (FE-SEM) at 5000, 10 000, 20 000 and 25 000 x magnification. Assistance with sample processing and SEM imaging were provided by Mr Martin Fuller, Astbury Centre for Structural Molecular Biology and Mr Stuart Micklethwaite, Leeds Electron Microscopy and Spectroscopy Centre, The University of Leeds. Selected images were false-coloured using Adobe Photoshop CC version.

5.2.11 Statistical analysis and graphical software

Statistical analysis was performed using IBM SPSS Statistics 22 for Windows. Co-culture data were analysed using a Mann-Whitney U test. Poly cultures, the effect of pH on *C. difficile* biofilm formation and all co-cultures involving

supernatants were analysed with the Kruskal Wallis one-way analysis of variance with a pairwise comparison. *P* values of ≤ 0.05 were considered statistically significant. GraphPad Prism 5 for Windows, version 5.03 and Microsoft Excel 2013 were used to generate figures.

5.3 Results

5.3.1 Characterisation of the *C. difficile* biofilm

The ability of hyper-virulent *C. difficile* ribotype 027 strains R20291 and 210 to form a biofilm *in vitro* were compared. TVC and spore counts were performed to gain an insight into the composition of these biofilms. R20291 was used as it is known produce a robust biofilm (Dawson *et al.*, 2012), these results were compared with 210 strain as the latter strain was used in the *in vitro* gut model experiments, thus assessing its ability to form biofilms was necessary. The semi-quantitative crystal violet assay was used to measure the total biofilm biomass. Crystal violet is able to non-specifically bind to negatively charged molecules and therefore is capable of binding to live and dead cells, and to certain negatively charged components of the biofilm EPS matrix (Pitts *et al.*, 2003, Petrachi *et al.*, 2017). Results from the CV assay demonstrated that R20291 formed a biofilm with significantly increased biofilm biomass compared with strain 210 (median absorbance of 10.0 and 8.5 AU, respectively, $p = 0.012$) (Figure 5-3 a). Enumeration of cells within the biofilms revealed no significant difference in TVC between the two strains (median \log_{10} CFU/mL of 7.6 and 7.7, respectively, $p = 0.924$); however, R20291 formed considerably more spores than 210 (median \log_{10} CFU/mL of 6.7 and 5.7, respectively, $p < 0.001$) (Figure 5-3 b). As the difference in biofilm biomass seen in the CV assay could not be attributed to an increase *C. difficile* growth, it is possible that a larger degree of cell death or an increase in EPS production in R20291, when compared to 210, could be responsible. Mono culture biofilms of *C. difficile* strain R20291 attached to glass coverslips were visualised by SEM after 3 days incubation. The image at x 5000 magnification revealed a mat of aggregated *C. difficile* vegetative cells and cell debris adherent to the abiotic surface and the presence of EPS matrix-like substance (Figure 5-4 a). Enlargement of images at x10 000 and x20 000 magnification revealed what appears to be an EPS matrix with a filamentous and web-like appearance, linking cells together (Figure 5-4 b-d) and anchoring them to the surface of the glass coverslip.

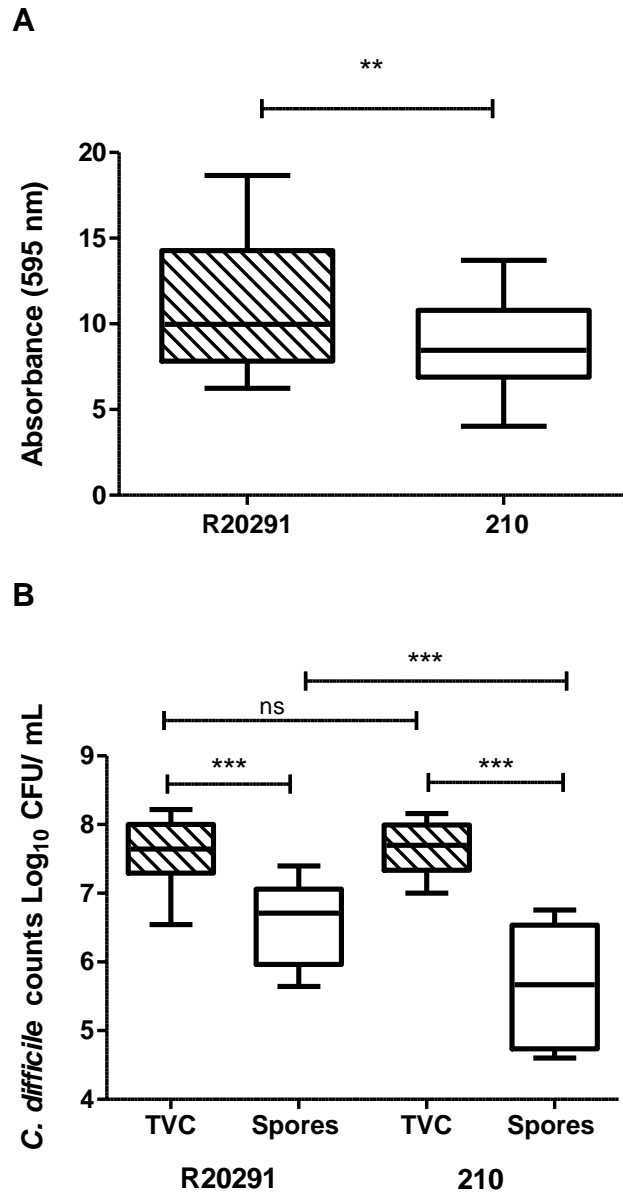


Figure 5-3 Crystal Violet staining and enumeration of *C. difficile* ribotype 027 strains R20291 and 210 biofilms. The biofilm produced by two *C. difficile* strains was analysed using (A) the semi-quantitative crystal violet assay (absorbance - AU) (R20291 – striped, 210 - clear) measured at 595 nm and (B) enumeration of total (striped) and spore (clear) counts in log₁₀ CFU/mL. R20291 produced significantly (** $p = 0.012$) more biofilm biomass when compared to 210 in the crystal violet assay. Similar levels of total counts were recovered between the two strains; however, R20291 produced significantly (** $p < 0.001$) more spores than 210. Results represent the median with interquartile range from at least three technical replicates from each of three biological replicates. TVC – total viable counts.

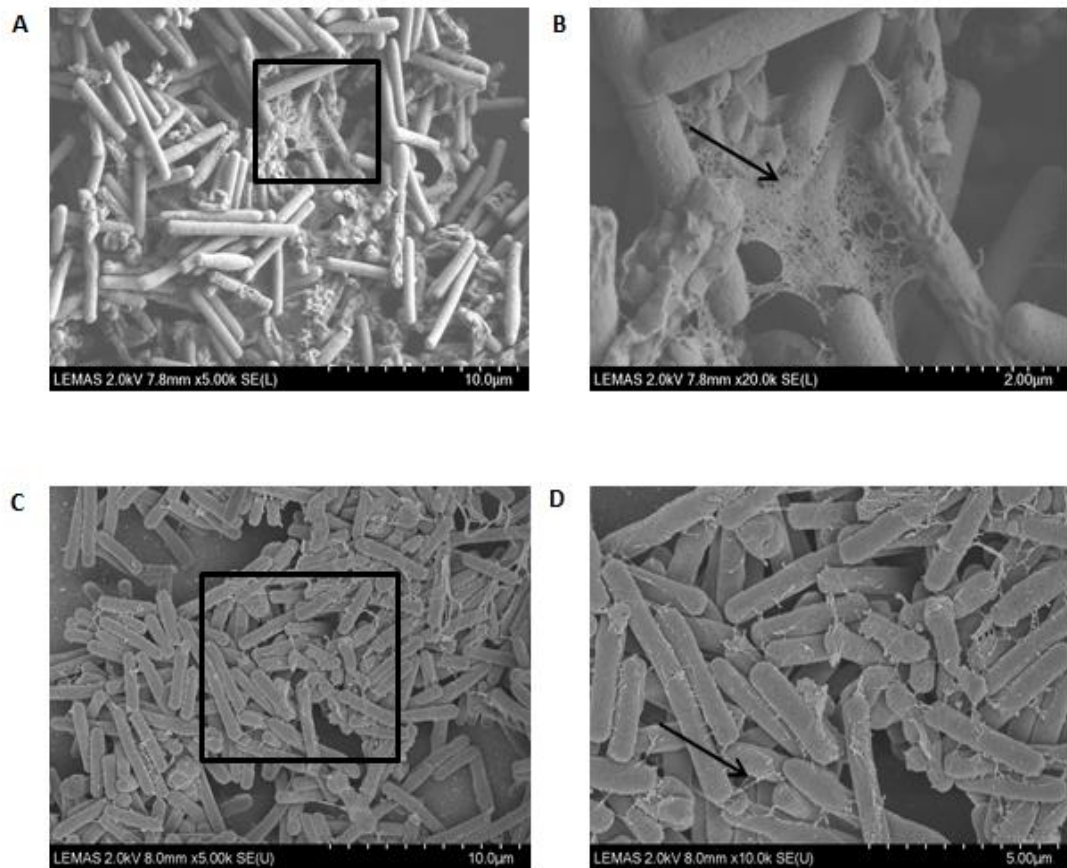


Figure 5-4 Scanning electron microscopy of *C. difficile* R20291 biofilms grown for 3 days. A) Robust *C. difficile* biofilm with a web-like extracellular polymeric substances and cell debris at x 5 000 magnification. B) Enlargement of image A at x 20 000 magnification clearly demonstrating the biofilm matrix linking the *C. difficile* cells and cell debris together. C) Mat of *C. difficile* R20291 vegetative cells and cell debris adherent to an abiotic surface, x 5 000 magnification. D) Enlargement of image C at x 10 000 magnification showing fibrous strings of matrix linking cells together. Black boxes indicate the enlarged sections, and the black arrows indicate the biofilm matrix linking cells together.

5.3.2 Impact of pH on biofilm formation

The ability of *C. difficile* R20291 to form a biofilm at pH 5, pH 7 and pH 9 was assessed using the crystal violet assay and enumeration of TVC and spores. The proximal colon has an acidic pH and therefore medium at pH 5 was used to mimic this environment. As the pH of the environment increased, this corresponded to an increase in biofilm formation from pH 5 to pH 9 (median absorbance of 1.1, 8.8 and 19.7 AU for pH 5, 7 and 9, respectively, $p \leq 0.001$) (Figure 5-5 a). This was accompanied with an increase TVCs of 7.0, 7.5 and 7.8 \log_{10} CFU/mL (Figure 5-5 b) and spores of 4.0, 5.4 and 6.3 \log_{10} CFU/mL for pH5, 7 and 9 (Figure 5-5 c), respectively ($p \leq 0.001$). As *C. difficile* infection is usually associated with the distal colon that has a pH closer to neutral, the results comparing biofilm formation at pH5 and pH 7 was expected.

The largest amount of biofilm biomass and growth was observed when the media was adjusted to pH 9 ($p < 0.001$). The clinical significance of this finding is not clear as the pH in the planktonic phase of the colon typically does not exceed pH 7; however, little is known regarding the pH levels within biofilms and pH gradients have been demonstrated previously in a mixed biofilm comprised of 10 oral bacteria ranging from pH 3 – pH 7.2 (Vroom *et al.*, 1999). However, members of the 'core' gut microbiome are generally associated with metabolic by-products that are acidic in nature (Oliphant and Allen-Vercoe, 2019) and therefore it is unlikely that the pH would rise to the level tested here (pH 9).

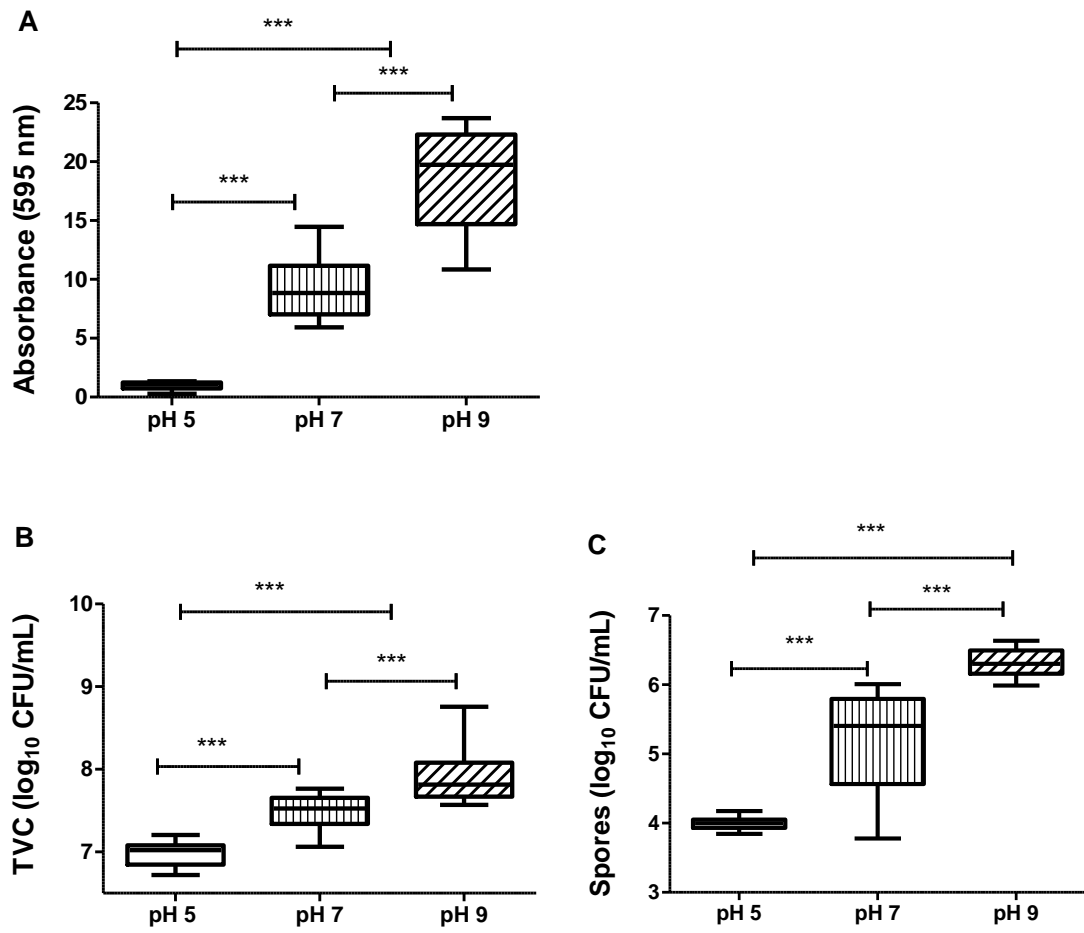


Figure 5-5 Crystal violet quantification and enumeration of *C. difficile* from biofilms formed in medium with different levels of pH. *C. difficile* biofilms were grown at pH 5, pH 7 and pH 9 were quantified using (a) the crystal violet assay (absorbance at 595nm) (b) enumeration of total viable counts (log₁₀ CFU/mL) and (c) enumeration of spores (log₁₀ CFU/mL). *C. difficile* biofilm biomass, total viable cells and spore recoveries increased with increasing pH. Results represented are the median with interquartile range for at least three technical replicates from each of three biological replicates. *** $p \leq 0.001$.

5.3.3 The effect of microorganisms isolated from the GI tract on *C. difficile* biofilm formation.

5.3.3.1 Initial screen of co-culture biofilms with *C. difficile* using the crystal violet assay.

To further understand the influence of biofilms on CDI, the impact of individual microorganisms on *C. difficile* biofilm formation was investigated. This was done by screening multiple microorganisms, isolated from the *in vitro* gut models (Chapter 3 and 4) and identified to a species level (section 2.2.13), for biofilm formation with *C. difficile* in co-culture. During initial co-culture biofilms, a mixture of obligate anaerobes and facultative anaerobes. For each experiment, a mono culture biofilm was grown for each microorganism as well as the co-culture biofilm with *C. difficile*. The crystal violet assay was used in this initial screen to identify microorganisms that would be used in further experiments. The tested microorganisms can be found listed in Table 5-2. This was done by comparing the co-culture biofilm result with the *C. difficile* mono culture biofilm. Co-culture biofilms of *C. difficile* together with *Klebsiella pneumoniae*, *Morganella morganii*, *Clostridium symbiosum*, *Bifidobacterium longum* ($p \leq 0.001$), *Bacteroides thetaiotaomicron*, *Clostridium butyricum* ($p \leq 0.02$), *Lactobacillus rhamnosus*, and *Clostridium celerecrescens* ($p \leq 0.05$), resulted in significantly less biofilm formed when compared with *C. difficile* mono-culture (Figure 5-6). The individual mono-culture data for each of these microorganisms suggests that these particular strains, in the conditions examined, are relatively poor biofilm formers. Co-culture biofilms of *C. difficile* together with *Staphylococcus warneri* ($p \leq 0.02$), *Clostridium paraputrificum* and *Fusobacterium polymorphum* ($p \leq 0.001$) resulted in significantly more biofilm formed when compared with *C. difficile* mono-culture. *M. morganii*, *B. longum*, *B. thetaiotaomicron*, *C. butyricum*, *L. rhamnosus*, *C. albicans*, *S. aureus* and *S. warneri* were selected to further investigate interactions with *C. difficile*. Although the co-culture of *C. difficile* with *C. paraputrificum* and *F. polymorphum* were significantly larger than *C. difficile* mono-culture, these microorganisms were not selected for further study. *F. polymorphum* is more relevant to the oral microbiota and therefore was not considered further. *C. paraputrificum* was not selected for follow up experiments due to inconsistencies in bacterial growth of overnight cultures. Even with agitation, *C.*

paraputrificum would form large aggregates in the overnight culture that would not readily disperse, resulting in difficulty adjusting the overnight growth concentration to 0.5 AU. The mono-culture results of *C. paraputrificum*, with a mean of 53 AU, far exceeded the mean 16 AU of *C. difficile*. It is therefore likely that the increase seen in biofilm co-cultures was as a result of *C. difficile* incorporation into the *C. paraputrificum* biofilm and not an example of interaction between the two species. Results from all mono and co-culture biofilm experiments are from at least three technical replicates of each of at least three biological replicates.

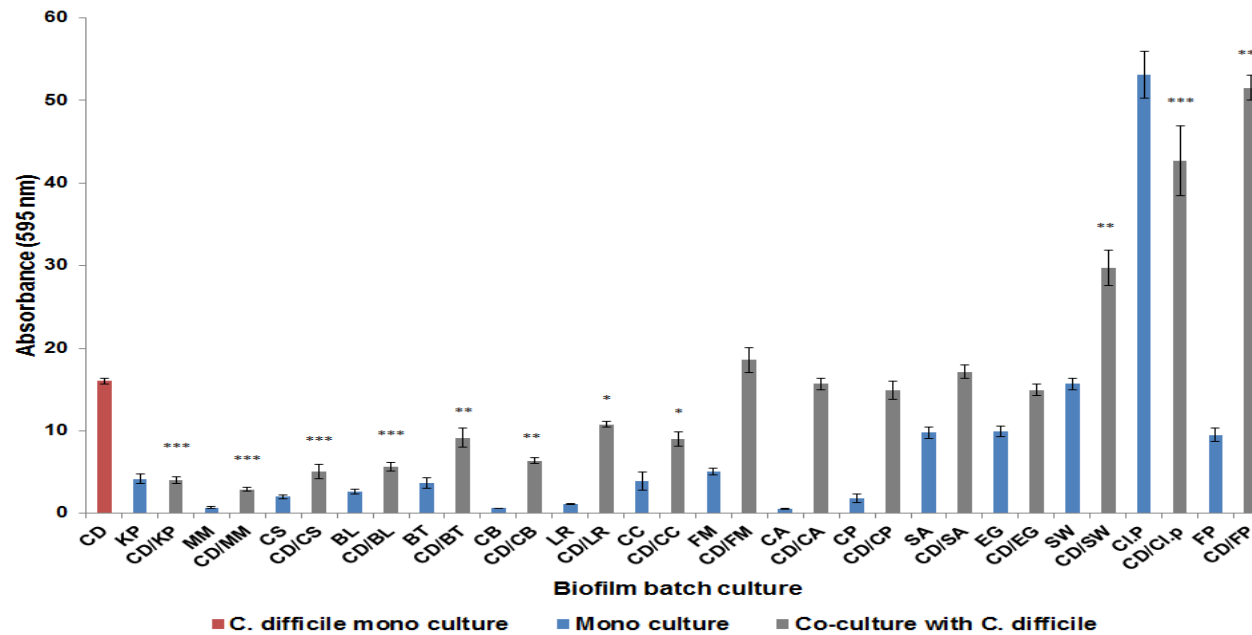


Figure 5-6 Quantification of mono and co-culture biofilms using the crystal violet assay. Biofilms were cultured in mono-culture (*C. difficile* – red, test microorganisms – blue) and in co-culture with *C. difficile* (grey) for three days before being analysed using the crystal violet assay (absorbance, AU with standard error). The absorbance of the co-culture was compared to the absorbance of the *C. difficile* mono-culture, and the interactions were assessed for significance using a Kruskal-Wallis test with pairwise comparisons (* $p \leq 0.05$, ** $p \leq 0.02$, *** $p \leq 0.001$). The majority of the microorganisms tested were poor biofilm formers and resulted in decreased amounts of biofilm produced in co-culture with *C. difficile* when compared with *C. difficile* mono-culture.

CD - *C. difficile*, KP – *K. pneumoniae*, MM – *M. morgani*, CS – *C. symbiosum*, BL – *B. longum*, BT – *B. thetaiotaomicron*, CB – *Clostridium butyricum*, LR – *L. rhamnosus*, CC – *Clostridium celerecrescens*, FM – *F. magna*, *Candida albicans*, CP – *Candida parapsilosis*, SA - *S. aureus*, EG – *Enterococcus galinarum*, SW - *S. warneri*, Cl.P - *Clostridium paraputrificum* and FP - *Fusobacterium polymorphum*.

5.3.3.2 Investigating the effect of cell-free supernatants (CFS) on *C. difficile* biofilm formation.

To further investigate the interactions of *C. difficile* with *L. rhamnosus*, *B. longum*, *S. warneri* and *S. aureus*, the co-culture biofilm assay was repeated using the cell free supernatant from the test microorganisms overnight culture to determine whether the effect seen in co-culture with *C. difficile* was as a result of cell viability or mediated by secreted factors and by-products. Additionally, as organic acid metabolic products of *L. rhamnosus* and *B. longum* are both known to reduce pH levels of the culture medium, this was measured to be pH 5.8 and pH 5.6 in overnight culture supernatants, respectively, a portion of the CFS was adjusted to pH 6.8 using 1M NaOH. A further co-culture biofilm experiment was done to include co-culture of *C. difficile* with the neutralised CFS (nCFS). In the CV assay, co-culture of *C. difficile* with *L. rhamnosus*, *L. rhamnosus* CFS and *L. rhamnosus* nCFS resulted in a significant decrease in biofilm formation in all conditions tested ($p < 0.001$), with largest decrease seen in co-culture with the CFS, resulting in a mean decrease of 8.4 AU vs the 3.6 RU decrease seen in nCFS, indicating that pH was partly responsible for the decrease seen in the co-culture (Figure 5-7 a). The TVC data shows a significant difference between *C. difficile* counts in the co-culture biofilm with *L. rhamnosus* when compared to mono-culture, with an approximate $3 \log_{10}$ CFU/mL decrease in *C. difficile* TVCs in co-culture ($p < 0.001$) (Figure 5-7 b). The TVC from *L. rhamnosus* indicates an increase in counts in co-culture vs mono-culture, despite the reduced biomass of the biofilm. TVC of *C. difficile* in co-culture with *L. rhamnosus* CFS and nCFS were not significantly different from the *C. difficile* mono culture TVC, suggesting that viable *L. rhamnosus* cells are required to inhibit *C. difficile* growth. *C. difficile* cytotoxin testing was performed on these biofilms and results were consistent with TVC values, with toxin levels in co-culture with *L. rhamnosus* decreasing from 3.5 RU in mono-cultures to 1.75 RU in co-culture ($p = 0.01$), whereas in co-cultures with the CFS and nCFS, there was no significant difference when compared to the mono-culture (3.6 and 3.5 RU, respectively) (Figure 5-9). The data suggests that the decrease in *C. difficile* toxin levels in co-culture were most likely a result of decreased cell numbers in the presence of *L. rhamnosus* viable cells.

Co-cultures of *C. difficile* with *B. longum* resulted in a significant decrease in biofilm formation (absorbance reduced by 9.2 AU, $p < 0.001$), when compared to the *C. difficile* monoculture (Figure 5-8 a). There was no significant difference in biofilm biomass in co-cultures of *C. difficile* with either the CFS or the nCFS. TVC revealed a significant decrease in *C. difficile* counts in co-culture with *B. longum* viable cells (decrease of 1.2 Log₁₀ CFU/mL, $p = 0.01$) (Figure 5-8 b). In line with the results in the crystal violet assay, there was no significant difference in TVC in the co-cultures of *C. difficile* with either *B. longum* CFS or nCFS. Cytotoxin testing demonstrated a reduction in toxin levels in co-culture with *B. longum* effect on *C. difficile* toxin levels. Co-culture of *C. difficile* from 3.5 RU in mono-culture to 2 RU in co-culture with *B. longum*, whereas co-culture with either the CFS or nCFS had no effect on toxin levels (Figure 5-9). From this data, it appears that *B. longum* viable cells are required to reduce *C. difficile* growth and biofilm biomass.

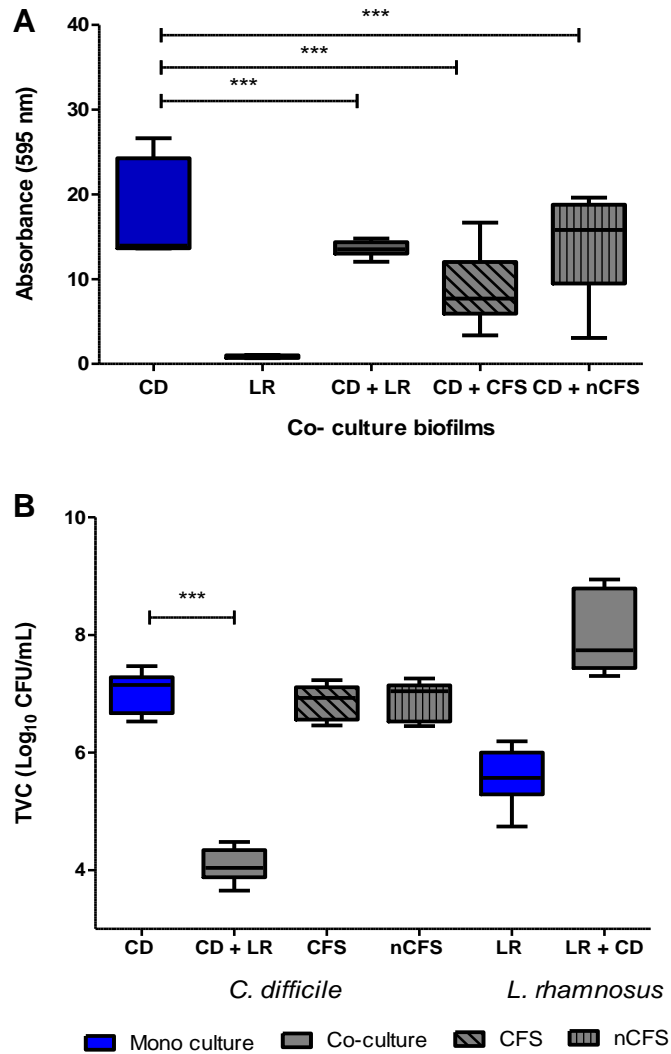


Figure 5-7 Co-culture biofilm experiments between *C. difficile* and *L. rhamnosus*. *C. difficile* and *L. rhamnosus* biofilms were cultured alone (blue) and in co-culture (grey), alongside *C. difficile* biofilm co-cultures with *L. rhamnosus* cell free supernatant (CFS – grey, diagonal pattern) and neutralised cell free supernatant (nCFS – grey, vertical pattern). Results were analysed using (a) the crystal violet assay (absorbance, AU) and (b) total viable counts (log₁₀ CFU/mL). There was a significant decrease in biofilm biomass in each co-culture when compared with the *C. difficile* mono culture in the crystal violet assay ($p \leq 0.001$) and in the total counts when *L. rhamnosus* viable cells were present ($p \leq 0.001$). Results represent median and interquartile range from at least three technical replicates of each of three biological replicates. CD- *C. difficile*, LR – *L. rhamnosus*, CFS – cell free supernatant, nCFS – neutralised cell free supernatant, TVC – total viable counts.

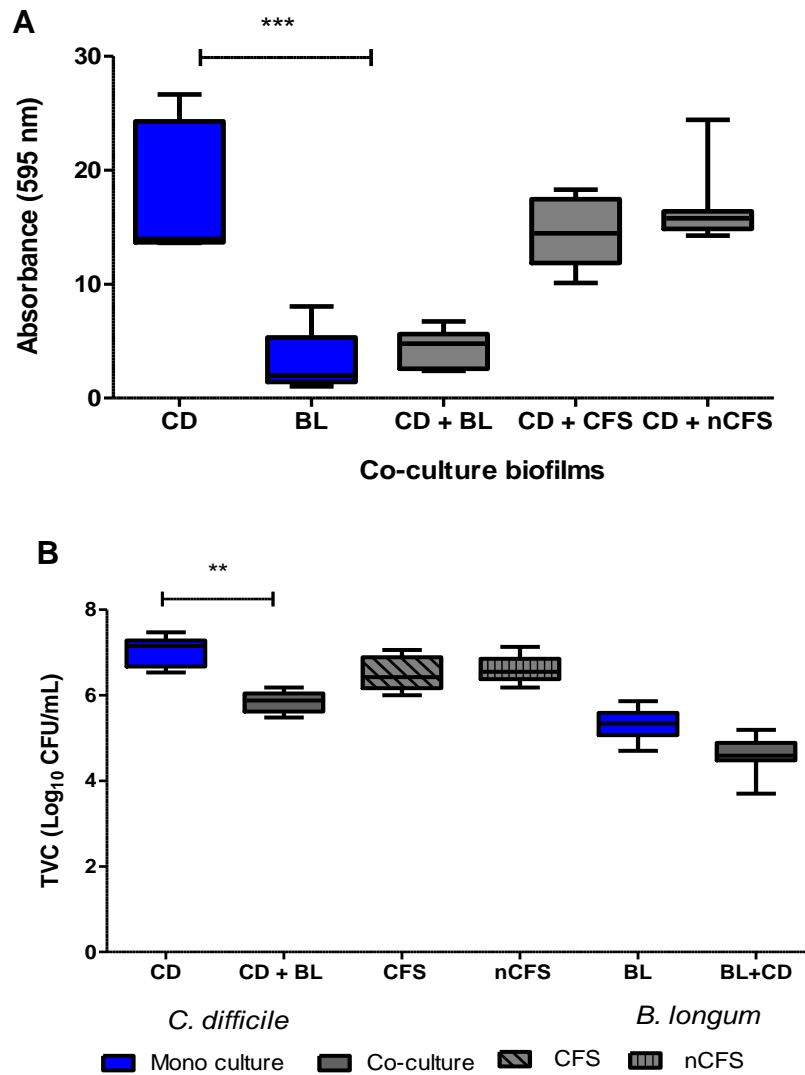


Figure 5-8 Co-culture biofilm experiments between *C. difficile* and *B.*

***longum*.** *C. difficile* and *B. longum* biofilms were cultured alone (blue) and in co-culture (grey), alongside *C. difficile* biofilm co-cultures with *B. longum* cell free supernatant (CFS – grey, diagonal pattern) and neutralised cell free supernatant (nCFS – grey, vertical pattern). Results were analysed using (a) the crystal violet assay (absorbance, AU) and (b) total viable counts (log₁₀ CFU/mL). There was a significant decrease in biofilm biomass and total counts when *C. difficile* was co-cultured with *B. longum* viable cells ($p \leq 0.001$ and $p \leq 0.01$, respectively). Results represent median and interquartile range from at least three technical replicates of each of three biological replicates. CD- *C. difficile*, BL – *B. longum*, CFS – cell free supernatant, nCFS – neutralised cell free supernatant, TVC – total viable counts.

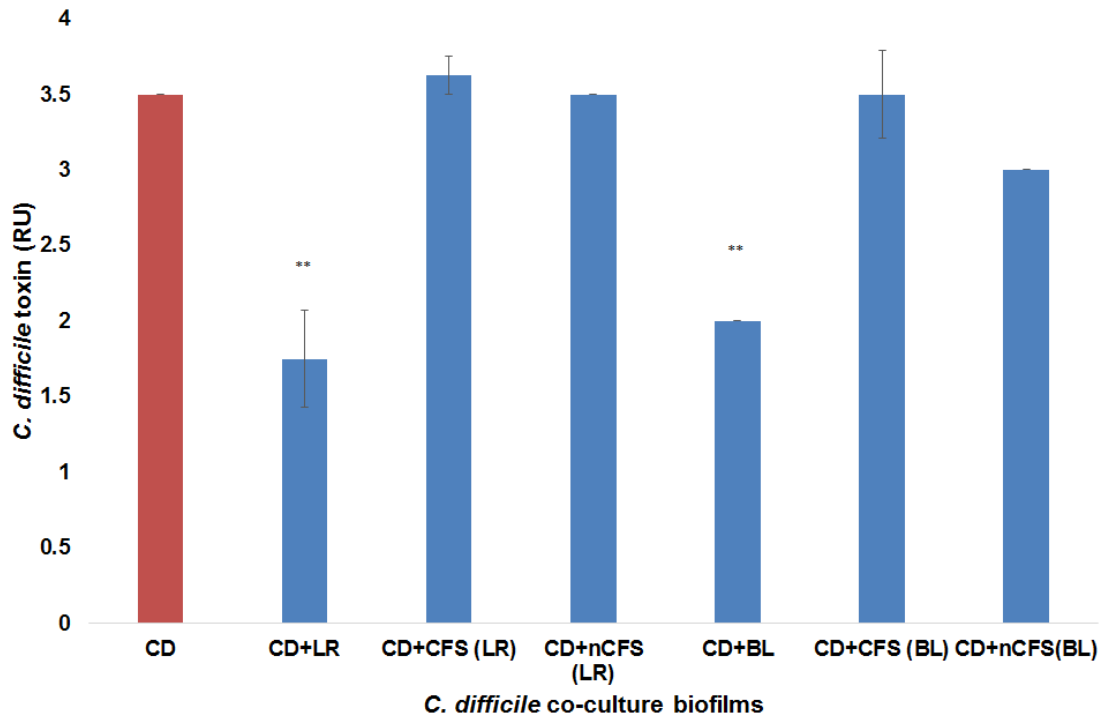


Figure 5-9 *C. difficile* toxin production in co-culture biofilms. Levels of *C. difficile* toxin were measured using the Vero cell cytotoxicity assay (measured in relative units – RU) in co-culture biofilms with *L. rhamnosus* and *B. longum*, as well as co-cultures with the cell free supernatant (CFS) and the neutralised cell free supernatant (nCFS) from each. There was a significant decrease in toxin production in co-cultures of *C. difficile* with *L. rhamnosus* and *B. longum* viable cells ($p \leq 0.01$). Data represents three technical replicates of three biological replicates. CD – *C. difficile*, LR – *L. rhamnosus*, BL – *B. longum*, CFS – cell free supernatant, nCFS – neutralised cell free supernatant.

5.3.4 Effect of poly-culture biofilms on *C. difficile* biofilm formation

In nature, biofilms are comprised of communities of microorganisms and the presence of additional species to the biofilm can potentially change its structure and function. To evaluate the effect of more than one micro-organism on *C. difficile* biofilm formation, poly-microbial biofilm cultures were conducted comprising of *C. difficile* cultured together in equal quantities with two other microorganisms isolated from the *in vitro* gut models. Briefly, each of the three microorganisms were cultured in mono-culture biofilms. *C. difficile* was then co-cultured with each of the two microorganisms selected and finally all three microorganisms were cultured together. Two of the poly-culture experiments were comprised of two sets of microorganisms that demonstrated reduced biofilm formation when in co-culture with *C. difficile*, namely *B. longum* and *B. thetaiotaomicron*; and *C. butyricum* and *M. morgani*. The latter poly-culture was chosen as an observation from culture plates from the *in vitro* gut models that revealed *C. butyricum* growing intimately associated with *M. morgani*, often one colony on top of the other, therefore this relationship warranted further investigation. As interactions between *C. difficile* and yeasts are not well documented, poly-cultures of *C. difficile* and *C. albicans* with *S. aureus* or *L. rhamnosus* were investigated.

The poly-culture of *C. difficile*, *B. longum* and *B. thetaiotaomicron* had a median absorbance of 3.1 AU in the CV assay. This value was not significantly different from the median values from co-cultures of *C. difficile* with *B. longum* (2.5 AU) and *B. thetaiotaomicron* (5.4 AU); however, it was significantly different from the *C. difficile* mono-culture of 17.3 AU ($p < 0.001$) (Figure 5-10 a). TVCs from the co-cultures experiments revealed a decrease of 1.1 – 1.3 \log_{10} CFU/mL which was significantly less than that of the *C. difficile* mono-culture ($p < 0.001$), for *B. longum* and *B. thetaiotaomicron*, respectively. TVCs from the poly-culture demonstrated a reduction in *C. difficile* numbers of 2.3 \log_{10} CFU/mL ($p < 0.001$) when compared to *C. difficile* mono-culture (Figure 5-10 b). These results suggest that there is a larger reduction in *C. difficile* biofilm biomass and growth within a biofilm when cultured with *B. longum* and *B. thetaiotaomicron* together than when in co-culture.

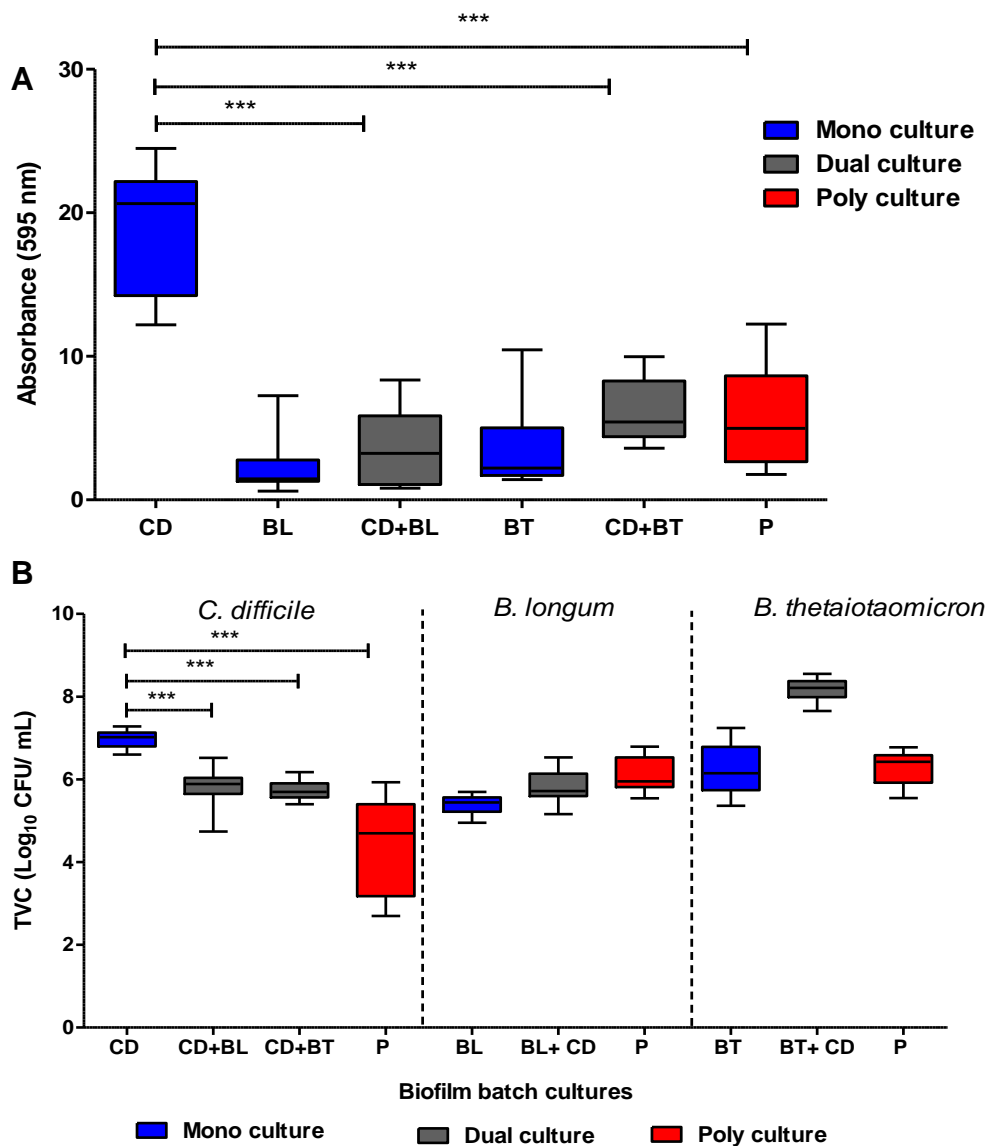


Figure 5-10 Poly-microbial biofilm culture of *C. difficile* with *B. longum* and *B. thetaiotaomicron*. Mono-culture (blue), co-culture (grey) and poly-culture (red) biofilms are shown for *C. difficile*, *B. longum* and *B. thetaiotaomicron* for (a) the crystal violet assay (absorbance – AU) and (b) total viable counts (log₁₀ CFU/mL). In both the co- and poly-culture biofilms, there was a significant reduction in *C. difficile* biofilm biomass and cell growth when compared to the mono-culture biofilm. Results represent the median and interquartile range of three technical replicates of each of three biological replicates. *** p ≤ 0.001. CD- *C. difficile*, BL – *B. longum*, BT – *B. thetaiotaomicron*, P – poly-culture, TVC – total viable counts.

The combined effect of co-culture of *C. butyricum* and *M. morgani* with *C. difficile* maintained a reductive effect, but the median value of the poly-culture was between that of the co-cultures with absorbance values of 7.4, 2.4 and 5.8 AU for co-culture with *C. butyricum*, co-culture, with *M. morgani*, and the poly-culture, respectively. All were significantly less than that of the measured absorbance for *C. difficile* mono-culture (11.8 AU, $p \leq 0.002$) (Figure 5-11 a). *C. difficile* TVCs from co-cultures were approximately 1 \log_{10} CFU/mL lower ($p < 0.01$) when compared to the *C. difficile* mono-culture; however, the *C. difficile* TVCs from the poly-culture were not significantly different from the mono-culture (Figure 5-11 b). *C. butyricum* TVCs increased in both co-and poly-cultures whereas *M. morgani* TVC was unaffected in co culture with *C. difficile* but decreased in the poly-culture.

The biofilm biomass of the poly-culture between *S. aureus*, *C. albicans* and *C. difficile* was not significantly different from the *C. difficile* mono-culture biofilms ($p \leq 0.3$) (Figure 5-12 a). There was a significant decrease in *C. difficile* TVC in co-culture with *S. aureus* ($p \leq 0.01$), but this effect was lost in poly-culture (Figure 5-12 b). Although the quantity of biofilm recovered was not significantly different, observations from SEM imaging revealed a change in the nature of the observed EPS matrix. SEM imaging of *C. difficile* mono-culture biofilms revealed an EPS matrix that is filamentous and web-like in nature, whereas *Candida spp.* mono-culture biofilm has an EPS matrix that has a dense, granular appearance (Figure 5-13 a and b). The poly-microbial biofilm formed between *C. difficile*, *Staphylococcus spp.* and *Candida spp.*, shows all three closely interacting with each other, where both types of EPS matrix are present, indicated by the white arrows, and contribute to the biofilm (Figure 5-13 c and d). This indicates that although the amount of biofilm biomass or micro-organism growth may not have changed, the nature of the interactions, spatial organisation and the appearance EPS matrix have altered. It is acknowledged that the nature of the processing of biofilms samples for SEM imaging affects the EPS matrix; however, differences in the appearance of the matrix between the different cultures is clearly seen.

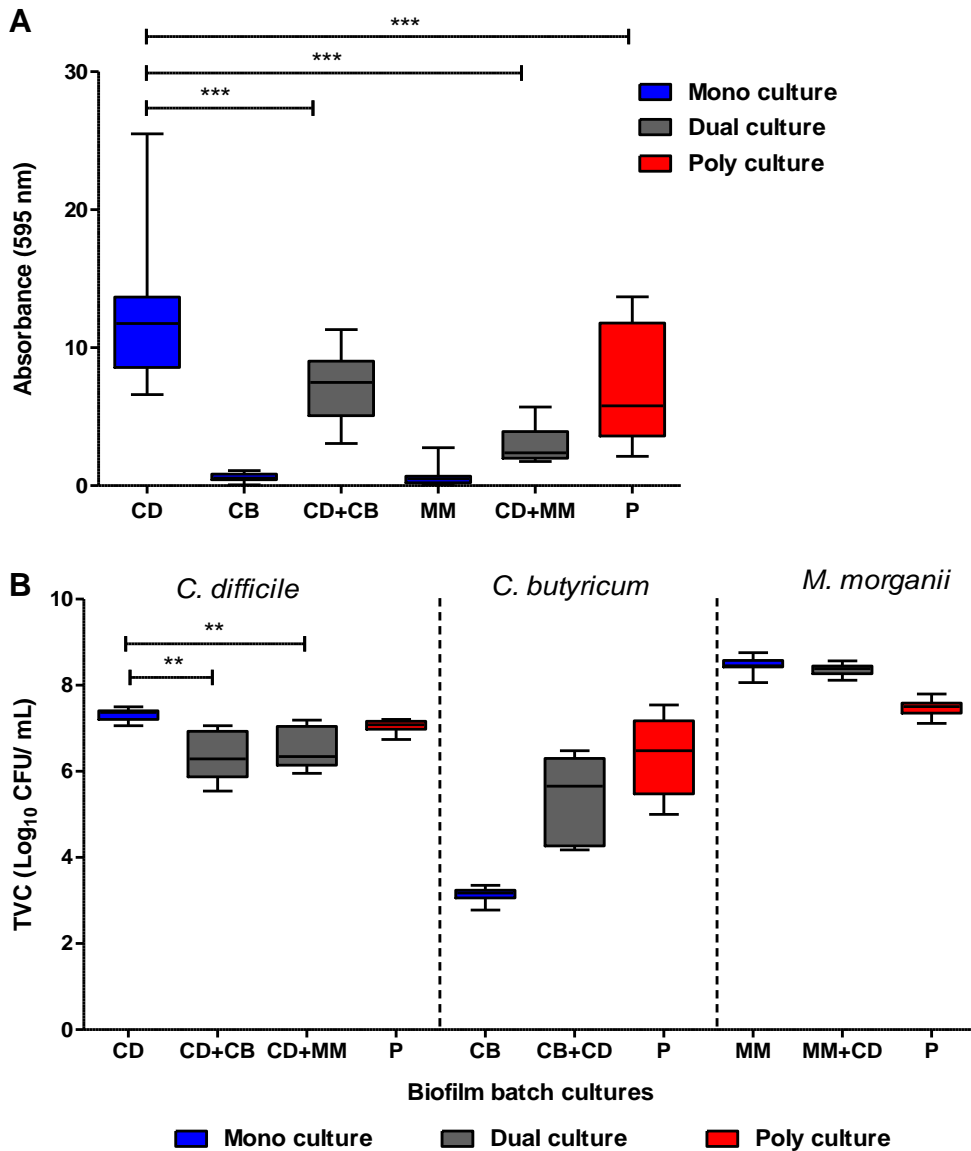


Figure 5-11 Poly-microbial biofilm culture of *C. difficile* with *C. butyricum* and *M. morganii*. Mono-culture (blue), co-culture (grey) and poly-culture (red) biofilms are shown for *C. difficile*, *B. butyricum* and *M. morganii* for (a) the crystal violet assay (absorbance – AU) and (b) total viable counts (log₁₀ CFU/mL). The crystal violet assay revealed a significant decrease in biofilm biomass in all cultures examined when compared to the *C. difficile* mono-culture ($***P \leq 0.002$), whereas the total counts revealed a significant decrease in *C. difficile* growth in both co-cultures but not in poly-culture ($**P \leq 0.01$). Results represent the median and interquartile range of three technical replicates of each of three biological replicates. CD- *C. difficile*, CB – *C. butyricum*, MM – *M. morganii*, P – poly-culture, TVC – total viable counts.

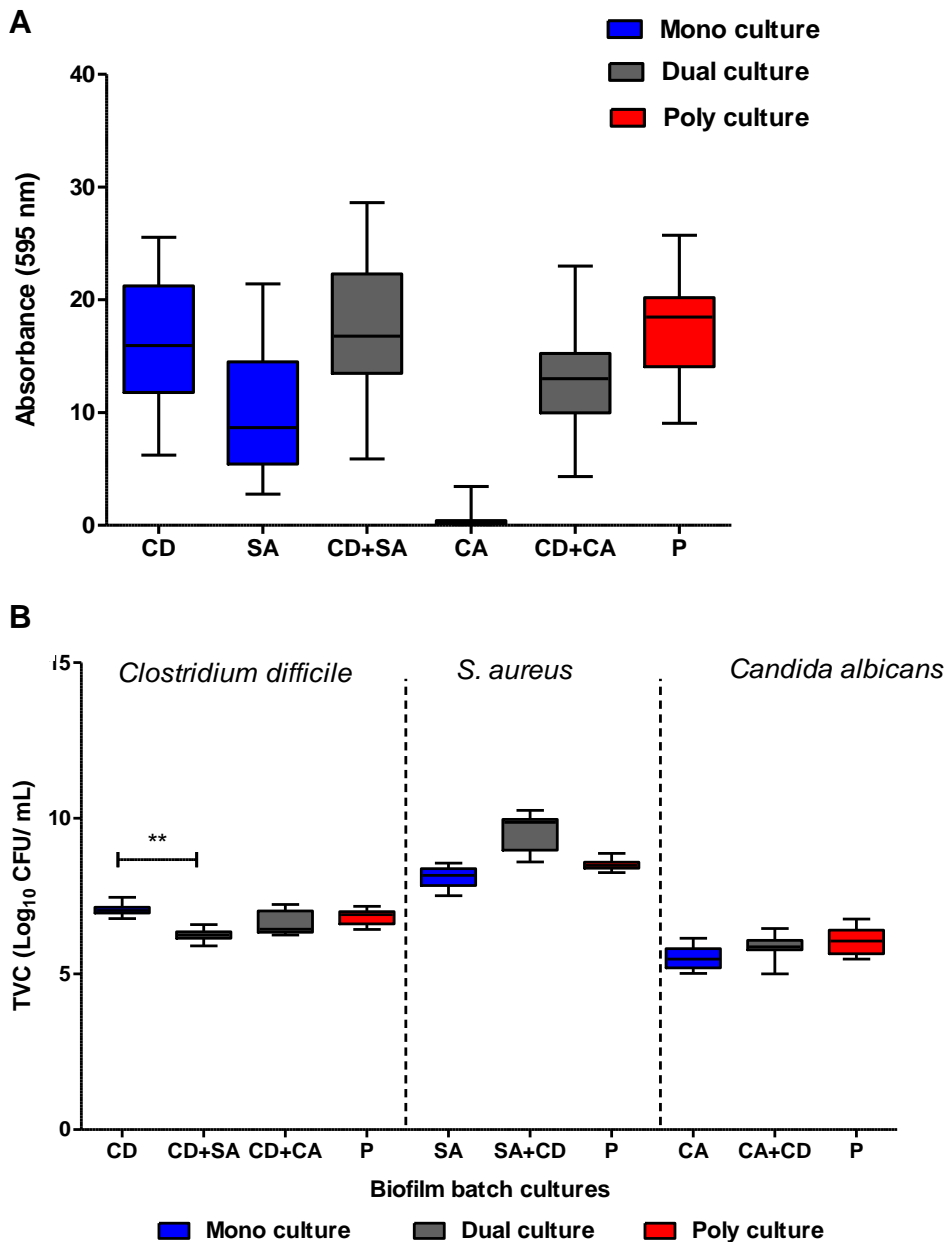


Figure 5-12 Poly-microbial biofilm culture of *Clostridium difficile* with *S. aureus* and *Candida albicans*. Mono-culture (blue), co-culture (grey) and poly-culture (red) biofilms are shown for *C. difficile*, *S. aureus* and *C. albicans* for (a) the crystal violet assay (absorbance – AU) and (b) total viable counts (log_{10} CFU/mL). There was a significant difference in *C. difficile* total counts in co-culture with *S. aureus* when compared to *C. difficile* mono-cultures (** $P \leq 0.01$). This reduction in *C. difficile* growth was not seen in the poly-culture. Results represent the median and interquartile range of three technical replicates of each of three biological replicates. CD- *C. difficile*, SA – *S. aureus*, CA – *C. albicans*, P – poly-culture, TVC – total viable counts.

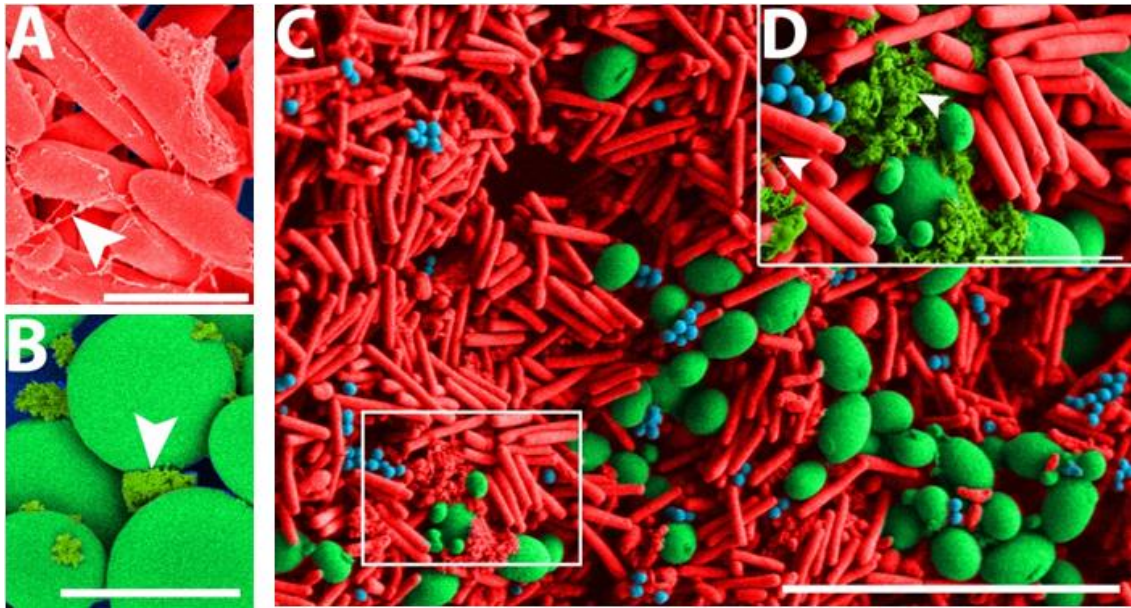


Figure 5-13 False-coloured scanning electron microscopy image of 3 day old mono- and poly-microbial biofilms. (a) *C. difficile* mono culture biofilm, scale bar 2µm) (b) *Candida sp.*, mono culture biofilm, scale bar 5µm and (c) poly-microbial biofilm comprised of *C. difficile* (red cells), *Staphylococcus spp.*, (blue cells) and *Candida spp.*, (green cells, (scale bar 20µm)). (d) insert of the extracellular matrix at a higher magnification, scale bar 2µm. Arrows show the different appearance of the extracellular matrix from *C. difficile* and *C. albicans*.

As the presence of *C. albicans* appeared to inhibit the ability of *S. aureus* to reduce *C. difficile* growth in the poly-culture biofilm, another poly-microbial culture was conducted that included *L. rhamnosus*, *C. albicans* and *C. difficile*. This was done to determine whether *C. albicans* could negate the effect seen in *L. rhamnosus* co-cultures as it did with *S. aureus*. In this poly-culture, there was a significant reduction of 8.7 AU in biofilm biomass when compared with *C. difficile* mono-culture biofilms ($p < 0.001$) (Figure 5-14 a). Co-culture TVCs with *L. rhamnosus* resulted in a 3.5 log₁₀ CFU/mL decrease in *C. difficile* counts ($p < 0.001$) whereas in the poly culture only a reduction of 0.3 log₁₀ CFU/mL was seen ($p > 0.05$) (Figure 5-14 b). These results indicate that although the biofilm biomass decreased, the presence of *C. albicans* in the biofilm prevented the reduction of *C. difficile* growth in the biofilm by *L. rhamnosus*, as seen in the poly-culture biofilm with *S. aureus*.

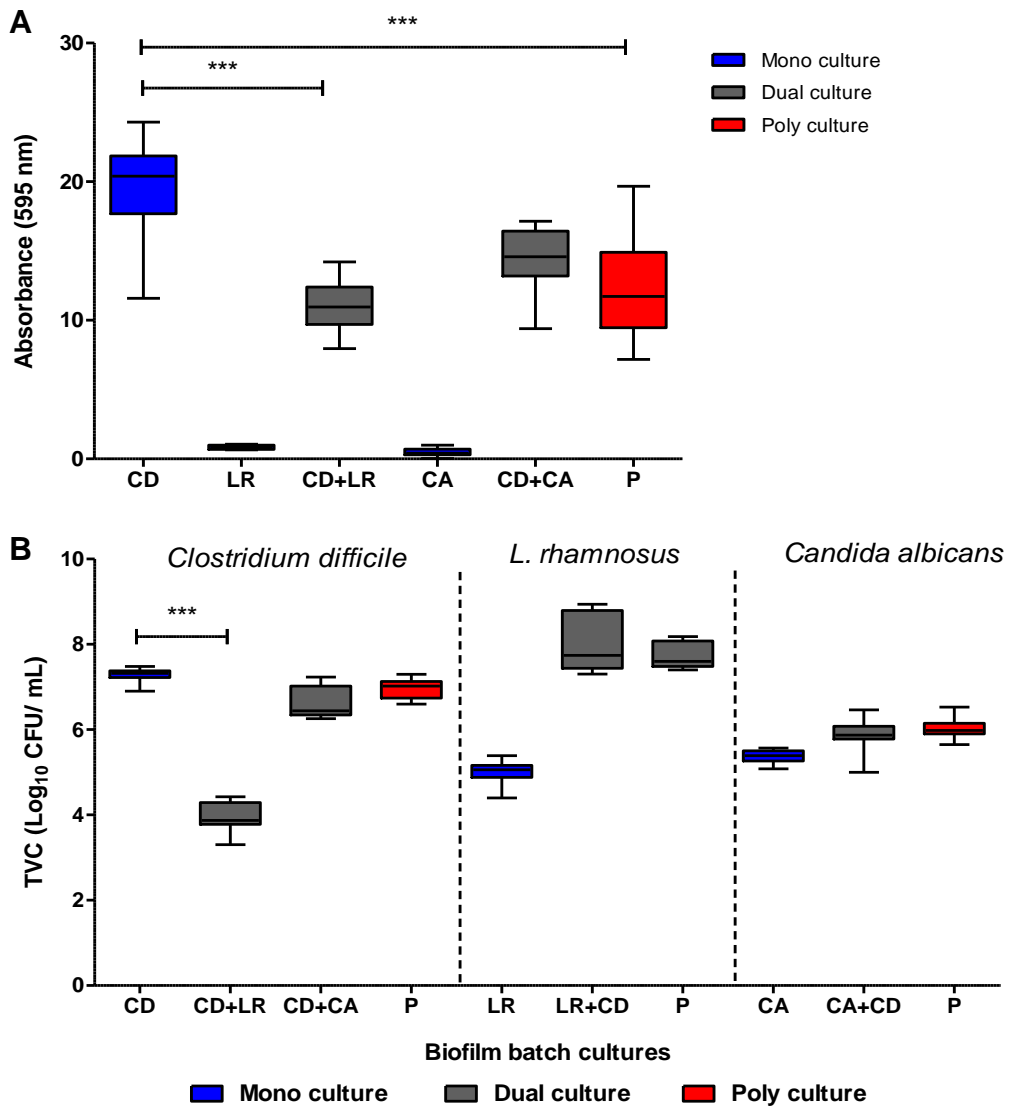


Figure 5-14 Poly-microbial biofilm culture of *Clostridium difficile* with *L.*

rhamnosus* and *Candida albicans*.** Mono-culture (blue), co-culture (grey) and poly-culture (red) biofilms are shown for *C. difficile*, *L. rhamnosus* and *C. albicans* for (a) the crystal violet assay (absorbance – AU) and (b) total viable counts (log₁₀ CFU/mL). There was a significant difference in absorbance (AU) between the *C. difficile* mono-culture when compared to the co-culture with *L. rhamnosus* and the poly-culture (p* ≤ 0.009). *C. difficile* total counts were reduced in co-culture with *L. rhamnosus* but not in poly-culture (***p* ≤ 0.009). Results represent the median and interquartile range of three technical replicates of each of three biological replicates. CD- *C. difficile*, LR – *L. rhamnosus*, CA – *C. albicans*, P – poly-culture, TVC – total viable counts.

5.4 Discussion

In this chapter, the effect of different microbial species on biofilm formation of *C. difficile* was investigated. The ability of *C. difficile* to form biofilms *in vitro* has been previously demonstrated (Dawson *et al.*, 2012, Đapa *et al.*, 2013, Semenyuk *et al.*, 2014), showing significant strain variation in the amount of biofilm formed, such as the increased biofilm formation of the 027 ribotype when compared with strain 630 (Đapa *et al.*, 2013). Using the CV assay to quantify biofilm biomass, it was demonstrated that strains 027 R20291 and 027 210 form robust biofilms on glass coverslips, with reduced turbidity of the culture medium and no fluid surface biofilm formation, in agreement with Dawson *et al.* (2012) and Đapa *et al.* (2013). The hypervirulent R20291 strain formed significantly more biofilm than the 210 strain. Biofilms from both strains were comprised of vegetative cells and spores, with R20291 forming significantly more spores than the 210 strain. Strain dependent variations in biofilm forming ability and composition have previously been demonstrated, with the hypervirulent strains generally forming larger biofilms than other clinical isolates (Đapa and Unnikrishnan, 2013, Hammond *et al.*, 2014, Pantaléon *et al.*, 2014), which highlights the potential of biofilms in virulence. Indeed, R20291 was found to display unique behaviour in a mouse model by forming numerous aggregates associated with the mucus layer (Lawley *et al.*, 2009a, Buckley *et al.*, 2011, Soavelomandroso *et al.*, 2017).

Donelli *et al.* (2012) was the first to show that *C. difficile* was capable of forming dual culture biofilms with another species, and that the interaction between *C. difficile* and *F. magna* changed the overall size and structure of the biofilm, indicating a co-operative relationship. *C. difficile* was also found as a minority member in the mucosal communities in a mouse model (Semenyuk *et al.*, 2015). During *in vitro* gut model experiments seeded with human faeces, the presence of *C. difficile* spores and vegetative cells within the multispecies biofilm was demonstrated, in agreement with Crowther *et al.* (2014b). Biofilms in nature exist as complex multispecies communities and the composition of these biofilms is integral to the function of the biofilm. Little is known about the relationship of different sessile species and *C. difficile*, including its recruitment into the biofilm and how variation in the microbial composition of mucosal

biofilm may alter virulence. In addition to identifying species present in the biofilm during CDI, it is also important to characterise the interactions of these organisms with *C. difficile* in a biofilm. To further understand the interaction of *C. difficile* with other commensal microorganisms in biofilms, a number of different microorganisms that co-existed with *C. difficile* as part of a multispecies biofilm from our gut models were isolated and identified. A selection of these microorganisms were then co-cultured alongside *C. difficile* to determine their impact on *C. difficile* biofilm formation.

As previous gut model results have shown a decrease in sessile *Bifidobacterium* spp., *Bacteroides* spp, and *Clostridium* spp. after antimicrobial therapy and leading to CDI, representative strains from each of these species were used in co-culture experiments with *C. difficile* to determine if they had an inhibitory effect on *C. difficile* biofilm formation. *B. longum* was consistently isolated during the gut models and has also been extensively studied as a potential probiotic strain to prevent and treat antibiotic-associated diarrhoea (AAD) (Valdes-Varela *et al.*, 2016) and therefore we used this bacterium in a number of co-culture and poly-culture experiments. Overall, *C. difficile* co-culture with *B. longum* resulted in a decrease in both biofilm production and *C. difficile* cell and toxin production in the biofilm. Similar results were seen with *L. rhamnosus*. Both *B. longum* and *L. rhamnosus* have been suggested as potential probiotic strains due to their ability to reduce the expression of *C. difficile* toxin; however, in contrast to the results presented here, there was no reduction in *C. difficile* growth in co-culture (Trejo *et al.*, 2010). It was believed that the production of organic acids (and so reduced media pH) may account for the inhibitory effect of these two bacteria. In line with this theory, experiments here examining *C. difficile* biofilm formation in culture media with various pH levels revealed diminished *C. difficile* biofilm production and vegetative cell proliferation in an acidic environment. By neutralising the CFS from overnight cultures of *B. longum* and *L. rhamnosus*, this pH effect was negated. Co-culture of *C. difficile* with *L. rhamnosus* CFS and neutralised CFS had similar effects, with a reduction in biofilm formation but no change in the number of *C. difficile* cells. As no significant reductions were seen in the number of sessile cells observed in the absence of *L. rhamnosus*, the decrease in CV absorbance could be due to a decrease in biofilm biomass, specifically

EPS production. This indicated that secreted factors may affect the *C. difficile* biofilm biomass; however, viable *L. rhamnosus* cells are required to reduce the growth of *C. difficile* in the biofilm. CFS and nCFS of *B. longum* had no effect on *C. difficile* biofilm formation or cell recovery and therefore the reduction of *C. difficile* biofilm formation and growth by *B. longum* is most likely mediated by the presence of viable cells and not metabolic by-products. This confirms results by Valdes-Varela *et al.* (2016) who showed that viability of *B. longum* is required to exert protective effects against clostridial toxins.

Another probiotic strain that we used in co-culture experiments was *C. butyricum*. *C. butyricum* has been previously shown to reduce the toxicity of *C. difficile* CFS (Woo *et al.*, 2011) and was found to be antagonistic to CDI in mice (Kamiya *et al.*, 1997). Clinical trials using concomitant *C. butyricum* with antibiotics resulted in reduced disturbance in commensal flora and subsequently reduced AAD in patients (Seki *et al.*, 2003). This protective effect to the commensal flora was also seen when *C. butyricum* was used after *Helicobacter pylori* eradication therapy and in the treatment and prevention of on Enterohemorrhagic *Escherichia coli* (EHEC) 0157:H7, resulting in less disruption to obligate anaerobic populations and subsequent reduced levels of AAD (Takahashi *et al.*, 2004, Imase *et al.*, 2008). *C. butyricum* has also been shown to support the growth of endemic *Lactobacillus* populations (Ichikawa *et al.*, 1999). The results presented here suggest that *C. butyricum* is able to reduce *C. difficile* biofilm formation and its growth in a biofilm, providing another potential mechanism of *C. butyricum* antagonism to CDI.

As *Bacteroides* was highlighted as a potential key genus in CDI during the *in vitro* gut models, *B. thetaiotaomicron* was selected as a representative species from this genus. *B. thetaiotaomicron* was one of the predominant strains isolated in the sessile populations, which is consistent with Macfarlane *et al.* (2005) who found that *Bacteroides* was a major genus in mucosal biofilms. Co-culture of *B. thetaiotaomicron* with *C. difficile* resulted in both a decrease in biofilm production and *C. difficile* growth in the biofilm. Similar results were reported by Slater *et al.* (2019), who found that the presence of *Bacteroides fragilis* resulted in a decrease in biofilm biomass and *C. difficile* cell numbers in co-culture biofilms, further supporting the theory that the *Bacteroides* genus plays a potential role in the prevention of CDI. In contrast to results from

biofilm formation and growth within a biofilm, *B. thetaiotaomicron* has been found to be beneficial for planktonic *C. difficile* germination and growth after antimicrobial therapy in mice (Ferreya *et al.*, 2014). This relationship is based on *B. thetaiotaomicron* producing high levels of the metabolite succinate (Curtis *et al.*, 2014). Succinate is not normally seen in a healthy gut due to cross-feeding of the commensal flora; however, perturbations of the gut facilitates succinate accumulation which has been implicated in *C. difficile* spore germination (Lawley *et al.*, 2009b). The complexity of this system was not replicated here, which highlights an important danger of drawing conclusions from simple batch culture experiments, as they are unable to account for the dynamics seen in a complex systems such as antimicrobial-induced dysbiosis and its subsequent metabolic shifts.

One of the main limitations of the study presented here was the use of the same culture conditions for each of the microorganisms. For optimum biofilm formation, appropriate growth conditions should be established for each microorganism studied, including the choice of growth medium, substratum, time of incubation and environment (O'Toole, 2011). Here, conditions optimised for *C. difficile* growth were used such as anaerobic incubation, a glass substratum and BHISC medium, which could have had an impact on the ability of the other microorganisms selected to form a biofilm. This was reflected in the relatively poor biofilm formation of *K. pneumoniae* and *M. morgani* demonstrated here, in contrast to other studies with aerobic growth on a plastic substratum (Seifi *et al.*, 2016, Zheng *et al.*, 2018). In an attempt to provide a culture medium more reflective of the gut model that the strains were isolated from, the complex growth medium from the gut model experiments was attempted in batch culture biofilms; however, the mono culture control biofilm did not form well and increased sedimentation from the medium interfered with CV staining (data not shown). Additionally, the strains selected were isolated from the *in vitro* gut models and therefore it is possible that they are more adapted to living as a community and not alone in a biofilm. Conversely, the particular strains used may not have been proficient biofilm producers.

Although limited, data from these simple batch culture experiments can offer important insight into the interactions in biofilms. Co-culture experiments of *C. difficile* with *L. rhamnosus* resulted in decrease in biofilm biomass and a

significant reduction in *C. difficile* growth in the biofilm; however, in poly-cultures with the addition *C. albicans*, the reduction of biofilm biomass was still seen but the suppression of *C. difficile* growth was completely lost. This was also seen with *S. aureus* cultures with *C. difficile*, where the effect was lost in poly-culture with *C. albicans*. Biofilm co-culture with *C. albicans* has previously been shown to confer an advantage to *C. difficile* survival in aerobic conditions (van Leeuwen *et al.*, 2016). *C. difficile* metabolism was also shown to influence *C. albicans* virulence and mode of growth. This illustrates the importance of studying the community dynamics and interspecies interactions within biofilms and how the different composition of microorganisms can influence the characteristics of the biofilm. Thus, data from experiments examining the effects of single bacterial species, labelled as probiotics, on *C. difficile* can be misleading once the interactions in complex community scenarios are considered.

In conclusion, the interactions of selected commensal microorganisms and their effect on *C. difficile* biofilm formation in batch co-culture experiments was examined. Using mixed microbial biofilms from *in vitro* gut models simulating CDI, target commensal microorganisms originating in these sessile communities were isolated and identified. In co- and poly-microbial biofilms, selected microorganisms were able to either increase or decrease *C. difficile* biofilm biomass, as well as reduce *C. difficile* growth within the biofilm. *B. longum* and *L. rhamnosus* were shown to reduce *C. difficile* biofilm formation, and reduce growth and toxin production within the biofilm. Poly-culture experiments with *B. longum* and *B. thetaiotaomicron* displayed a greater reduction in biofilm formation than seen in individual co-culture biofilms. Interactions of *C. difficile* with *L. rhamnosus* and *B. longum* were further characterised by neutralising the possible antagonistic effect of metabolic organic acids, demonstrating that cell viability was required to mediate the reduction of *C. difficile* biofilm formation and growth by both *B. longum* and *L. rhamnosus*. The microorganisms *S. warneri*, *F. polymorphum* and *C. paraputrificum* were also demonstrated to increase *C. difficile* biofilm formation. SEM imaging confirmed close interactions between the different species in poly culture biofilms, with the sharing of EPS matrix to anchor the different species together in a dense and heterogeneous layer. These results demonstrate that

C. difficile interacts with different members of the sessile community, which likely influences its growth and virulence in biofilms.

Chapter 6 Sessile *C. difficile* cells can contribute towards recurrent disease

6.1 Background

The incidence of disease recurrence following antimicrobial therapy occurs in up to 20 – 30% of CDI cases (Kelly and LaMont, 2008, Cornely *et al.*, 2012b) with the risk of further recurrence increasing with each subsequent episode (McFarland *et al.*, 1994, McFarland *et al.*, 2002). In the majority of rCDI cases, it was found that disease was caused by the strain responsible for the initial episode, indicating disease relapse as opposed to reinfection with a different strain (Durovic *et al.*, 2017). This suggests that *C. difficile* can occupy a protective niche whereby antimicrobial therapy is ineffective. Biofilms represent such a niche and *C. difficile* has been demonstrated to form a biofilm *in vitro* (Dawson *et al.*, 2012, Donelli *et al.*, 2012, Đapa *et al.*, 2013, Hammond *et al.*, 2014, Semenyuk *et al.*, 2014) and *in vivo* (Buckley *et al.*, 2011, Semenyuk *et al.*, 2015, Soavelomandroso *et al.*, 2017), displaying an altered gene expression profile from planktonic cells (Poquet *et al.*, 2018). *C. difficile* can also interact with commensal microorganisms as part of a multispecies biofilm (Donelli *et al.*, 2012, Crowther *et al.*, 2014a, Slater *et al.*, 2019) which has also been demonstrated here in continuous (Chapter 3 and 4) and batch biofilm cultures (Chapter 5).

A biofilm offers the residing microorganisms protection from external stress conditions such as the hosts immune response and antimicrobial treatment, making biofilm-associated infections particularly resilient. Increasing evidence suggests an important role for biofilms in chronic infections, especially in disease persistence and relapse. It is believed that roughly 65% of all bacterial infections and 80% of chronic infections are associated with biofilm formation (Percival *et al.*, 2015, Jamal *et al.*, 2018). Often these infections are characterised by their slow, progressive nature and are inherently difficult to treat, requiring aggressive and sustained antimicrobial therapy. This contrasts with the relatively rapid onset of acute infections resulting from infection with planktonic bacteria that are, in general, more responsive to antimicrobials (Bjarnsholt, 2013). Indeed, biofilms were found to be significantly tolerant to

antimicrobials when compared with their planktonic counterparts, and this reduced susceptibility contributes to the persistence of biofilm-associated infections (Nickel *et al.*, 1985, Stewart, 2002, Ahmed *et al.*, 2018). Dapa *et al.* (2013) demonstrated that three day old hyper-virulent *C. difficile* R20291 strain biofilms were able to tolerate exposure to vancomycin at 100 times the MIC usually effective against the planktonic cells. It was also found that exposure to sub-inhibitory levels of antimicrobial agent may promote increased biofilm formation in *C. difficile* (Vuotto *et al.*, 2015).

Biofilms have been associated with dental infections (Larsen and Fiehn, 2017), chronic wounds (Davis *et al.*, 2008), cystic fibrosis infections (Hoiby, 2011), chronic otitis media (Post, 2001), urinary tract infections (Hatt and Rather, 2008), infections involving indwelling devices (Donlan, 2001b) and they have also been implicated in chronic *Helicobacter pylori* infection (Hathroubi *et al.*, 2018). The life-cycle of biofilms include a number of highly regulated stages, including attachment, aggregation with EPS production, maturation and finally dispersal. Dispersal is characterised by an active phenotypic switch to a planktonic-like state and the subsequent release of free-floating bacteria or bacterial aggregates and cell clusters from either mono or mixed species biofilms (Stoodley *et al.*, 2001, Sauer *et al.*, 2004). This facilitates the dissemination of bacteria to colonise a new habitat leading to the persistence of infection (Kaplan, 2010).

6.1.1 Rationale

The mucosal populations in the GI tract have gathered much interest in health and disease (Macfarlane and Dillon, 2007), particularly the disruption and subsequent dispersal of biofilm-associated cells leading to disease development (Buret *et al.*, 2019). The chronic nature of rCDI and its recalcitrance to antimicrobial therapy leads to the speculation of biofilm involvement; however, biofilms have not yet been proven as a cause of rCDI. In our gut models, we found that vancomycin and microbiome-based therapies reduced planktonic *C. difficile*; however, these therapies failed to eradicate *C. difficile* cells from the biofilm. This was consistent with findings from Crowther *et al.* (2014a). Here, we set out to determine whether a biofilm harbouring *C. difficile* cells has the potential to disperse from the biofilm and repopulate the planktonic phase, which could lead to the relapse of CDI.

6.2 Materials and Methodology

Three gut models were used in this experiment to determine whether *C. difficile* spores originating in the biofilm can lead to repopulation of the planktonic phase and subsequent induction of CDI. Briefly, multispecies biofilms containing *C. difficile* cells were transplanted from a donor model, model D, into a susceptible recipient model, model R. A control model, model C, was run parallel with model R and dosed with *C. difficile* spores as a positive control model and to compare CDI from biofilm and planktonic origins.

6.2.1 Donor screening and slurry preparation

In this experiment, two separate faecal slurries were prepared; one for the donor model and another for the control and recipient models. Donors were recruited and screened as in section 2.2.2 and 2.2.3. Each slurry was freshly prepared at the start of each gut model using either 5 or 4 faecal donors for the donor model and the control/recipient models, respectively. The slurries were prepared by diluting the faeces to 10% (W/V) solution using pre-reduced PBS. The suspension was emulsified and filtered as per section 2.2.4, and approximately 160 mL was added to each vessel.

6.2.2 The *in vitro* gut model set up

All three models were set up according to section 2.2.8 with the exception of models R and C in which vessel two was comprised of biofilm vessels (Figure 6-1). This was done to accommodate the transplantation of biofilm rods from model D. *C. difficile* spores are normally added to vessel one, allowing time for colonisation throughout the model; however, in this case it was not possible to perform the biofilm transplantation in vessel one due to different volumes of the vessels. Additionally, transplanting the biofilm into vessel two and enumerating the lack of *C. difficile* populations in vessel one ensured there was no cross-contamination between the models R and C, thus acting as an internal control.

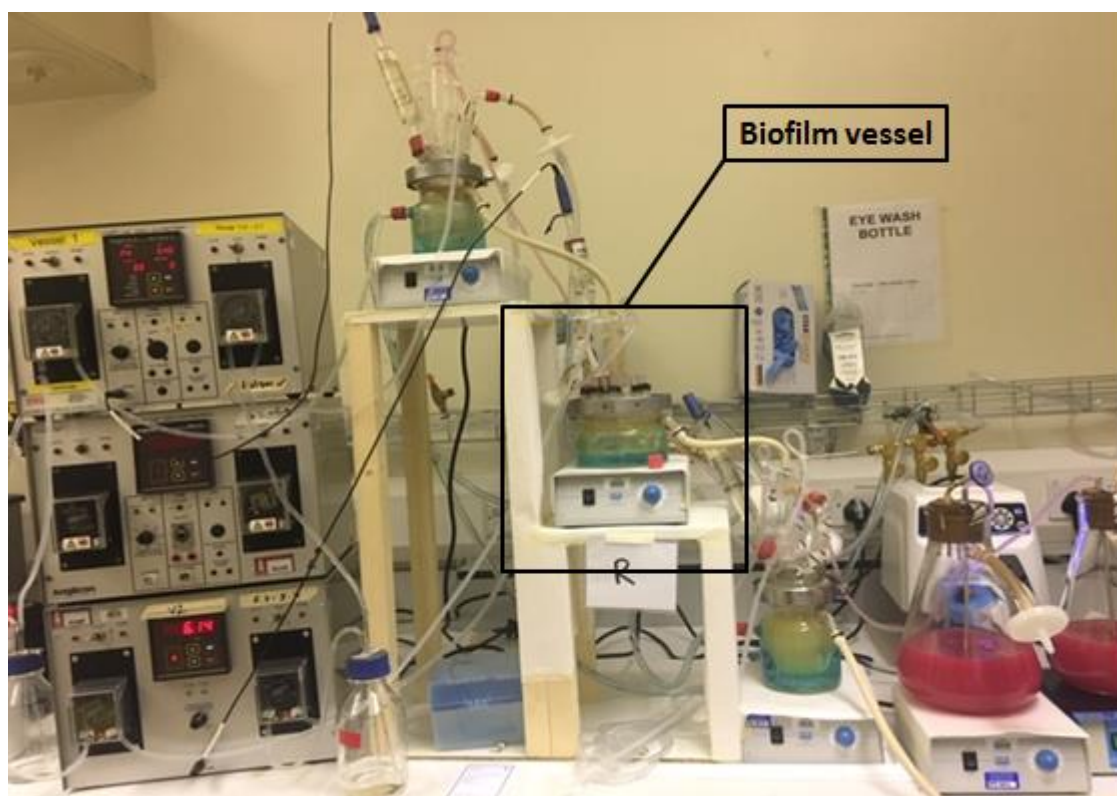


Figure 6-1 The Recipient and Control *in vitro* gut model set up. The recipient (model R) and control model (model C) were set up using a biofilm vessel for vessel two to facilitate the biofilm transplantation into model R.

6.2.3 Experimental design

The models followed the timeline in Figure 6-2 and in line with section 2.2.10. The donor model was set up first and had a two week steady state period followed by dosing with *C. difficile* spores (section 2.2.7) into vessel one. This was left for 7 days to ensure colonisation resistance in the model. A further spore dose was added to replenish the *C. difficile* spore reservoir before clindamycin dosing commenced for 7 days. The model was then monitored for the development of CDI using *C. difficile* total viable and spore counts, as well as cytotoxin testing (section 2.2.11 and 2.2.16). Once the model reached peak CDI, a sample from the biofilm was taken to enumerate the sessile *C. difficile* populations (one biofilm rod, processed according to section 2.2.12), before vancomycin was added to the model for 7 days.

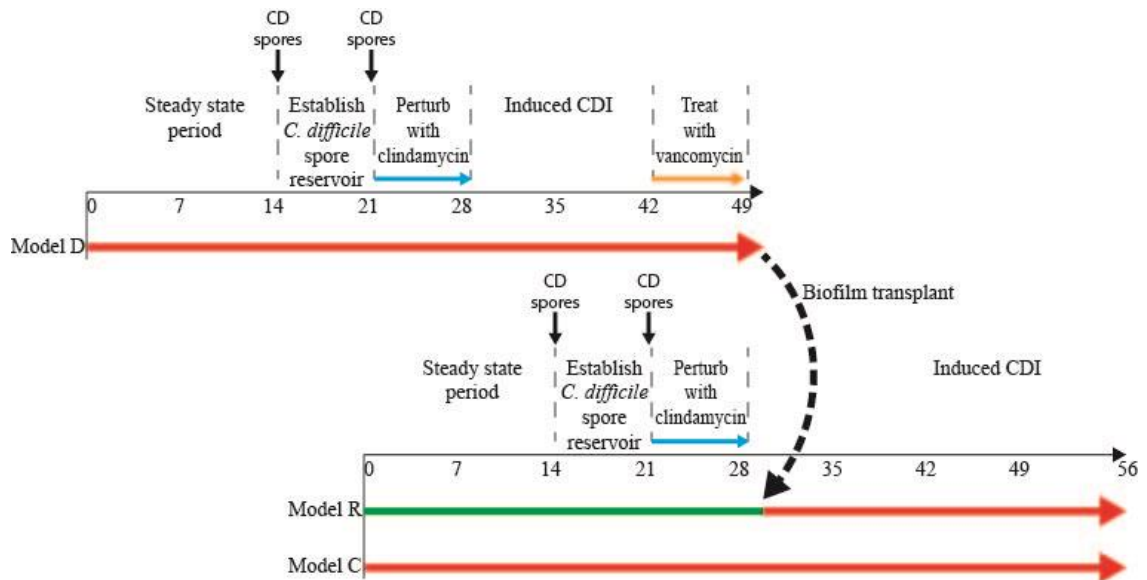


Figure 6-2 Model timeline of the biofilm transplant experiment. The biofilm support structures with associated multispecies biofilm were transplanted from Model D (top) into the *C. difficile* naïve (green line) model R, which had been exposed to clindamycin (blue arrow) to create an environment susceptible to *C. difficile* growth. Model C was run in parallel with Model R and infected with *C. difficile* spores as a positive control.

Models C and R were set up with a fresh faecal slurry when model D started clindamycin dosing. As per section 2.2.10, both models had a two week steady state period followed by two doses of *C. difficile* spores being added to vessel one of model C only, one week apart. Model R did not receive a *C. difficile* spore dose (indicated by the green arrow, Figure 6-2). Both models were then dosed with clindamycin for 7 days as per 2.2.10 to create an environment susceptible to CDI. To investigate the ability of sessile *C. difficile* to repopulate the planktonic phase and induce CDI, the biofilm from model D, harbouring *C. difficile* cells after vancomycin dosing, was transferred to the recipient model (Figure 6-3). Planktonic *C. difficile* levels in Model D dropped to below the limit of detection with vancomycin treatment, ensuring that the *C. difficile* transferred originated from the biofilm. The biofilm vessel lid (vessel three) from model D, and associated biofilm support structures, was carefully removed and transferred to the biofilm vessel (vessel two) of Model R (Figure 6-2 and Figure 6-3). At the time of biofilm rod transplantation, a sample of the biofilm was removed from the pH probe in vessel three of Model D to enumerate total *C.*

difficile biofilm populations post vancomycin treatment. This sample was processed according to section 2.2.12. Previously, biofilm samples from the pH probes and vessels walls were enumerated and found to be comparable to those from the biofilm support structures (results not shown). All planktonic populations were sampled as per section 2.2.11, on every alternate day from model commencement until the *C. difficile* reservoir stage and daily thereafter until biofilm transplantation. After biofilm transplantation, only *C. difficile* TVCs and spores were enumerated on every alternate day until model completion. Results from Model R were compared with Model C to determine the difference in CDI induction with *C. difficile* originating from the biofilm and from the planktonic phase (exogenous *C. difficile*). The *C. difficile* cytotoxin assay and antimicrobial bioassays were performed on all models as described in sections 2.2.16 and 2.2.17, respectively.

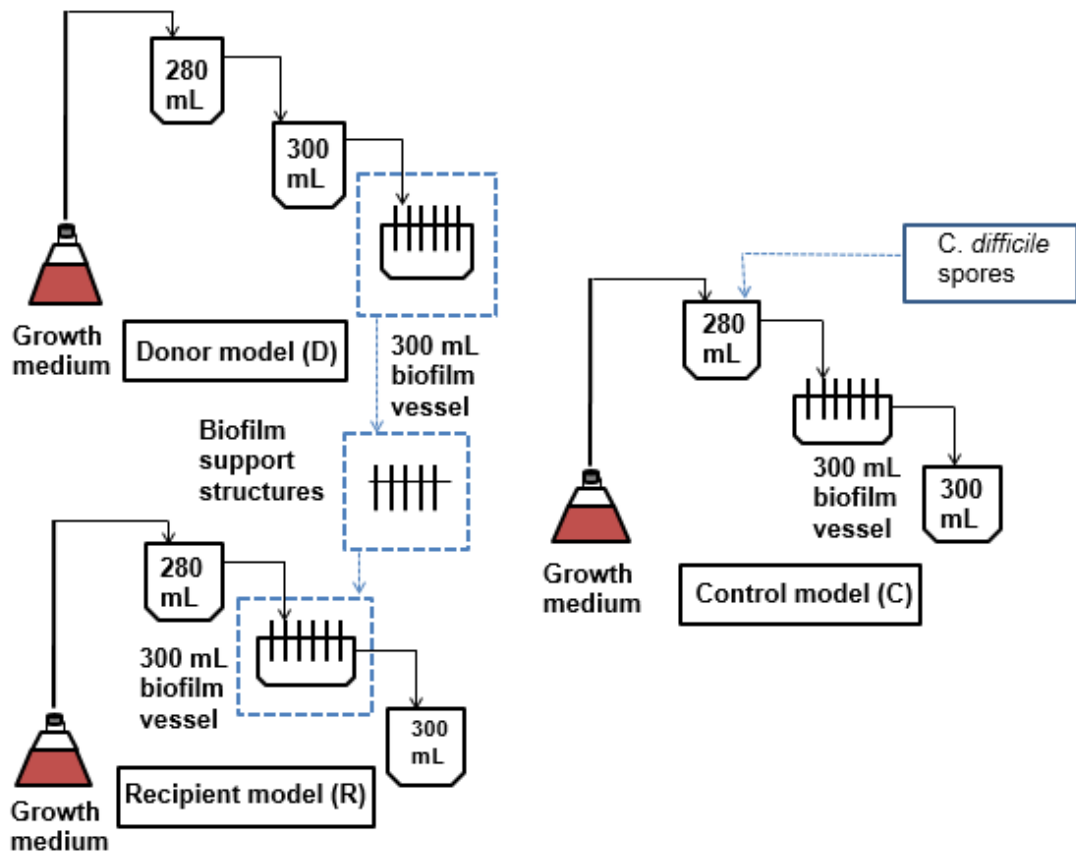


Figure 6-3 Diagram of the gut model set-up for the donor model, the recipient model and the control model, illustrating the transplantation of biofilm support structures. The biofilm support structures, located in vessel three of the donor model (top left), were transplanted into the second vessel of the recipient vessel (bottom left) after vancomycin treatment. The control model (right) was dosed with *C. difficile* spores into vessel one.

6.3 Results

To investigate the ability of *C. difficile* originating solely from a biofilm to re-populate the planktonic phase and induce CDI, a series of three gut models consisting of a biofilm donor model, a biofilm recipient model and a control model were used. The donor model was run to model CDI, mediated by clindamycin induced dysbiosis of the microbial communities, followed by the subsequent treatment with vancomycin to generate an environment susceptible to rCDI. This model was equipped with a vessel that enabled the formation and removal of the multispecies biofilm containing *C. difficile* cells for transplantation into the susceptible recipient model.

6.3.1 Donor model

Commensal planktonic populations were monitored throughout the Model D timeline. Following a two week steady state period in which populations were allowed to equilibrate, two doses of *C. difficile* spores were added to the model, 7 days apart, to ensure colonisation resistance in the model. The antimicrobial effect of clindamycin was consistent with previous models (Chapters 3 and 4), namely, *B. fragilis* gp., *Clostridium* spp., *Bifidobacterium* spp., and *Lactobacillus* spp., populations were reduced and an increase in total facultative anaerobes, LF Enterobacteriaceae and *Enterococcus* spp.. All populations recovered to pre-antibiotic levels soon after clindamycin cessation, with the exception of *Bifidobacterium* spp. that recovered more gradually and remained approximately 1 - 1.5 log₁₀ CFU/mL lower than steady state levels throughout CDI (Figure 6-4).

C. difficile total viable counts, spores and cytotoxin were closely monitored for evidence of CDI. Divergence of *C. difficile* total and spore counts were seen 7 days post-clindamycin, reaching peak levels of 5.5 log₁₀ CFU/mL with spore and TVC divergence of 1.5 log₁₀ CFU/mL, with the subsequent detection of *C. difficile* toxin reaching peak levels of 3 RU 3 weeks post-clindamycin (Figure 6-5 a).

At peak CDI, one biofilm rod was removed to enumerate the *C. difficile* populations in the multispecies biofilm. Based on the counts from this sample, *C. difficile* was found to be associated with the biofilm with levels of 5.32 log₁₀

CFU/g biofilm biomass (Figure 6-5 b), consistent with data from previous biofilm models (Chapter 3 and 4).

After peak CDI was assumed, the model was dosed with vancomycin for 7 days, causing a profound effect on the planktonic microbiota, with *B. fragilis* gp. recoveries reducing by approximately 8 log₁₀ CFU/mL with *Bifidobacterium* spp. and *Clostridia* spp. dropping below the limit of detection (Figure 6-4 a).

Planktonic *C. difficile* total and spore counts also dropped below the limit of detection after vancomycin treatment with undetectable levels of cytotoxin activity (Figure 6-5 a). These results were consistent with previous models (Chapter 3 and 4). Three days after vancomycin cessation, the biofilm rods from vessel 3 were transplanted into the recipient model. At the time of transplantation, a sample of biofilm was removed from the pH probe in vessel 3 of model D and *C. difficile* populations enumerated (Figure 6-5 c). Vancomycin treatment had caused an approximate 2 log log₁₀ CFU/g decrease in biofilm *C. difficile* counts, with the level of *C. difficile* in the biofilm being transplanted approximately 3.6 log₁₀ CFU/g biofilm weight. There were 15 biofilm rods remaining at the time of transplantation and based on average biofilm weight per rod across previous models, it was determined that approximately 1.6 g of biofilm was transferred from Model D to model R, with an estimated total amount of approximately 3.8 log₁₀ CFU *C. difficile* transferred.

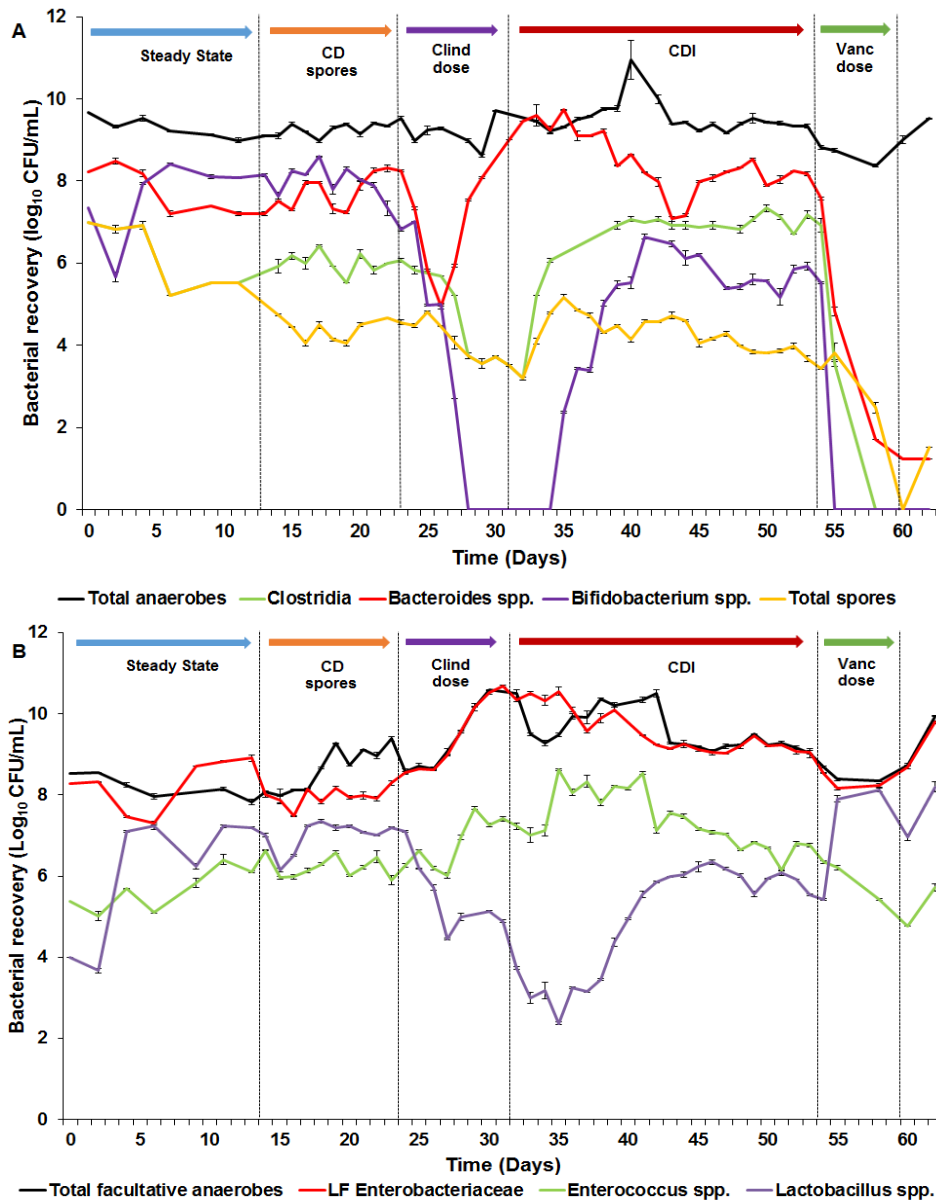


Figure 6-4 Enumeration of planktonic populations in the *in vitro* Donor gut model. (a) Bacterial enumeration of total anaerobes (black), *B. fragilis* gp. (red), *Clostridium* spp. (green), *Bifidobacterium* spp. (purple), and spores (yellow). (b) Bacterial enumeration of total facultative anaerobes (black), lactose fermenting (LF) Enterobacteriaceae (red), *Enterococcus* spp. (green), and *Lactobacillus* spp. (purple). Data demonstrates the disruption to the microbial populations when treated with clindamycin (purple arrow) and vancomycin (green arrow). Data shown are the mean \log_{10} CFU/mL \pm standard error from three technical replicates per day of the model timeline of one biological replicate. Different model stages are separated by vertical broken lines. CD – *C. difficile*, Clind – clindamycin, Vanc – vancomycin, CDI – *C. difficile* infection.

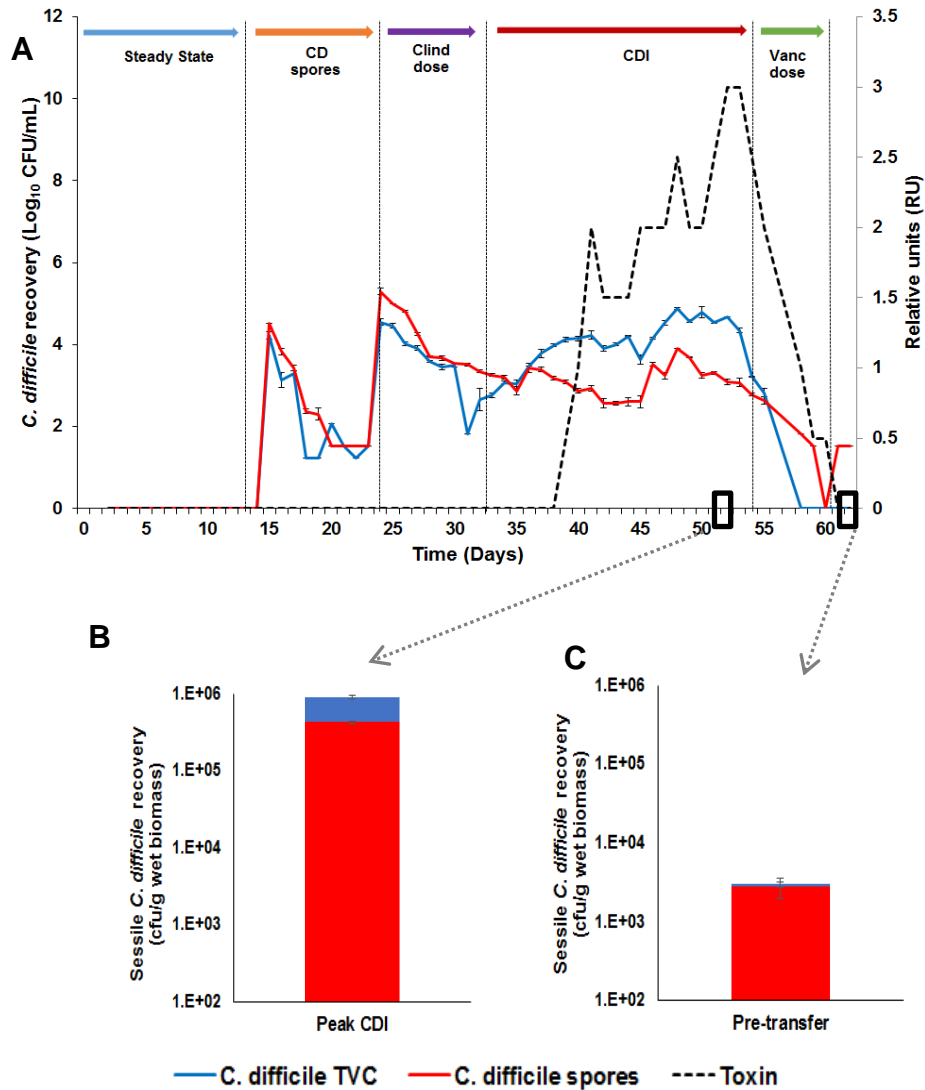


Figure 6-5 Enumeration of planktonic and sessile *C. difficile* total and spore counts in the *in vitro* Donor gut model. Enumerations of *C. difficile* spores (red) and total viable counts (blue) are represented the Donor model in mean log₁₀ CFU/mL and log₁₀ CFU/g ± standard error (left axis). *C. difficile* toxin (black broken line) is represented as log reciprocal units (RU, right axis). (a) Enumeration of planktonic *C. difficile* populations. Total and spore counts drop below the limit of detection after vancomycin instillation. (b) Enumeration of sessile *C. difficile* populations during peak CDI. (c) Enumeration of sessile *C. difficile* prior to biofilm transfer, showing predominantly spore populations remaining. Data shown are from three technical replicates per day of the model timeline from one biological replicate CD – *C. difficile*, Clind – clindamycin, Vanc – vancomycin, CDI – *C. difficile* infection.

6.3.2 Recipient Model (R) and Control Model (C)

The recipient model had an extended steady state period compared with the other two models as there was no *C. difficile* spore reservoir phase.

Populations stabilised around 6 days after model set up and remained so for the duration of steady state. Model C was given two doses of *C. difficile* spores, one week apart, before both models began clindamycin dosing. Despite a drop in *Clostridium* spp. and *Bifidobacterium* spp. leading up to clindamycin treatment, *C. difficile* spores showed no sign of germinating during the reservoir phase in Model C, suggesting colonisation resistance was established.

Bacterial recoveries from both models were comparable through this period, entering clindamycin treatment at similar levels. In both models, there was a decrease in *Clostridia* and *Bifidobacterium* recoveries; however, this did not compromise the colonisation resistance established. Furthermore, this demonstrated that the introduction of *C. difficile* spores to model C did not affect the microbiota. This was consistent with results from previous gut model experiments (Chapters 3 and 4). Clindamycin was introduced to both models, resulting in disruption to the commensal microflora. This was characterised by an approximately 3 - 3.5 log₁₀ CFU/mL reduction in *Clostridium* spp. and the *Bifidobacterium* spp. dropping to below the limit of detection in both models (Figure 6-6). Increases in bacterial recoveries for total facultative anaerobes, LF Enterobacteriaceae and *Enterococcus* spp. of approximately 1 log₁₀ CFU/mL were seen in both models (Figure 6-7). Similar levels of clindamycin were seen in both models, with peak levels of 128.3 mg/L and 120.0 mg/L detected in vessel one on day 6 of dosing for Model R and Model C, respectively. Four days after clindamycin cessation, the biofilm rods containing *C. difficile* cells associated with the multispecies biofilm were transplanted from Model D into Model R. From this point in both models, only *C. difficile* planktonic populations were monitored (Figure 6-8 and Figure 6-9).

In Model C, acting as a positive control in this experiment, *C. difficile* total and spore populations were recovered at equal measures of approximately 4 log₁₀ CFU/mL in each vessel during the *C. difficile* reservoir phase. Evidence of *C. difficile* spore germination was seen 10 days after clindamycin cessation in vessel three, with *C. difficile* TVCs reaching peak levels of 6.6 log₁₀ CFU/mL. *C. difficile* cytotoxin was detected 18 days post-clindamycin, with peak levels of

2 RU detected 21 days post-clindamycin, indicating active CDI (Figure 6-9). Germination and toxin production with similar levels were also seen in vessel 2 and although *C. difficile* was recovered from vessel one, no evidence of CDI in this vessel was found (data not shown). In Model R, vessel one remained *C. difficile* free for the entire experiment (data not shown). Transient *C. difficile* was recovered from vessel two approximately 5 days after the biofilm transplant, with evidence of stable planktonic population recoveries 15 days after transplantation from 1.5 – 3.4 log₁₀ CFU/mL (Figure 6-8 a). *C. difficile* was recovered from vessel three approximately 10 days after transplantation, with evidence of germination seen 15 days post-transplant with a 1 log₁₀ CFU/mL divergence in TVC and spore recoveries. This was accompanied with the detection of *C. difficile* cytotoxin at 0.25 RU corresponding with peak TVC recoveries of approximately 4 log₁₀ CFU/mL (Figure 6-8 b). Peak *C. difficile* recovery in Model R was approximately 3 log₁₀ CFU/mL lower than those recovered in Model C.

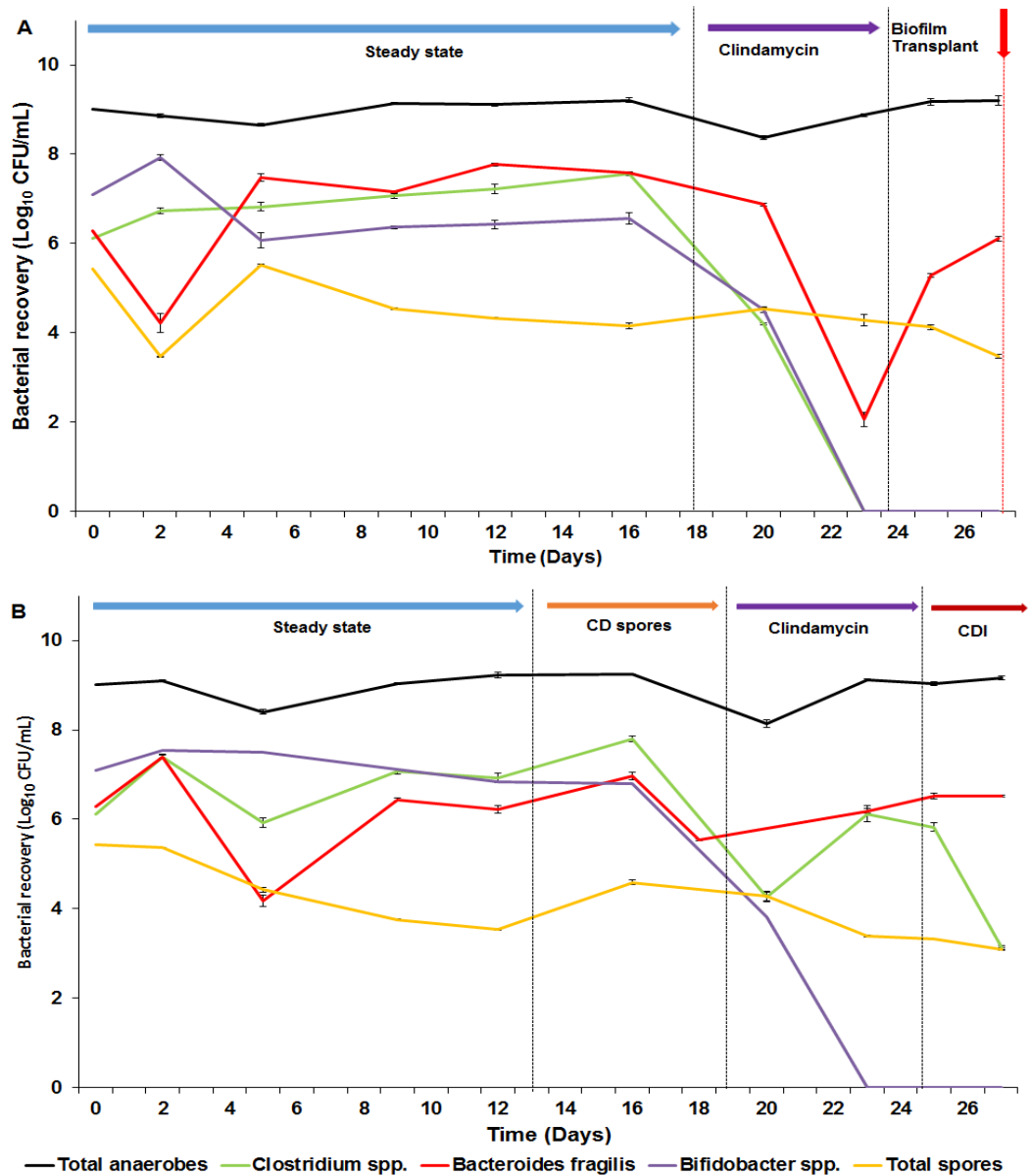


Figure 6-6 Enumeration of planktonic anaerobes in (a) the recipient model and (b) the control model. Bacterial enumeration of total anaerobes (black), *B. fragilis* sp. (red), *Clostridium* spp. (green), *Bifidobacterium* spp. (purple), and spores (yellow) of the recipient model (model R) and the control model (model C). Data shows the disruption to the microbiota during clindamycin instillation. Data shown are the mean log_{10} CFU/mL \pm standard error from three technical replicates on alternate days of the model timeline of one biological replicate. Different model stages are separated by vertical broken lines (grey; biofilm transplantation – red – model R only). CD – *C. difficile*, Clind – clindamycin, Vanc – vancomycin, CDI – *C. difficile* infection.

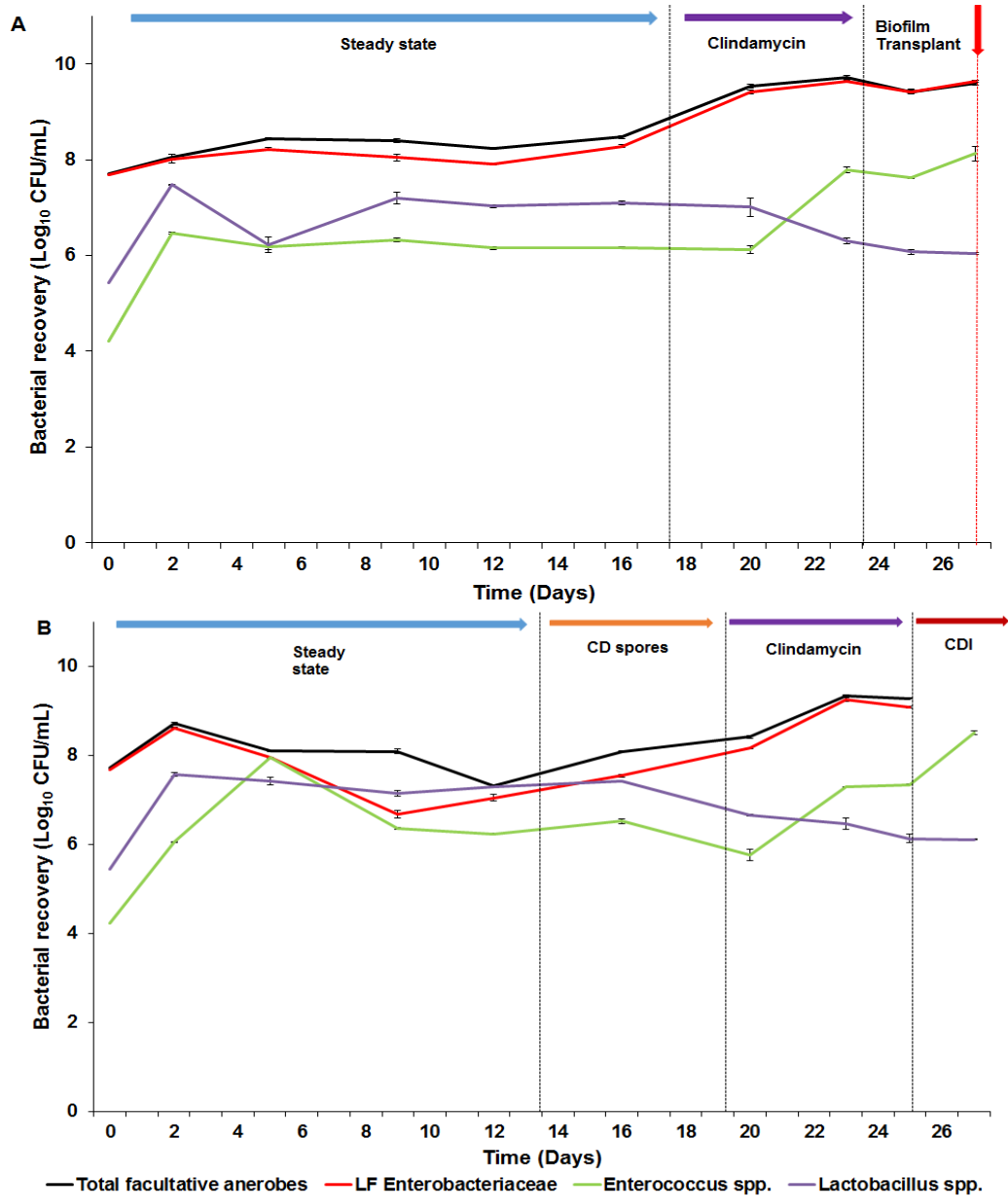


Figure 6-7 Enumeration of planktonic facultative anaerobes in (a) the recipient model and (b) the control model. Bacterial enumeration of total facultative anaerobes (black), lactose fermenting (LF) Enterobacteriaceae (red), *Enterococcus* spp. (green), and *Lactobacillus* spp. (purple) of the recipient model (model R) and the control model (model C). Data shows the disruption to the microbiota during clindamycin instillation. Data shown are the mean log_{10} CFU/mL \pm standard error from three technical replicates on alternate days of the model timeline of one biological replicate. Different model stages are separated by vertical broken lines (grey; biofilm transplantation – red – model R only). CD – *C. difficile*, Clind – clindamycin, Vanc – vancomycin, CDI – *C. difficile* infection.

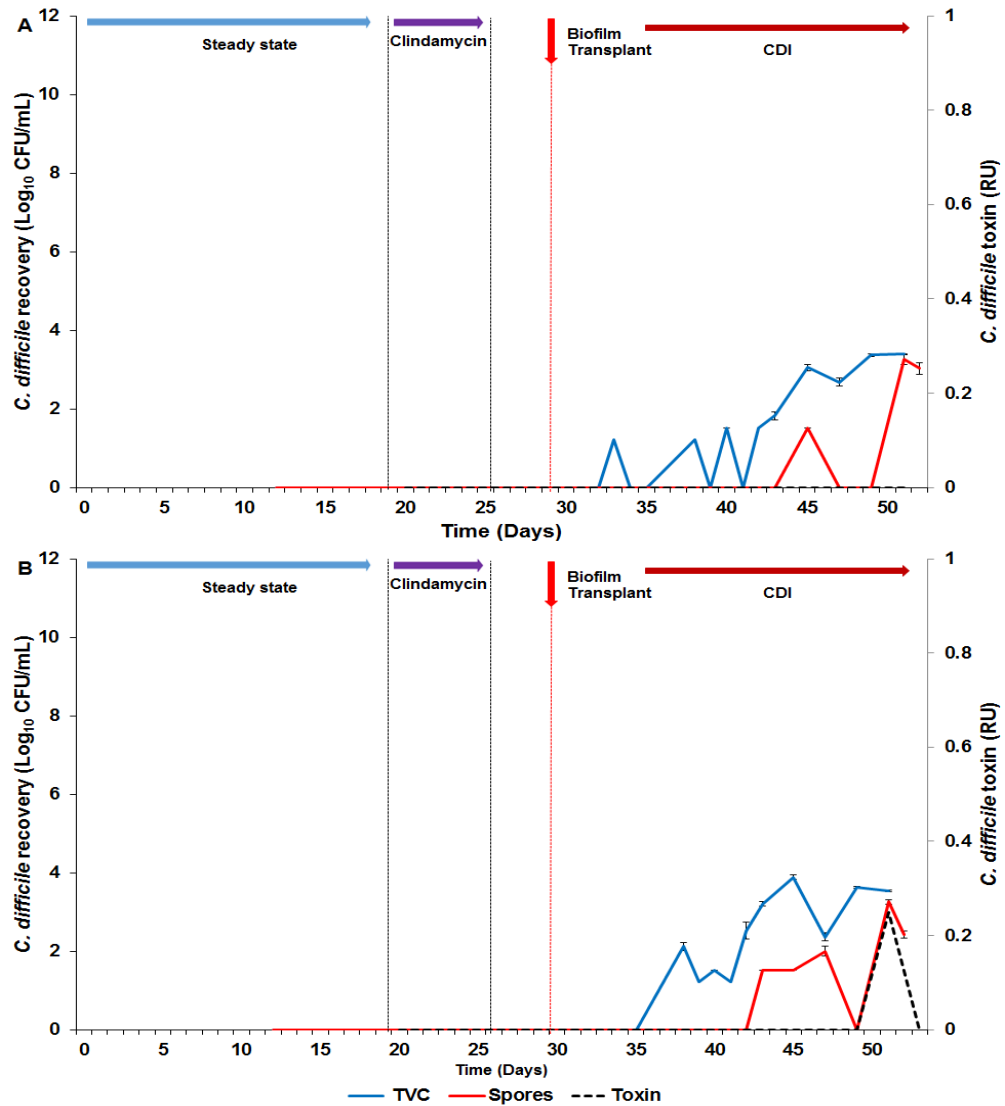


Figure 6-8 Enumeration of planktonic *C. difficile* total and spore counts in (a) vessel two and (b) vessel three of the recipient model (model R). Enumerations of *C. difficile* spores (red) and total viable counts (blue) are represented for vessels two and three in mean log₁₀ CFU/mL ± standard error (left axis). *C. difficile* toxin (black broken line) is represented as log reciprocal units (RU, right axis). Data represents *C. difficile* originating from the biofilm re-populating the planktonic phase with evidence of spore germination and toxin production in vessel three. Data shown are from three technical replicates on alternate days of the model timeline from one biological replicate. Different model stages are separated by vertical broken lines (grey; biofilm transplanted – red – model R only). CD – *C. difficile*, Clind – clindamycin, Vanc – vancomycin, CDI – *C. difficile* infection.

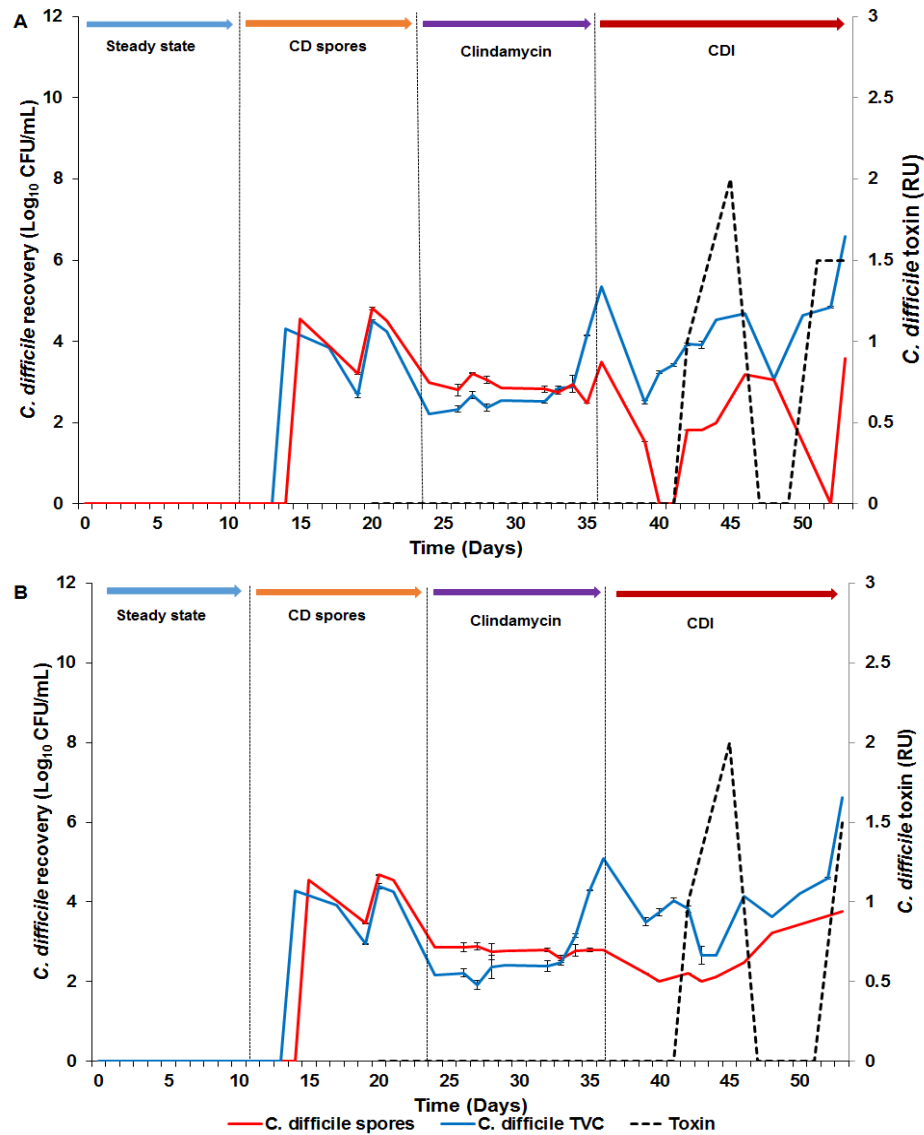


Figure 6-9 Enumeration of planktonic *C. difficile* total and spore counts in (a) vessel two and (b) vessel three of the control model (model C). Enumerations of *C. difficile* spores (red) and total viable counts (blue) are represented for vessels two and three in mean log₁₀ CFU/mL ± standard error (left axis). *C. difficile* toxin (black broken line) is represented as log reciprocal units (RU, right axis). Data represents *C. difficile* originating from spores added to vessel one, with evidence of *C. difficile* germination and toxin production in vessel two and three. Data shown are from three technical replicates on alternate days of the model timeline from one biological replicate. Different model stages are separated by vertical broken lines. CD – *C. difficile*, Clind – clindamycin, Vanc – vancomycin, CDI – *C. difficile* infection.

6.4 Discussion

Biofilms have been implicated in many chronic infections and the persistence of microbial pathogens; for example, *P. aeruginosa* infections in chronic otitis media and UTIs from indwelling urinary catheters, *Porphyromonas gingivalis* in periodontal infections and *Staphylococcus epidermidis* in prosthetic valve endocarditis. Increased tolerance to antimicrobial agents plays an important role biofilm-associated infections, with treatment failure and disease persistence a common occurrence (Stewart, 2015). Current recommendations for the treatment of primary CDI include the use metronidazole or vancomycin; however, in up 30 % of cases the disease relapses within 8 weeks and this is not linked to increased resistance of the infecting strain (Kelly and LaMont, 2008). Relapse with the initial strain during the primary episode of CDI is present in between 65 - 88% of recurrences (Kamboj *et al.*, 2011, Figueroa *et al.*, 2012). The risk of further recurrence was found to increase with each subsequent episode, (McFarland *et al.*, 1994), suggesting that *C. difficile* may exploit a protective niche in the GI tract where antimicrobial therapy is ineffective. We believe that biofilms offer such a niche and may facilitate rCDI. Although rCDI displays a number of characteristics normally associated with biofilm-mediated infections, the role of biofilms in rCDI has not been established.

C. difficile has been shown to form biofilms *in vitro* (Dawson *et al.*, 2012, Donelli *et al.*, 2012, Dapa and Unnikrishnan, 2013, Semenyuk *et al.*, 2014) and *in vivo* (Buckley *et al.*, 2011, Semenyuk *et al.*, 2015, Soavelomandroso *et al.*, 2017); however, the ability of sessile *C. difficile* to contribute towards pathogenesis and recurrence has not been demonstrated. The gut model used here provides an ideal opportunity to study the contribution of biofilms towards CDI. It is clinically relevant and accurately represents the different stages of the *C. difficile* disease process and facilitates the manipulation of the sessile populations independent of the planktonic populations. Consistent with findings from Crowther *et al.* (2014a), we demonstrated that treatment with vancomycin was ineffective against sessile *C. difficile* populations that formed part of a multispecies biofilm in a continuous flow model system of the human gut. Batch culture biofilm experiments support this increased tolerance of sessile *C.*

difficile to vancomycin therapy, with increased resistance rates of 100 times the MIC of the hypervirulent R20291 strain seen (Đapa *et al.*, 2013, Mathur *et al.*, 2016, James *et al.*, 2017). This increased antimicrobial tolerance extended to studies with metronidazole (Semenyuk *et al.*, 2014, James *et al.*, 2017) with sub-inhibitory concentrations resulting in an increase in biofilm formation (Vuotto *et al.*, 2015). It was found that fidaxomicin displayed increased effectiveness against *in vitro* *C. difficile* biofilms, resulting in biofilm disruption and a reduction in *C. difficile* numbers (James *et al.*, 2017). The increased efficacy of fidaxomicin against sessile *C. difficile* may, in addition to microbiota sparing properties due to its narrow spectrum of activity (Crawford *et al.*, 2012), contribute towards the reduced recurrence rates associated with fidaxomicin when compared to vancomycin therapy (Cornely *et al.*, 2012b). The ability of biofilm-dwelling microorganisms to either actively or passively disperse from a biofilm to colonise new niches and spread infection has been demonstrated (Boyd and Chakrabarty, 1994, Lee *et al.*, 1996, Kaplan *et al.*, 2003, Kaplan, 2010); however, dispersal and seeding from *C. difficile* biofilms has not been well studied.

In previous gut model experiments, *C. difficile* spores added to the models rapidly became associated with the biofilm. The incorporation of the spores into the biofilm may involve the presence of a mature exosporium layer, with hair-like protrusions and hydrophobicity mediating adhesion to matrix components (Henriques and Charles P. Moran, 2007, Barra-Carrasco *et al.*, 2013, Mora-Uribe *et al.*, 2016). This incorporation into the biofilm enabled the survival of sessile *C. difficile* populations during vancomycin dosing, suggesting a colonisation niche for *C. difficile* and a potential reservoir to facilitate rCDI. Indeed, disease relapse was demonstrated despite planktonic levels of *C. difficile* falling to below the limit of detection. To further explore the relationship of sessile *C. difficile* and rCDI, we transplanted sessile *C. difficile* into a naive model treated with clindamycin to create a susceptible environment for CDI. At the time of donation, planktonic recoveries of *C. difficile* in the Donor Model were below the level of detection, ensuring that the *C. difficile* transplanted was from a sessile origin. Enumeration of the biofilm indicated levels of sessile *C. difficile* of 3.1 log₁₀ CFU/g, which is consistent with results from previous models after vancomycin treatment. We monitored the *C. difficile* recoveries in

the planktonic phase seeded from the transplanted biofilm for the duration of the experiment. We ran a positive control model alongside this model with the addition of a *C. difficile* spore preparation into vessel one. Levels of clindamycin in vessel one were comparable between the models, reaching peak levels on day 6 of dosing. Disruption to the microflora was similar and consistent with previous and induced CDI was deemed present in Model C when evidence of *C. difficile* spore germination was seen approximately 10 days after clindamycin cessation, accompanied by vegetative cell outgrowth and toxin production. In Model R, the biofilm was transplanted three days after clindamycin cessation into vessel two. This time lag was to ensure levels of clindamycin had dropped below the level of detection at the time of biofilm introduction. Transient recoveries of planktonic *C. difficile* was detected in vessel two five days after transplantation, with stable *C. difficile* populations recovered after 15 days in vessel two and after 10 days in vessel three. Peak levels of *C. difficile* recovered from vessel three were 4 log₁₀ CFU/mL, with evidence of germination and toxin production detected 23 days after transplantation; however, the toxin levels detected did not reach levels associated with simulated CDI. The biofilm in this experiment was transplanted from a recurrence model into a model that had been prepared for acute infection, and therefore it should be acknowledged that the end point comparison is not the equivalent; however, the overall objective was to re-establish *C. difficile* colonisation from sessile origins, which was clearly demonstrated.

Although full CDI was not established in this model, there was clear evidence of *C. difficile* seeding from the transplanted biofilm and subsequent colonisation of the planktonic phase. In our gut models, biofilms also form on the walls of the vessels and the composition of which has been shown to be equivalent to that formed on the biofilm support structures. Thus the amount of biofilm transplanted here represents a small proportion of the *C. difficile*-containing biofilm that would normally seed the planktonic phase. As we were only able to transplant a very small portion of the biofilm in the form of biofilm support structures, the number of *C. difficile* cells seeded from the biofilm were only a fraction of what could be seen, which could account for the low levels of cells recovered from planktonic populations. It was estimated that approximately 3.8 log₁₀ CFU *C. difficile* was transferred to the recipient model. These numbers

are significantly lower than the two doses of $7 \log_{10}$ CFU/mL that was added to the Control Model. The effect of different infective doses was seen in mouse models where a dose – response relationship was seen between environmental spore concentration and the development of CDI (Lawley *et al.*, 2010).

In previous models, *Clostridium* spp. and *B. fragilis* gp. recoveries increased to pre-antibiotic levels just prior to clindamycin cessation, with the rest of the microbiota taking approximately 10 – 14 days to recover from clindamycin dosing. The delay between clindamycin cessation and biofilm transplantation could have allowed the partial recovery of colonisation resistance of the microbiota, potentially inhibiting the ability of sessile populations to effectively colonise the niche generated by clindamycin. Another factor to consider is the transplantation into vessel two where normally *C. difficile* spores are introduced to the model in vessel one. There is an abundance of biofilm formed on the walls of vessel one, with previous models demonstrating sessile associated *C. difficile* at levels comparable to those recovered in vessels two and three (data not shown). The *C. difficile* associated with biofilm in vessel one could potentially seed the subsequent vessels at a higher rate than our transplant in vessel two. As the *C. difficile* from this model originated from the biofilm, this decreased transition time may have had a significant effect on the outcome as *C. difficile* spores from biofilms display reduced germination efficiencies compared with conventional spores, and therefore may have required increased time to fully germinate and proliferate (Semenyuk *et al.*, 2014).

Here, we saw clear evidence of *C. difficile* dispersal from the transplanted biofilm that resulted in planktonic seeding and subsequent colonisation. This was accompanied by low level spore germination, outgrowth and toxin production. The increased survival of *C. difficile* associated with a biofilm has significant repercussions for the development of rCDI. Although simulated CDI did not result, the potential of the biofilm to provide a protective niche for *C. difficile* survival during antibiotic therapy, and the subsequent dispersal from the biofilm in a susceptible environment to re-establish CDI, was clearly demonstrated.

Chapter 7 Conclusions

This research aimed to determine whether multispecies biofilms play a role in the recurrence of CDI and to explore the characterisation of *C. difficile* with commensal microorganisms in these structures. The recurrence and persistence of CDI, despite appropriate antimicrobial therapy, led us to hypothesise that biofilms in the gut may act as a reservoir to *C. difficile* and potentially facilitate rCDI. Currently, there is a lack of knowledge regarding intestinal biofilms and their contribution to disease persistence, mainly due to the invasive nature of mucosal sampling and the lack of suitable *in vitro* models. Using a combination of continuous flow and batch culture biofilms models, we showed that *C. difficile* was incorporated into a multispecies biofilm, which provided a protective niche against antimicrobial and microbiome therapies. This facilitated the repopulation of the planktonic phase under susceptible conditions, potentially contributing to rCDI.

Here, a triple stage gut model was used that has been shown to be microbiologically and physio-chemically reflective of the human colon (Macfarlane *et al.*, 1998) and has been used previously to accurately reflect clinical outcomes, in terms of the propensity of drugs to induce and treat simulated CDI (Freeman *et al.*, 2003, Baines *et al.*, 2006, Chilton *et al.*, 2014a). The ability to longitudinally sample biofilm populations in this model provided a valuable opportunity to delineate the contributions of sessile and planktonic populations with respect to disease recurrence. With the clinical success of FMT and increased interest in microbiome-restoration therapy, we simulated FMT in our models to determine whether this could accurately predict clinical outcome of microbiome-based therapeutics. In our models, a combination of vancomycin treatment followed by FMT instillation successfully prevented rCDI for up to 35 days. Vancomycin treatment alone failed to prevent rCDI, with peak *C. difficile* recovered at 6.4 log CFU/ml 28 days post antibiotic treatment, accompanied with toxin detection at 3 RU. Antimicrobial therapy was associated with a higher ratio of primary bile acids compared with secondary bile acids, and this ratio was prolonged in the vancomycin only model. The bile acid ratio upon FMT instillation was characterised by a lower ratio of primary to secondary bile acids. This demonstrated the microbiome-mediated restoration

of bile acid metabolism after FMT therapy. These results were consistent with clinical findings (Weingarden *et al.*, 2014, Winston and Theriot, 2016), indicating that these models could provide a valuable tool in the development of microbiome-based therapies and determining the mechanisms of efficacy. To this end, we evaluated two different dosing regimens of the spore-based therapeutic SER-109, an undefined spore consortium derived from human faeces. In a Phase 2 clinical trial, the relative risk of CDI recurrence for placebo compared with SER-109 recipients was not statistically significant. We established that a single SER-109 dose was insufficient to prevent rCDI whereas a triple dose on sequential days successfully prevented rCDI. These results supported one of the conclusions from the Phase 2 post-trial analysis regarding under-dosing of SER-109. Using data from Phase 1 clinical studies and my results, SER-109 has progressed to Phase 3 clinical trials.

These models provided the first characterisation of biofilm composition and profiling during FMT and microbiome-based therapies. Bacterial culture and taxonomic sequencing of the biofilm populations revealed that these sessile populations were not affected by antibiotics to the same degree as seen in planktonic populations, highlighting the resilience of biofilms towards external pressures, such as antimicrobial therapy. A highly significant finding from these experiments was the inability of vancomycin or FMT and other microbiome-based therapies to displace *C. difficile* from the biofilm in my models. After antibiotic treatment, planktonic *C. difficile* levels dropped to below the level of detection, whereas the biofilm populations remained between approximately 3 – 4 log CFU/g for the duration of the model runs. This suggested that the biofilm provided a protective niche for *C. difficile* during antibiotic treatment which, in the vancomycin-only model, potentially facilitated the re-population of the planktonic phase and the subsequent development of rCDI. This also raised the possibility that patients which undergo FMT and other microbiome-based therapies could potentially remain at further risk of rCDI with subsequent antimicrobial therapy. The biofilm niche we described could be responsible for the CDI recurrence in up to 18 % of patients at 18-22 months post-FMT (Mamo *et al.*, 2018, Allegretti *et al.*, 2019). The use of antibiotics after successful FMT significantly increased the risk of rCDI. Although the gut model has been shown to reflect the conditions of the human colon, this model has some limitations,

especially with regard to biofilm communities. It has been demonstrated that planktonic based culture systems may not be representative of sessile states in the colon due to lower cell densities coupled with the washout of less competitive or slow growing microorganisms (Lacroix *et al.*, 2015). This can be overcome using immobilised faecal microbiota trapped in gel beads or colonisation of mucin gels (Macfarlane *et al.*, 2005, Fehlbauer *et al.*, 2015); however, these methods were not appropriate for the use in the models here and did not facilitate periodic sampling. The use of glass biofilm support structures used here facilitated the formation of a multispecies biofilm that provided the opportunity for longitudinal sampling and analysis, with populations distinct from that of the planktonic phase (Crowther *et al.*, 2014a, Crowther *et al.*, 2014b). Due to inaccessibility of mucosal populations in the gut, comparisons between these and the sessile populations formed in the model are difficult. It is likely that, as the microbiota is unique on an individual basis, the same will ring true for the sessile populations.

As *C. difficile* has been demonstrated to form a biofilm *in vitro* (Dawson *et al.*, 2012, Donelli *et al.*, 2012, Dapa *et al.*, 2013), a set of biofilm batch culture experiments were conducted to explore the interactions of *C. difficile* with commensal microorganisms isolated from the gut models. This utilised the crystal violet assay for the semi-quantitative analysis of biofilm formation together with total viable counts to assess growth in the biofilm. The crystal violet assay is an inexpensive, high-throughput assay used here as an initial screen to identify potential interactions with *C. difficile*. It was optimised for *C. difficile* growth and therefore conditions may not have been suitable for all microorganisms examined (O'Toole, 2011) and also only a limited number of microbial species were assessed in co-culture biofilms, whereas there would be a plethora of species in sessile communities interacting in the gut. Therefore caution is required when extrapolating results as the simple nature of this assay does not encompass the complexity of interactions and biogeography *in vivo*. Members of the genus *Lactobacillus*, *Bifidobacterium* and *Bacteroides* all reduced *C. difficile* biofilm formation in co-culture. This result is noteworthy as, during the gut model experiments, we demonstrated a decreased abundance of these bacterial families in the biofilm after exposure to clindamycin and vancomycin. Thus, these therapeutics may influence commensal bacteria that

reduce *C. difficile* biofilm formation and, despite the ability of FMT and microbiome-based therapies to restore diversity of sessile bacteria, they failed to displace *C. difficile* from the biofilm.

To determine whether the biofilm-associated *C. difficile* was responsible for the recurrence of CDI, we transplanted the biofilm support structures containing multispecies biofilm with *C. difficile*, into a susceptible, *C. difficile* naïve model. Ten days after the transplant, *C. difficile* was recovered from the planktonic populations and evidence of germination/proliferation was seen 18 days post-transplant, with peak *C. difficile* levels of 3.9 log₁₀ CFU/mL recovered accompanied by toxin levels of 0.25 RU. Although the toxin levels recovered were not clinically significant, implications of the re-population of the planktonic phase leading to *C. difficile* germination and proliferation solely derived from the biofilm is striking. This demonstrated that biofilm-associated *C. difficile* was capable of dispersing from the biofilm, and upon encountering an environment conducive for CDI, facilitated the colonisation of the planktonic phase, with the potential to cause CDI. This is the first clear evidence demonstrating the influence of biofilms in driving rCDI.

This thesis presents evidence to the involvement of biofilms in the recurrence of CDI. These results highlight the importance of evaluating the efficacy of CDI therapeutics and future microbiome therapies to target both planktonic and biofilm *C. difficile* populations. Additionally, it suggests that patients undergoing FMT therapy remain at risk of rCDI from subsequent antimicrobial use.

7.1 Study limitations and further work

In this body of work, the focus was on measuring bacterial populations and their potential association with *C. difficile* in a biofilm. It is important to remember that other microorganisms have the potential to affect *C. difficile* levels. Indeed, we observed a positive correlation in *C. difficile* biofilm formation with *Candida* species. The importance of the enteric virome was demonstrated by Zuo *et al.* (2018b) and Draper *et al.* (2018) in the context of CDI. They established that the enteric virome was altered in CDI when compared with healthy controls, resulting in enteric virome dysbiosis. FMT treatment resulted in an increase in both bacterial and virome diversity that closely matched the donors, indicating that bacteriophages may play a role in the efficacy of FMT in CDI cases. Bacteriophages have also been investigated for the use in the treatment of CDI with specific combinations of bacteriophages resulting in the complete lysis and eradication of *C. difficile* after 24 hours, leaving the commensal microorganisms unaffected (Nale *et al.*, 2016, Nale *et al.*, 2018). Using large-scale metagenomics sequencing (MGS) together with the Human Virome Protein Cluster Database (HVPC) (Elbehery *et al.*, 2018) and the Human Gut Virome Database (GVD)(Gregory *et al.*, 2019), the virome potential, including the active and silent virome, could be monitored in the gut models. Alongside the virome, the mycobiome has also been implicated in CDI. Marked enrichment of fungi were found in CDI patients but not in CDI negative controls (Sangster *et al.*, 2016, Lamendella *et al.*, 2018) and an over-abundance of *C. albicans* in recipients was associated with FMT failure (Zuo *et al.*, 2018a). Fungal sequencing could be performed on the gut model contents using primers for the nuclear ribosomal internal transcribed spacer (ITS) and the QIIME (Caporaso *et al.*, 2010) and UNITE (Koljalg *et al.*, 2013) softwares/databases. Analysing the virome and mycobiome alongside the bacteriome could provide valuable information on the dynamics of microbiome changes during CDI and CDI therapy and allow a better understanding of interspecies dynamics during health and disease.

To further explore the role of biofilms in rCDI, it would be beneficial to repeat the experiment of the biofilm transplantation with an additional transplantation of the planktonic phase. This would serve two purposes, namely to replicate

these results by transferring the biofilm support structures into a susceptible model as well as provide an opportunity to transfer the planktonic phase, after vancomycin treatment, to seed a new model in place of a faecal slurry. This would remove the influence of the biofilm populations and determine whether any residual *C. difficile* in the planktonic phase is sufficient to cause rCDI. This experiment would require a donor model in which simulated CDI was treated with vancomycin. The biofilm from vessel 2 and 3 would be transplanted from this model into a *C. difficile* naïve after clindamycin treatment (as seen in Chapter 6, with the exception of transferring additional biofilm support structures) and the planktonic phase would be transferred from each vessel to an empty model to ensure the biofilm on the vessel walls could not contribute any biofilm-associated *C. difficile*. Both models would be monitored for evidence of *C. difficile* germination and outgrowth. A control model would be used to ensure successful CDI induction using a *C. difficile* spore preparation.

Currently, the biofilm support structures used in the models are composed of glass. I believe these structures could be redesigned to be more reflective of the *in vivo* environment. Therefore, we have set out to redesign the biofilm support structures to more closely mimic the intestinal environment. This includes plans to replace the glass rods with semi-permeable structures linked with a mucin reservoir to simulate the action of goblet cells and facilitate the secretion of mucin. The structures will be 3D printed using biocompatible materials (such as poly lactic acid from corn starch and collagen) and printing will include the addition of a textured appearance to mimic microvilli. Although the models do not represent interactions with the host, these suggested alterations should provide an environment that more closely reflects those found in the intestinal tract, and so could provide vital information on the formation of biofilm in a more dynamic environment.

During gut model experiments, the presence of the AI-2 quorum sensing molecule was detected in the multispecies biofilm. These levels decreased in accordance with antimicrobial therapy and recovered with an increase in species abundance and diversity. Recent work by Slater *et al.* (2019) described the effect of a *C. difficile* AI-2 (*luxS* mutant strain) deficient strain on biofilm formation. They found that this QS mutant was defective for biofilm formation *in vitro*; however, in co-culture, the antagonistic effect of *Bacteroides fragilis* on *C.*

difficile biofilm formation was alleviated with the *luxS* mutant. To further explore inter-species communication of *C. difficile* with other commensal microorganisms, we successfully created a *C. difficile* quorum sensing mutant using homologous recombination by allele exchange of the *luxS* gene (appendix A6). The use of this mutant in biofilm co-culture biofilm experiments could provide valuable insights into the role of quorum sensing in *C. difficile* biofilm formation and interactions with other commensal microorganisms. The use of this mutant in gut model experiments has distinct limitations due to the production of AI-2 by other biofilm-dwelling microorganisms and therefore an additional *C. difficile* AI-2 sensing mutant would be required.

References

- ACKERMANN, G., LÖFFLER, B., ADLER, D. & RODLOFF, A. C. 2004. *In vitro* activity of OPT-80 against *Clostridium difficile*. *Antimicrobial Agents and Chemotherapy*, 48, 2280-2282.
- ADAMS, S. D. & MERCER, D. W. 2007. Fulminant *Clostridium difficile* colitis. *Current Opinion in Critical Care*, 13, 450-5.
- AGOSTINHO, A. M., HARTMAN, A., LIPP, C., PARKER, A. E., STEWART, P. S. & JAMES, G. A. 2011. An *in vitro* model for the growth and analysis of chronic wound MRSA biofilms. *Journal of Applied Microbiology*, 111, 1275-1282.
- AGUILAR, C., VLAMAKIS, H., GUZMAN, A., LOSICK, R. & KOLTER, R. 2010. KinD is a checkpoint protein linking spore formation to extracellular-matrix production in *Bacillus subtilis* biofilms. *mBio*, 1, 00035-10.
- AHMED, M. N., PORSE, A., SOMMER, M. O. A., HOIBY, N. & CIOFU, O. 2018. Evolution of Antibiotic Resistance in Biofilm and Planktonic *Pseudomonas aeruginosa* Populations Exposed to Subinhibitory Levels of Ciprofloxacin. *Antimicrobial Agents and Chemotherapy*, 62, e00320-18.
- ÅKERLUND, T., PERSSON, I., UNEMO, M., NORÉN, T., SVENUNGSSON, B., WULLT, M. & BURMAN, L. G. 2008. Increased Sporulation Rate of Epidemic *Clostridium difficile* Type 027/NAP1. *Journal of Clinical Microbiology*, 46, 1530-1533.
- AKTORIES, K., SCHWAN, C. & JANK, T. 2017. *Clostridium difficile* Toxin Biology. *Annual Review of Microbiology*, 71, 281-307.
- AKTORIES, K. & WEGNER, A. 1989. ADP-ribosylation of actin by clostridial toxins. *Journal of Cell Biology*, 109, 1385-7.
- AL MOMANI, L. A., ABUGHANIMEH, O., BOONPHENG, B., GABRIEL, J. G. & YOUNG, M. 2018. Fidaxomicin vs Vancomycin for the Treatment of a First Episode of *Clostridium Difficile* Infection: A Meta-analysis and Systematic Review. *Cureus Journal of Medical Science*, 10, e2778-e2778.
- ALDAPE, M. J., PACKHAM, A. E., NUTE, D. W., BRYANT, A. E. & STEVENS, D. L. 2013. Effects of ciprofloxacin on the expression and production of exotoxins by *Clostridium difficile*. *Journal of Medical Microbiology*, 62, 741-7.
- ALHEDE, M., QVORTRUP, K., LIEBRECHTS, R., HØIBY, N., GIVSKOV, M. & BJARNSHOLT, T. 2012. Combination of microscopic techniques reveals

a comprehensive visual impression of biofilm structure and composition. *FEMS Immunology and Medical Microbiology*, 65, 335-342.

- ALLEGRETTI, J. R., KAO, D., PHELPS, E., ROACH, B., SMITH, J., GANAPINI, V. C., KASSAM, Z., XU, H. & FISCHER, M. 2019. Risk of *Clostridium difficile* Infection with Systemic Antimicrobial Therapy Following Successful Fecal Microbiota Transplant: Should We Recommend Anti-*Clostridium difficile* Antibiotic Prophylaxis? *Digestive Diseases and Sciences*, 64, 1668-1671.
- ALLEGRETTI, J. R., KEARNEY, S., LI, N., BOGART, E., BULLOCK, K., GERBER, G. K., BRY, L., CLISH, C. B., ALM, E. & KORZENIK, J. 2016. Recurrent *Clostridium difficile* Infection Associates with Distinct Bile Acid and Microbiome Profiles. *Alimentary pharmacology & therapeutics*, 43, 1142-1153.
- ALLISON, D. G., RUIZ, B., SANJOSE, C., JASPE, A. & GILBERT, P. 1998. Extracellular products as mediators of the formation and detachment of *Pseudomonas fluorescens* biofilms. *FEMS Microbiology Letters*, 167, 179-84.
- ALVAREZ, G., GONZÁLEZ, M., ISABAL, S., BLANC, V. & LEÓN, R. 2013. Method to quantify live and dead cells in multi-species oral biofilm by real-time PCR with propidium monoazide. *AMB Express*, 3, 1-1.
- ANASTASIADIS, P., MOJICA, K. D. A., ALLEN, J. S. & MATTER, M. L. 2014. Detection and quantification of bacterial biofilms combining high-frequency acoustic microscopy and targeted lipid microparticles. *Journal of nanobiotechnology*, 12, 24-24.
- ANDERL, J. N., FRANKLIN, M. J. & STEWART, P. S. 2000. Role of Antibiotic Penetration Limitation in *Klebsiella pneumoniae* Biofilm Resistance to Ampicillin and Ciprofloxacin. *Antimicrobial Agents and Chemotherapy*, 44, 1818-1824.
- ANDERL, J. N., ZÄHLLER, J., ROE, F. & STEWART, P. S. 2003. Role of Nutrient Limitation and Stationary-Phase Existence in *Klebsiella pneumoniae* Biofilm Resistance to Ampicillin and Ciprofloxacin. *Antimicrobial Agents and Chemotherapy*, 47, 1251-1256.
- ANJUWON-FOSTER, B. R. & TAMAYO, R. 2017. A genetic switch controls the production of flagella and toxins in *Clostridium difficile*. *PLOS Genetics*, 13, e1006701.
- ANJUWON-FOSTER, B. R. & TAMAYO, R. 2018. Phase variation of *Clostridium difficile* virulence factors. *Gut Microbes*, 9, 76-83.
- ANTUNES, A., CAMIADE, E., MONOT, M., COURTOIS, E., BARBUT, F., SERNOVA, N. V., RODIONOV, D. A., MARTIN-VERSTRAETE, I. & DUPUY, B. 2012. Global transcriptional control by glucose and carbon

regulator CcpA in *Clostridium difficile*. *Nucleic Acids Research*, 40, 10701-18.

- APEWOKIN, S., PRADHAN, S., FRERICK, M. & WEISS, A. 2017. Induced Human Intestinal Organoids (iHIOs) as Model Systems for Chemotherapy-associated *Clostridium difficile* (CD) Infections. *Open Forum Infectious Diseases*, 4, S382-S382.
- ARNON, S. S., MILLS, D. C., DAY, P. A., HENRICKSON, R. V., SULLIVAN, N. M. & WILKINS, T. D. 1984. Rapid death of infant rhesus monkeys injected with *Clostridium difficile* toxins A and B: Physiologic and pathologic basis. *The Journal of Pediatrics*, 104, 34-40.
- ASAHI, Y., MIURA, J., TSUDA, T., KUWABATA, S., TSUNASHIMA, K., NOIRI, Y., SAKATA, T., EBISU, S. & HAYASHI, M. 2015. Simple observation of *Streptococcus mutans* biofilm by scanning electron microscopy using ionic liquids. *AMB Express*, 5, 6-6.
- AUBRY, A., HUSSACK, G., CHEN, W., KUOLEE, R., TWINE, S. M., FULTON, K. M., FOOTE, S., CARRILLO, C. D., TANHA, J. & LOGAN, S. M. 2012. Modulation of toxin production by the flagellar regulon in *Clostridium difficile*. *Infection and Immunity*, 80, 3521-32.
- AZEREDO, J., AZEVEDO, N. F., BRIANDET, R., CERCA, N., COENYE, T., COSTA, A. R., DESVAUX, M., DI BONAVENTURA, G., HÉBRAUD, M., JAGLIC, Z., KAČÁNIOVÁ, M., KNØCHEL, S., LOURENÇO, A., MERGULHÃO, F., MEYER, R. L., NYCHAS, G., SIMÕES, M., TRESSE, O. & STERNBERG, C. 2017. Critical review on biofilm methods. *Critical Reviews in Microbiology*, 43, 313-351.
- BABAN, S. T., KUEHNE, S. A., BARKETI-KLAI, A., CARTMAN, S. T., KELLY, M. L., HARDIE, K. R., KANSAU, I., COLLIGNON, A. & MINTON, N. P. 2013. The role of flagella in *Clostridium difficile* pathogenesis: comparison between a non-epidemic and an epidemic strain. *PLoS One*, 8, e73026.
- BABCOCK, G. J., BROERING, T. J., HERNANDEZ, H. J., MANDELL, R. B., DONAHUE, K., BOATRIGHT, N., STACK, A. M., LOWY, I., GRAZIANO, R., MOLRINE, D., AMBROSINO, D. M. & THOMAS, W. D., JR. 2006. Human monoclonal antibodies directed against toxins A and B prevent *Clostridium difficile*-induced mortality in hamsters. *Infection and Immunity*, 74, 6339-47.
- BAINES, S. D., CROWTHER, G. S., TODHUNTER, S. L., FREEMAN, J., CHILTON, C. H., FAWLEY, W. N. & WILCOX, M. H. 2013. Mixed infection by *Clostridium difficile* in an *in vitro* model of the human gut. *Journal of Antimicrobial Chemotherapy*, 68, 1139-1143.
- BAINES, S. D., FREEMAN, J. & WILCOX, M. H. 2005. Effects of piperacillin/tazobactam on *Clostridium difficile* growth and toxin

- production in a human gut model. *Journal of Antimicrob Chemotherapy*, 55, 974-82.
- BAINES, S. D., O'CONNOR, R., SAXTON, K., FREEMAN, J. & WILCOX, M. H. 2009. Activity of vancomycin against epidemic *Clostridium difficile* strains in a human gut model. *Journal of Antimicrob Chemotherapy*, 63, 520-5.
- BAINES, S. D., SAXTON, K., FREEMAN, J. & WILCOX, M. H. 2006. Tigecycline does not induce proliferation or cytotoxin production by epidemic *Clostridium difficile* strains in a human gut model. *Journal of Antimicrob Chemotherapy*, 58, 1062-5.
- BAKKEN, J. S., BORODY, T., BRANDT, L. J., BRILL, J. V., DEMARCO, D. C., FRANZOS, M. A., KELLY, C., KHORUTS, A., LOUIE, T., MARTINELLI, L. P., MOORE, T. A., RUSSELL, G., SURAWICZ, C. & FECAL MICROBIOTA TRANSPLANTATION, W. 2011. Treating *Clostridium difficile* infection with fecal microbiota transplantation. *Clinical gastroenterology and hepatology*, 9, 1044-1049.
- BAKKER, D., SMITS, W. K., KUIJPER, E. J. & CORVER, J. 2012. TcdC does not significantly repress toxin expression in *Clostridium difficile* 630DeltaErm. *PLoS One*, 7, e43247.
- BANG, B. W., PARK, J. S., KIM, H. K., SHIN, Y. W., KWON, K. S., KWON, H. Y., BAEK, J. H. & LEE, J. S. 2017. Fecal Microbiota Transplantation for Refractory and Recurrent *Clostridium difficile* Infection: A Case Series of Nine Patients. *Korean Journal of Gastroenterology*, 69, 226-231.
- BARKETI-KLAI, A., HOYS, S., LAMBERT-BORDES, S., COLLIGNON, A. & KANSAU, I. 2011. Role of fibronectin-binding protein A in *Clostridium difficile* intestinal colonization. *Journal of Medical Microbiology*, 60, 1155-61.
- BARRA-CARRASCO, J., OLGUÍN-ARANEDA, V., PLAZA-GARRIDO, A., MIRANDA-CÁRDENAS, C., COFRÉ-ARANEDA, G., PIZARRO-GUAJARDO, M., SARKER, M. R. & PAREDES-SABJA, D. 2013. The *Clostridium difficile* exosporium cysteine (CdeC)-rich protein is required for exosporium morphogenesis and coat assembly. *Journal of bacteriology*, 195, 3863-3875.
- BARTH, H., AKTORIES, K., POPOFF, M. R. & STILES, B. G. 2004. Binary bacterial toxins: biochemistry, biology, and applications of common *Clostridium* and *Bacillus* proteins. *Microbiology and Molecular Biology Reviews*, 68, 373-402.
- BARTLETT, J. G., CHANG, T., TAYLOR, N. S. & ONDERDONK, A. B. 1979. Colitis induced by *Clostridium difficile*. *Reviews of Infectious Diseases*, 1, 370-8.

- BARTLETT, J. G., CHANG, T. W., GURWITH, M., GORBACH, S. L. & ONDERDONK, A. B. 1978. Antibiotic-associated pseudomembranous colitis due to toxin-producing clostridia. *The New England Journal of Medicine*, 298, 531-4.
- BARTLETT, J. G. & GERDING, D. N. 2008. Clinical recognition and diagnosis of *Clostridium difficile* infection. *Clinical Infectious Diseases*, 46 Suppl 1, S12-8.
- BARTLETT, J. G., ONDERDONK, A. B., CISNEROS, R. L. & KASPER, D. L. 1977. Clindamycin-associated colitis due to a toxin-producing species of *Clostridium* in hamsters. *Journal of Infectious Diseases*, 136, 701-5.
- BARTLETT, J. G., TAYLOR, N. S., CHANG, T. & DZINK, J. 1980. Clinical and laboratory observations in *Clostridium difficile* colitis. *American Journal of Clinical Nutrition*, 33, 2521-6.
- BASSLER, B. L., GREENBERG, E. P. & STEVENS, A. M. 1997. Cross-species induction of luminescence in the quorum-sensing bacterium *Vibrio harveyi*. *Journal of Bacteriology*, 179, 4043-5.
- BASSLER, B. L., WRIGHT, M., SHOWALTER, R. E. & SILVERMAN, M. R. 1993. Intercellular signalling in *Vibrio harveyi*: sequence and function of genes regulating expression of luminescence. *Molecular Microbiology*, 9, 773-86.
- BASSLER, B. L., WRIGHT, M. & SILVERMAN, M. R. 1994. Multiple signalling systems controlling expression of luminescence in *Vibrio harveyi*: sequence and function of genes encoding a second sensory pathway. *Molecular Microbiology*, 13, 273-286.
- BATTESTI, A., MAJDALANI, N. & GOTTESMAN, S. 2011. The RpoS-mediated general stress response in *Escherichia coli*. *Annual Review of Microbiology*, 65, 189-213.
- BAUMGART, D. C. & CARDING, S. R. 2007. Inflammatory bowel disease: cause and immunobiology. *Lancet*, 369, 1627-40.
- BAXTER, M., AHMAD, T., COLVILLE, A. & SHERIDAN, R. 2015. Fatal Aspiration Pneumonia as a Complication of Fecal Microbiota Transplant. *Clinical Infectious Diseases*, 61, 136-137.
- BAXTER, M. & COLVILLE, A. 2016. Adverse events in faecal microbiota transplant: a review of the literature. *Journal of Hospital Infections*, 92, 117-27.
- BECHINGER, B. & GORR, S. U. 2017. Antimicrobial Peptides: Mechanisms of Action and Resistance. *Journal of Dental Research*, 96, 254-260.
- BERNEY, M., HAMMES, F., BOSSHARD, F., WEILENMANN, H. U. & EGLI, T. 2007. Assessment and interpretation of bacterial viability by using the

LIVE/DEAD BacLight Kit in combination with flow cytometry. *Applied Environmental Microbiology*, 73, 3283-90.

BEST, E. L., FAWLEY, W. N., PARNELL, P. & WILCOX, M. H. 2010. The Potential for Airborne Dispersal of *Clostridium difficile* from Symptomatic Patients. *Clinical Infectious Diseases*, 50, 1450-1457.

BEST, E. L., FREEMAN, J. & WILCOX, M. H. 2012. Models for the study of *Clostridium difficile* infection. *Gut Microbes*, 3, 145-167.

BIAZZO, M., CIONCADA, R., FIASCHI, L., TEDDE, V., SPIGAGLIA, P., MASTRANTONIO, P., PIZZA, M., BAROCCHI, M. A., SCARSELLI, M. & GALEOTTI, C. L. 2013. Diversity of *cwp* loci in clinical isolates of *Clostridium difficile*. *Journal of Medical Microbiology*, 62, 1444-52.

BIEN, J., PALAGANI, V. & BOZKO, P. 2013. The intestinal microbiota dysbiosis and *Clostridium difficile* infection: is there a relationship with inflammatory bowel disease? *Therapeutic Advances in Gastroenterology*, 6, 53-68.

BIRCH, L., DAWSON, C. E., CORNETT, J. H. & KEER, J. T. 2001. A comparison of nucleic acid amplification techniques for the assessment of bacterial viability. *Letters in Applied Microbiology*, 33, 296-301.

BJARNSHOLT, T. 2013. The role of bacterial biofilms in chronic infections. *APMIS*, 121, 1-58.

BOLES, B. R., THOENDEL, M. & SINGH, P. K. 2004. Self-generated diversity produces "insurance effects" in biofilm communities. *Proceedings of the National Academy of Sciences of the United States of America*, 101, 16630-16635.

BORDELEAU, E., FORTIER, L.-C., MALOUIN, F. & BURRUS, V. 2011. c-di-GMP Turn-Over in *Clostridium difficile* Is Controlled by a Plethora of Diguanylate Cyclases and Phosphodiesterases. *PLOS Genetics*, 7, e1002039.

BORDELEAU, E., PURCELL, E. B., LAFONTAINE, D. A., FORTIER, L.-C., TAMAYO, R. & BURRUS, V. 2015. Cyclic Di-GMP Riboswitch-Regulated Type IV Pili Contribute to Aggregation of *Clostridium difficile*. *Journal of Bacteriology*, 197, 819-832.

BORRIELLO, S. P. & BARCLAY, F. E. 1986. An *in-vitro* model of colonisation resistance to *Clostridium difficile* infection. *Journal of Medical Microbiology*, 21, 299-309.

BORRIELLO, S. P., DAVIES, H. A. & BARCLAY, F. E. 1988a. Detection of fimbriae amongst strains of *Clostridium difficile*. *FEMS Microbiology Letters*, 49, 65-67.

- BORRIELLO, S. P., WELCH, A. R., BARCLAY, F. E. & DAVIES, H. A. 1988b. Mucosal association by *Clostridium difficile* in the hamster gastrointestinal tract. *Journal of Medical Microbiology*, 25, 191-6.
- BOUILLAUT, L., DUBOIS, T., SONENSHEIN, A. L. & DUPUY, B. 2015. Integration of metabolism and virulence in *Clostridium difficile*. *Research in Microbiology*, 166, 375-383.
- BOYD, A. & CHAKRABARTY, A. M. 1994. Role of alginate lyase in cell detachment of *Pseudomonas aeruginosa*. *Applied and Environmental Microbiology*, 60, 2355-9.
- BRAUN, V., HUNDSBERGER, T., LEUKEL, P., SAUERBORN, M. & VON EICHEL-STREIBER, C. 1996. Definition of the single integration site of the pathogenicity locus in *Clostridium difficile*. *Gene*, 181, 29-38.
- BRIDIER, A., DUBOIS-BRISSENET, F., BOUBETRA, A., THOMAS, V. & BRIANDET, R. 2010. The biofilm architecture of sixty opportunistic pathogens deciphered using a high throughput CLSM method. *Journal of Microbiological Methods*, 82, 64-70.
- BRILEYA, K. A., CAMILLERI, L. B., ZANE, G. M., WALL, J. D. & FIELDS, M. W. 2014. Biofilm growth mode promotes maximum carrying capacity and community stability during product inhibition syntrophy. *Frontiers in Microbiology*, 5, 693.
- BROWN, A. W. W. & WILSON, R. B. 2018. *Clostridium difficile* colitis and zoonotic origins-a narrative review. *Gastroenterology report*, 6, 157-166.
- BROWN, E., TALBOT, G. H., AXELROD, P., PROVENCHER, M. & HOEGG, C. 1990. Risk factors for *Clostridium difficile* toxin-associated diarrhea. *Infection Control and Hospital Epidemiology*, 11, 283-90.
- BUCKLEY, A. M., SPENCER, J., CANDLISH, D., IRVINE, J. J. & DOUCE, G. R. 2011. Infection of hamsters with the UK *Clostridium difficile* ribotype 027 outbreak strain R20291. *Journal of Medical Microbiology*, 60, 1174-1180.
- BUCKLEY, A. M., SPENCER, J., MACLELLAN, L. M., CANDLISH, D., IRVINE, J. J. & DOUCE, G. R. 2013. Susceptibility of Hamsters to *Clostridium difficile* Isolates of Differing Toxinotype. *PLOS ONE*, 8, e64121.
- BUFFIE, C. G., BUCCI, V., STEIN, R. R., MCKENNEY, P. T., LING, L., GOBOURNE, A., NO, D., LIU, H., KINNEBREW, M., VIALE, A., LITTMANN, E., VAN DEN BRINK, M. R., JENQ, R. R., TAUR, Y., SANDER, C., CROSS, J. R., TOUSSAINT, N. C., XAVIER, J. B. & PAMER, E. G. 2015. Precision microbiome reconstitution restores bile acid mediated resistance to *Clostridium difficile*. *Nature*, 517, 205-8.
- BUFFIE, C. G., JARCHUM, I., EQUINDA, M., LIPUMA, L., GOBOURNE, A., VIALE, A., UBEDA, C., XAVIER, J. & PAMER, E. G. 2012. Profound

alterations of intestinal microbiota following a single dose of clindamycin results in sustained susceptibility to *Clostridium difficile*-induced colitis. *Infection and Immunity*, 80, 62-73.

- BURET, A. G., MOTTA, J. P., ALLAIN, T., FERRAZ, J. & WALLACE, J. L. 2019. Pathobiont release from dysbiotic gut microbiota biofilms in intestinal inflammatory diseases: a role for iron? *Journal of Biomedical Science*, 26, 1.
- BURMØLLE, M., REN, D., BJARNSHOLT, T. & SØRENSEN, S. J. 2014. Interactions in multispecies biofilms: do they actually matter? *Trends in Microbiology*, 22, 84-91.
- BURNS, D. A., HEAP, J. T. & MINTON, N. P. 2010. The diverse sporulation characteristics of *Clostridium difficile* clinical isolates are not associated with type. *Anaerobe*, 16, 618-622.
- BURNS, D. A., HEEG, D., CARTMAN, S. T. & MINTON, N. P. 2011. Reconsidering the Sporulation Characteristics of Hypervirulent *Clostridium difficile* BI/NAP1/027. *PLOS ONE*, 6, e24894.
- BUTEL, M. J., ROLAND, N., HIBERT, A., POPOT, F., FAVRE, A., TESSEDE, A. C., BENSADA, M., RIMBAULT, A. & SZYLIT, O. 1998. Clostridial pathogenicity in experimental necrotising enterocolitis in gnotobiotic quails and protective role of bifidobacteria. *Journal of Medical Microbiology*, 47, 391-9.
- CAFARDI, V., BIAGINI, M., MARTINELLI, M., LEUZZI, R., RUBINO, J. T., CANTINI, F., NORAI, N., SCARSELLI, M., SERRUTO, D. & UNNIKRISSHANNAN, M. 2013. Identification of a novel zinc metalloprotease through a global analysis of *Clostridium difficile* extracellular proteins. *PLoS One*, 8, e81306.
- CALABI, E., CALABI, F., PHILLIPS, A. D. & FAIRWEATHER, N. F. 2002. Binding of *Clostridium difficile* Surface Layer Proteins to Gastrointestinal Tissues. *Infection and Immunity*, 70, 5770-5778.
- CALLAHAN, B. J., MCMURDIE, P. J., ROSEN, M. J., HAN, A. W., JOHNSON, A. J. & HOLMES, S. P. 2016. DADA2: High-resolution sample inference from Illumina amplicon data. *Nature Methods*, 13, 581-3.
- CAMMAROTA, G., IANIRO, G. & GASBARRINI, A. 2014. Fecal microbiota transplantation for the treatment of *Clostridium difficile* infection: a systematic review. *Journal of Clinical Gastroenterology*, 48, 693-702.
- CAMMAROTA, G., MASUCCI, L., IANIRO, G., BIBBO, S., DINOI, G., COSTAMAGNA, G., SANGUINETTI, M. & GASBARRINI, A. 2015. Randomised clinical trial: faecal microbiota transplantation by colonoscopy vs. vancomycin for the treatment of recurrent *Clostridium difficile* infection. *Alimentary Pharmacology and Therapeutics*, 41, 835-43.

- CANI, P. D., BIBILONI, R., KNAUF, C., WAGET, A., NEYRINCK, A. M., DELZENNE, N. M. & BURCELIN, R. 2008. Changes in gut microbiota control metabolic endotoxemia-induced inflammation in high-fat diet-induced obesity and diabetes in mice. *Diabetes*, 57, 1470-81.
- CAPORASO, J. G., KUCZYNSKI, J., STOMBAUGH, J., BITTINGER, K., BUSHMAN, F. D., COSTELLO, E. K., FIERER, N., PEÑA, A. G., GOODRICH, J. K., GORDON, J. I., HUTTLEY, G. A., KELLEY, S. T., KNIGHTS, D., KOENIG, J. E., LEY, R. E., LOZUPONE, C. A., MCDONALD, D., MUEGGE, B. D., PIRRUNG, M., REEDER, J., SEVINSKY, J. R., TURNBAUGH, P. J., WALTERS, W. A., WIDMANN, J., YATSUNENKO, T., ZANEVELD, J. & KNIGHT, R. 2010. QIIME allows analysis of high-throughput community sequencing data. *Nature Methods*, 7, 335-6.
- CARDING, S., VERBEKE, K., VIPOND, D. T., CORFE, B. M. & OWEN, L. J. 2015. Dysbiosis of the gut microbiota in disease. *Microbial ecology in health and disease*, 26, 26191-26191.
- CARTER, G. P., DOUCE, G. R., GOVIND, R., HOWARTH, P. M., MACKIN, K. E., SPENCER, J., BUCKLEY, A. M., ANTUNES, A., KOTSANAS, D., JENKIN, G. A., DUPUY, B., ROOD, J. I. & LYRAS, D. 2011. The anti-sigma factor TcdC modulates hypervirulence in an epidemic BI/NAP1/027 clinical isolate of *Clostridium difficile*. *PLoS Pathog*, 7, e1002317.
- CARTER, G. P., LYRAS, D., ALLEN, D. L., MACKIN, K. E., HOWARTH, P. M., O'CONNOR, J. R. & ROOD, J. I. 2007. Binary Toxin Production in *Clostridium difficile* Is Regulated by CdtR, a LytTR Family Response Regulator. *Journal of Bacteriology*, 189, 7290-7301.
- CARTER, G. P., PURDY, D., WILLIAMS, P. & MINTON, N. P. 2005. Quorum sensing in *Clostridium difficile*: analysis of a luxS-type signalling system. *Journal of Medical Microbiology*, 54, 119-27.
- CARTMAN, S. T., KELLY, M. L., HEEG, D., HEAP, J. T. & MINTON, N. P. 2012. Precise manipulation of the *Clostridium difficile* chromosome reveals a lack of association between the tcdC genotype and toxin production. *Applied Environmental Microbiology*, 78, 4683-90.
- CARVALHO, F. G. D., PUPPIN-RONTANI, R. M., FÚCIO, S. B. P. D., NEGRINI, T. D. C., CARLO, H. L. & GARCIA-GODOY, F. 2012. Analysis by confocal laser scanning microscopy of the MDPB bactericidal effect on *S. mutans* biofilm CLSM analysis of MDPB bactericidal effect on biofilm. *Journal of applied oral science : revista FOB*, 20, 568-575.
- CASTAGLIUOLO, I., KEATES, A. C., QIU, B., KELLY, C. P., NIKULASSON, S., LEEMAN, S. E. & POTHOUKAKIS, C. 1997. Increased substance P responses in dorsal root ganglia and intestinal macrophages during

Clostridium difficile toxin A enteritis in rats. *Proceedings of the National Academy of Sciences of the United States of America*, 94, 4788-93.

- CERCA, F., FRANÇA, Â., GUIMARÃES, R., HINZMANN, M., CERCA, N., LOBO DA CUNHA, A., AZEREDO, J. & VILANOVA, M. 2011. Modulation of poly-N-acetylglucosamine accumulation within mature *Staphylococcus epidermidis* biofilms grown in excess glucose. *Microbiology and Immunity*, 55, 673-682.
- CERI, H., OLSON, M. E., STREMICK, C., READ, R. R., MORCK, D. & BURET, A. 1999. The Calgary Biofilm Device: New Technology for Rapid Determination of Antibiotic Susceptibilities of Bacterial Biofilms. *Journal of Clinical Microbiology*, 37, 1771-1776.
- CERQUETTI, M., SERAFINO, A., SEBASTIANELLI, A. & MASTRANTONIO, P. 2002. Binding of *Clostridium difficile* to Caco-2 epithelial cell line and to extracellular matrix proteins. *FEMS Immunology and Medical Microbiology*, 32, 211-8.
- CHANDRASEKARAN, R., KENWORTHY, A. K. & LACY, D. B. 2016. *Clostridium difficile* Toxin A Undergoes Clathrin-Independent, PACSIN2-Dependent Endocytosis. *PLoS Pathogens*, 12, e1006070.
- CHANG, C. J., LIN, T. L., TSAI, Y. L., WU, T. R., LAI, W. F., LU, C. C. & LAI, H. C. 2019. Next generation probiotics in disease amelioration. *Journal of Food and Drug Analysis*, 27, 615-622.
- CHANG, J. Y., ANTONOPOULOS, D. A., KALRA, A., TONELLI, A., KHALIFE, W. T., SCHMIDT, T. M. & YOUNG, V. B. 2008. Decreased diversity of the fecal Microbiome in recurrent *Clostridium difficile*-associated diarrhea. *Journal of Infectious Diseases*, 197, 435-8.
- CHARACKLIS, W. G., TRULEAR, M. G., BRYERS, J. D. & ZELVER, N. 1982. Dynamics of biofilm processes: methods. *Water Research*, 16, 1207-1216.
- CHAVANT, P., GAILLARD-MARTINIE, B., TALON, R., HÉBRAUD, M. & BERNARDI, T. 2007. A new device for rapid evaluation of biofilm formation potential by bacteria. *Journal of Microbiological Methods*, 68, 605-12.
- CHAVES-OLARTE, E., WEIDMANN, M., EICHEL-STREIBER, C. & THELESTAM, M. 1997. Toxins A and B from *Clostridium difficile* differ with respect to enzymatic potencies, cellular substrate specificities, and surface binding to cultured cells. *Journal of Clinical Investigation*, 100, 1734-1741.
- CHEN, X., KATCHAR, K., GOLDSMITH, J. D., NANTHAKUMAR, N., CHEKNIS, A., GERDING, D. N. & KELLY, C. P. 2008. A mouse model of *Clostridium difficile*-associated disease. *Gastroenterology*, 135, 1984-92.

- CHIANG, J. Y. 2009. Bile acids: regulation of synthesis. *J Lipid Res*, 50, 1955-66.
- CHILTON, C. H., CROWTHER, G. S., BAINES, S. D., TODHUNTER, S. L., FREEMAN, J., LOCHER, H. H., ATHANASIOU, A. & WILCOX, M. H. 2014a. *In vitro* activity of cadazolid against clinically relevant *Clostridium difficile* isolates and in an *in vitro* gut model of *C. difficile* infection. *Journal of Antimicrobial Chemotherapy*, 69, 697-705.
- CHILTON, C. H., CROWTHER, G. S., FREEMAN, J., TODHUNTER, S. L., NICHOLSON, S., LONGSHAW, C. M. & WILCOX, M. H. 2014b. Successful treatment of simulated *Clostridium difficile* infection in a human gut model by fidaxomicin first line and after vancomycin or metronidazole failure. *Journal of Antimicrobial Chemotherapy*, 69, 451-62.
- CHILTON, C. H., CROWTHER, G. S., ŚPIEWAK, K., BRINDELL, M., SINGH, G., WILCOX, M. H. & MONAGHAN, T. M. 2016. Potential of lactoferrin to prevent antibiotic-induced *Clostridium difficile* infection. *Journal of Antimicrobial Chemotherapy*, 71, 975-985.
- CHILTON, C. H., CROWTHER, G. S., TODHUNTER, S. L., ASHWIN, H., LONGSHAW, C. M., KARAS, A. & WILCOX, M. H. 2015. Efficacy of alternative fidaxomicin dosing regimens for treatment of simulated *Clostridium difficile* infection in an *in vitro* human gut model. *Journal of Antimicrobial Chemotherapy*, 70, 2598-607.
- CHIRAKKAL, H., O'ROURKE, M., ATRIH, A., FOSTER, S. J. & MOIR, A. 2002. Analysis of spore cortex lytic enzymes and related proteins in *Bacillus subtilis* endospore germination. *Microbiology*, 148, 2383-92.
- CHRISTENSEN, G. D., SIMPSON, W. A., YOUNGER, J. J., BADDOUR, L. M., BARRETT, F. F., MELTON, D. M. & BEACHEY, E. H. 1985. Adherence of coagulase-negative staphylococci to plastic tissue culture plates: a quantitative model for the adherence of staphylococci to medical devices. *Journal of clinical microbiology*, 22, 996-1006.
- CHUMBLER, N. M., RUTHERFORD, S. A., ZHANG, Z., FARROW, M. A., LISHER, J. P., FARQUHAR, E., GIEDROC, D. P., SPILLER, B. W., MELNYK, R. A. & LACY, D. B. 2016. Crystal structure of *Clostridium difficile* toxin A. *Nature Microbiology*, 1, 15002.
- CIFTCI, Y., GIRINATHAN, B. P., DHUNGEL, B. A., HASAN, M. K. & GOVIND, R. 2019. *Clostridioides difficile* SinR' regulates toxin, sporulation and motility through protein-protein interaction with SinR. *Anaerobe*, 59, 1-7.
- COENYE, T., KJELLERUP, B., STOODLEY, P. & BJARNSHOLT, T. 2020. The future of biofilm research – Report on the '2019 Biofilm Bash'. *Biofilm*, 2, 100012.

- COENYE, T. & NELIS, H. J. 2010. *In vitro* and *in vivo* model systems to study microbial biofilm formation. *Journal of Microbiological Methods*, 83, 89-105.
- COLLIGNON, A. 2010. Methods for working with the mouse model. *Methods in Molecular Biology*, 646, 229-37.
- COLLINS, J., AUCTIONG, J. M., SCHAEFER, L., EATON, K. A. & BRITTON, R. A. 2015. Humanized microbiota mice as a model of recurrent *Clostridium difficile* disease. *Microbiome*, 3, 35.
- CORNELY, O. A., CROOK, D. W., ESPOSITO, R., POIRIER, A., SOMERO, M. S., WEISS, K., SEARS, P. & GORBACH, S. 2012a. Fidaxomicin versus vancomycin for infection with *Clostridium difficile* in Europe, Canada, and the USA: a double-blind, non-inferiority, randomised controlled trial. *Lancet Infectious Diseases*, 12, 281-9.
- CORNELY, O. A., MILLER, M. A., LOUIE, T. J., CROOK, D. W. & GORBACH, S. L. 2012b. Treatment of first recurrence of *Clostridium difficile* infection: fidaxomicin versus vancomycin. *Clinical infectious diseases : an official publication of the Infectious Diseases Society of America*, 55 Suppl 2, S154-S161.
- COSTELLO, S. P., CONLON, M. A., VUARAN, M. S., ROBERTS-THOMSON, I. C. & ANDREWS, J. M. 2015. Faecal microbiota transplant for recurrent *Clostridium difficile* infection using long-term frozen stool is effective: clinical efficacy and bacterial viability data. *Alimentary Pharmacology and Therapeutics*, 42, 1011-8.
- COSTERTON, J. W., LEWANDOWSKI, Z., CALDWELL, D. E., KORBER, D. R. & LAPPIN-SCOTT, H. M. 1995. Microbial biofilms. *Annual Review of Microbiology*, 49, 711-45.
- COSTERTON, J. W., STEWART, P. S. & GREENBERG, E. P. 1999. Bacterial biofilms: a common cause of persistent infections. *Science*, 284, 1318-22.
- CRAWFORD, T., HUESGEN, E. & DANZIGER, L. 2012. Fidaxomicin: a novel macrocyclic antibiotic for the treatment of *Clostridium difficile* infection. *American Journal of Health-System Pharmacy*, 69, 933-43.
- CROBACH, M. J., PLANCHE, T., ECKERT, C., BARBUT, F., TERVEER, E. M., DEKKERS, O. M., WILCOX, M. H. & KUIJPER, E. J. 2016. European Society of Clinical Microbiology and Infectious Diseases: update of the diagnostic guidance document for *Clostridium difficile* infection. *Clinical Microbiology and Infection*, 22 Suppl 4, S63-81.
- CROWTHER, G. S., CHILTON, C. H., LONGSHAW, C., TODHUNTER, S. L., EWIN, D., VERNON, J., KARAS, A. & WILCOX, M. H. 2016. Efficacy of vancomycin extended-dosing regimens for treatment of simulated

Clostridium difficile infection within an in vitro human gut model. *Journal of Antimicrobial Chemotherapy*, 71, 986-991.

CROWTHER, G. S., CHILTON, C. H., TODHUNTER, S. L., NICHOLSON, S., FREEMAN, J., BAINES, S. D. & WILCOX, M. H. 2014a. Comparison of planktonic and biofilm-associated communities of *Clostridium difficile* and indigenous gut microbiota in a triple-stage chemostat gut model. *Journal of Antimicrobial Chemotherapy*, 69, 2137-47.

CROWTHER, G. S., CHILTON, C. H., TODHUNTER, S. L., NICHOLSON, S., FREEMAN, J., BAINES, S. D. & WILCOX, M. H. 2014b. Development and validation of a chemostat gut model to study both planktonic and biofilm modes of growth of *Clostridium difficile* and human microbiota. *PLoS One*, 9, e88396.

CROWTHER, G. S., CHILTON, C. H., TODHUNTER, S. L., NICHOLSON, S., FREEMAN, J. & WILCOX, M. H. 2015. Recurrence of dual-strain *Clostridium difficile* infection in an in vitro human gut model. *Journal of Antimicrobial Chemotherapy*, 70, 2316-21.

CUCARELLA, C., TORMO, M. A., KNECHT, E., AMORENA, B., LASA, I., FOSTER, T. J. & PENADÉS, J. R. 2002. Expression of the biofilm-associated protein interferes with host protein receptors of *Staphylococcus aureus* and alters the infective process. *Infection and immunity*, 70, 3180-3186.

CURTIS, M. M., HU, Z., KLIMKO, C., NARAYANAN, S., DEBERARDINIS, R. & SPERANDIO, V. 2014. The gut commensal *Bacteroides thetaiotaomicron* exacerbates enteric infection through modification of the metabolic landscape. *Cell host & microbe*, 16, 759-769.

CZEPIEL, J., DRÓŹDŹ, M., PITUCH, H., KUIJPER, E. J., PERUCKI, W., MIELIMONKA, A., GOLDMAN, S., WULTAŃSKA, D., GARLICKI, A. & BIESIADA, G. 2019. *Clostridium difficile* infection: review. *European journal of clinical microbiology & infectious diseases : official publication of the European Society of Clinical Microbiology*, 38, 1211-1221.

DABARD, J., DUBOS, F., MARTINET, L. & DUCLUZEAU, R. 1979. Experimental reproduction of neonatal diarrhea in young gnotobiotic hares simultaneously associated with *Clostridium difficile* and other *Clostridium* strains. *Infection and Immunity*, 24, 7-11.

DALLAL, R. M., HARBRECHT, B. G., BOUJOUKAS, A. J., SIRIO, C. A., FARKAS, L. M., LEE, K. K. & SIMMONS, R. L. 2002. Fulminant *Clostridium difficile*: An Underappreciated and Increasing Cause of Death and Complications. *Annals of Surgery*, 235, 363-372.

ĐAPA, T., LEUZZI, R., NG, Y. K., BABAN, S. T., ADAMO, R., KUEHNE, S. A., SCARSELLI, M., MINTON, N. P., SERRUTO, D. & UNNIKRIISHNAN, M. 2013. Multiple Factors Modulate Biofilm Formation by the Anaerobic Pathogen *Clostridium difficile*. *Journal of Bacteriology*, 195, 545-555.

- DAPA, T. & UNNIKRISHNAN, M. 2013. Biofilm formation by *Clostridium difficile*. *Gut Microbes*, 4, 397-402.
- DAQUIGAN, N., SEEKATZ, A. M., GREATHOUSE, K. L., YOUNG, V. B. & WHITE, J. R. 2017. High-resolution profiling of the gut microbiome reveals the extent of *Clostridium difficile* burden. *NPJ Biofilms Microbiomes*, 3, 35.
- DARKOH, C., DUPONT, H. L., NORRIS, S. J. & KAPLAN, H. B. 2015. Toxin Synthesis by *Clostridium difficile* Is Regulated through Quorum Signaling. *mBio*, 6, e02569-14.
- DAVEY, H. M. 2011. Life, death, and in-between: meanings and methods in microbiology. *Applied and environmental microbiology*, 77, 5571-5576.
- DAVIES, K. A., ASHWIN, H., LONGSHAW, C. M., BURNS, D. A., DAVIS, G. L., WILCOX, M. H. & GROUP, O. B. O. T. E. S. 2016. Diversity of *Clostridium difficile* PCR ribotypes in Europe: results from the European, multicentre, prospective, biannual, point-prevalence study of *Clostridium difficile* infection in hospitalised patients with diarrhoea (EUCLID), 2012 and 2013. *Eurosurveillance*, 21, 30294.
- DAVIS, S. C., RICOTTI, C., CAZZANIGA, A., WELSH, E., EAGLSTEIN, W. H. & MERTZ, P. M. 2008. Microscopic and physiologic evidence for biofilm-associated wound colonization *in vivo*. *Wound Repair and Regeneration*, 16, 23-9.
- DAWSON, L. F., VALIENTE, E., FAULDS-PAIN, A., DONAHUE, E. H. & WREN, B. W. 2012. Characterisation of *Clostridium difficile* biofilm formation, a role for Spo0A. *PLoS One*, 7, e50527.
- DE LA RIVA, L., WILLING, S. E., TATE, E. W. & FAIRWEATHER, N. F. 2011. Roles of cysteine proteases Cwp84 and Cwp13 in biogenesis of the cell wall of *Clostridium difficile*. *Journal of Bacteriology*, 193, 3276-85.
- DE LALLA, F., PRIVITERA, G., ORTISI, G., RIZZARDINI, G., SANTORO, D., PAGANO, A., RINALDI, E. & SCARPELLINI, P. 1989. Third generation cephalosporins as a risk factor for *Clostridium difficile*-associated disease: a four-year survey in a general hospital. *Journal of Antimicrobial Chemotherapy*, 23, 623-31.
- DE VOS, W. M. 2015. Microbial biofilms and the human intestinal microbiome. *Npj Biofilms And Microbiomes*, 1, 15005.
- DEBAST, S. B., BAUER, M. P. & KUIJPER, E. J. 2014. European Society of Clinical Microbiology and Infectious Diseases: update of the treatment guidance document for *Clostridium difficile* infection. *Clinical Microbiology and Infection*, 20 Suppl 2, 1-26.

- DEFILIPP, Z., BLOOM, P. P., TORRES SOTO, M., MANSOUR, M. K., SATER, M. R. A., HUNTLEY, M. H., TURBETT, S., CHUNG, R. T., CHEN, Y. B. & HOHMANN, E. L. 2019. Drug-Resistant *E. coli* Bacteremia Transmitted by Fecal Microbiota Transplant. *New England Journal of Medicine*, 381, 2043-2050.
- DEMBEK, M., BARQUIST, L., BOINETT, C. J., CAIN, A. K., MAYHO, M., LAWLEY, T. D., FAIRWEATHER, N. F. & FAGAN, R. P. 2015. High-throughput analysis of gene essentiality and sporulation in *Clostridium difficile*. *mBio*, 6, e02383-e02383.
- DI MARTINO, P. 2018. Extracellular polymeric substances, a key element in understanding biofilm phenotype. *AIMS Microbiology*, 4, 274-288.
- DÍAZ-GONZÁLEZ, F., MILANO, M., OLGUIN-ARANEDA, V., PIZARRO-CERDA, J., CASTRO-CÓRDOVA, P., TZENG, S.-C., MAIER, C. S., SARKER, M. R. & PAREDES-SABJA, D. 2015. Protein composition of the outermost exosporium-like layer of *Clostridium difficile* 630 spores. *Journal of Proteomics*, 123, 1-13.
- DINEEN, S. S., MCBRIDE, S. M. & SONENSHEIN, A. L. 2010. Integration of metabolism and virulence by *Clostridium difficile* CodY. *Journal of Bacteriology*, 192, 5350-62.
- DOMINGUEZ-BENETTON, X., SEVDA, S., VANBROEKHOVEN, K. & PANT, D. 2012. The accurate use of impedance analysis for the study of microbial electrochemical systems. *Chemical Society Reviews*, 41, 7228-46.
- DOMKA, J., LEE, J., BANSAL, T. & WOOD, T. K. 2007. Temporal gene-expression in *Escherichia coli* K-12 biofilms. *Environ Microbiology*, 9, 332-46.
- DONELLI, G., VUOTTO, C., CARDINES, R. & MASTRANTONIO, P. 2012. Biofilm-growing intestinal anaerobic bacteria. *FEMS Immunology and Medical Microbiology*, 65, 318-25.
- DONLAN, R. M. 2001a. Biofilm Formation: A Clinically Relevant Microbiological Process. *Clinical Infectious Diseases*, 33, 1387-1392.
- DONLAN, R. M. 2001b. Biofilms and device-associated infections. *Emerging infectious diseases*, 7, 277-281.
- DONLAN, R. M. 2002. Biofilms: Microbial Life on Surfaces. *Emerging Infectious Diseases*, 8, 881-890.
- DONLAN, R. M. & COSTERTON, J. W. 2002. Biofilms: Survival Mechanisms of Clinically Relevant Microorganisms. *Clinical Microbiology Reviews*, 15, 167-193.

- DRAPER, L. A., RYAN, F. J., SMITH, M. K., JALANKA, J., MATTILA, E., ARKKILA, P. A., ROSS, R. P., SATOKARI, R. & HILL, C. 2018. Long-term colonisation with donor bacteriophages following successful faecal microbial transplantation. *Microbiome*, 6, 220.
- DRUDY, D., O'DONOGHUE, D. P., BAIRD, A., FENELON, L. & O'FARRELLY, C. 2001. Flow cytometric analysis of *Clostridium difficile* adherence to human intestinal epithelial cells. *Journal of Medical Microbiology*, 50, 526-34.
- DUAN, Q., ZHOU, M., ZHU, L. & ZHU, G. 2013. Flagella and bacterial pathogenicity. *Journal of Basic Microbiology*, 53, 1-8.
- DUBBERKE, E. R., LEE, C. H., ORENSTEIN, R., KHANNA, S., HECHT, G. & GERDING, D. N. 2018. Results From a Randomized, Placebo-Controlled Clinical Trial of a RBX2660-A Microbiota-Based Drug for the Prevention of Recurrent *Clostridium difficile* Infection. *Clinical Infectious Diseases*, 67, 1198-1204.
- DUPUY, B. & SONENSHEIN, A. L. 1998. Regulated transcription of *Clostridium difficile* toxin genes. *Molecular Microbiology*, 27, 107-20.
- DURACK, D. T. 1975. Experimental bacterial endocarditis. IV. Structure and evolution of very early lesions. *Journal of Pathology*, 115, 81-9.
- DUROVIC, A., WIDMER, A. F., FREI, R. & TSCHUDIN-SUTTER, S. 2017. Distinguishing *Clostridium difficile* Recurrence From Reinfection: Independent Validation of Current Recommendations. *Infection Control and Hospital Epidemiology*, 38, 891-896.
- DYER, C., HUTT, L. P., BURKY, R. & JOSHI, L. T. 2019. Biocide Resistance and Transmission of *Clostridium difficile* Spores Spiked onto Clinical Surfaces from an American Health Care Facility. *Applied Environmental Microbiology*, 85, e01090-19.
- ECKERT, C., EMIRIAN, A., LE MONNIER, A., CATHALA, L., DE MONTCLOS, H., GORET, J., BERGER, P., PETIT, A., DE CHEVIGNY, A., JEAN-PIERRE, H., NEBBAD, B., CAMIADE, S., MECKENSTOCK, R., LALANDE, V., MARCHANDIN, H. & BARBUT, F. 2015. Prevalence and pathogenicity of binary toxin-positive *Clostridium difficile* strains that do not produce toxins A and B. *New Microbes and New Infections*, 3, 12-17.
- EDWARDS, A. N., KARIM, S. T., PASCUAL, R. A., JOWHAR, L. M., ANDERSON, S. E. & MCBRIDE, S. M. 2016. Chemical and Stress Resistances of *Clostridium difficile* Spores and Vegetative Cells. *Frontiers in Microbiology*, 7, 1698.
- EDWARDS, A. N., NAWROCKI, K. L. & MCBRIDE, S. M. 2014. Conserved oligopeptide permeases modulate sporulation initiation in *Clostridium difficile*. *Infection and immunity*, 82, 4276-4291.

- EGERER, M., GIESEMANN, T., JANK, T., SATCHELL, K. J. & AKTORIES, K. 2007. Auto-catalytic cleavage of *Clostridium difficile* toxins A and B depends on cysteine protease activity. *Journal of Biological Chemistry*, 282, 25314-21.
- EISEMAN, B., SILEN, W., BASCOM, G. S. & KAUVAR, A. J. 1958. Fecal enema as an adjunct in the treatment of pseudomembranous enterocolitis. *Surgery*, 44, 854-9.
- EL MEOUCHE, I., PELTIER, J., MONOT, M., SOUTOURINA, O., PESTEL-CARON, M., DUPUY, B. & PONS, J. L. 2013. Characterization of the SigD regulon of *C. difficile* and its positive control of toxin production through the regulation of tcdR. *PLoS One*, 8, e83748.
- ELBEHERY, A. H. A., FEICHTMAYER, J., SINGH, D., GRIEBLER, C. & DENG, L. 2018. The Human Virome Protein Cluster Database (HVPC): A Human Viral Metagenomic Database for Diversity and Function Annotation. *Frontiers in microbiology*, 9, 1110-1110.
- ENGEVIK, M. A., ENGEVIK, K. A., YACYSHYN, M. B., WANG, J., HASSETT, D. J., DARIEN, B., YACYSHYN, B. R. & WORRELL, R. T. 2015. Human *Clostridium difficile* infection: inhibition of NHE3 and microbiota profile. *American Journal of Physiology- Gastrointestinal and Liver Physiology*, 308, G497-509.
- EVAIN, S., BOURIGAULT, C., JUVIN, M. E., CORVEC, S. & LEPELLETIER, D. 2019. Carbapenemase-producing Enterobacteriaceae digestive carriage at hospital readmission and the role of antibiotic exposure. *Journal of Hospital Infection*, 102, 25-30.
- FAIR, K. L., COLQUHOUN, J. & HANNAN, N. R. F. 2018. Intestinal organoids for modelling intestinal development and disease. *Philosophical Transactions of the Royal Society of London. Series B, Biological Sciences*, 373, 1750.
- FAROOQ, P. D., URRUNAGA, N. H., TANG, D. M. & VON ROSENVINGE, E. C. 2015. Pseudomembranous Colitis. *Disease-a-month : DM*, 61, 181-206.
- FARROW, M. A., CHUMBLER, N. M., LAPIERRE, L. A., FRANKLIN, J. L., RUTHERFORD, S. A., GOLDENRING, J. R. & LACY, D. B. 2013. *Clostridium difficile* toxin B-induced necrosis is mediated by the host epithelial cell NADPH oxidase complex. *Proceedings of the National Academy of Sciences of the United States of America*, 110, 18674-9.
- FAULDS-PAIN, A., TWINE, S. M., VINOGRADOV, E., STRONG, P. C. R., DELL, A., BUCKLEY, A. M., DOUCE, G. R., VALIENTE, E., LOGAN, S. M. & WREN, B. W. 2014. The post-translational modification of the *Clostridium difficile* flagellin affects motility, cell surface properties and virulence. *Molecular Microbiology*, 94, 272-289.

- FAWLEY, W. N., UNDERWOOD, S., FREEMAN, J., BAINES, S. D., SAXTON, K., STEPHENSON, K., OWENS, R. C. & WILCOX, M. H. 2007. Efficacy of Hospital Cleaning Agents and Germicides Against Epidemic *Clostridium difficile* Strains. *Infection Control & Hospital Epidemiology*, 28, 920-925.
- FEHLBAUM, S., CHASSARD, C., HAUG, M. C., FOURMESTRAUX, C., DERRIEN, M. & LACROIX, C. 2015. Design and Investigation of PolyFermS *In Vitro* Continuous Fermentation Models Inoculated with Immobilized Fecal Microbiota Mimicking the Elderly Colon. *PLOS ONE*, 10, e0142793.
- FEHLBAUM, S., CHASSARD, C., POEKER, S. A., DERRIEN, M., FOURMESTRAUX, C. & LACROIX, C. 2016. *Clostridium difficile* colonization and antibiotics response in PolyFermS continuous model mimicking elderly intestinal fermentation. *Gut pathogens*, 8, 63-63.
- FEKETY, R. & SHAH, A. B. 1993. Diagnosis and treatment of *Clostridium difficile* colitis. *Jama*, 269, 71-5.
- FEKETY, R., SILVA, J., TOSHNIWAL, R., ALLO, M., ARMSTRONG, J., BROWNE, R., EBRIGHT, J. & RIFKIN, G. 1979. Antibiotic-associated colitis: effects of antibiotics on *Clostridium difficile* and the disease in hamsters. *Reviews of Infectious Diseases*, 1, 386-97.
- FERREYRA, J. A., WU, K. J., HRYCKOWIAN, A. J., BOULEY, D. M., WEIMER, B. C. & SONNENBURG, J. L. 2014. Gut microbiota-produced succinate promotes *C. difficile* infection after antibiotic treatment or motility disturbance. *Cell host & microbe*, 16, 770-777.
- FIGUEROA, I., JOHNSON, S., SAMBOL, S. P., GOLDSTEIN, E. J., CITRON, D. M. & GERDING, D. N. 2012. Relapse versus reinfection: recurrent *Clostridium difficile* infection following treatment with fidaxomicin or vancomycin. *Clinical Infectious Diseases*, 55 Suppl 2, S104-9.
- FINEGOLD, S. M., MOLITORIS, D., VAISANEN, M. L., SONG, Y., LIU, C. & BOLANOS, M. 2004. *In vitro* activities of OPT-80 and comparator drugs against intestinal bacteria. *Antimicrobial Agents and Chemotherapy*, 48, 4898-902.
- FINNEY, J. M. 1983. Gastroenterostomy for cicatrizing ulcer of pylorus. *Bulletin Johns Hopkins Hospital*, 4, 53.
- FLEMMING, H.-C. & WINGENDER, J. 2010. The biofilm matrix. *Nature Reviews Microbiology*, 8, 623-633.
- FOLKERS, B. L., SCHURING, C., ESSMANN, M. & LARSEN, B. 2010. Quantitative real time PCR detection of *Clostridium difficile* growth inhibition by probiotic organisms. *North American Journal of Medical Sciences*, 2, 5-10.

- FRANCIS, M. B., ALLEN, C. A., SHRESTHA, R. & SORG, J. A. 2013. Bile acid recognition by the *Clostridium difficile* germinant receptor, CspC, is important for establishing infection. *PLoS Pathogens*, 9, e1003356.
- FREEMAN, J., BAINES, S. D., JABES, D. & WILCOX, M. H. 2005. Comparison of the efficacy of ramoplanin and vancomycin in both *in vitro* and *in vivo* models of clindamycin-induced *Clostridium difficile* infection. *Journal of Antimicrobial Chemotherapy*, 56, 717-725.
- FREEMAN, J., BAINES, S. D., SAXTON, K. & WILCOX, M. H. 2007. Effect of metronidazole on growth and toxin production by epidemic *Clostridium difficile* PCR ribotypes 001 and 027 in a human gut model. *Journal of Antimicrobial Chemotherapy*, 60, 83-91.
- FREEMAN, J., BAUER, M. P., BAINES, S. D., CORVER, J., FAWLEY, W. N., GOORHUIS, B., KUIJPER, E. J. & WILCOX, M. H. 2010. The Changing Epidemiology of *Clostridium difficile* Infections. *Clinical Microbiology Reviews*, 23, 529-549.
- FREEMAN, J., O'NEILL, F. J. & WILCOX, M. H. 2003. Effects of cefotaxime and desacetylcefotaxime upon *Clostridium difficile* proliferation and toxin production in a triple-stage chemostat model of the human gut. *Journal of Antimicrobial Chemotherapy*, 52, 96-102.
- FROSSARD, A., HAMMES, F. & GESSNER, M. O. 2016. Flow Cytometric Assessment of Bacterial Abundance in Soils, Sediments and Sludge. *Frontiers in Microbiology*, 7, 903.
- GAMBELLO, M. J. & IGLEWSKI, B. H. 1991. Cloning and characterization of the *Pseudomonas aeruginosa* lasR gene, a transcriptional activator of elastase expression. *Journal of Bacteriology*, 173, 3000-9.
- GEORGE, R. H., SYMONDS, J. M., DIMOCK, F., BROWN, J. D., ARABI, Y., SHINAGAWA, N., KEIGHLEY, M. R., ALEXANDER-WILLIAMS, J. & BURDON, D. W. 1978a. Identification of *Clostridium difficile* as a cause of pseudomembranous colitis. *British Medical Journal*, 1, 695-695.
- GEORGE, W. L., SUTTER, V. L., GOLDSTEIN, E. J., LUDWIG, S. L. & FINEGOLD, S. M. 1978b. Aetiology of antimicrobial-agent-associated colitis. *Lancet*, 1, 802-3.
- GERDING, D. N., JOHNSON, S., RUPNIK, M. & AKTORIES, K. 2014. *Clostridium difficile* binary toxin CDT: mechanism, epidemiology, and potential clinical importance. *Gut Microbes*, 5, 15-27.
- GERHARD, R., NOTTROT, S., SCHOENTAUBE, J., TATGE, H., OLLING, A. & JUST, I. 2008. Glucosylation of Rho GTPases by *Clostridium difficile* toxin A triggers apoptosis in intestinal epithelial cells. *Journal of Medical Microbiology*, 57, 765-70.

- GILL, S. R., POP, M., DEBOY, R. T., ECKBURG, P. B., TURNBAUGH, P. J., SAMUEL, B. S., GORDON, J. I., RELMAN, D. A., FRASER-LIGGETT, C. M. & NELSON, K. E. 2006. Metagenomic Analysis of the Human Distal Gut Microbiome. *Science*, 312, 1355-1359.
- GIRINATHAN, B. P., OU, J., DUPUY, B. & GOVIND, R. 2018. Pleiotropic roles of *Clostridium difficile* *sin* locus. *PLOS Pathogens*, 14, e1006940.
- GOERES, D. M., HAMILTON, M. A., BECK, N. A., BUCKINGHAM-MEYER, K., HILYARD, J. D., LOETTERLE, L. R., LORENZ, L. A., WALKER, D. K. & STEWART, P. S. 2009. A method for growing a biofilm under low shear at the air-liquid interface using the drip flow biofilm reactor. *Nature Protocols*, 4, 783-8.
- GOLDENBERG, S. D., CLIFF, P. R., SMITH, S., MILNER, M. & FRENCH, G. L. 2010. Two-step glutamate dehydrogenase antigen real-time polymerase chain reaction assay for detection of toxigenic *Clostridium difficile*. *Journal of Hospital Infections*, 74, 48-54.
- GÓMEZ-SUÁREZ, C., BUSSCHER, H. J. & VAN DER MEI, H. C. 2001. Analysis of bacterial detachment from substratum surfaces by the passage of air-liquid interfaces. *Applied Environmental Microbiology*, 67, 2531-7.
- GONÇALVES, C., DECRÉ, D., BARBUT, F., BURGHOFFER, B. & PETIT, J.-C. 2004. Prevalence and Characterization of a Binary Toxin (Actin-Specific ADP-Ribosyltransferase) from *Clostridium difficile*. *Journal of Clinical Microbiology*, 42, 1933-1939.
- GONZÁLEZ-MACHADO, C., CAPITA, R., RIESCO-PELÁEZ, F. & ALONSO-CALLEJA, C. 2018. Visualization and quantification of the cellular and extracellular components of *Salmonella agona* biofilms at different stages of development. *PLOS One*, 13, e0200011.
- GORBACH, S. L. 2014. John G. Bartlett: Contributions to the discovery of *Clostridium difficile* antibiotic-associated diarrhea. *Clinical Infectious Diseases*, 59 Suppl 2, S66-70.
- GOUGH, E., SHAIKH, H. & MANGES, A. R. 2011. Systematic Review of Intestinal Microbiota Transplantation (Fecal Bacteriotherapy) for Recurrent *Clostridium difficile* Infection. *Clinical Infectious Diseases*, 53, 994-1002.
- GOULDING, D., THOMPSON, H., EMERSON, J., FAIRWEATHER, N. F., DOUGAN, G. & DOUCE, G. R. 2009. Distinctive profiles of infection and pathology in hamsters infected with *Clostridium difficile* strains 630 and B1. *Infection and Immunity*, 77, 5478-85.
- GOVIND, R. & DUPUY, B. 2012. Secretion of *Clostridium difficile* toxins A and B requires the holin-like protein TcdE. *PLoS Pathogens*, 8, e1002727.

- GRAND, I., BELLON-FONTAINE, M. N., HERRY, J. M., HILAIRE, D., MORICONI, F. X. & NAÏTALI, M. 2011. Possible overestimation of surface disinfection efficiency by assessment methods based on liquid sampling procedures as demonstrated by *in situ* quantification of spore viability. *Applied and environmental microbiology*, 77, 6208-6214.
- GREGORY, A. C., ZABLOCKI, O., HOWELL, A., BOLDOC, B. & SULLIVAN, M. B. 2019. The human gut virome database. *BioRxiv*, 655910.
- GUILBAUD, M., PIVETEAU, P., DESVAUX, M., BRISSE, S. & BRIANDET, R. 2015. Exploring the diversity of *Listeria monocytogenes* biofilm architecture by high-throughput confocal laser scanning microscopy and the predominance of the honeycomb-like morphotype. *Applied and environmental microbiology*, 81, 1813-1819.
- GULKE, I., PFEIFER, G., LIESE, J., FRITZ, M., HOFMANN, F., AKTORIES, K. & BARTH, H. 2001. Characterization of the enzymatic component of the ADP-ribosyltransferase toxin CDTa from *Clostridium difficile*. *Infection and Immunity*, 69, 6004-11.
- GUPTA, S. B., MEHTA, V., DUBBERKE, E. R., ZHAO, X., DORR, M. B., GURIS, D., MOLRINE, D., LENEY, M., MILLER, M., DUPIN, M. & MAST, T. C. 2016. Antibodies to Toxin B Are Protective Against *Clostridium difficile* Infection Recurrence. *Clinical Infectious Diseases*, 63, 730-734.
- HAAGENSEN, J. A., KLAUSEN, M., ERNST, R. K., MILLER, S. I., FOLKESSON, A., TOLKER-NIELSEN, T. & MOLIN, S. 2007. Differentiation and distribution of colistin- and sodium dodecyl sulfate-tolerant cells in *Pseudomonas aeruginosa* biofilms. *Journal of Bacteriology*, 189, 28-37.
- HAIKO, J. & WESTERLUND-WIKSTRÖM, B. 2013. The Role of the Bacterial Flagellum in Adhesion and Virulence. *Biology*, 2, 1242-1267.
- HALE, M. L., MARVAUD, J. C., POPOFF, M. R. & STILES, B. G. 2004. Detergent-resistant membrane microdomains facilitate I_b oligomer formation and biological activity of *Clostridium perfringens* iota-toxin. *Infection and Immunity*, 72, 2186-93.
- HALL-STOODLEY, L., COSTERTON, J. W. & STOODLEY, P. 2004. Bacterial biofilms: from the Natural environment to infectious diseases. *Nature Reviews Microbiology*, 2, 95-108.
- HALL-STOODLEY, L. & STOODLEY, P. 2009. Evolving concepts in biofilm infections. *Cell Microbiology*, 11, 1034-43.
- HALL, I. C. & O'TOOLE, E. 1935. Intestinal flora in new-born infants: With a description of a new pathogenic anaerobe, bacillus difficilis. *American Journal of Diseases of Children*, 49, 390-402.

- HAMM, E. E., VOTH, D. E. & BALLARD, J. D. 2006. Identification of *Clostridium difficile* toxin B cardiotoxicity using a zebrafish embryo model of intoxication. *Proceedings of the National Academy of Science of the United States of America*, 103, 14176-81.
- HAMMOND, E., DONKOR, E. & BROWN, C. 2014. Biofilm formation of *Clostridium difficile* and susceptibility to Manuka Honey. *BMC Complementary and Alternative Medicine*, 14, 1-6.
- HAMMOND, G. A. & JOHNSON, J. L. 1995. The toxigenic element of *Clostridium difficile* strain VPI 10463. *Microbial Pathogenesis*, 19, 203-13.
- HARRIOTT, M. M. & NOVERR, M. C. 2010. Ability of *Candida albicans* mutants to induce *Staphylococcus aureus* vancomycin resistance during polymicrobial biofilm formation. *Antimicrobial Agents and Chemotherapy*, 54, 3746-55.
- HATHROUBI, S., SERVETAS, S. L., WINDHAM, I., MERRELL, D. S. & OTTEMANN, K. M. 2018. *Helicobacter pylori* Biofilm Formation and Its Potential Role in Pathogenesis. *Microbiology and molecular biology reviews : MMBR*, 82, e00001-18.
- HATT, J. K. & RATHER, P. N. 2008. Role of bacterial biofilms in urinary tract infections. *Current Topics in Microbiology and Immunology*, 322, 163-92.
- HAUG, G., AKTORIES, K. & BARTH, H. 2004. The host cell chaperone Hsp90 is necessary for cytotoxic action of the binary iota-like toxins. *Infection and Immunity*, 72, 3066-8.
- HECHT, D. W., GALANG, M. A., SAMBOL, S. P., OSMOLSKI, J. R., JOHNSON, S. & GERDING, D. N. 2007. *In vitro* activities of 15 antimicrobial agents against 110 toxigenic *Clostridium difficile* clinical isolates collected from 1983 to 2004. *Antimicrobial Agents Chemotherapy*, 51, 2716-9.
- HECHT, G., KOUTSOURIS, A., POTHOUKAKIS, C., LAMONT, J. T. & MADARA, J. L. 1992. *Clostridium difficile* toxin B disrupts the barrier function of T84 monolayers. *Gastroenterology*, 102, 416-23.
- HENNEQUIN, C., JANOIR, C., BARC, M. C., COLLIGNON, A. & KARJALAINEN, T. 2003. Identification and characterization of a fibronectin-binding protein from *Clostridium difficile*. *Microbiology*, 149, 2779-87.
- HENRIQUES, A. O. & CHARLES P. MORAN, J. 2007. Structure, Assembly, and Function of the Spore Surface Layers. *Annual Review of Microbiology*, 61, 555-588.
- HENSBERGEN, P. J., KLYCHNIKOV, O. I., BAKKER, D., VAN WINDEN, V. J., RAS, N., KEMP, A. C., CORDFUNKE, R. A., DRAGAN, I., DEELDER, A.

- M., KUIJPER, E. J., CORVER, J., DRIJFHOUT, J. W. & VAN LEEUWEN, H. C. 2014. A novel secreted metalloprotease (CD2830) from *Clostridium difficile* cleaves specific proline sequences in LPXTG cell surface proteins. *Molecular and Cellular Proteomics*, 13, 1231-44.
- HILL, D. R. & SPENCE, J. R. 2016. Gastrointestinal Organoids: Understanding the Molecular Basis of the Host-Microbe Interface. *Cellular and molecular gastroenterology and hepatology*, 3, 138-149.
- HIPPENSTIEL, S., SCHMECK, B., N'GUESSAN, P. D., SEYBOLD, J., KRULL, M., PREISSNER, K., EICHEL-STREIBER, C. V. & SUTTORP, N. 2002. Rho protein inactivation induced apoptosis of cultured human endothelial cells. *American Journal of Physiology-Lung Cellular and Molecular Physiology*, 283, L830-8.
- HIROTA, S. A., FINES, K., NG, J., TRABOULSI, D., LEE, J., IHARA, E., LI, Y., WILLMORE, W. G., CHUNG, D., SCULLY, M. M., LOUIE, T., MEDLICOTT, S., LEJEUNE, M., CHADEE, K., ARMSTRONG, G., COLGAN, S. P., MURUVE, D. A., MACDONALD, J. A. & BECK, P. L. 2010. Hypoxia-inducible factor signaling provides protection in *Clostridium difficile*-induced intestinal injury. *Gastroenterology*, 139, 259-69.e3.
- HO, T. D., WILLIAMS, K. B., CHEN, Y., HELM, R. F., POPHAM, D. L. & ELLERMEIER, C. D. 2014. *Clostridium difficile* extracytoplasmic function sigma factor sigmaV regulates lysozyme resistance and is necessary for pathogenesis in the hamster model of infection. *Infection and Immunity*, 82, 2345-55.
- HOFFMANN, B., ESCHBAUMER, M. & BEER, M. 2009. Real-Time Quantitative Reverse Transcription-PCR Assays Specifically Detecting Bluetongue Virus Serotypes 1, 6, and 8. *Journal of Clinical Microbiology*, 47, 2992-2994.
- HOIBY, N. 2011. Recent advances in the treatment of *Pseudomonas aeruginosa* infections in cystic fibrosis. *BMC Medicine*, 9, 32.
- HOLD, G. L., PRYDE, S. E., RUSSELL, V. J., FURRIE, E. & FLINT, H. J. 2002. Assessment of microbial diversity in human colonic samples by 16S rDNA sequence analysis. *FEMS Microbiology Ecology*, 39, 33-9.
- HOPKINS, M. J. & MACFARLANE, G. T. 2003. Nondigestible oligosaccharides enhance bacterial colonization resistance against *Clostridium difficile* *in vitro*. *Applied Environmental Microbiology*, 69, 1920-7.
- HORVAT, S., MAHNIC, A., BRESKVAR, M., DZEROSKI, S. & RUPNIK, M. 2017. Evaluating the effect of *Clostridium difficile* conditioned medium on fecal microbiota community structure. *Scientific Reports*, 7, 16448.

- HORVAT, S. & RUPNIK, M. 2018. Interactions Between *Clostridioides difficile* and Fecal Microbiota in *in Vitro* Batch Model: Growth, Sporulation, and Microbiota Changes. *Frontiers in microbiology*, 9, 1633-1633.
- HUGON, P., DUFOUR, J. C., COLSON, P., FOURNIER, P. E., SALLAH, K. & RAOULT, D. 2015. A comprehensive repertoire of prokaryotic species identified in human beings. *Lancet Infectious Diseases*, 15, 1211-1219.
- HUNDSBERGER, T., BRAUN, V., WEIDMANN, M., LEUKEL, P., SAUERBORN, M. & VON EICHEL-STREIBER, C. 1997. Transcription analysis of the genes *tcdA-E* of the pathogenicity locus of *Clostridium difficile*. *European Journal of Biochemistry*, 244, 735-42.
- HUTTNER, B. D., DE LASTOURS, V., WASSENBERG, M., MAHARSHAK, N., MAURIS, A., GALPERINE, T., ZANICHELLI, V., KAPEL, N., BELLANGER, A., OLEARO, F., DUVAL, X., ARMAND-LEFEVRE, L., CARMELI, Y., BONTEN, M., FANTIN, B. & HARBARTH, S. 2019. A 5-day course of oral antibiotics followed by faecal transplantation to eradicate carriage of multidrug-resistant Enterobacteriaceae: a randomized clinical trial. *Clinical Microbiology and Infection*, 25, 830-838.
- HUTTON, M. L., MACKIN, K. E., CHAKRAVORTY, A. & LYRAS, D. 2014. Small animal models for the study of *Clostridium difficile* disease pathogenesis. *FEMS Microbiology Letters*, 352, 140-149.
- ICHIKAWA, H., KUROIWA, T., INAGAKI, A., SHINEHA, R., NISHIHARA, T., SATOMI, S. & SAKATA, T. 1999. Probiotic bacteria stimulate gut epithelial cell proliferation in rat. *Digestive Diseases and Sciences*, 44, 2119-23.
- IMASE, K., TAKAHASHI, M., TANAKA, A., TOKUNAGA, K., SUGANO, H., TANAKA, M., ISHIDA, H., KAMIYA, S. & TAKAHASHI, S. 2008. Efficacy of *Clostridium butyricum* preparation concomitantly with *Helicobacter pylori* eradication therapy in relation to changes in the intestinal microbiota. *Microbiology and Immunology*, 52, 156-61.
- JAFFE, A. B. & HALL, A. 2005. Rho GTPases: biochemistry and biology. *Annual Review of Cell Developmental Biology*, 21, 247-69.
- JAIN, S., SMYTH, D., O'HAGAN, B. M. G., HEAP, J. T., MCMULLAN, G., MINTON, N. P. & TERNAN, N. G. 2017. Inactivation of the *dnaK* gene in *Clostridium difficile* 630 Δ erm yields a temperature-sensitive phenotype and increases biofilm-forming ability. *Scientific Reports*, 7, 17522.
- JAKUBOVICS, N. S., GILL, S. R., IOBST, S. E., VICKERMAN, M. M. & KOLENBRANDER, P. E. 2008. Regulation of gene expression in a mixed-genus community: stabilized arginine biosynthesis in *Streptococcus gordonii* by coaggregation with *Actinomyces naeslundii*. *Journal of Bacteriology*, 190, 3646-57.

- JAMAL, M., AHMAD, W., ANDLEEB, S., JALIL, F., IMRAN, M., NAWAZ, M. A., HUSSAIN, T., ALI, M., RAFIQ, M. & KAMIL, M. A. 2018. Bacterial biofilm and associated infections. *Journal of the Chinese Medical Association*, 81, 7-11.
- JAMES, G. A., CHESNEL, L., BOEGLI, L., DELANCEY PULCINI, E., FISHER, S. & STEWART, P. S. 2017. Analysis of *Clostridium difficile* biofilms: imaging and antimicrobial treatment. *Journal of Antimicrobial Chemotherapy*, 73, 102-108.
- JANK, T. & AKTORIES, K. 2008. Structure and mode of action of clostridial glucosylating toxins: the ABCD model. *Trends in Microbiology*, 16, 222-229.
- JANOIR, C., PECHINE, S., GROSDIDIER, C. & COLLIGNON, A. 2007. Cwp84, a surface-associated protein of *Clostridium difficile*, is a cysteine protease with degrading activity on extracellular matrix proteins. *Journal of Bacteriology*, 189, 7174-80.
- JENSEN, P., KOLPEN, M., KRAGH, K. N. & KÜHL, M. 2017. Microenvironmental characteristics and physiology of biofilms in chronic infections of CF patients are strongly affected by the host immune response. *Apmis*, 125, 276-288.
- JOHNSON, S., LOUIE, T. J., GERDING, D. N., CORNELLY, O. A., CHASANTABER, S., FITTS, D., GELONE, S. P., BROOM, C. & DAVIDSON, D. M. 2014. Vancomycin, metronidazole, or tolevamer for *Clostridium difficile* infection: results from two multinational, randomized, controlled trials. *Clinical Infectious Diseases*, 59, 345-54.
- JOUHTEN, H., MATTILA, E., ARKKILA, P. & SATOKARI, R. 2016. Reduction of Antibiotic Resistance Genes in Intestinal Microbiota of Patients With Recurrent *Clostridium difficile* Infection After Fecal Microbiota Transplantation. *Clinical Infectious Diseases*, 63, 710-711.
- JUST, I., SELZER, J., WILM, M., VON EICHEL-STREIBER, C., MANN, M. & AKTORIES, K. 1995a. Glucosylation of Rho proteins by *Clostridium difficile* toxin B. *Nature*, 375, 500-3.
- JUST, I., WILM, M., SELZER, J., REX, G., VON EICHEL-STREIBER, C., MANN, M. & AKTORIES, K. 1995b. The enterotoxin from *Clostridium difficile* (ToxA) monoglucosylates the Rho proteins. *Journal of Biological Chemistry*, 270, 13932-6.
- KAATZ, G. W., GITLIN, S. D., SCHABERG, D. R., WILSON, K. H., KAUFFMAN, C. A., SEO, S. M. & FEKETY, R. 1988. Acquisition of *Clostridium difficile* from the hospital environment. *American Journal of Epidemiology*, 127, 1289-94.
- KAISER, E., KROLL, C., ERNST, K., SCHWAN, C., POPOFF, M., FISCHER, G., BUCHNER, J., AKTORIES, K. & BARTH, H. 2011. Membrane

translocation of binary actin-ADP-ribosylating toxins from *Clostridium difficile* and *Clostridium perfringens* is facilitated by cyclophilin A and Hsp90. *Infection and Immunity*, 79, 3913-21.

- KALAMARA, M., SPACAPAN, M., MANDIC-MULEC, I. & STANLEY-WALL, N. R. 2018. Social behaviours by *Bacillus subtilis*: quorum sensing, kin discrimination and beyond. *Molecular Microbiology*, 110, 863-878.
- KAMBOJ, M., KHOSA, P., KALTSAS, A., BABADY, N. E., SON, C. & SEPKOWITZ, K. A. 2011. Relapse versus reinfection: surveillance of *Clostridium difficile* infection. *Clinical infectious diseases : an official publication of the Infectious Diseases Society of America*, 53, 1003-1006.
- KAMIYA, S., TAGUCHI, H., YAMAGUCHI, H., OSAKI, T., TAKAHASHI, M. & NAKAMURA, S. 1997. Bacteriophylaxis using *Clostridium butyricum* for lethal caecitis by *Clostridium difficile* in gnotobiotic mice. *Reviews in Medical Microbiology*, 8, S60.
- KAPLAN, J. B. 2010. Biofilm dispersal: mechanisms, clinical implications, and potential therapeutic uses. *Journal of dental research*, 89, 205-218.
- KAPLAN, J. B., RAGUNATH, C., RAMASUBBU, N. & FINE, D. H. 2003. Detachment of *Actinobacillus actinomycescomitans* biofilm cells by an endogenous beta-hexosaminidase activity. *Journal of Bacteriology*, 185, 4693-4698.
- KARJALAINEN, T., BARC, M. C., COLLIGNON, A., TROLLÉ, S., BOUREAU, H., COTTE-LAFFITTE, J. & BOURLIOUX, P. 1994. Cloning of a genetic determinant from *Clostridium difficile* involved in adherence to tissue culture cells and mucus. *Infection and Immunity*, 62, 4347-4355.
- KARLSSON, S., LINDBERG, A., NORIN, E., BURMAN, L. G. & AKERLUND, T. 2000. Toxins, butyric acid, and other short-chain fatty acids are coordinately expressed and down-regulated by cysteine in *Clostridium difficile*. *Infection and Immunity*, 68, 5881-8.
- KARLSTROM, O., FRYKLUND, B., TULLUS, K. & BURMAN, L. G. 1998. A prospective nationwide study of *Clostridium difficile*-associated diarrhea in Sweden. The Swedish *C. difficile* Study Group. *Clinical Infectious Diseases*, 26, 141-5.
- KASSAM, Z., LEE, C. H., YUAN, Y. & HUNT, R. H. 2013. Fecal microbiota transplantation for *Clostridium difficile* infection: systematic review and meta-analysis. *American Journal of Gastroenterology*, 108, 500-8.
- KEAN, R., RAJENDRAN, R., HAGGARTY, J., TOWNSEND, E. M., SHORT, B., BURGESS, K. E., LANG, S., MILLINGTON, O., MACKAY, W. G., WILLIAMS, C. & RAMAGE, G. 2017. *Candida albicans* Mycofilms Support *Staphylococcus aureus* Colonization and Enhances Miconazole

Resistance in Dual-Species Interactions. *Frontiers in Microbiology*, 8, 258.

- KELLINGRAY, L., GALL, G. L., DEFERNEZ, M., BEALES, I. L. P., FRANSLEM-ELUMOGO, N. & NARBAD, A. 2018. Microbial taxonomic and metabolic alterations during faecal microbiota transplantation to treat *Clostridium difficile* infection. *Journal of Infection*, 77, 107-118.
- KELLY, C. P., BECKER, S., LINEVSKY, J. K., JOSHI, M. A., O'KEANE, J. C., DICKEY, B. F., LAMONT, J. T. & POTHOUKAKIS, C. 1994. Neutrophil recruitment in *Clostridium difficile* toxin A enteritis in the rabbit. *The Journal of Clinical Investigation*, 93, 1257-1265.
- KELLY, C. P. & LAMONT, J. T. 2008. *Clostridium difficile* — More Difficult Than Ever. *New England Journal of Medicine*, 359, 1932-1940.
- KELLY, C. R., IHUNNAH, C., FISCHER, M., KHORUTS, A., SURAWICZ, C., AFZALI, A., ARONIADIS, O., BARTO, A., BORODY, T., GIOVANELLI, A., GORDON, S., GLUCK, M., HOHMANN, E. L., KAO, D., KAO, J. Y., MCQUILLEN, D. P., MELLOW, M., RANK, K. M., RAO, K., RAY, A., SCHWARTZ, M. A., SINGH, N., STOLLMAN, N., SUSKIND, D. L., VINDIGNI, S. M., YOUNGSTER, I. & BRANDT, L. 2014. Fecal microbiota transplant for treatment of *Clostridium difficile* infection in immunocompromised patients. *American Journal of Gastroenterology*, 109, 1065-71.
- KELLY, C. R., KHORUTS, A., STALEY, C., SADOWSKY, M. J., ABD, M., ALANI, M., BAKOW, B., CURRAN, P., MCKENNEY, J., TISCH, A., REINERT, S. E., MACHAN, J. T. & BRANDT, L. J. 2016. Effect of Fecal Microbiota Transplantation on Recurrence in Multiply Recurrent *Clostridium difficile* Infection: A Randomized Trial. *Annals of Internal Medicine*, 165, 609-616.
- KHANNA, S., PARDI, D., GERDING, D., BLOUNT, K., JONES, C., SHANNON, B. & DEYCH, E. 2018. RBX7455 - a Non-Frozen, Lyophilized, Oral Microbiota Reduces *Clostridium difficile* Infection Recurrence and Restores Patients' Microbiomes. *American Journal of Gastroenterology*, 188, 113, S107.
- KHANNA, S., PARDI, D. S., GERDING, D. N., BLOUNT, K., JONES, C. R., SHANNON, B. & DEYCH, E. 2019. Tu1880 2013; Durable Freedom from *Clostridium difficile* Infection Recurrence and Microbiome Restoration During Six-Month Follow-Up For a Phase 1 Clinical Trial of Rbx7455, An Investigational Room Temperature-Stable, Oral Microbiotabased Therapeutic. *Gastroenterology*, 156, S-1158.
- KHANNA, S., PARDI, D. S., KELLY, C. R., KRAFT, C. S., DHERE, T., HENN, M. R., LOMBARDO, M. J., VULIC, M., OHSUMI, T., WINKLER, J., PINDAR, C., MCGOVERN, B. H., POMERANTZ, R. J., AUNINS, J. G., COOK, D. N. & HOHMANN, E. L. 2016. A Novel Microbiome Therapeutic Increases Gut Microbial Diversity and Prevents Recurrent

Clostridium difficile Infection. *Journal of Infectious Diseases*, 214, 173-81.

KHORUTS, A., DICKSVED, J., JANSSON, J. K. & SADOWSKY, M. J. 2010. Changes in the composition of the human fecal microbiome after bacteriotherapy for recurrent *Clostridium difficile*-associated diarrhea. *Journal of Clinical Gastroenterology*, 44, 354-60.

KHORUTS, A. & SADOWSKY, M. J. 2016. Understanding the mechanisms of faecal microbiota transplantation. *Nature Reviews Gastroenterology & Hepatology*, 13, 508-16.

KIM, H. J., BOEDICKER, J. Q., CHOI, J. W. & ISMAGILOV, R. F. 2008. Defined spatial structure stabilizes a synthetic multispecies bacterial community. *Proceedings of the National Academy of Sciences of the United States of America*, 105, 18188-93.

KIM, K. H., FEKETY, R., BATTS, D. H., BROWN, D., CUDMORE, M., SILVA, J., JR. & WATERS, D. 1981. Isolation of *Clostridium difficile* from the environment and contacts of patients with antibiotic-associated colitis. *Journal of Infectious Diseases*, 143, 42-50.

KLAYMAN, B. J., VOLDEN, P. A., STEWART, P. S. & CAMPER, A. K. 2009. *Escherichia coli* O157:H7 requires colonizing partner to adhere and persist in a capillary flow cell. *Environmental Science & Technology*, 43, 2105-11.

KOBAN, I., MATTHES, R., HÜBNER, N.-O., WELK, A., SIETMANN, R., LADEMANN, J., KRAMER, A. & KOCHER, T. 2012. XTT assay of *ex vivo* saliva biofilms to test antimicrobial influences. *GMS Krankenhaushygiene interdisziplinär*, 7, Doc06.

KOH, K. S., LAM, K. W., ALHEDE, M., QUECK, S. Y., LABBATE, M., KJELLEBERG, S. & RICE, S. A. 2007. Phenotypic Diversification and Adaptation of *Serratia marcescens* MG1 Biofilm-Derived Morphotypes. *Journal of Bacteriology*, 189, 119-130.

KOLJALG, U., NILSSON, R. H., ABARENKOV, K., TEDERSOO, L., TAYLOR, A. F., BAHRAM, M., BATES, S. T., BRUNS, T. D., BENGTSSON-PALME, J., CALLAGHAN, T. M., DOUGLAS, B., DRENKHAN, T., EBERHARDT, U., DUENAS, M., GREBENC, T., GRIFFITH, G. W., HARTMANN, M., KIRK, P. M., KOHOUT, P., LARSSON, E., LINDAHL, B. D., LUCKING, R., MARTIN, M. P., MATHENY, P. B., NGUYEN, N. H., NISKANEN, T., OJA, J., PEAY, K. G., PEINTNER, U., PETERSON, M., POLDMAA, K., SAAG, L., SAAR, I., SCHUSSLER, A., SCOTT, J. A., SENES, C., SMITH, M. E., SUIJA, A., TAYLOR, D. L., TELLERIA, M. T., WEISS, M. & LARSSON, K. H. 2013. Towards a unified paradigm for sequence-based identification of fungi. *Molecular Ecology*, 22, 5271-7.

- KOVACS-SIMON, A., LEUZZI, R., KASENDRA, M., MINTON, N., TITBALL, R. W. & MICHELL, S. L. 2014. Lipoprotein CD0873 is a novel adhesin of *Clostridium difficile*. *Journal of Infectious Diseases*, 210, 274-84.
- KUMAR, R., YI, N., ZHI, D., EIPERS, P., GOLDSMITH, K. T., DIXON, P., CROSSMAN, D. K., CROWLEY, M. R., LEFKOWITZ, E. J., RODRIGUEZ, J. M. & MORROW, C. D. 2017. Identification of donor microbe species that colonize and persist long term in the recipient after fecal transplant for recurrent *Clostridium difficile*. *NPJ Biofilms Microbiomes*, 3, 12.
- KYNE, L., WARNY, M., QAMAR, A. & KELLY, C. P. 2001. Association between antibody response to toxin A and protection against recurrent *Clostridium difficile* diarrhoea. *Lancet*, 357, 189-93.
- LACROIX, C., DE WOUTERS, T. & CHASSARD, C. 2015. Integrated multi-scale strategies to investigate nutritional compounds and their effect on the gut microbiota. *Current Opinion in Biotechnology*, 32, 149-155.
- LAFRANCE, M. E., FARROW, M. A., CHANDRASEKARAN, R., SHENG, J., RUBIN, D. H. & LACY, D. B. 2015. Identification of an epithelial cell receptor responsible for *Clostridium difficile* TcdB-induced cytotoxicity. *Proceedings of the National Academy of Sciences of the United States of America*, 112, 7073-8.
- LAMENDELLA, R., WRIGHT, J. R., HACKMAN, J., MCLIMANS, C., TOOLE, D. R., BERNARD RUBIO, W., DRUCKER, R., WONG, H. T., SABEY, K., HEGARTY, J. P. & STEWART, D. B., SR. 2018. Antibiotic Treatments for *Clostridium difficile* Infection Are Associated with Distinct Bacterial and Fungal Community Structures. *mSphere*, 3, e00572-17.
- LANDELLE, C., VERACHTEN, M., LEGRAND, P., GIROU, E., BARBUT, F. & BUISSON, C. B. 2014. Contamination of Healthcare workers hands with *Clostridium difficile* spores after Caring for Patients with *C. difficile* Infection. *Infection Control and Hospital Epidemiology*, 35, 10-15.
- LANDRY, R. M., AN, D., HUPP, J. T., SINGH, P. K. & PARSEK, M. R. 2006. Mucin-Pseudomonas aeruginosa interactions promote biofilm formation and antibiotic resistance. *Molecular Microbiology*, 59, 142-51.
- LARSEN, T. & FIEHN, N. E. 2017. Dental biofilm infections - an update. *Apmis*, 125, 376-384.
- LARSON, H. E. & BORRIELLO, S. P. 1990. Quantitative study of antibiotic-induced susceptibility to *Clostridium difficile* enterocolitis in hamsters. *Antimicrobial Agents and Chemotherapy*, 34, 1348-53.
- LARSON, H. E., PARRY, J. V., PRICE, A. B., DAVIES, D. R., DOLBY, J. & TYRRELL, D. A. 1977. Undescribed toxin in pseudomembranous colitis. *BMJ*, 1, 1246-8.

- LARSON, H. E. & PRICE, A. B. 1977. Pseudomembranous colitis: Presence of clostridial toxin. *Lancet*, 2, 1312-4.
- LARSON, H. E. & WELCH, A. 1993. *In-vitro* and *in-vivo* characterisation of resistance to colonisation with *Clostridium difficile*. *Journal of Medical Microbiology*, 38, 103-8.
- LAU, H. Y. & ASHBOLT, N. J. 2009. The role of biofilms and protozoa in Legionella pathogenesis: implications for drinking water. *Journal of Applied Microbiology*, 107, 368-78.
- LAVELLE, A., LENNON, G., O'SULLIVAN, O., DOCHERTY, N., BALFE, A., MAGUIRE, A., MULCAHY, H. E., DOHERTY, G., O'DONOGHUE, D., HYLAND, J., ROSS, R. P., COFFEY, J. C., SHEAHAN, K., COTTER, P. D., SHANAHAN, F., WINTER, D. C. & O'CONNELL, P. R. 2015. Spatial variation of the colonic microbiota in patients with ulcerative colitis and control volunteers. *Gut*, 64, 1553-61.
- LAWLEY, T. D., CLARE, S., DEAKIN, L. J., GOULDING, D., YEN, J. L., RAISEN, C., BRANDT, C., LOVELL, J., COOKE, F., CLARK, T. G. & DOUGAN, G. 2010. Use of purified *Clostridium difficile* spores to facilitate evaluation of health care disinfection regimens. *Applied Environmental Microbiology*, 76, 6895-900.
- LAWLEY, T. D., CLARE, S., WALKER, A. W., GOULDING, D., STABLER, R. A., CROUCHER, N., MASTROENI, P., SCOTT, P., RAISEN, C., MOTTRAM, L., FAIRWEATHER, N. F., WREN, B. W., PARKHILL, J. & DOUGAN, G. 2009a. Antibiotic treatment of *clostridium difficile* carrier mice triggers a supershedder state, spore-mediated transmission, and severe disease in immunocompromised hosts. *Infection and Immunity*, 77, 3661-9.
- LAWLEY, T. D., CLARE, S., WALKER, A. W., STARES, M. D., CONNOR, T. R., RAISEN, C., GOULDING, D., RAD, R., SCHREIBER, F., BRANDT, C., DEAKIN, L. J., PICKARD, D. J., DUNCAN, S. H., FLINT, H. J., CLARK, T. G., PARKHILL, J. & DOUGAN, G. 2012. Targeted restoration of the intestinal microbiota with a simple, defined bacteriotherapy resolves relapsing *Clostridium difficile* disease in mice. *PLoS Pathogens*, 8, e1002995.
- LAWLEY, T. D., CROUCHER, N. J., YU, L., CLARE, S., SEBAIHIA, M., GOULDING, D., PICKARD, D. J., PARKHILL, J., CHOUDHARY, J. & DOUGAN, G. 2009b. Proteomic and genomic characterization of highly infectious *Clostridium difficile* 630 spores. *Journal of Bacteriology*, 191, 5377-86.
- LAWLEY, T. D. & YOUNG, V. B. 2013. Murine models to study *Clostridium difficile* infection and transmission. *Anaerobe*, 24, 94-97.

- LAWRENCE, J. R., SWERHONE, G. D. W., KUHLCHE, U. & NEU, T. R. 2007. *In situ* evidence for microdomains in the polymer matrix of bacterial microcolonies. *Canadian Journal of Microbiology*, 53, 450-458.
- LAWSON, P. A., CITRON, D. M., TYRRELL, K. L. & FINEGOLD, S. M. 2016. Reclassification of *Clostridium difficile* as *Clostridioides difficile* (Hall and O'Toole 1935) Prévot 1938. *Anaerobe*, 40, 95-99.
- LEBEER, S., VANDERLEYDEN, J. & DE KEERSMAECKER, S. C. 2008. Genes and molecules of lactobacilli supporting probiotic action. *Microbiology and Molecular Biology Reviews*, 72, 728-64.
- LEE, A. S. & SONG, K. P. 2005. LuxS/autoinducer-2 quorum sensing molecule regulates transcriptional virulence gene expression in *Clostridium difficile*. *Biochemical and Biophysical Research Communications*, 335, 659-66.
- LEE, C. H., STEINER, T., PETROF, E. O., SMIEJA, M., ROSCOE, D., NEMATALLAH, A., WEESE, J. S., COLLINS, S., MOAYYEDI, P., CROWTHER, M., ROPELESKI, M. J., JAYARATNE, P., HIGGINS, D., LI, Y., RAU, N. V. & KIM, P. T. 2016. Frozen vs Fresh Fecal Microbiota Transplantation and Clinical Resolution of Diarrhea in Patients With Recurrent *Clostridium difficile* Infection: A Randomized Clinical Trial. *Jama*, 315, 142-9.
- LEE, S. F., LI, Y. H. & BOWDEN, G. H. 1996. Detachment of *Streptococcus mutans* biofilm cells by an endogenous enzymatic activity. *Infection and Immunity*, 64, 1035-1038.
- LEFFLER, D. A. & LAMONT, J. T. 2015. *Clostridium difficile* infection. *New England Journal of Medicine*, 372, 1539-48.
- LEMBKE, C., PODBIELSKI, A., HIDALGO-GRASS, C., JONAS, L., HANSKI, E. & KREIKEMEYER, B. 2006. Characterization of Biofilm Formation by Clinically Relevant Serotypes of Group A Streptococci. *Applied and Environmental Microbiology*, 72, 2864-2875.
- LESLIE, J. L., HUANG, S., OPP, J. S., NAGY, M. S., KOBAYASHI, M., YOUNG, V. B. & SPENCE, J. R. 2015. Persistence and toxin production by *Clostridium difficile* within human intestinal organoids result in disruption of epithelial paracellular barrier function. *Infection and Immunity*, 83, 138-45.
- LEWANDOWSKI, Z., BEYENAL, H. & STOOKEY, D. 2004. Reproducibility of biofilm processes and the meaning of steady state in biofilm reactors. *Water Science & Technology*, 49, 359-64.
- LEWIS, K. 2008. Multidrug tolerance of biofilms and persister cells. *Current Topics in Microbiology and Immunology*, 322, 107-31.

- LEY, R. E., TURNBAUGH, P. J., KLEIN, S. & GORDON, J. I. 2006. Microbial ecology: human gut microbes associated with obesity. *Nature*, 444, 1022-3.
- LI, Y. H., LAU, P. C., LEE, J. H., ELLEN, R. P. & CVITKOVITCH, D. G. 2001. Natural genetic transformation of *Streptococcus mutans* growing in biofilms. *Journal of Bacteriology*, 183, 897-908.
- LI, Y. H. & TIAN, X. 2012. Quorum sensing and bacterial social interactions in biofilms. *Sensors (Basel)*, 12, 2519-38.
- LIN, Y.-P., KUO, C.-J., KOLECI, X., MCDONOUGH, S. P. & CHANG, Y.-F. 2011. Manganese Binds to *Clostridium difficile* Fbp68 and Is Essential for Fibronectin Binding. *Journal of Biological Chemistry*, 286, 3957-3969.
- LINDSAY, D. & VON HOLY, A. 2006. Bacterial biofilms within the clinical setting: what healthcare professionals should know. *Journal of Hospital Infection*, 64, 313-325.
- LIU, W., RØDER, H. L., MADSEN, J. S., BJARNSHOLT, T., SØRENSEN, S. J. & BURMØLLE, M. 2016. Interspecific Bacterial Interactions are Reflected in Multispecies Biofilm Spatial Organization. *Frontiers in microbiology*, 7, 1366-1366.
- LLOYD-PRICE, J., MAHURKAR, A., RAHNAVARD, G., CRABTREE, J., ORVIS, J., HALL, A. B., BRADY, A., CREASY, H. H., MCCRACKEN, C., GIGLIO, M. G., MCDONALD, D., FRANZOSA, E. A., KNIGHT, R., WHITE, O. & HUTTENHOWER, C. 2017. Strains, functions and dynamics in the expanded Human Microbiome Project. *Nature*, 550, 61-66.
- LOMBARDIA, E., ROVETTO, A. J., ARABOLAZA, A. L. & GRAU, R. R. 2006. A LuxS-dependent cell-to-cell language regulates social behavior and development in *Bacillus subtilis*. *Journal of Bacteriology*, 188, 4442-52.
- LOPETUSO, L. R., SCALDAFERRI, F., PETITO, V. & GASBARRINI, A. 2013. Commensal Clostridia: leading players in the maintenance of gut homeostasis. *Gut Pathogens*, 5, 23-23.
- LORITE, G. S., RODRIGUES, C. M., DE SOUZA, A. A., KRANZ, C., MIZAIKOFF, B. & COTTA, M. A. 2011. The role of conditioning film formation and surface chemical changes on *Xylella fastidiosa* adhesion and biofilm evolution. *Journal of Colloid and Interface Science*, 359, 289-295.
- LOUIE, T. J., MILLER, M. A., MULLANE, K. M., WEISS, K., LENTNEK, A., GOLAN, Y., GORBACH, S., SEARS, P. & SHUE, Y. K. 2011. Fidaxomicin versus vancomycin for *Clostridium difficile* infection. *New England Journal of Medicine*, 364, 422-31.

- LYERLY, D. M., SAUM, K. E., MACDONALD, D. K. & WILKINS, T. D. 1985. Effects of *Clostridium difficile* toxins given intragastrically to animals. *Infection and Immunity*, 47, 349-52.
- LYNCH, M., WALSH, T. A., MARSZALOWSKA, I., WEBB, A. E., MACAOGAIN, M., ROGERS, T. R., WINDLE, H., KELLEHER, D., O'CONNELL, M. J. & LOSCHER, C. E. 2017. Surface layer proteins from virulent *Clostridium difficile* ribotypes exhibit signatures of positive selection with consequences for innate immune response. *BMC Evolutionary Biology*, 17, 90.
- LYNCH, S. V. & PEDERSEN, O. 2016. The Human Intestinal Microbiome in Health and Disease. *New England Journal of Medicine*, 375, 2369-2379.
- LYRA, A., FORSSTEN, S., ROLNY, P., WETTERGREN, Y., LAHTINEN, S. J., SALLI, K., CEDGÅRD, L., ODIN, E., GUSTAVSSON, B. & OUWEHAND, A. C. 2012. Comparison of bacterial quantities in left and right colon biopsies and faeces. *World journal of gastroenterology*, 18, 4404-4411.
- LYRAS, D., O'CONNOR, J. R., HOWARTH, P. M., SAMBOL, S. P., CARTER, G. P., PHUMOONNA, T., POON, R., ADAMS, V., VEDANTAM, G., JOHNSON, S., GERDING, D. N. & ROOD, J. I. 2009. Toxin B is essential for virulence of *Clostridium difficile*. *Nature*, 458, 1176-1179.
- LYTE, M., LI, W., OPITZ, N., GAYKEMA, R. P. & GOEHLER, L. E. 2006. Induction of anxiety-like behavior in mice during the initial stages of infection with the agent of murine colonic hyperplasia *Citrobacter rodentium*. *Physiology & Behavior*, 89, 350-7.
- MACCANNELL, D. R., LOUIE, T. J., GREGSON, D. B., LAVERDIERE, M., LABBE, A. C., LAING, F. & HENWICK, S. 2006. Molecular analysis of *Clostridium difficile* PCR ribotype 027 isolates from Eastern and Western Canada. *Journal of Clinical Microbiology*, 44, 2147-52.
- MACFARLANE, G. T., MACFARLANE, S. & GIBSON, G. R. 1998. Validation of a Three-Stage Compound Continuous Culture System for Investigating the Effect of Retention Time on the Ecology and Metabolism of Bacteria in the Human Colon. *Microbial Ecology*, 35, 180-187.
- MACFARLANE, S. & DILLON, J. F. 2007. Microbial biofilms in the human gastrointestinal tract. *Journal of Applied Microbiology*, 102, 1187-96.
- MACFARLANE, S., WOODMANSEY, E. J. & MACFARLANE, G. T. 2005. Colonization of mucin by human intestinal bacteria and establishment of biofilm communities in a two-stage continuous culture system. *Applied and Environmental Microbiology*, 71, 7483-7492.
- MACKIN, K. E., CARTER, G. P., HOWARTH, P., ROOD, J. I. & LYRAS, D. 2013. Spo0A differentially regulates toxin production in evolutionarily diverse strains of *Clostridium difficile*. *PLoS One*, 8, e79666.

- MALDARELLI, G. A., PIEPENBRINK, K. H., SCOTT, A. J., FREIBERG, J. A., SONG, Y., ACHERMANN, Y., ERNST, R. K., SHIRTLIFF, M. E., SUNDBERG, E. J., DONNENBERG, M. S. & VON ROSENVINGE, E. C. 2016. Type IV pili promote early biofilm formation by *Clostridium difficile*. *Pathogens and disease*, 74, ftw061.
- MALHOTRA, R., DHAWAN, B., GARG, B., SHANKAR, V. & NAG, T. C. 2019. A Comparison of Bacterial Adhesion and Biofilm Formation on Commonly Used Orthopaedic Metal Implant Materials: An *In vitro* Study. *Indian journal of orthopaedics*, 53, 148-153.
- MAMO, Y., WOODWORTH, M. H., WANG, T., DHERE, T. & KRAFT, C. S. 2018. Durability and Long-term Clinical Outcomes of Fecal Microbiota Transplant Treatment in Patients With Recurrent *Clostridium difficile* Infection. *Clinical Infectious Diseases*, 66, 1705-1711.
- MANI, N. & DUPUY, B. 2001. Regulation of toxin synthesis in *Clostridium difficile* by an alternative RNA polymerase sigma factor. *Proceedings of the National Academy of Sciences of the United States of America*, 98, 5844-5849.
- MANI, N., LYRAS, D., BARROSO, L., HOWARTH, P., WILKINS, T., ROOD, J. I., SONENSHEIN, A. L. & DUPUY, B. 2002. Environmental response and autoregulation of *Clostridium difficile* TxeR, a sigma factor for toxin gene expression. *Journal of Bacteriology*, 184, 5971-8.
- MARSH, J. W., ARORA, R., SCHLACKMAN, J. L., SHUTT, K. A., CURRY, S. R. & HARRISON, L. H. 2012. Association of Relapse of *Clostridium difficile* Disease with BI/NAP1/027. *Journal of Clinical Microbiology*, 50, 4078-4082.
- MARTIN, M., HÖLSCHER, T., DRAGOŠ, A., COOPER, V. S. & KOVÁCS, Á. T. 2016. Laboratory Evolution of Microbial Interactions in Bacterial Biofilms. *Journal of Bacteriology*, 198, 2564-2571.
- MARTÍN, R., CHAMIGNON, C., MHEDBI-HAJRI, N., CHAIN, F., DERRIEN, M., ESCRIBANO-VÁZQUEZ, U., GARAU, P., COTILLARD, A., PHAM, H. P., CHERVAUX, C., BERMÚDEZ-HUMARÁN, L. G., SMOKVINA, T. & LANGELLA, P. 2019. The potential probiotic *Lactobacillus rhamnosus* CNCM I-3690 strain protects the intestinal barrier by stimulating both mucus production and cytoprotective response. *Scientific Reports*, 9, 5398.
- MATAMOUROS, S., ENGLAND, P. & DUPUY, B. 2007. *Clostridium difficile* toxin expression is inhibited by the novel regulator TcdC. *Molecular Microbiology*, 64, 1274-88.
- MATHUR, H., REA, M. C., COTTER, P. D., HILL, C. & ROSS, R. P. 2016. The efficacy of thuricin CD, tigecycline, vancomycin, teicoplanin, rifampicin and nitazoxanide, independently and in paired combinations against *Clostridium difficile* biofilms and planktonic cells. *Gut Pathogens*, 8, 20.

- MAURI, P. L., PIETTA, P. G., MAGGIONI, A., CERQUETTI, M., SEBASTIANELLI, A. & MASTRANTONIO, P. 1999. Characterization of surface layer proteins from *Clostridium difficile* by liquid chromatography/electrospray ionization mass spectrometry. *Rapid Communications in Mass Spectrometry*, 13, 695-703.
- MCBRIDE, S. M. & SONENSHEIN, A. L. 2011a. The dlt operon confers resistance to cationic antimicrobial peptides in *Clostridium difficile*. *Microbiology (Reading, England)*, 157, 1457-1465.
- MCBRIDE, S. M. & SONENSHEIN, A. L. 2011b. Identification of a genetic locus responsible for antimicrobial peptide resistance in *Clostridium difficile*. *Infection and Immunity*, 79, 167-76.
- MCCOY, W. F., BRYERS, J. D., ROBBINS, J. & COSTERTON, J. W. 1981. Observations of fouling biofilm formation. *Canadian Journal of Microbiology*, 27, 910-917.
- MCDONALD, J. A. K., MULLISH, B. H., PECHLIVANIS, A., LIU, Z., BRIGNARDELLO, J., KAO, D., HOLMES, E., LI, J. V., CLARKE, T. B., THURSZ, M. R. & MARCHESI, J. R. 2018a. Inhibiting Growth of *Clostridioides difficile* by Restoring Valerate, Produced by the Intestinal Microbiota. *Gastroenterology*, 155, 1495-1507.e15.
- MCDONALD, L. C., GERDING, D. N., JOHNSON, S., BAKKEN, J. S., CARROLL, K. C., COFFIN, S. E., DUBBERKE, E. R., GAREY, K. W., GOULD, C. V., KELLY, C., LOO, V., SHAKLEE SAMMONS, J., SANDORA, T. J. & WILCOX, M. H. 2018b. Clinical Practice Guidelines for *Clostridium difficile* Infection in Adults and Children: 2017 Update by the Infectious Diseases Society of America (IDSA) and Society for Healthcare Epidemiology of America (SHEA). *Clinical Infectious Diseases*, 66, e1-e48.
- MCFARLAND, L. V., ELMER, G. W. & SURAWICZ, C. M. 2002. Breaking the cycle: treatment strategies for 163 cases of recurrent *Clostridium difficile* disease. *American Journal of Gastroenterology*, 97, 1769-75.
- MCFARLAND, L. V., MULLIGAN, M. E., KWOK, R. Y. & STAMM, W. E. 1989. Nosocomial acquisition of *Clostridium difficile* infection. *New England Journal of Medicine*, 320, 204-10.
- MCFARLAND, L. V., SURAWICZ, C. M., GREENBERG, R. N., FEKETY, R., ELMER, G. W., MOYER, K. A., MELCHER, S. A., BOWEN, K. E., COX, J. L., NOORANI, Z. & ET AL. 1994. A randomized placebo-controlled trial of *Saccharomyces boulardii* in combination with standard antibiotics for *Clostridium difficile* disease. *Jama*, 271, 1913-8.
- MCFARLAND, L. V., SURAWICZ, C. M., RUBIN, M., FEKETY, R., ELMER, G. W. & GREENBERG, R. N. 1999. Recurrent *Clostridium difficile* disease:

epidemiology and clinical characteristics. *Infection Control & Hospital Epidemiology*, 20, 43-50.

- MEADOR-PARTON, J. & POPHAM, D. L. 2000. Structural Analysis of *Bacillus subtilis* Spore Peptidoglycan during Sporulation. *Journal of Bacteriology*, 182, 4491-4499.
- MERRIGAN, M., VENUGOPAL, A., MALLOZZI, M., ROXAS, B., VISWANATHAN, V. K., JOHNSON, S., GERDING, D. N. & VEDANTAM, G. 2010. Human Hypervirulent *Clostridium difficile* Strains Exhibit Increased Sporulation as Well as Robust Toxin Production. *Journal of Bacteriology*, 192, 4904-4911.
- MERRIGAN, M. M., VENUGOPAL, A., ROXAS, J. L., ANWAR, F., MALLOZZI, M. J., ROXAS, B. A., GERDING, D. N., VISWANATHAN, V. K. & VEDANTAM, G. 2013. Surface-layer protein A (SlpA) is a major contributor to host-cell adherence of *Clostridium difficile*. *PLoS One*, 8, e78404.
- MERRITT, J. H., KADOURI, D. E. & O'TOOLE, G. A. 2005. Growing and analyzing static biofilms. *Current Protocols in Microbiology*, Chapter 1.
- MILANI, C., TICINESI, A., GERRITSEN, J., NOUVENNE, A., LUGLI, G. A., MANCABELLI, L., TURRONI, F., DURANTI, S., MANGIFESTA, M., VIAPPANI, A., FERRARIO, C., MAGGIO, M., LAURETANI, F., DEVOS, W., VAN SINDEREN, D., MESCHI, T. & VENTURA, M. 2016. Gut microbiota composition and *Clostridium difficile* infection in hospitalized elderly individuals: a metagenomic study. *Scientific Reports*, 6, 25945.
- MILLAN, B., PARK, H., HOTTE, N., MATHIEU, O., BURGUIERE, P., TOMPKINS, T. A., KAO, D. & MADSEN, K. L. 2016. Fecal Microbial Transplants Reduce Antibiotic-resistant Genes in Patients With Recurrent *Clostridium difficile* Infection. *Clinical Infectious Diseases*, 62, 1479-1486.
- MITCHELL, T. J., KETLEY, J. M., HASLAM, S. C., STEPHEN, J., BURDON, D. W., CANDY, D. C. & DANIEL, R. 1986. Effect of toxin A and B of *Clostridium difficile* on rabbit ileum and colon. *Gut*, 27, 78-85.
- MOELLER, R., SETLOW, P., REITZ, G. & NICHOLSON, W. L. 2009. Roles of Small, Acid-Soluble Spore Proteins and Core Water Content in Survival of *Bacillus subtilis* Spores Exposed to Environmental Solar UV Radiation. *Applied and Environmental Microbiology*, 75, 5202-5208.
- MOGG, G. A., KEIGHLEY, M. R., BURDON, D. W., ALEXANDER-WILLIAMS, J., YOUNGS, D., JOHNSON, M., BENTLEY, S. & GEORGE, R. H. 1979. Antibiotic-associated colitis--a review of 66 cases. *British Journal of Surgery*, 66, 738-42.

- MOLIN, S. & TOLKER-NIELSEN, T. 2003. Gene transfer occurs with enhanced efficiency in biofilms and induces enhanced stabilisation of the biofilm structure. *Current Opinion in Biotechnology*, 14, 255-261.
- MONTANARO, L., POGGI, A., VISAI, L., RAVAIOLI, S., CAMPOCCIA, D., SPEZIALE, P. & ARCIOLA, C. R. 2011. Extracellular DNA in biofilms. *International Journal of Artificial Organs*, 34, 824-31.
- MORA-URIBE, P., MIRANDA-CARDENAS, C., CASTRO-CORDOVA, P., GIL, F., CALDERON, I., FUENTES, J. A., RODAS, P. I., BANAWAS, S., SARKER, M. R. & PAREDES-SABJA, D. 2016. Characterization of the Adherence of *Clostridium difficile* Spores: The Integrity of the Outermost Layer Affects Adherence Properties of Spores of the Epidemic Strain R20291 to Components of the Intestinal Mucosa. *Frontiers in Cellular and Infection Microbiology*, 6, 99.
- MORGAN, X. C., TICKLE, T. L., SOKOL, H., GEVERS, D., DEVANEY, K. L., WARD, D. V., REYES, J. A., SHAH, S. A., LELEIKO, N., SNAPPER, S. B., BOUSVAROS, A., KORZENIK, J., SANDS, B. E., XAVIER, R. J. & HUTTENHOWER, C. 2012. Dysfunction of the intestinal microbiome in inflammatory bowel disease and treatment. *Genome Biology*, 13, R79.
- MOURA, I. B., BUCKLEY, A. M., EWIN, D., SHEARMAN, S., CLARK, E., WILCOX, M. H. & CHILTON, C. H. 2019. Omadacycline Gut Microbiome Exposure Does Not Induce *Clostridium difficile* Proliferation or Toxin Production in a Model That Simulates the Proximal, Medial, and Distal Human Colon. *Antimicrob Agents Chemother*, 63, e01581-18.
- MULLER, E. L., PITT, H. A. & GEORGE, W. L. 1987. Prairie dog model for antimicrobial agent-induced *Clostridium difficile* diarrhea. *Infection and immunity*, 55, 198-200.
- MÜLLER, P., GUGGENHEIM, B., ATTIN, T., MARLINGHAUS, E. & SCHMIDLIN, P. R. 2011. Potential of shock waves to remove calculus and biofilm. *Clinical Oral Investigations*, 15, 959-965.
- MULLISH, B. H., MCDONALD, J. A. K., PECHLIVANIS, A., ALLEGRETTI, J. R., KAO, D., BARKER, G. F., KAPILA, D., PETROF, E. O., JOYCE, S. A., GAHAN, C. G. M., GLEGOLA-MADEJSKA, I., WILLIAMS, H. R. T., HOLMES, E., CLARKE, T. B., THURSZ, M. R. & MARCHESI, J. R. 2019. Microbial bile salt hydrolases mediate the efficacy of faecal microbiota transplant in the treatment of recurrent *Clostridioides difficile* infection. *Gut*, 68, 1791-1800.
- NA, X., KIM, H., MOYER, M. P., POTHOUKAKIS, C. & LAMONT, J. T. 2008. gp96 is a human colonocyte plasma membrane binding protein for *Clostridium difficile* toxin A. *Infection and Immunity*, 76, 2862-71.
- NAABER, P., LEHTO, E., SALMINEN, S. & MIKELSAAR, M. 1996. Inhibition of adhesion of *Clostridium difficile* to Caco-2 cells. *FEMS Immunology and Medical Microbiology*, 14, 205-9.

- NADELL, C. D., DRESCHER, K. & FOSTER, K. R. 2016. Spatial structure, cooperation and competition in biofilms. *Nature Reviews Microbiology*, 14, 589.
- NAGAHAMA, M., SAKAGUCHI, Y., KOBAYASHI, K., OCHI, S. & SAKURAI, J. 2000. Characterization of the enzymatic component of *Clostridium perfringens* iota-toxin. *Journal of Bacteriology*, 182, 2096-103.
- NALE, J. Y., REDGWELL, T. A., MILLARD, A. & CLOKIE, M. R. J. 2018. Efficacy of an Optimised Bacteriophage Cocktail to Clear *Clostridium difficile* in a Batch Fermentation Model. *Antibiotics (Basel, Switzerland)*, 7, 13.
- NALE, J. Y., SPENCER, J., HARGREAVES, K. R., BUCKLEY, A. M., TRZEPINSKI, P., DOUCE, G. R. & CLOKIE, M. R. 2016. Bacteriophage Combinations Significantly Reduce *Clostridium difficile* Growth *In Vitro* and Proliferation *In Vivo*. *Antimicrobial Agents and Chemotherapy*, 60, 968-81.
- NEU, T. R. & LAWRENCE, J. R. 2014. Investigation of microbial biofilm structure by laser scanning microscopy. *Advances in Biochemical Engineering/Biotechnology*, 146, 1-51.
- NEWMAN, J. A., RODRIGUES, C. & LEWIS, R. J. 2013. Molecular basis of the activity of SinR protein, the master regulator of biofilm formation in *Bacillus subtilis*. *Journal of Biological Chemistry*, 288, 10766-78.
- NG, J., HIROTA, S. A., GROSS, O., LI, Y., ULKE-LEMEE, A., POTENTIER, M. S., SCHENCK, L. P., VILAYSANE, A., SEAMONE, M. E., FENG, H., ARMSTRONG, G. D., TSCHOPP, J., MACDONALD, J. A., MURUVE, D. A. & BECK, P. L. 2010. *Clostridium difficile* toxin-induced inflammation and intestinal injury are mediated by the inflammasome. *Gastroenterology*, 139, 542-52, 552.e1-3.
- NG, K. M., FERREYRA, J. A., HIGGINBOTTOM, S. K., LYNCH, J. B., KASHYAP, P. C., GOPINATH, S., NAIDU, N., CHOUDHURY, B., WEIMER, B. C., MONACK, D. M. & SONNENBURG, J. L. 2013. Microbiota-liberated host sugars facilitate post-antibiotic expansion of enteric pathogens. *Nature*, 502, 96-9.
- NICHOLSON, W. L., SETLOW, B. & SETLOW, P. 1990. Binding of DNA in vitro by a small, acid-soluble spore protein from *Bacillus subtilis* and the effect of this binding on DNA topology. *Journal of Bacteriology*, 172, 6900-6.
- NICKEL, J. C., COSTERTON, J. W., MCLEAN, R. J. & OLSON, M. 1994. Bacterial biofilms: influence on the pathogenesis, diagnosis and treatment of urinary tract infections. *Journal of Antimicrobial Chemotherapy*, 33 Suppl A, 31-41.

- NICKEL, J. C., RUSESKA, I., WRIGHT, J. B. & COSTERTON, J. W. 1985. Tobramycin resistance of *Pseudomonas aeruginosa* cells growing as a biofilm on urinary catheter material. *Antimicrobial Agents and Chemotherapy*, 27, 619-624.
- NOCKER, A., MAZZA, A., MASSON, L., CAMPER, A. K. & BROUSSEAU, R. 2009. Selective detection of live bacteria combining propidium monoazide sample treatment with microarray technology. *Journal of Microbiological Methods*, 76, 253-61.
- NOCKER, A., SOSSA-FERNANDEZ, P., BURR, M. D. & CAMPER, A. K. 2007. Use of propidium monoazide for live/dead distinction in microbial ecology. *Applied and environmental microbiology*, 73, 5111-5117.
- NUSRAT, A., GIRY, M., TURNER, J. R., COLGAN, S. P., PARKOS, C. A., CARNES, D., LEMICHEZ, E., BOQUET, P. & MADARA, J. L. 1995. Rho protein regulates tight junctions and perijunctional actin organization in polarized epithelia. *Proceedings of the National Academy of Sciences of the United States of America*, 92, 10629-10633.
- NUSRAT, A., VON EICHEL-STREIBER, C., TURNER, J. R., VERKADE, P., MADARA, J. L. & PARKOS, C. A. 2001. *Clostridium difficile* toxins disrupt epithelial barrier function by altering membrane microdomain localization of tight junction proteins. *Infection and Immunity*, 69, 1329-36.
- O'LOUGHLIN, C. T., MILLER, L. C., SIRYAPORN, A., DRESCHER, K., SEMMELHACK, M. F. & BASSLER, B. L. 2013. A quorum-sensing inhibitor blocks *Pseudomonas aeruginosa* virulence and biofilm formation. *Proceedings of the National Academy of Sciences of the United States of America*, 110, 17981-6.
- O'TOOLE, G. A. 2011. Microtiter dish biofilm formation assay. *Journal of visualized experiments : JoVE*, 2437.
- O'TOOLE, G. A. & KOLTER, R. 1998a. Flagellar and twitching motility are necessary for *Pseudomonas aeruginosa* biofilm development. *Molecular Microbiology*, 30, 295-304.
- O'TOOLE, G. A. & KOLTER, R. 1998b. Initiation of biofilm formation in *Pseudomonas fluorescens* WCS365 proceeds via multiple, convergent signalling pathways: a genetic analysis. *Molecular Microbiology*, 28, 449-61.
- OFORI, E., RAMAI, D., DHAWAN, M., MUSTAFA, F., GASPERINO, J. & REDDY, M. 2018. Community-acquired *Clostridium difficile*: epidemiology, ribotype, risk factors, hospital and intensive care unit outcomes, and current and emerging therapies. *Journal of Hospital Infection*, 99, 436-442.

- OKSHEVSKY, M. & MEYER, R. L. 2015. The role of extracellular DNA in the establishment, maintenance and perpetuation of bacterial biofilms. *Critical Reviews Microbiology*, 41, 341-52.
- OLIPHANT, K. & ALLEN-VERCOE, E. 2019. Macronutrient metabolism by the human gut microbiome: major fermentation by-products and their impact on host health. *Microbiome*, 7, 91.
- OLIVEIRA, A. C., PASQUAL, M., BRUZI, A. T., PIO, L. A., MENDONÇA, P. M. & SOARES, J. D. 2015. Flow cytometry reliability analysis and variations in sugarcane DNA content. *Genetics and Molecular Research*, 14, 7172-83.
- OLLING, A., GOY, S., HOFFMANN, F., TATGE, H., JUST, I. & GERHARD, R. 2011. The repetitive oligopeptide sequences modulate cytopathic potency but are not crucial for cellular uptake of *Clostridium difficile* toxin A. *PLoS One*, 6, e17623.
- OLSEN, M. A., YAN, Y., RESKE, K. A., ZILBERBERG, M. D. & DUBBERKE, E. R. 2015. Recurrent *Clostridium difficile* infection is associated with increased mortality. *Clinical Microbiology Infection*, 21, 164-70.
- ONDERDONK, A. B., JOHNSTON, J., MAYHEW, J. W. & GORBACH, S. L. 1976. Effect of dissolved oxygen and Eh and *Bacteroides fragilis* during continuous culture. *Applied Environmental Microbiology*, 31, 168-72.
- ONDERDONK, A. B., LOWE, B. R. & BARTLETT, J. G. 1979. Effect of environmental stress on *Clostridium difficile* toxin levels during continuous cultivation. *Applied Environmental Microbiology*, 38, 637-41.
- OOTANI, A., LI, X., SANGIORGI, E., HO, Q. T., UENO, H., TODA, S., SUGIHARA, H., FUJIMOTO, K., WEISSMAN, I. L., CAPECCHI, M. R. & KUO, C. J. 2009. Sustained *in vitro* intestinal epithelial culture within a Wnt-dependent stem cell niche. *Nature medicine*, 15, 701-706.
- OTT, S. J., WAETZIG, G. H., REHMAN, A., MOLTZAU-ANDERSON, J., BHARTI, R., GRASIS, J. A., CASSIDY, L., THOLEY, A., FICKENSCHER, H., SEEGER, D., ROSENSTIEL, P. & SCHREIBER, S. 2017. Efficacy of Sterile Fecal Filtrate Transfer for Treating Patients With *Clostridium difficile* Infection. *Gastroenterology*, 152, 799-811.e7.
- OTTLINGER, M. E. & LIN, S. 1988. *Clostridium difficile* toxin B induces reorganization of actin, vinculin, and talin in cultured cells. *Experimental Cell Research*, 174, 215-29.
- PALMER, R. J., JR. & WHITE, D. C. 1997. Developmental biology of biofilms: implications for treatment and control. *Trends in Microbiology*, 5, 435-40.
- PAMP, S. J., STERNBERG, C. & TOLKER-NIELSEN, T. 2009. Insight into the microbial multicellular lifestyle via flow-cell technology and confocal microscopy. *Cytometry Part A*, 75A, 90-103.

- PANTALÉON, V., BOUTTIER, S., SOAVELOMANDROSO, A. P., JANOIR, C. & CANDELA, T. 2014. Biofilms of *Clostridium* species. *Anaerobe*, 30, 193-198.
- PANTALEON, V., SOAVELOMANDROSO, A. P., BOUTTIER, S., BRIANDET, R., ROXAS, B., CHU, M., COLLIGNON, A., JANOIR, C., VEDANTAM, G. & CANDELA, T. 2015. The *Clostridium difficile* Protease Cwp84 Modulates both Biofilm Formation and Cell-Surface Properties. *PLoS One*, 10, e0124971.
- PAPATHEODOROU, P., CARETTE, J. E., BELL, G. W., SCHWAN, C., GUTTENBERG, G., BRUMMELKAMP, T. R. & AKTORIES, K. 2011. Lipolysis-stimulated lipoprotein receptor (LSR) is the host receptor for the binary toxin *Clostridium difficile* transferase (CDT). *Proceedings of the National Academy of Sciences of the United States of America*, 108, 16422-7.
- PAPATHEODOROU, P., ZAMBOGLOU, C., GENISYUERK, S., GUTTENBERG, G. & AKTORIES, K. 2010. Clostridial glucosylating toxins enter cells via clathrin-mediated endocytosis. *PLoS One*, 5, e10673.
- PAPENFORT, K. & BASSLER, B. L. 2016. Quorum sensing signal-response systems in Gram-negative bacteria. *Nature reviews. Microbiology*, 14, 576-588.
- PAREDES-SABJA, D., SHEN, A. & SORG, J. A. 2014. *Clostridium difficile* spore biology: sporulation, germination, and spore structural proteins. *Trends in microbiology*, 22, 406-416.
- PASSMORE, I. J., LETERTRE, M. P. M., PRESTON, M. D., BIANCONI, I., HARRISON, M. A., NASHER, F., KAUR, H., HONG, H. A., BAINES, S. D., CUTTING, S. M., SWANN, J. R., WREN, B. W. & DAWSON, L. F. 2018. Para-cresol production by *Clostridium difficile* affects microbial diversity and membrane integrity of Gram-negative bacteria. *PLOS Pathogens*, 14, e1007191.
- PAWLOWSKI, S. W., CALABRESE, G., KOLLING, G. L., PLATTS-MILLS, J., FREIRE, R., ALCANTARAWARREN, C., LIU, B., SARTOR, R. B. & GUERRANT, R. L. 2010. Murine model of *Clostridium difficile* infection with aged gnotobiotic C57BL/6 mice and a BI/NAP1 strain. *Journal of Infectious Diseases*, 202, 1708-12.
- PELTIER, J., COURTIN, P., EL MEOUCHE, I., LEMEE, L., CHAPOT-CHARTIER, M. P. & PONS, J. L. 2011. *Clostridium difficile* has an original peptidoglycan structure with a high level of N-acetylglucosamine deacetylation and mainly 3-3 cross-links. *Journal of Biological Chemistry*, 286, 29053-62.

- PEPIN, J., SAHEB, N., COULOMBE, M. A., ALARY, M. E., CORRIVEAU, M. P., AUTHIER, S., LEBLANC, M., RIVARD, G., BETTEZ, M., PRIMEAU, V., NGUYEN, M., JACOB, C. E. & LANTHIER, L. 2005. Emergence of fluoroquinolones as the predominant risk factor for *Clostridium difficile*-associated diarrhea: a cohort study during an epidemic in Quebec. *Clinical Infectious Diseases*, 41, 1254-60.
- PERCIVAL, S. L., MALIC, S., CRUZ, H. & WILLIAMS, D. W. 2011. Introduction to Biofilms. In: PERCIVAL, S., KNOTTENBELT, D. & COCHRANE, C. (eds.) *Biofilms and Veterinary Medicine*. Berlin, Heidelberg: Springer Berlin Heidelberg.
- PERCIVAL, S. L. & SULEMAN, L. 2014. Biofilms and *Helicobacter pylori*: Dissemination and persistence within the environment and host. *World Journal of Gastrointestinal Pathophysiology*, 5, 122-132.
- PERCIVAL, S. L., SULEMAN, L., VUOTTO, C. & DONELLI, G. 2015. Healthcare-associated infections, medical devices and biofilms: risk, tolerance and control. *Journal of Medical Microbiology*, 64, 323-334.
- PERELLE, S., GIBERT, M., BOURLIOUX, P., CORTIER, G. & POPOFF, M. R. 1997. Production of a complete binary toxin (actin-specific ADP-ribosyltransferase) by *Clostridium difficile* CD196. *Infection and Immunity*, 65, 1402-7.
- PETRACHI, T., RESCA, E., PICCINNO, M. S., BIAGI, F., STRUSI, V., DOMINICI, M. & VERONESI, E. 2017. An Alternative Approach to Investigate Biofilm in Medical Devices: A Feasibility Study. *International journal of environmental research and public health*, 14, 1587.
- PIOTROWSKI, M., KARPINSKI, P., PITUCH, H., VAN BELKUM, A. & OBUCH-WOSZCZATYNSKI, P. 2017. Antimicrobial effects of Manuka honey on *in vitro* biofilm formation by *Clostridium difficile*. *European Journal of Clinical Microbiology and Infectious Diseases*, 36, 1661-1664.
- PITTS, B., HAMILTON, M. A., ZELVER, N. & STEWART, P. S. 2003. A microtiter-plate screening method for biofilm disinfection and removal. *Journal of Microbiological Methods*, 54, 269-76.
- POQUET, I., SAUJET, L., CANETTE, A., MONOT, M., MIHAJLOVIC, J., GHIGO, J.-M., SOUTOURINA, O., BRIANDET, R., MARTIN-VERSTRAETE, I. & DUPUY, B. 2018. *Clostridium difficile* Biofilm: Remodeling Metabolism and Cell Surface to Build a Sparse and Heterogeneously Aggregated Architecture. *Frontiers in Microbiology*, 9.
- POST, J. C. 2001. Direct evidence of bacterial biofilms in otitis media. *Laryngoscope*, 111, 2083-94.
- POTERA, C. 1999. Forging a link between biofilms and disease. *Science*, 283, 1837, 1839.

- PRICE, A. B., LARSON, H. E. & CROW, J. 1979. Morphology of experimental antibiotic-associated enterocolitis in the hamster: a model for human pseudomembranous colitis and antibiotic-associated diarrhoea. *Gut*, 20, 467-75.
- PRUITT, R. N., CHAMBERS, M. G., NG, K. K., OHI, M. D. & LACY, D. B. 2010. Structural organization of the functional domains of *Clostridium difficile* toxins A and B. *Proceedings of the National Academy of Sciences of the United States of America*, 107, 13467-72.
- PULTZ, N. J. & DONSKEY, C. J. 2005. Effect of antibiotic treatment on growth of and toxin production by *Clostridium difficile* in the cecal contents of mice. *Antimicrobial Agents and Chemotherapy*, 49, 3529-32.
- PURCELL, E. B., MCKEE, R. W., BORDELEAU, E., BURRUS, V. & TAMAYO, R. 2016. Regulation of Type IV Pili Contributes to Surface Behaviors of Historical and Epidemic Strains of *Clostridium difficile*. *Journal of Bacteriology*, 198, 565-77.
- PURCELL, E. B., MCKEE, R. W., COURSON, D. S., GARRETT, E. M., MCBRIDE, S. M., CHENEY, R. E. & TAMAYO, R. 2017. A Nutrient-Regulated Cyclic Diguanylate Phosphodiesterase Controls *Clostridium difficile* Biofilm and Toxin Production during Stationary Phase. *Infection and Immunity*, 85, e00347-17.
- PURCELL, E. B., MCKEE, R. W., MCBRIDE, S. M., WATERS, C. M. & TAMAYO, R. 2012. Cyclic diguanylate inversely regulates motility and aggregation in *Clostridium difficile*. *Journal of Bacteriology*, 194, 3307-16.
- QUAST, C., PRUESSE, E., YILMAZ, P., GERKEN, J., SCHWEER, T., YARZA, P., PEPLIES, J. & GLOCKNER, F. O. 2013. The SILVA ribosomal RNA gene database project: improved data processing and web-based tools. *Nucleic Acids Research*, 41, D590-6.
- RAKOFF-NAHOUM, S., FOSTER, K. R. & COMSTOCK, L. E. 2016. The evolution of cooperation within the gut microbiota. *Nature*, 533, 255-259.
- RATNER, M. 2016. Seres's pioneering microbiome drug fails mid-stage trial. *Nature Biotechnology*, 34, 1004-1005.
- RAZAQ, N., SAMBOL, S., NAGARO, K., ZUKOWSKI, W., CHEKNIS, A., JOHNSON, S. & GERDING, D. N. 2007. Infection of Hamsters with Historical and Epidemic BI Types of *Clostridium difficile*. *The Journal of Infectious Diseases*, 196, 1813-1819.
- REEVES, A. E., KOENIGSKNECHT, M. J., BERGIN, I. L. & YOUNG, V. B. 2012. Suppression of *Clostridium difficile* in the gastrointestinal tracts of germfree mice inoculated with a murine isolate from the family Lachnospiraceae. *Infection and Immunity*, 80, 3786-94.

- REEVES, A. E., THERIOT, C. M., BERGIN, I. L., HUFFNAGLE, G. B., SCHLOSS, P. D. & YOUNG, V. B. 2011. The interplay between microbiome dynamics and pathogen dynamics in a murine model of *Clostridium difficile* Infection. *Gut Microbes*, 2, 145-58.
- REN, Y., WANG, C., CHEN, Z., ALLAN, E., VAN DER MEI, H. C. & BUSSCHER, H. J. 2018. Emergent heterogeneous microenvironments in biofilms: substratum surface heterogeneity and bacterial adhesion force-sensing. *FEMS Microbiology Reviews*, 42, 259-272.
- REYNOLDS, C. B., EMERSON, J. E., DE LA RIVA, L., FAGAN, R. P. & FAIRWEATHER, N. F. 2011. The *Clostridium difficile* Cell Wall Protein CwpV is Antigenically Variable between Strains, but Exhibits Conserved Aggregation-Promoting Function. *PLoS Pathogens*, 7, e1002024.
- RIEGLER, M., SEDIVY, R., POTHOUKAKIS, C., HAMILTON, G., ZACHERL, J., BISCHOF, G., COSENTINI, E., FEIL, W., SCHIESSEL, R. & LAMONT, J. T. 1995. *Clostridium difficile* toxin B is more potent than toxin A in damaging human colonic epithelium *in vitro*. *Journal of Clinical Investigation*, 95, 2004-2011.
- RIFKIN, G. D., FEKETY, F. R., SILVA, J. J. & SACK, R. B. 1977. Antibiotic-induced colitis implication of a toxin neutralised by *Clostridium sordellii* antitoxin. *The Lancet*, 310, 1103-1106.
- ROBERTS, M. E. & STEWART, P. S. 2004. Modeling Antibiotic Tolerance in Biofilms by Accounting for Nutrient Limitation. *Antimicrobial Agents and Chemotherapy*, 48, 48-52.
- ROLFE, R. D. & SONG, W. 1993. Purification of a functional receptor for *Clostridium difficile* toxin A from intestinal brush border membranes of infant hamsters. *Clinical Infectious Diseases*, 16 Suppl 4, S219-27.
- ROONEY, C. M., SHEPPARD, A. E., CLARK, E., DAVIES, K., HUBBARD, A. T. M., SEBRA, R., CROOK, D. W., WALKER, A. S., WILCOX, M. H. & CHILTON, C. H. 2019. Dissemination of multiple carbapenem resistance genes in an *in vitro* gut model simulating the human colon. *Journal of Antimicrobial Chemotherapy*, 74, 1876-1883.
- ROSHAN, N., HAMMER, K. A. & RILEY, T. V. 2018. Non-conventional antimicrobial and alternative therapies for the treatment of *Clostridium difficile* infection. *Anaerobe*, 49, 103-111.
- RUPNIK, M., WILCOX, M. H. & GERDING, D. N. 2009. *Clostridium difficile* infection: new developments in epidemiology and pathogenesis. *Nature Reviews Microbiology*, 7, 526-36.
- RUTHERFORD, S. T. & BASSLER, B. L. 2012. Bacterial quorum sensing: its role in virulence and possibilities for its control. *Cold Spring Harbor perspectives in medicine*, 2, a012427.

- SAAVEDRA, P. H. V., HUANG, L., GHAZAVI, F., KOURULA, S., VANDEN BERGHE, T., TAKAHASHI, N., VANDENABEELE, P. & LAMKANFI, M. 2018. Apoptosis of intestinal epithelial cells restricts *Clostridium difficile* infection in a model of pseudomembranous colitis. *Nature Communications*, 9, 4846.
- SABAEIFARD, P., ABDI-ALI, A., SOUDI, M. R. & DINARVAND, R. 2014. Optimization of tetrazolium salt assay for *Pseudomonas aeruginosa* biofilm using microtiter plate method. *Journal of Microbiological Methods*, 105, 134-140.
- SAMBOL, S. P., TANG, J. K., MERRIGAN, M. M., JOHNSON, S. & GERDING, D. N. 2001. Infection of hamsters with epidemiologically important strains of *Clostridium difficile*. *Journal of Infectious Diseases*, 183, 1760-6.
- SANGSTER, W., HEGARTY, J. P., SCHIEFFER, K. M., WRIGHT, J. R., HACKMAN, J., TOOLE, D. R., LAMENDELLA, R. & STEWART, D. B., SR. 2016. Bacterial and Fungal Microbiota Changes Distinguish *C. difficile* Infection from Other Forms of Diarrhea: Results of a Prospective Inpatient Study. *Frontiers in Microbiology*, 7, 789.
- SATO, T. & CLEVERS, H. 2013. Growing self-organizing mini-guts from a single intestinal stem cell: mechanism and applications. *Science*, 340, 1190-4.
- SATO, T., VRIES, R. G., SNIPPERT, H. J., VAN DE WETERING, M., BARKER, N., STANGE, D. E., VAN ES, J. H., ABO, A., KUJALA, P., PETERS, P. J. & CLEVERS, H. 2009. Single Lgr5 stem cells build crypt-villus structures *in vitro* without a mesenchymal niche. *Nature*, 459, 262-265.
- SATTAR, A., THOMMES, P., PAYNE, L., WARN, P. & VICKERS, R. J. 2015. SMT19969 for *Clostridium difficile* infection (CDI): *in vivo* efficacy compared with fidaxomicin and vancomycin in the hamster model of CDI. *Journal of Antimicrobial Chemotherapy*, 70, 1757-1762.
- SAUER, K., CAMPER, A. K., EHRLICH, G. D., COSTERTON, J. W. & DAVIES, D. G. 2002. *Pseudomonas aeruginosa* Displays Multiple Phenotypes during Development as a Biofilm. *Journal of Bacteriology*, 184, 1140-1154.
- SAUER, K., CULLEN, M. C., RICKARD, A. H., ZEEF, L. A., DAVIES, D. G. & GILBERT, P. 2004. Characterization of nutrient-induced dispersion in *Pseudomonas aeruginosa* PAO1 biofilm. *Journal of Bacteriology*, 186, 7312-26.
- SAVIDGE, T. C., PAN, W. H., NEWMAN, P., O'BRIEN, M., ANTON, P. M. & POTHOUKAKIS, C. 2003. *Clostridium difficile* toxin B is an inflammatory enterotoxin in human intestine. *Gastroenterology*, 125, 413-20.

- SAXTON, K., BAINES, S., FREEMAN, J., O'CONNOR, R. & WILCOX, M. 2008. Effects of Exposure of *Clostridium difficile* PCR Ribotypes 027 and 001 to Fluoroquinolones in a Human Gut Model. *Antimicrobial agents and chemotherapy*, 53, 412-20.
- SCHIESSL, K. T., HU, F., JO, J., NAZIA, S. Z., WANG, B., PRICE-WHELAN, A., MIN, W. & DIETRICH, L. E. P. 2019. Phenazine production promotes antibiotic tolerance and metabolic heterogeneity in *Pseudomonas aeruginosa* biofilms. *Nature Communications*, 10, 762.
- SCHOSTER, A., KOKOTOVIC, B., PERMIN, A., PEDERSEN, P. D., BELLO, F. D. & GUARDABASSI, L. 2013. *In vitro* inhibition of *Clostridium difficile* and *Clostridium perfringens* by commercial probiotic strains. *Anaerobe*, 20, 36-41.
- SCHUBERT, A. M., SINANI, H. & SCHLOSS, P. D. 2015. Antibiotic-Induced Alterations of the Murine Gut Microbiota and Subsequent Effects on Colonization Resistance against *Clostridium difficile*. *mBIO*, 6, e00974-15.
- SCHWAN, A., SJOLIN, S., TROTTESTAM, U. & ARONSSON, B. 1983. Relapsing *Clostridium difficile* enterocolitis cured by rectal infusion of homologous faeces. *Lancet*, 2, 845.
- SCHWAN, C., STECHER, B., TZIVELEKIDIS, T., VAN HAM, M., ROHDE, M., HARDT, W. D., WEHLAND, J. & AKTORIES, K. 2009. *Clostridium difficile* toxin CDT induces formation of microtubule-based protrusions and increases adherence of bacteria. *PLoS Pathog*, 5, e1000626.
- SCOTT, A. J., NICHOLSON, G. I. & KERR, A. R. 1973. Lincomycin as a cause of pseudomembranous colitis. *Lancet*, 2, 1232-4.
- SEBAIHIA, M., WREN, B. W., MULLANY, P., FAIRWEATHER, N. F., MINTON, N., STABLER, R., THOMSON, N. R., ROBERTS, A. P., CERDEÑO-TÁRRAGA, A. M., WANG, H., HOLDEN, M. T. G., WRIGHT, A., CHURCHER, C., QUAIL, M. A., BAKER, S., BASON, N., BROOKS, K., CHILLINGWORTH, T., CRONIN, A., DAVIS, P., DOWD, L., FRASER, A., FELTWELL, T., HANCE, Z., HOLROYD, S., JAGELS, K., MOULE, S., MUNGALL, K., PRICE, C., RABBINOWITSCH, E., SHARP, S., SIMMONDS, M., STEVENS, K., UNWIN, L., WHITEHEAD, S., DUPUY, B., DOUGAN, G., BARRELL, B. & PARKHILL, J. 2006. The multidrug-resistant human pathogen *Clostridium difficile* has a highly mobile, mosaic genome. *Nature Genetics*, 38, 779.
- SEDDON, S. V., HEMINGWAY, I. & BORRIELLO, S. P. 1990. Hydrolytic enzyme production by *Clostridium difficile* and its relationship to toxin production and virulence in the hamster model. *Journal of Medical Microbiology*, 31, 169-74.
- SEEKATZ, A. M., THERIOT, C. M., RAO, K., CHANG, Y. M., FREEMAN, A. E., KAO, J. Y. & YOUNG, V. B. 2018. Restoration of short chain fatty acid

and bile acid metabolism following fecal microbiota transplantation in patients with recurrent *Clostridium difficile* infection. *Anaerobe*, 53, 64-73.

- SEIFI, K., KAZEMIAN, H., HEIDARI, H., REZAGHOLIZADEH, F., SAAE, Y., SHIRVANI, F. & HOURI, H. 2016. Evaluation of Biofilm Formation Among *Klebsiella pneumoniae* Isolates and Molecular Characterization by ERIC-PCR. *Jundishapur journal of microbiology*, 9, e30682-e30682.
- SEKI, H., SHIOHARA, M., MATSUMURA, T., MIYAGAWA, N., TANAKA, M., KOMIYAMA, A. & KURATA, S. 2003. Prevention of antibiotic-associated diarrhea in children by *Clostridium butyricum* MIYAIRI. *Pediatrics International*, 45, 86-90.
- SEKULOVIC, O. & FORTIER, L. C. 2015. Global transcriptional response of *Clostridium difficile* carrying the CD38 prophage. *Applied Environmental Microbiology*, 81, 1364-74.
- SEMENYUK, E. G., LANING, M. L., FOLEY, J., JOHNSTON, P. F., KNIGHT, K. L., GERDING, D. N. & DRIKS, A. 2014. Spore Formation and Toxin Production in *Clostridium difficile* Biofilms. *PLoS ONE*, 9, e87757.
- SEMENYUK, E. G., POROYKO, V. A., JOHNSTON, P. F., JONES, S. E., KNIGHT, K. L., GERDING, D. N. & DRIKS, A. 2015. Analysis of Bacterial Communities during *Clostridium difficile* Infection in the Mouse. *Infection and Immunity*, 83, 4383-4391.
- SERRA, D. O., RICHTER, A. M., KLAUCK, G., MIKA, F. & HENGGE, R. 2013. Microanatomy at Cellular Resolution and Spatial Order of Physiological Differentiation in a Bacterial Biofilm. *mBio*, 4, e00103-13.
- SETHI, A. K., AL-NASSIR, W. N., NERANDZIC, M. M. & DONSKEY, C. J. 2009. Skin and environmental contamination with vancomycin-resistant Enterococci in patients receiving oral metronidazole or oral vancomycin treatment for *Clostridium difficile*-associated disease. *Infection Control & Hospital Epidemiology*, 30, 13-7.
- SETLOW, B., ATLURI, S., KITCHEL, R., KOZIOL-DUBE, K. & SETLOW, P. 2006. Role of Dipicolinic Acid in Resistance and Stability of Spores of *Bacillus subtilis* with or without DNA-Protective α/β -Type Small Acid-Soluble Proteins. *Journal of Bacteriology*, 188, 3740-3747.
- SETLOW, B. & SETLOW, P. 1993. Binding of small, acid-soluble spore proteins to DNA plays a significant role in the resistance of *Bacillus subtilis* spores to hydrogen peroxide. *Applied Environmental Microbiology*, 59, 3418-23.
- SHARP, S. E., RUDEN, L. O., POHL, J. C., HATCHER, P. A., JAYNE, L. M. & IVIE, W. M. 2010. Evaluation of the C.Diff Quik Chek Complete Assay, a new glutamate dehydrogenase and A/B toxin combination lateral flow

assay for use in rapid, simple diagnosis of *Clostridium difficile* disease. *Journal of Clinical Microbiology*, 48, 2082-2086.

- SHEN, A., LUPARDUS, P. J., GERSCH, M. M., PURI, A. W., ALBROW, V. E., GARCIA, K. C. & BOGYO, M. 2011. Defining an allosteric circuit in the cysteine protease domain of *Clostridium difficile* toxins. *Nature Structural & Molecular Biology*, 18, 364-71.
- SHETH, P. M., DOUCHANT, K., UYANWUNE, Y., LAROCQUE, M., ANANTHARAJAH, A., BORGUNDVAAG, E., DALES, L., MCCREIGHT, L., MCNAUGHT, L., MOORE, C., RAGAN, K., MCGEER, A. & BROUKHANSKI, G. 2019. Evidence of transmission of *Clostridium difficile* in asymptomatic patients following admission screening in a tertiary care hospital. *PLOS One*, 14, e0207138.
- SHIGETA, M., TANAKA, G., KOMATSUZAWA, H., SUGAI, M., SUGINAKA, H. & USUI, T. 1997. Permeation of antimicrobial agents through *Pseudomonas aeruginosa* biofilms: a simple method. *Chemotherapy*, 43, 340-5.
- SHIN, N. R., WHON, T. W. & BAE, J. W. 2015. Proteobacteria: microbial signature of dysbiosis in gut microbiota. *Trends in Biotechnology*, 33, 496-503.
- SIEGRIST, S. E. & DOE, C. Q. 2007. Microtubule-induced cortical cell polarity. *Genes and Development*, 21, 483-96.
- SIM, S. T. V., SUWARNO, S. R., CHONG, T. H., KRANTZ, W. B. & FANE, A. G. 2013. Monitoring membrane biofouling via ultrasonic time-domain reflectometry enhanced by silica dosing. *Journal of Membrane Science*, 428, 24-37.
- SIMM, R., MORR, M., KADER, A., NIMTZ, M. & ROMLING, U. 2004. GGDEF and EAL domains inversely regulate cyclic di-GMP levels and transition from sessility to motility. *Molecular Microbiology*, 53, 1123-34.
- SINGH, R., RAY, P., DAS, A. & SHARMA, M. 2010. Penetration of antibiotics through *Staphylococcus aureus* and *Staphylococcus epidermidis* biofilms. *Journal of Antimicrobial Chemotherapy*, 65, 1955-1958.
- SIRARD, S., VALIQUETTE, L. & FORTIER, L.-C. 2011. Lack of Association between Clinical Outcome of *Clostridium difficile* Infections, Strain Type, and Virulence-Associated Phenotypes. *Journal of Clinical Microbiology*, 49, 4040-4046.
- SKOGMAN, M. E., VUORELA, P. M. & FALLARERO, A. 2012. Combining biofilm matrix measurements with biomass and viability assays in susceptibility assessments of antimicrobials against *Staphylococcus aureus* biofilms. *Journal of Antibiotics (Tokyo)*, 65, 453-9.

- SLADE, E. A., THORN, R. M. S., YOUNG, A. & REYNOLDS, D. M. 2019. An *in vitro* collagen perfusion wound biofilm model; with applications for antimicrobial studies and microbial metabolomics. *BMC Microbiology*, 19, 310.
- SLATER, R. T., FROST, L. R., JOSSI, S. E., MILLARD, A. D. & UNNIKRISHNAN, M. 2019. *Clostridioides difficile* LuxS mediates inter-bacterial interactions within biofilms. *Scientific reports*, 9, 9903-9903.
- SMITH, A. 2005. Outbreak of *Clostridium difficile* infection in an English hospital linked to hypertoxin-producing strains in Canada and the US. *European Surveilence*, 10, E050630.2.
- SMITH, J. A., COOKE, D. L., HYDE, S., BORRIELLO, S. P. & LONG, R. G. 1997. *Clostridium difficile* toxin A binding to human intestinal epithelial cells. *Journal of Medical Microbiology*, 46, 953-8.
- SMITS, W. K., LYRAS, D., LACY, D. B., WILCOX, M. H. & KUIJPER, E. J. 2016. *Clostridium difficile* infection. *Nature Reviews Disease Primers*, 2, 16020.
- SNYDER, M. L. 1937. Further Studies on *Bacillus Difficilis* (Hall and O'Toole). *The Journal of Infectious Diseases*, 60, 223-231.
- SOAVELOMANDROSO, A. P., GAUDIN, F., HOYS, S., NICOLAS, V., VEDANTAM, G., JANOIR, C. & BOUTTIER, S. 2017. Biofilm Structures in a Mono-Associated Mouse Model of *Clostridium difficile* Infection. *Frontiers in microbiology*, 8, 2086-2086.
- SOMMERFELD ROSS, S., TU, M. H., FALSETTA, M. L., KETTERER, M. R., KIEDROWSKI, M. R., HORSWILL, A. R., APICELLA, M. A., REINHARDT, J. M. & FIEGEL, J. 2014. Quantification of confocal images of biofilms grown on irregular surfaces. *Journal of microbiological methods*, 100, 111-120.
- SONG, Z., CAI, Y., LAO, X., WANG, X., LIN, X., CUI, Y., KALAVAGUNTA, P. K., LIAO, J., JIN, L., SHANG, J. & LI, J. 2019. Taxonomic profiling and populational patterns of bacterial bile salt hydrolase (BSH) genes based on worldwide human gut microbiome. *Microbiome*, 7, 9.
- SORBARA, M. T. & PAMER, E. G. 2019. Interbacterial mechanisms of colonization resistance and the strategies pathogens use to overcome them. *Mucosal Immunology*, 12, 1-9.
- SORG, J. A. & SONENSHEIN, A. L. 2008. Bile Salts and Glycine as Cogerminants for *Clostridium difficile* Spores. *Journal of Bacteriology*, 190, 2505-2512.
- SPENCE, J. R., MAYHEW, C. N., RANKIN, S. A., KUCHAR, M. F., VALLANCE, J. E., TOLLE, K., HOSKINS, E. E., KALINICHENKO, V. V., WELLS, S. I., ZORN, A. M., SHROYER, N. F. & WELLS, J. M. 2011. Directed

differentiation of human pluripotent stem cells into intestinal tissue *in vitro*. *Nature*, 470, 105-109.

SPENCER, J., LEUZZI, R., BUCKLEY, A., IRVINE, J., CANDLISH, D., SCARSELLI, M. & DOUCE, G. R. 2014. Vaccination against *Clostridium difficile* using toxin fragments: Observations and analysis in animal models. *Gut Microbes*, 5, 225-232.

SPENCER, R. C. 1998. The role of antimicrobial agents in the aetiology of *Clostridium difficile*-associated disease. *Journal of Antimicrobial Chemotherapy*, 41 Suppl C, 21-7.

SPIGAGLIA, P., BARKETI-KLAI, A., COLLIGNON, A., MASTRANTONIO, P., BARBANTI, F., RUPNIK, M., JANEZIC, S. & KANSAU, I. 2013. Surface-layer (S-layer) of human and animal *Clostridium difficile* strains and their behaviour in adherence to epithelial cells and intestinal colonization. *Journal of Medical Microbiology*, 62, 1386-93.

SPOERING, A. L. & LEWIS, K. 2001. Biofilms and Planktonic Cells of *Pseudomonas aeruginosa* Have Similar Resistance to Killing by Antimicrobials. *Journal of Bacteriology*, 183, 6746-6751.

STABLER, R. A., HE, M., DAWSON, L., MARTIN, M., VALIENTE, E., CORTON, C., LAWLEY, T. D., SEBAIHIA, M., QUAIL, M. A., ROSE, G., GERDING, D. N., GIBERT, M., POPOFF, M. R., PARKHILL, J., DOUGAN, G. & WREN, B. W. 2009. Comparative genome and phenotypic analysis of *Clostridium difficile* 027 strains provides insight into the evolution of a hypervirulent bacterium. *Genome Biology*, 10, R102.

STALEY, C., HAMILTON, M. J., VAUGHN, B. P., GRAIZIGER, C. T., NEWMAN, K. M., KABAGE, A. J., SADOWSKY, M. J. & KHORUTS, A. 2017a. Successful Resolution of Recurrent *Clostridium difficile* Infection using Freeze-Dried, Encapsulated Fecal Microbiota; Pragmatic Cohort Study. *American Journal of Gastroenterology*, 112, 940-947.

STALEY, C., KAISER, T., VAUGHN, B. P., GRAIZIGER, C., HAMILTON, M. J., KABAGE, A. J., KHORUTS, A. & SADOWSKY, M. J. 2019. Durable Long-Term Bacterial Engraftment following Encapsulated Fecal Microbiota Transplantation To Treat *Clostridium difficile* Infection. *mBio*, 10, e01586-19.

STALEY, C., VAUGHN, B. P., GRAIZIGER, C. T., SINGROY, S., HAMILTON, M. J., YAO, D., CHEN, C., KHORUTS, A. & SADOWSKY, M. J. 2017b. Community dynamics drive punctuated engraftment of the fecal microbiome following transplantation using freeze-dried, encapsulated fecal microbiota. *Gut Microbes*, 8, 276-288.

STARE, B. G., DELMEE, M. & RUPNIK, M. 2007. Variant forms of the binary toxin CDT locus and *tcdC* gene in *Clostridium difficile* strains. *Journal of Medical Microbiology*, 56, 329-35.

- STEELE, J., FENG, H., PARRY, N. & TZIPORI, S. 2010. Piglet models of acute or chronic *Clostridium difficile* illness. *The Journal of infectious diseases*, 201, 428-434.
- STEFFEN, E. K. & HENTGES, D. J. 1981. Hydrolytic enzymes of anaerobic bacteria isolated from human infections. *Journal of Clinical Microbiology*, 14, 153-6.
- STEPANOVIĆ, S., VUKOVIĆ, D., HOLA, V., DI BONAVENTURA, G., DJUKIĆ, S., CIRKOVIĆ, I. & RUZICKA, F. 2007. Quantification of biofilm in microtiter plates: overview of testing conditions and practical recommendations for assessment of biofilm production by staphylococci. *Apmis*, 115, 891-9.
- STERNBERG, C., CHRISTENSEN, B. B., JOHANSEN, T., TOFTGAARD NIELSEN, A., ANDERSEN, J. B., GIVSKOV, M. & MOLIN, S. 1999. Distribution of Bacterial Growth Activity in Flow-Chamber Biofilms. 65, 4108-4117.
- STEWART, P. S. 2002. Mechanisms of antibiotic resistance in bacterial biofilms. *International Journal of Medical Microbiology*, 292, 107-13.
- STEWART, P. S. 2015. Antimicrobial Tolerance in Biofilms. *Microbiology spectrum*, 3, 10.1128/microbiolspec.MB-0010-2014.
- STIEFEL, P., ROSENBERG, U., SCHNEIDER, J., MAUERHOFER, S., MANIURA-WEBER, K. & REN, Q. 2016. Is biofilm removal properly assessed? Comparison of different quantification methods in a 96-well plate system. *Applied microbiology and biotechnology*, 100, 4135-4145.
- STOODLEY, P., SAUER, K., DAVIES, D. G. & COSTERTON, J. W. 2002. Biofilms as complex differentiated communities. *Annual Review of Microbiology*, 56, 187-209.
- STOODLEY, P., WILSON, S., HALL-STOODLEY, L., BOYLE, J. D., LAPPIN-SCOTT, H. M. & COSTERTON, J. W. 2001. Growth and Detachment of Cell Clusters from Mature Mixed-Species Biofilms. *Applied and Environmental Microbiology*, 67, 5608-5613.
- STRÄUBER, H. & MÜLLER, S. 2010. Viability states of bacteria--specific mechanisms of selected probes. *Cytometry A*, 77, 623-34.
- SUDARSAN, N., LEE, E. R., WEINBERG, Z., MOY, R. H., KIM, J. N., LINK, K. H. & BREAKER, R. R. 2008. Riboswitches in eubacteria sense the second messenger cyclic di-GMP. *Science*, 321, 411-3.
- SUN, X., WANG, H., ZHANG, Y., CHEN, K., DAVIS, B. & FENG, H. 2011. Mouse relapse model of *Clostridium difficile* infection. *Infection and immunity*, 79, 2856-2864.

- SUNDRIYAL, A., ROBERTS, A. K., SHONE, C. C. & ACHARYA, K. R. 2009. Structural basis for substrate recognition in the enzymatic component of ADP-ribosyltransferase toxin CDTa from *Clostridium difficile*. *Journal of Biological Chemistry*, 284, 28713-9.
- TACK, K. J. & SABATH, L. D. 1985. Increased minimum inhibitory concentrations with anaerobiasis for tobramycin, gentamicin, and amikacin, compared to latamoxef, piperacillin, chloramphenicol, and clindamycin. *Chemotherapy*, 31, 204-10.
- TAKAHASHI, M., TAGUCHI, H., YAMAGUCHI, H., OSAKI, T., KOMATSU, A. & KAMIYA, S. 2004. The effect of probiotic treatment with *Clostridium butyricum* on enterohemorrhagic *Escherichia coli* O157:H7 infection in mice. *FEMS Immunology and Medical Microbiology*, 41, 219-26.
- TAMAYO, R., PRATT, J. T. & CAMILLI, A. 2007. Roles of cyclic diguanylate in the regulation of bacterial pathogenesis. *Annual Review of Microbiology*, 61, 131-48.
- TAN, K. S., WEE, B. Y. & SONG, K. P. 2001. Evidence for holin function of tcdE gene in the pathogenicity of *Clostridium difficile*. *Journal of Medical Microbiology*, 50, 613-9.
- TAO, L., ZHANG, J., MERANER, P., TOVAGLIERI, A., WU, X., GERHARD, R., ZHANG, X., STALLCUP, W. B., MIAO, J., HE, X., HURDLE, J. G., BREAU, D. T., BRASS, A. L. & DONG, M. 2016. Frizzled proteins are colonic epithelial receptors for *C. difficile* toxin B. *Nature*, 538, 350-355.
- TARIQ, R., PARDI, D. S., BARTLETT, M. G. & KHANNA, S. 2018. Low Cure Rates in Controlled Trials of Fecal Microbiota Transplantation for Recurrent *Clostridium difficile* Infection: A Systematic Review and Meta-analysis. *Clinical Infectious Diseases*, 68, 1351-1358.
- TARIQ, R., SINGH, S., GUPTA, A., PARDI, D. S. & KHANNA, S. 2017. Association of Gastric Acid Suppression With Recurrent *Clostridium difficile* Infection: A Systematic Review and Meta-analysis. *JAMA Internal Medicine*, 177, 784-791.
- TASTEYRE, A., BARC, M.-C., KARJALAINEN, T., DODSON, P., HYDE, S., BOURLIOUX, P. & BORRIELLO, P. 2000. A *Clostridium difficile* gene encoding flagellin. *Microbiology*, 146, 957-966.
- TASTEYRE, A., BARC, M. C., COLLIGNON, A., BOUREAU, H. & KARJALAINEN, T. 2001a. Role of FliC and FliD flagellar proteins of *Clostridium difficile* in adherence and gut colonization. *Infection and Immunity*, 69, 7937-40.
- TASTEYRE, A., KARJALAINEN, T., AVESANI, V., DELMÉE, M., COLLIGNON, A., BOURLIOUX, P. & BARC, M.-C. 2001b. Molecular Characterization of fliD Gene Encoding Flagellar Cap and Its Expression among

Clostridium difficile Isolates from Different Serogroups. *Journal of Clinical Microbiology*, 39, 1178-1183.

- TEASLEY, D., OLSON, M., GEBHARD, R., GERDING, D., PETERSON, L., SCHWARTZ, M. & LEE, J. 1983. Prospective Randomised Trial of Metronidazole Verses Vancomycin for *Clostridium difficile*-associated Diarrhoea and Colitis. *The Lancet*, 322, 1043-1046.
- TEDESCO, F. J., BARTON, R. W. & ALPERS, D. H. 1974. Clindamycin-associated colitis. A prospective study. *Annals of Internal Medicine*, 81, 429-33.
- TENEBERG, S., LONNROTH, I., TORRES LOPEZ, J. F., GALILI, U., HALVARSSON, M. O., ANGSTROM, J. & KARLSSON, K. A. 1996. Molecular mimicry in the recognition of glycosphingolipids by Gal alpha 3 Gal beta 4 GlcNAc beta-binding *Clostridium difficile* toxin A, human natural anti alpha-galactosyl IgG and the monoclonal antibody Gal-13: characterization of a binding-active human glycosphingolipid, non-identical with the animal receptor. *Glycobiology*, 6, 599-609.
- THERIOT, C. M., BOWMAN, A. A., YOUNG, V. B. & ELLERMEIER, C. D. 2016. Antibiotic-induced alterations of the gut microbiota alter secondary bile acid production and allow for *Clostridium difficile* spore germination and outgrowth in the large intestine. *mSphere.*, 1, e00045-15.
- THERIOT, C. M., KOENIGSKNECHT, M. J., CARLSON, P. E., JR., HATTON, G. E., NELSON, A. M., LI, B., HUFFNAGLE, G. B., J, Z. L. & YOUNG, V. B. 2014. Antibiotic-induced shifts in the mouse gut microbiome and metabolome increase susceptibility to *Clostridium difficile* infection. *Nature Communications*, 5, 3114.
- THERIOT, C. M., KOUMPOURAS, C. C., CARLSON, P. E., BERGIN, II, ARONOFF, D. M. & YOUNG, V. B. 2011. Cefoperazone-treated mice as an experimental platform to assess differential virulence of *Clostridium difficile* strains. *Gut Microbes*, 2, 326-34.
- THERIOT, C. M. & YOUNG, V. B. 2015. Interactions Between the Gastrointestinal Microbiome and *Clostridium difficile*. *Annual review of microbiology*, 69, 445-461.
- THOMPSON, F. L., GOMEZ-GIL, B., VASCONCELOS, A. T. & SAWABE, T. 2007. Multilocus sequence analysis reveals that *Vibrio harveyi* and *V. campbellii* are distinct species. *Applied Environmental Microbiology*, 73, 4279-85.
- THURSBY, E. & JUGE, N. 2017. Introduction to the human gut microbiota. *The Biochemical journal*, 474, 1823-1836.
- TONG, H., CHEN, W., SHI, W., QI, F. & DONG, X. 2008. SO-LAAO, a novel L-amino acid oxidase that enables *Streptococcus oligofermentans* to

outcompete *Streptococcus mutans* by generating H₂O₂ from peptone. *Journal of Bacteriology*, 190, 4716-21.

- TREJO, F. M., PÉREZ, P. F. & DE ANTONI, G. L. 2010. Co-culture with potentially probiotic microorganisms antagonises virulence factors of *Clostridium difficile* in vitro. *Antonie van Leeuwenhoek*, 98, 19-29.
- TRIADAFILOPOULOS, G., POTHOUKAKIS, C., O'BRIEN, M. J. & LAMONT, J. T. 1987. Differential effects of *Clostridium difficile* toxins A and B on rabbit ileum. *Gastroenterology*, 93, 273-9.
- TRZASKO, A., LEEDS, J. A., PRAESTGAARD, J., LAMARCHE, M. J. & MCKENNEY, D. 2012. Efficacy of LFF571 in a hamster model of *Clostridium difficile* infection. *Antimicrobial agents and chemotherapy*, 56, 4459-4462.
- TUCKER, K. D. & WILKINS, T. D. 1991. Toxin A of *Clostridium difficile* binds to the human carbohydrate antigens I, X, and Y. *Infection and Immunity*, 59, 73-78.
- TULLI, L., MARCHI, S., PETRACCA, R., SHAW, H. A., FAIRWEATHER, N. F., SCARSELLI, M., SORIANI, M. & LEUZZI, R. 2013. CbpA: a novel surface exposed adhesin of *Clostridium difficile* targeting human collagen. *Cellular Microbiology*, 15, 1674-87.
- TVEDE, M. & RASK-MADSEN, J. 1989. Bacteriotherapy for chronic relapsing *Clostridium difficile* diarrhoea in six patients. *Lancet*, 1, 1156-60.
- TWINE, S. M., REID, C. W., AUBRY, A., MCMULLIN, D. R., FULTON, K. M., AUSTIN, J. & LOGAN, S. M. 2009. Motility and Flagellar Glycosylation in *Clostridium difficile*. *Journal of Bacteriology*, 191, 7050-7062.
- TYERMAN, J. G., PONCIANO, J. M., JOYCE, P., FORNEY, L. J. & HARMON, L. J. 2013. The evolution of antibiotic susceptibility and resistance during the formation of *Escherichia coli* biofilms in the absence of antibiotics. *BMC Evolutionary Biology*, 13, 1-7.
- VALDÉS-VARELA, L., ALONSO-GUERVOS, M., GARCÍA-SUÁREZ, O., GUEIMONDE, M. & RUAS-MADIEDO, P. 2016. Screening of Bifidobacteria and Lactobacilli Able to Antagonize the Cytotoxic Effect of *Clostridium difficile* upon Intestinal Epithelial HT29 Monolayer. *Frontiers in Microbiology*, 7, 577-577.
- VALDES-VARELA, L., HERNANDEZ-BARRANCO, A. M., RUAS-MADIEDO, P. & GUEIMONDE, M. 2016. Effect of *Bifidobacterium* upon *Clostridium difficile* Growth and Toxicity When Co-cultured in Different Prebiotic Substrates. *Frontiers in Microbiology*, 7, 738.
- VALENTINI, M. & FILLoux, A. 2016. Biofilms and Cyclic di-GMP (c-di-GMP) Signaling: Lessons from *Pseudomonas aeruginosa* and Other Bacteria. *Journal of Biological Chemistry*, 291, 12547-55.

- VALLE, J., TOLEDO-ARANA, A., BERASAIN, C., GHIGO, J. M., AMORENA, B., PENADÉS, J. R. & LASA, I. 2003. SarA and not sigmaB is essential for biofilm development by *Staphylococcus aureus*. *Molecular Microbiology*, 48, 1075-87.
- VAN DEN ABEELE, P., BELZER, C., GOOSSENS, M., KLEEREBEZEM, M., DE VOS, W. M., THAS, O., DE WEIRD, R., KERCKHOF, F. M. & VAN DE WIELE, T. 2013. Butyrate-producing *Clostridium* cluster XIVa species specifically colonize mucins in an *in vitro* gut model. *ISME Journal*, 7, 949-61.
- VAN DEN DRIESSE, F., RIGOLE, P., BRACKMAN, G. & COENYE, T. 2014. Optimization of resazurin-based viability staining for quantification of microbial biofilms. *Journal of Microbiological Methods*, 98, 31-4.
- VAN DER WAAIJ, D., BERGHUIS-DE VRIES, J. M. & LEKKERKERK, L.-V. 1971. Colonization resistance of the digestive tract in conventional and antibiotic-treated mice. *Journal of Hygiene (Lond)*, 69, 405-11.
- VAN LEEUWEN, P. T., VAN DER PEET, J. M., BIKKER, F. J., HOOGENKAMP, M. A., OLIVEIRA PAIVA, A. M., KOSTIDIS, S., MAYBORODA, O. A., SMITS, W. K. & KROM, B. P. 2016. Interspecies Interactions between *Clostridium difficile* and *Candida albicans*. *mSphere*, 1, e00187-16.
- VAN NOOD, E., DIJKGRAAF, M. G. & KELLER, J. J. 2013. Duodenal infusion of feces for recurrent *Clostridium difficile*. *New England Journal of Medicine*, 368, 2145.
- VARDAKAS, K. Z., KONSTANTELIAS, A. A., LOIZIDIS, G., RAFAILIDIS, P. I. & FALAGAS, M. E. 2012. Risk factors for development of *Clostridium difficile* infection due to BI/NAP1/027 strain: a meta-analysis. *International Journal of Infectious Diseases*, 16, e768-e773.
- VEDANTAM, G., CLARK, A., CHU, M., MCQUADE, R., MALLOZZI, M. & VISWANATHAN, V. K. 2012. *Clostridium difficile* infection: Toxins and non-toxin virulence factors, and their contributions to disease establishment and host response. *Gut Microbes*, 3, 121-134.
- VERBEKE, F., DE CRAEMER, S., DEBUNNE, N., JANSSENS, Y., WYNENDAELE, E., VAN DE WIELE, C. & DE SPIEGELEER, B. 2017. Peptides as Quorum Sensing Molecules: Measurement Techniques and Obtained Levels *In vitro* and *In vivo*. *Frontiers in Neuroscience*, 11, 183.
- VESTEINSDOTTIR, I., GUDLAUGSDOTTIR, S., EINARSDOTTIR, R., KALAITZAKIS, E., SIGURDARDOTTIR, O. & BJORNSSON, E. S. 2012. Risk factors for *Clostridium difficile* toxin-positive diarrhea: a population-based prospective case-control study. *European Journal of Clinical Microbiology and Infectious Diseases*, 31, 2601-10.

- VITAL, M., RUD, T., RATH, S., PIEPER, D. H. & SCHLÜTER, D. 2019. Diversity of Bacteria Exhibiting Bile Acid-inducible 7 α -dehydroxylation Genes in the Human Gut. *Computational and Structural Biotechnology Journal*, 17, 1016-1019.
- VON EICHEL-STREIBER, C., LAUFENBERG-FELDMANN, R., SARTINGEN, S., SCHULZE, J. & SAUERBORN, M. 1992. Comparative sequence analysis of the *Clostridium difficile* toxins A and B. *Molecular Genetics and Genomics*, 233, 260-8.
- VROOM, J. M., DE GRAUW, K. J., GERRITSEN, H. C., BRADSHAW, D. J., MARSH, P. D., WATSON, G. K., BIRMINGHAM, J. J. & ALLISON, C. 1999. Depth Penetration and Detection of pH Gradients in Biofilms by Two-Photon Excitation Microscopy. *Applied and Environmental Microbiology*, 65, 3502-3511.
- VUOTTO, C., MOURA, I., BARBANTI, F., DONELLI, G. & SPIGAGLIA, P. 2015. Subinhibitory concentrations of metronidazole increase biofilm formation in *Clostridium difficile* strains. *Pathogens and Disease*, 74.
- WAGNER, R. D. 2008. Effects of microbiota on GI health: gnotobiotic research. *Advances in Experimental Medicine and Biology*, 635, 41-56.
- WALIGORA, A.-J., HENNEQUIN, C., MULLANY, P., BOURLIOUX, P., COLLIGNON, A. & KARJALAINEN, T. 2001. Characterization of a Cell Surface Protein of *Clostridium difficile* with Adhesive Properties. *Infection and Immunity*, 69, 2144-2153.
- WALLACH, T. E. & BAYRER, J. R. 2017. Intestinal Organoids: New Frontiers in the Study of Intestinal Disease and Physiology. *Journal of pediatric gastroenterology and nutrition*, 64, 180-185.
- WALTERS, M. C., 3RD, ROE, F., BUGNICOURT, A., FRANKLIN, M. J. & STEWART, P. S. 2003. Contributions of antibiotic penetration, oxygen limitation, and low metabolic activity to tolerance of *Pseudomonas aeruginosa* biofilms to ciprofloxacin and tobramycin. *Antimicrobial Agents and Chemotherapy*, 47, 317-23.
- WANG, Q., GARRITY, G. M., TIEDJE, J. M. & COLE, J. R. 2007. Naïve Bayesian Classifier for Rapid Assignment of rRNA Sequences into the New Bacterial Taxonomy. *Applied and Environmental Microbiology*, 73, 5261-5267.
- WANG, S., XU, M., WANG, W., CAO, X., PIAO, M., KHAN, S., YAN, F., CAO, H. & WANG, B. 2016. Systematic Review: Adverse Events of Fecal Microbiota Transplantation. *PLOS ONE*, 11, e0161174.
- WANG, X., GIBSON, G. R., SAILER, M., THEIS, S. & RASTALL, R. A. 2020. Prebiotics Inhibit Proteolysis by Gut Bacteria in a Host Diet-Dependent Manner: a Three-Stage Continuous *In Vitro* Gut Model Experiment. *Applied and Environmental Microbiology*, 86, e02730-19.

- WARNY, M., PEPIN, J., FANG, A., KILLGORE, G., THOMPSON, A., BRAZIER, J., FROST, E. & MCDONALD, L. C. 2005. Toxin production by an emerging strain of *Clostridium difficile* associated with outbreaks of severe disease in North America and Europe. *Lancet*, 366, 1079-84.
- WEBER, D. J., ANDERSON, D. J., SEXTON, D. J. & RUTALA, W. A. 2013. Role of the environment in the transmission of *Clostridium difficile* in health care facilities. *American Journal of Infection Control*, 41, S105-S110.
- WEINGARDEN, A. R., CHEN, C., BOBR, A., YAO, D., LU, Y., NELSON, V. M., SADOWSKY, M. J. & KHORUTS, A. 2014. Microbiota transplantation restores normal fecal bile acid composition in recurrent *Clostridium difficile* infection. *American Journal of Physiology-Gastrointestinal and Liver Physiology*, 306, G310-9.
- WEISS, W., PULSE, M. & VICKERS, R. 2014. *In vivo* assessment of SMT19969 in a hamster model of clostridium difficile infection. *Antimicrobial agents and chemotherapy*, 58, 5714-5718.
- WENISCH, C., PARSchALK, B., HASENHÜNDL, M., HIRSCHL, A. M. & GRANINGER, W. 1996. Comparison of Vancomycin, Teicoplanin, Metronidazole, and Fusidic Acid for the Treatment of *Clostridium difficile*—Associated Diarrhea. *Clinical Infectious Diseases*, 22, 813-818.
- WILCOX, M. H., AHIR, H., COIA, J. E., DODGSON, A., HOPKINS, S., LLEWELYN, M. J., SETTLE, C., MCLAIN-SMITH, S. & MARCELLA, S. W. 2017a. Impact of recurrent *Clostridium difficile* infection: hospitalization and patient quality of life. *Journal of Antimicrobial Chemotherapy*, 72, 2647-2656.
- WILCOX, M. H., GERDING, D. N., POXTON, I. R., KELLY, C., NATHAN, R., BIRCH, T., CORNELLY, O. A., RAHAV, G., BOUZA, E., LEE, C., JENKIN, G., JENSEN, W., KIM, Y.-S., YOSHIDA, J., GABRYELSKI, L., PEDLEY, A., EVES, K., TIPPING, R., GURIS, D., KARTSONIS, N. & DORR, M.-B. 2017b. Bezlotoxumab for Prevention of Recurrent *Clostridium difficile* Infection. *New England Journal of Medicine*, 376, 305-317.
- WILCOX, M. H., SHETTY, N., FAWLEY, W. N., SHEMKO, M., COEN, P., BIRTLES, A., CAIRNS, M., CURRAN, M. D., DODGSON, K. J., GREEN, S. M., HARDY, K. J., HAWKEY, P. M., MAGEE, J. G., SAILS, A. D. & WREN, M. W. D. 2012. Changing Epidemiology of *Clostridium difficile* Infection Following the Introduction of a National Ribotyping-Based Surveillance Scheme in England. *Clinical Infectious Diseases*, 55, 1056-1063.
- WILLING, S. E., CANDELA, T., SHAW, H. A., SEAGER, Z., MESNAGE, S., FAGAN, R. P. & FAIRWEATHER, N. F. 2015. *Clostridium difficile* surface proteins are anchored to the cell wall using CWB2 motifs that

recognise the anionic polymer PSII. *Molecular Microbiology*, 96, 596-608.

- WILSON, K. H. & PERINI, F. 1988. Role of competition for nutrients in suppression of *Clostridium difficile* by the colonic microflora. *Infection and Immunity*, 56, 2610-4.
- WILSON, K. H., SHEAGREN, J. N., FRETER, R., WEATHERBEE, L. & LYERLY, D. 1986. Gnotobiotic models for study of the microbial ecology of *Clostridium difficile* and *Escherichia coli*. *Journal of Infectious Diseases*, 153, 547-51.
- WILSON, K. H., SILVA, J. & FEKETY, F. R. 1981. Suppression of *Clostridium difficile* by normal hamster cecal flora and prevention of antibiotic-associated cecitis. *Infection and Immunity*, 34, 626-8.
- WINSTON, J. A. & THERIOT, C. M. 2016. Impact of microbial derived secondary bile acids on colonization resistance against *Clostridium difficile* in the gastrointestinal tract. *Anaerobe*, 41, 44-50.
- WOO, T. D., OKA, K., TAKAHASHI, M., HOJO, F., OSAKI, T., HANAWA, T., KURATA, S., YONEZAWA, H. & KAMIYA, S. 2011. Inhibition of the cytotoxic effect of *Clostridium difficile* *in vitro* by *Clostridium butyricum* MIYAIRI 588 strain. *Journal of Medical Microbiology*, 60, 1617-25.
- WOOD, T. K., KNABEL, S. J. & KWAN, B. W. 2013. Bacterial Persister Cell Formation and Dormancy. *Applied and Environmental Microbiology*, 79, 7116-7121.
- XAVIER, K. B. & BASSLER, B. L. 2003. LuxS quorum sensing: more than just a numbers game. *Current Opinion Microbiology*, 6, 191-7.
- XIA, Y., HU, H. Z., LIU, S., POTHOUKAKIS, C. & WOOD, J. D. 2000. *Clostridium difficile* toxin A excites enteric neurones and suppresses sympathetic neurotransmission in the guinea pig. *Gut*, 46, 481-6.
- XIE, H., COOK, G. S., COSTERTON, J. W., BRUCE, G., ROSE, T. M. & LAMONT, R. J. 2000. Intergeneric communication in dental plaque biofilms. *Journal of Bacteriology*, 182, 7067-9.
- XIE, H., LIN, X., WANG, B.-Y., WU, J. & LAMONT, R. J. 2007. Identification of a signalling molecule involved in bacterial intergeneric communication. *Microbiology*, 153, 3228-3234.
- YAMAMOTO-OSAKI, T., KAMIYA, S., SAWAMURA, S., KAI, M. & OZAWA, A. 1994. Growth inhibition of *Clostridium difficile* by intestinal flora of infant faeces in continuous flow culture. *Journal of Medical Microbiology*, 40, 179-87.
- YAMAMOTO, M., YAMAGUCHI, R., MUNAKATA, K., TAKASHIMA, K., NISHIYAMA, M., HIOKI, K., OHNISHI, Y., NAGASAKI, M., IMOTO, S.,

- MIYANO, S., ISHIGE, A. & WATANABE, K. 2012. A microarray analysis of gnotobiotic mice indicating that microbial exposure during the neonatal period plays an essential role in immune system development. *BMC genomics*, 13, 335-335.
- YARWOOD, J. M., BARTELS, D. J., VOLPER, E. M. & GREENBERG, E. P. 2004. Quorum sensing in *Staphylococcus aureus* biofilms. *Journal of Bacteriology*, 186, 1838-1850.
- YOUNGSTER, I., MAHABAMUNUGE, J., SYSTROM, H. K., SAUK, J., KHALILI, H., LEVIN, J., KAPLAN, J. L. & HOHMANN, E. L. 2016. Oral, frozen fecal microbiota transplant (FMT) capsules for recurrent *Clostridium difficile* infection. *BMC Medicine*, 14, 134.
- YOUNGSTER, I., SAUK, J., PINDAR, C., WILSON, R. G., KAPLAN, J. L., SMITH, M. B., ALM, E. J., GEVERS, D., RUSSELL, G. H. & HOHMANN, E. L. 2014. Fecal Microbiota Transplant for Relapsing *Clostridium difficile* Infection Using a Frozen Inoculum From Unrelated Donors: A Randomized, Open-Label, Controlled Pilot Study. *Clinical Infectious Diseases: An Official Publication of the Infectious Diseases Society of America*, 58, 1515-1522.
- YUAN, P., ZHANG, H., CAI, C., ZHU, S., ZHOU, Y., YANG, X., HE, R., LI, C., GUO, S., LI, S., HUANG, T., PEREZ-CORDON, G., FENG, H. & WEI, W. 2015. Chondroitin sulfate proteoglycan 4 functions as the cellular receptor for *Clostridium difficile* toxin B. *Cell Research*, 25, 157-68.
- ZACHOS, N. C., KOVBASNJUK, O., FOULKE-ABEL, J., IN, J., BLUTT, S. E., DE JONGE, H. R., ESTES, M. K. & DONOWITZ, M. 2016. Human Enteroids/Colonoids and Intestinal Organoids Functionally Recapitulate Normal Intestinal Physiology and Pathophysiology. *Journal of Biological Chemistry*, 291, 3759-66.
- ZAR, F. A., BAKKANAGARI, S. R., MOORTHI, K. M. L. S. T. & DAVIS, M. B. 2007. A Comparison of Vancomycin and Metronidazole for the Treatment of *Clostridium difficile*-Associated Diarrhea, Stratified by Disease Severity. *Clinical Infectious Diseases*, 45, 302-307.
- ZHANEL, G. G., WALKTY, A. J. & KARLOWSKY, J. A. 2015. Fidaxomicin: A novel agent for the treatment of *Clostridium difficile* infection. *Canadian Journal of Infectious Diseases and Medical Microbiology*, 26, 305-12.
- ZHENG, J. X., LIN, Z. W., CHEN, C., CHEN, Z., LIN, F. J., WU, Y., YANG, S. Y., SUN, X., YAO, W. M., LI, D. Y., YU, Z. J., JIN, J. L., QU, D. & DENG, Q. W. 2018. Biofilm Formation in *Klebsiella pneumoniae* Bacteremia Strains Was Found to be Associated with CC23 and the Presence of *wcaG*. *Frontiers in Cellular and Infection Microbiology*, 8, 21.
- ZHU, Z., SCHNELL, L., MÜLLER, B., MÜLLER, M., PAPTAEODOROU, P. & BARTH, H. 2019. The Antibiotic Bacitracin Protects Human Intestinal Epithelial Cells and Stem Cell-Derived Intestinal Organoids from

Clostridium difficile Toxin TcdB. *Stem Cells International*, 2019, 4149762.

ZOBELL, C. E. 1943. The Effect of Solid Surfaces upon Bacterial Activity. *Journal of Bacteriology*, 46, 39-56.

ZOETENDAL, E. G., VON WRIGHT, A., VILPPONEN-SALMELA, T., BEN-AMOR, K., AKKERMANS, A. D. & DE VOS, W. M. 2002. Mucosa-associated bacteria in the human gastrointestinal tract are uniformly distributed along the colon and differ from the community recovered from feces. *Applied and Environmental Microbiology*, 68, 3401-7.

ZOTTOLA, E. A. & SASAHARA, K. C. 1994. Microbial biofilms in the food processing industry--should they be a concern? *International Journal of Food Microbiology*, 23, 125-48.

ZUO, T., WONG, S. H., CHEUNG, C. P., LAM, K., LUI, R., CHEUNG, K., ZHANG, F., TANG, W., CHING, J. Y. L., WU, J. C. Y., CHAN, P. K. S., SUNG, J. J. Y., YU, J., CHAN, F. K. L. & NG, S. C. 2018a. Gut fungal dysbiosis correlates with reduced efficacy of fecal microbiota transplantation in *Clostridium difficile* infection. *Nature Communications*, 9, 3663.

ZUO, T., WONG, S. H., LAM, K., LUI, R., CHEUNG, K., TANG, W., CHING, J. Y. L., CHAN, P. K. S., CHAN, M. C. W., WU, J. C. Y., CHAN, F. K. L., YU, J., SUNG, J. J. Y. & NG, S. C. 2018b. Bacteriophage transfer during faecal microbiota transplantation in *Clostridium difficile* infection is associated with treatment outcome. *Gut*, 67, 634-643.

Appendix

A.1 Ethical approval



UNIVERSITY OF LEEDS

Faculty of Medicine and Health Research Office
School of Medicine Research Ethics Committee (SoMREC)

Room 10.111b, level 10
Worsley Building
Clarendon Way
Leeds, LS2 9NL
United Kingdom

☎ +44 (0) 113 343 1642

04 April 2016

Dr Caroline Chilton
University Academic Fellow
Molecular Gastroenterology, LIBACS
Medicine and Health
Microbiology R&D
Old Medical School
Leeds General Infirmary
Thoresby Place
LEEDS LS1 3EX

Dear Caroline

Ref no: MREC15-070

Title: Investigation of the Interplay between Commensal Intestinal Organisms and Pathogenic Bacteria

Your research application has been reviewed by the School of Medicine Ethics Committee (SoMREC) and we can confirm that ethics approval is granted based on the following documentation received from you:

Document	Version	Date Submitted
Chilton_2016_gut_model_ethics_application_revised	2.0	02/03/2016
The Human Gut Model v2.1_revisions_highlighted	2.1	02/03/2016
uni_loneworking_risk_assessment_form	1.0	26/01/2016

Please notify the committee if you intend to make any amendments to the original research ethics application or documentation. All changes must receive ethics approval prior to implementation. Please contact the Faculty Research Ethics Administrator for further information (fmhuniethics@leeds.ac.uk)

Ethics approval does not infer you have the right of access to any member of staff or student or documents and the premises of the University of Leeds. Nor does it imply any right of access to the premises of any other organisation, including clinical areas. The committee takes no responsibility for you gaining access to staff, students and/or premises prior to, during or following your research activities.

Please note: You are expected to keep a record of all your approved documentation, as well as documents such as sample consent forms, and other documents relating to the study. This should be kept in your study file, which should be readily available for audit purposes. You will be given a two week notice period if your project is to be audited.

It is our policy to remind everyone that it is your responsibility to comply with Health and Safety, Data Protection and any other legal and/or professional guidelines there may be.

Re-Issued 16/06/2016



09 June 2016

Dr Anthony Buckley
 Microbiology, Old Medical School
 Leeds General Infirmary
 Leeds
 LS1 3EX

Dear Dr Buckley,

Study title:	Long-term storage of donor faecal samples for use in an in vitro gut model.
REC reference:	16/EM/0263
IRAS project ID:	206781

The Proportionate Review Sub-committee of the East Midlands - Leicester South Research Ethics Committee reviewed the above application on 09 June 2016.

We plan to publish your research summary wording for the above study on the HRA website, together with your contact details. Publication will be no earlier than three months from the date of this favourable opinion letter. The expectation is that this information will be published for all studies that receive an ethical opinion but should you wish to provide a substitute contact point, wish to make a request to defer, or require further information, please contact the REC Manager, Rebecca Morledge, NRESCcommittee.EastMidlands-LeicesterSouth@nhs.net. Under very limited circumstances (e.g. for student research which has received an unfavourable opinion), it may be possible to grant an exemption to the publication of the study.

Ethical opinion

On behalf of the Committee, the sub-committee gave a favourable ethical opinion of the above research on the basis described in the application form, protocol and supporting documentation, subject to the conditions specified below.

Conditions of the favourable opinion

The REC favourable opinion is subject to the following conditions being met prior to the start of the study.

Management permission must be obtained from each host organisation prior to the start of the study at the site concerned.

A.2 Participant recruitment and information sheet

The Human Gut Model



What is it?

The Human Gut Model is a research tool at Leeds University, used to study the normal bacterial populations of the gut and important pathogens that can cause healthcare associated infections such as *Clostridium difficile* or Antibiotic Resistant organisms.

It is used to mimic infection or gut colonisation in a patient, and we monitor the normal gut bacteria, and the pathogenic bacteria throughout a simulated infection.

We can use this platform to test potential new treatment agents, and also to see which antibiotics are risk factors for causing or increasing the spread of healthcare associated infections.

In order to set up the model with normal gut bacteria, we use human poo from volunteers.

Who can be a volunteer?

Any healthy person (over 18) can be a volunteer unless you have taken any antibiotics in the last 3 months (as this will affect your normal gut bacteria).

Because patients over the age of 60 are most at risk from *C. difficile* infection, we try to get volunteers from this age group when investigating this pathogen. For other experiments, age is not a factor, so anyone can donate.

In order to get an average 'picture' of gut bacteria we need 5 different volunteers for each run.

You are being invited to take part in a research project. Before you decide it is important for you to understand why the research is being done and what it will involve. Please take time to read this information sheet carefully and discuss it with others if you wish. Ask us if there is anything that is not clear or if you would like more information. Take time to decide whether or not you wish to take part. This study has been approved by an NHS ethics committee.

What is involved?

Volunteers will be provided with a poo collection kit that consists of:

- A disposable bowl
- 3 x screw top containers
- Wooden spatula
- 1 AnaeroGen anaerobic pouch
- Sealable bag
- Large plastic bag
- Disposable gloves

Instructions:

- Poo into disposable bowl
- Scoop poo into containers and loosely screw shut
- Put containers into bag with anaerobic pouch and seal
- Everything else can be put in the plastic bag and disposed of in normal household waste (as you would a nappy) or returned to us for disposal.

By providing us with a sample, you are consenting to it being used for the gut model.

Please note:

Samples are only used for setting up the gut model.

Volunteer's samples remain anonymous throughout the process.

Pooled samples can be stored for a maximum of 2 years.

Samples will be collected in person by either Tony Buckley or Caroline Chilton.

Once we have received your sample, you cannot withdraw your consent, however, you may choose not to give further samples whenever you wish.

If you have any questions, please contact us;
Telephone: 0113 392 8663

Healthcare Associated Infections Research Group
Microbiology R&D
Old Medical School, Leeds General Infirmary,

Caroline Chilton - c.h.chilton@leeds.ac.uk
Tony Buckley - a.buckley1@leeds.ac.uk

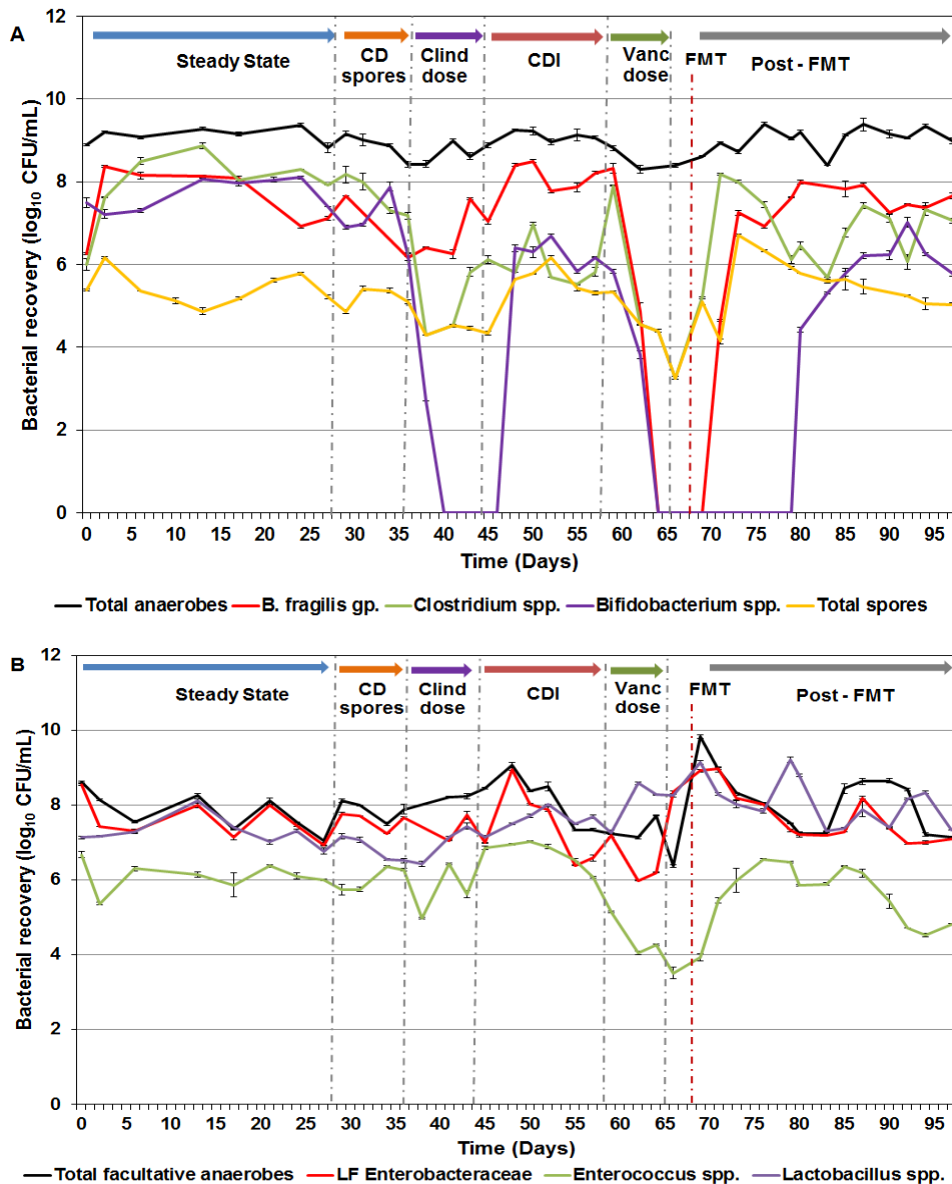
A.3 Constituents of the culture media used to enumerate microbial populations

Agar	Typical formula	Amount (g/ L)
Brazier's CCEY agar (LabM) – LAB160	Peptone Mix	23.0
	Sodium chloride	5.0
	Soluble starch	1.0
	Agar	12.0
	Sodium bicarbonate	0.4
	Glucose	1.0
	Sodium pyruvate	1.0
	Cysteine HCl	0.5
	Haemin	0.01
	Vitamin K	0.001
	L-arginine	1.0
	Soluble pyrophosphate	0.25
	Sodium succinate	0.5
	Cholic acid	1.0
p-Hydroxyphenylacetic acid	1.0	
Bile aesculin agar (Oxoid) – CM0888	Peptone	14.0
	Bile salts	15.0
	Ferric citrate	0.5
	Aesculin	1.0
	Agar	15.0
Columbia blood agar base (Oxoid) – CM0331	Special peptone	23.0
	Starch	1.0
	Sodium chloride	5.0
	Agar	10.0
Fastidious anaerobe agar with horse blood (Oxoid) – PB0225A	Peptone Mix	23.0
	Sodium chloride	5.0
	Soluble Starch	1.0
	Agar No.2	12.0
	Sodium bicarbonate	0.4
	Glucose	1.0
	Sodium pyruvate	1.0
	Cysteine HCl monohydrate	0.5
	Haemin	0.01
	Vitamin K	0.001
	L-Arginine	1.0
	Soluble pyrophosphate	0.25
	Sodium succinate	0.5
	Defibrinated horse blood	50 mL
Kanamycin aesculin azide	Tryptone	18.8

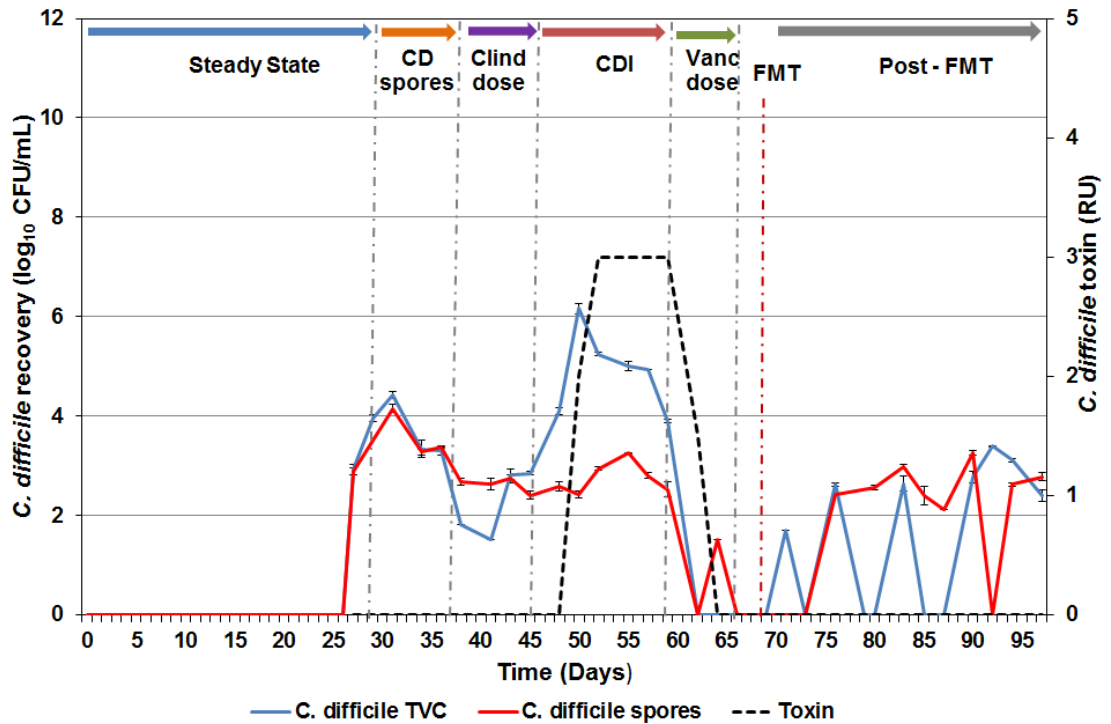
agar base (Oxoid) - CM0591	Yeast extract Sodium chloride Sodium citrate Aesculin Ferric ammonium citrate Sodium azide Starch Mix for Streptococci Agar	5.0 5.0 1.0 1.0 0.5 0.15 0.6 0.6 10.0
MacConkey agar No.3 (Oxoid) – PO0495A	Peptone Lactose Bile salts No. 3 Sodium chloride Neutral red Crystal violet Agar	20.0 10.0 1.5 5.0 0.03 0.001 15.0
MRS Broth (De Man, Rogosa, Sharpe, Oxoid) – CM0359	Peptone 'Lab-Lemco' powder Yeast extract Glucose Sorbitan mono-oleate Dipotassium hydrogen phosphate Sodium acetate 3H₂O Triammonium citrate Magnesium sulphate 7H₂O Manganese sulphate 4H₂O	10.0 8.0 4.0 20.0 1 mL 2.0 5.0 2.0 0.2 0.05
Nutrient agar (Oxoid) – PO0155A	Protease peptone Yeast extract Liver digest Sodium chloride Agar	15.0 5.0 2.5 5.0 12.0
Oxytetracycline glucose yeast extract agar (Oxoid) – PO0183	Yeast extract Glucose Agar Oxytetracycline	5.0 20.0 12.0 100 mg

CCEY – cefoxitin cycloserine egg yolk, FAA – Fastidious anaerobe agar, MRS – De Man, Rogosa, Sharpe

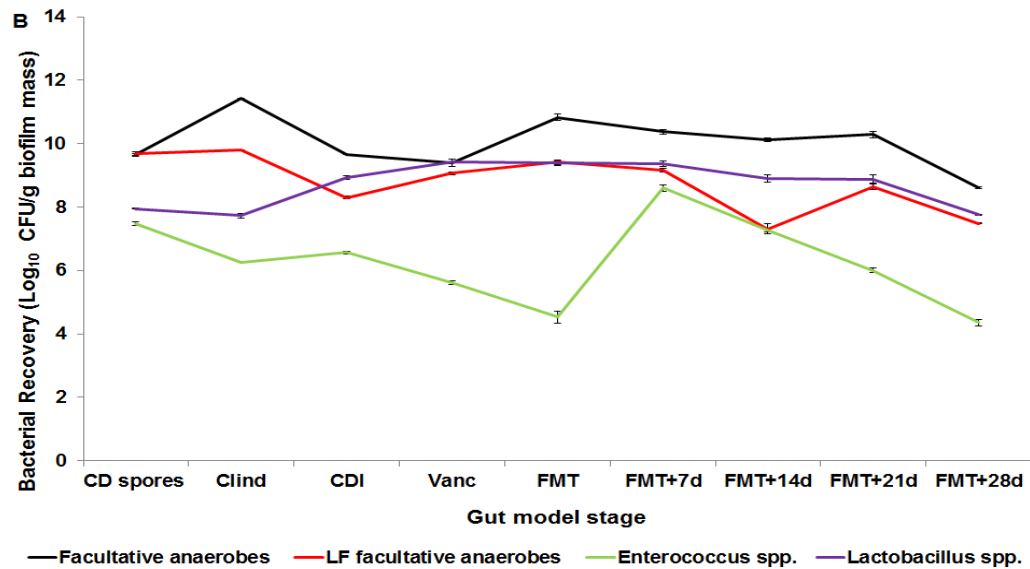
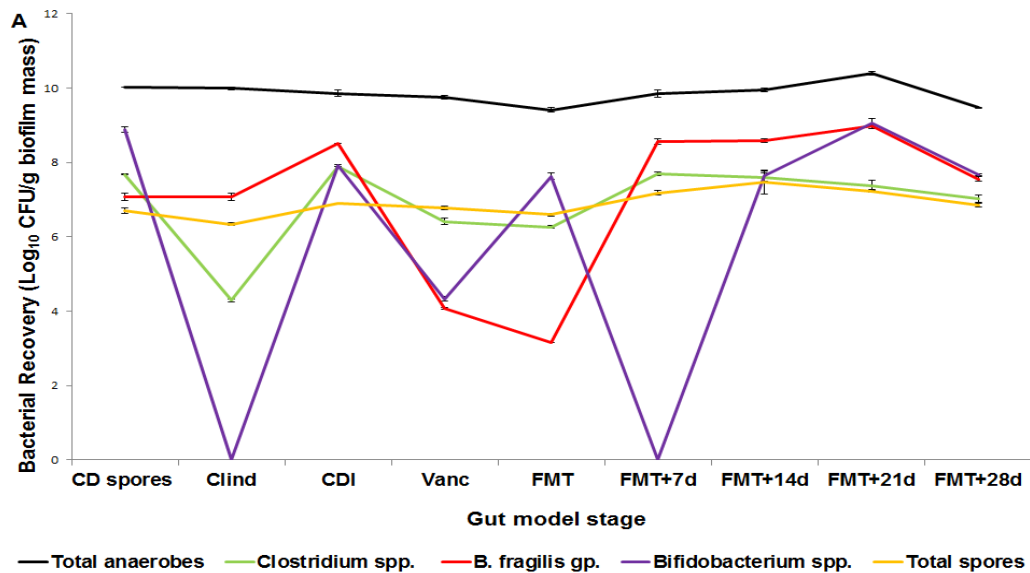
A.4 Repeat FMT model



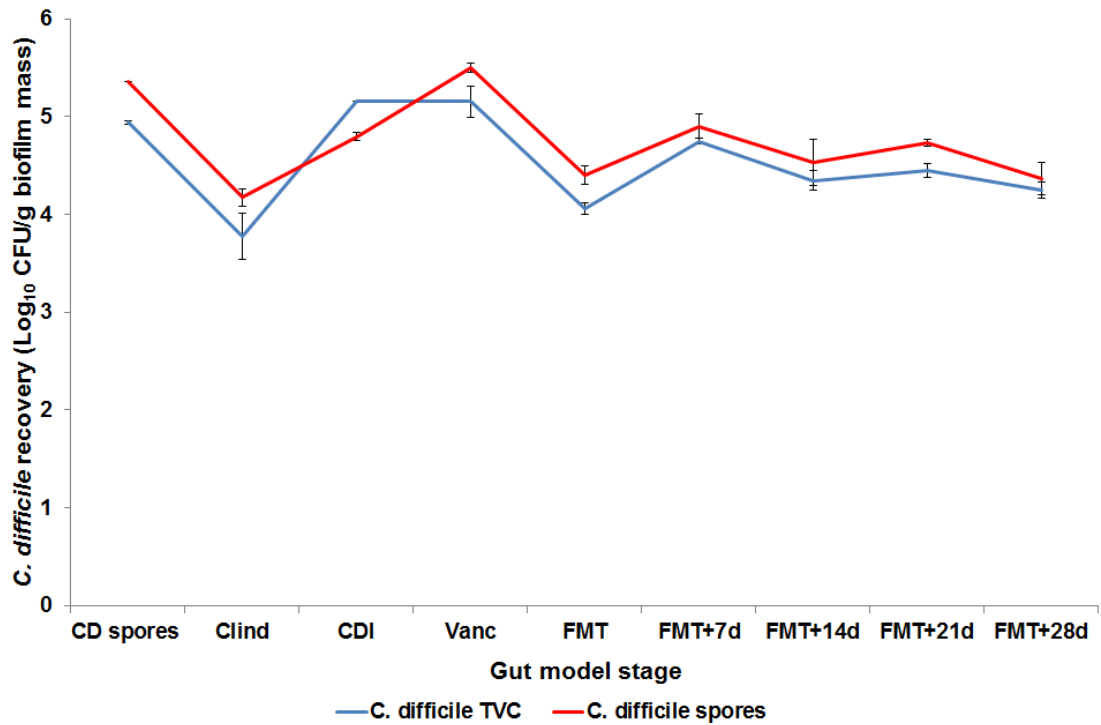
Enumeration of planktonic populations in the repeat faecal microbiota transplant model. (a) Enumeration of total anaerobes (black), *B. fragilis* gp. (red), *Clostridium* spp. (green), *Bifidobacterium* spp. (purple), and spores (yellow). (b) Enumeration of total facultative anaerobes (black), lactose fermenting (LF) Enterobacteriaceae (red), *Enterococcus* spp. (green), and *Lactobacillus* spp. (purple). Results show bacterial population changes in response to antimicrobial and faecal microbiota transplant therapy. Data shown are the mean \log_{10} CFU/mL \pm standard error from three technical replicates per day of the model timeline of a single biological replicate. Clind – clindamycin, Vanc – vancomycin, FMT – faecal microbiota transplantation, CDI – *C. difficile* infection.



Enumeration of planktonic *C. difficile* total and spore counts in repeat simulated faecal microbiota transplant model. Enumerations of *C. difficile* spores (red) and total viable counts (blue) are represented in mean \log_{10} CFU/mL \pm standard error (left axis). *C. difficile* toxin (black broken line) is represented as log reciprocal units (RU, right axis). No evidence of *C. difficile* recurrence is seen after the simulated faecal microbiota transplant. Different model stages are separated by vertical broken lines (grey; FMT instillation red). Clind – clindamycin, Vanc – vancomycin, FMT – faecal microbiota transplantation, CDI – *C. difficile* infection.

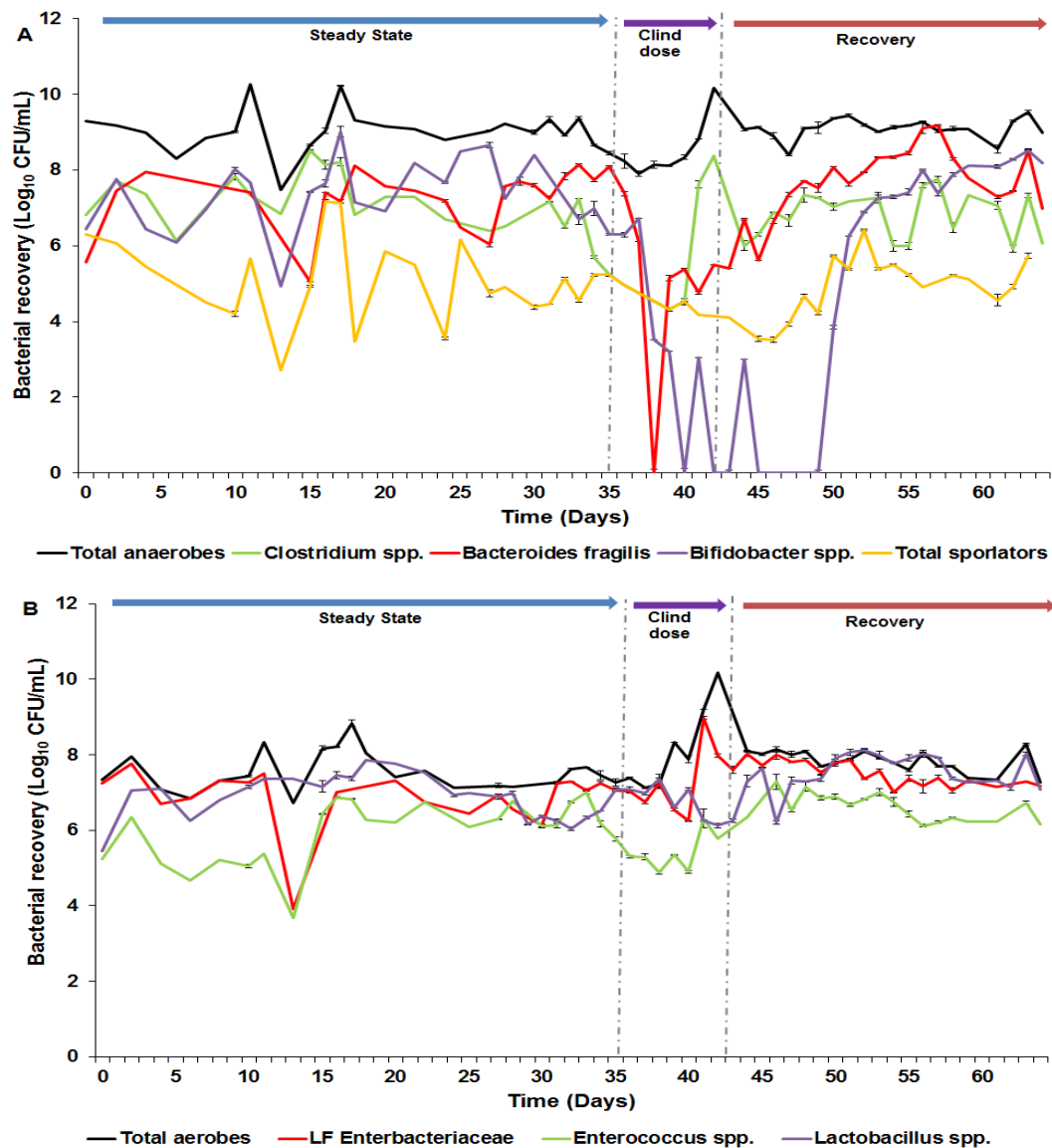


Enumeration of biofilm populations in the repeat faecal microbiota transplant model. (a) Enumeration of total anaerobes (black), *B. fragilis* gp. (red), *Clostridium* spp. (green), *Bifidobacterium* spp. (purple), and spores (yellow). (b) Enumeration of total facultative anaerobes (black), lactose fermenting (LF) Enterobacteriaceae (red), *Enterococcus* spp. (green), and *Lactobacillus* spp. (purple). Results show bacterial population changes in response to antimicrobial and faecal microbiota transplant therapy. Data shown are the mean log_{10} CFU/mL \pm standard error from three technical replicates at selected time points of a single biological replicate. Clind – clindamycin, Vanc – vancomycin, FMT – faecal microbiota transplantation, CDI – *C. difficile* infection.

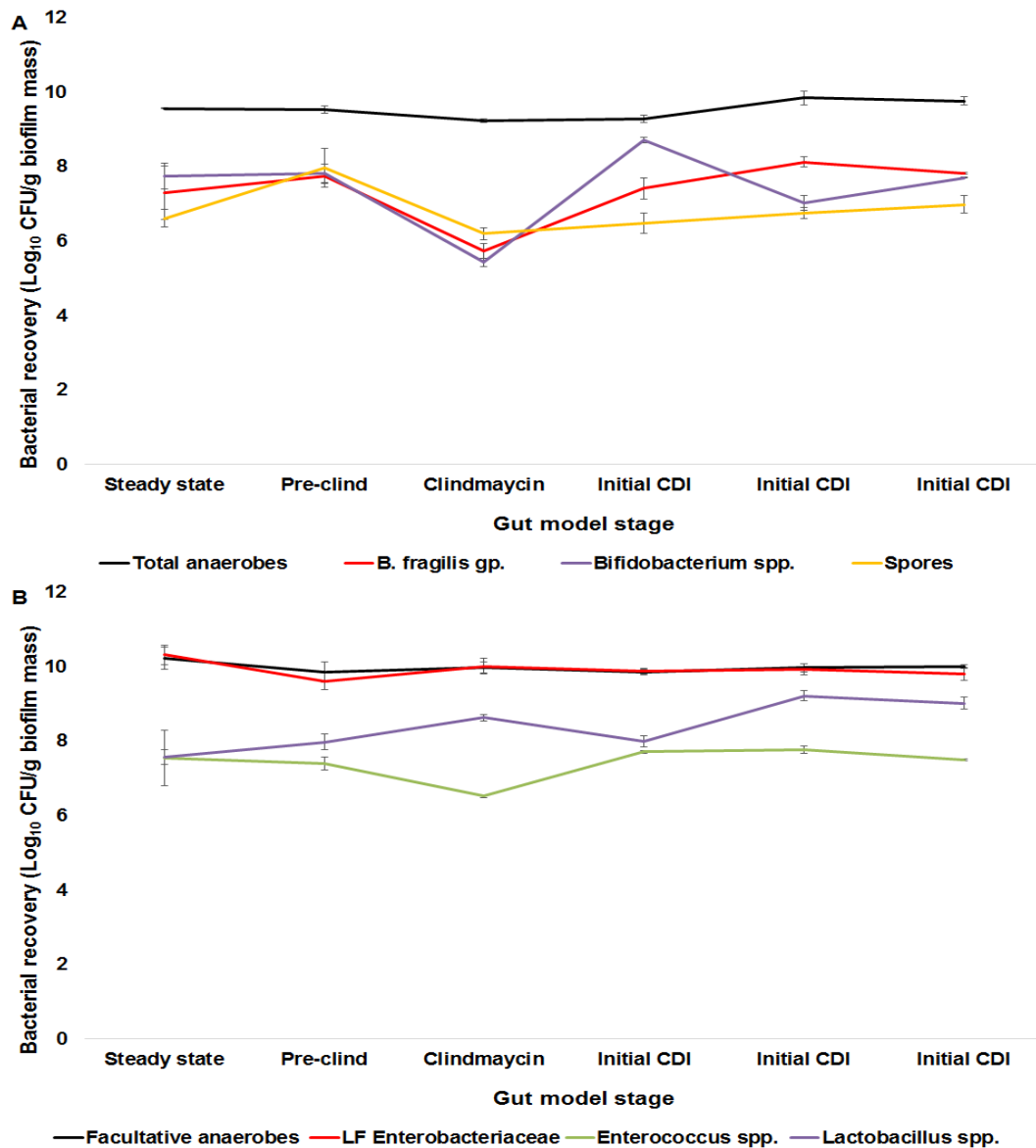


Enumeration of *C. difficile* total and spore counts recovered from the biofilm in the repeat faecal microbiota transplant model. Bacterial enumeration of *C. difficile* total viable counts (TVC - blue) and spore counts (red). Data demonstrates the persistence of *C. difficile* cells in the biofilm through antimicrobial and faecal microbiota transplant therapy. Data shown are the mean log₁₀ CFU/g biofilm mass ± standard error from three technical replicates at selected time points of a single biological replicate, at various stages throughout the model timeline. Clind – clindamycin, Vanc – vancomycin, FMT – faecal microbiota transplantation, CDI – *C. difficile* infection, d – days, wk – weeks, TVC – total viable counts.

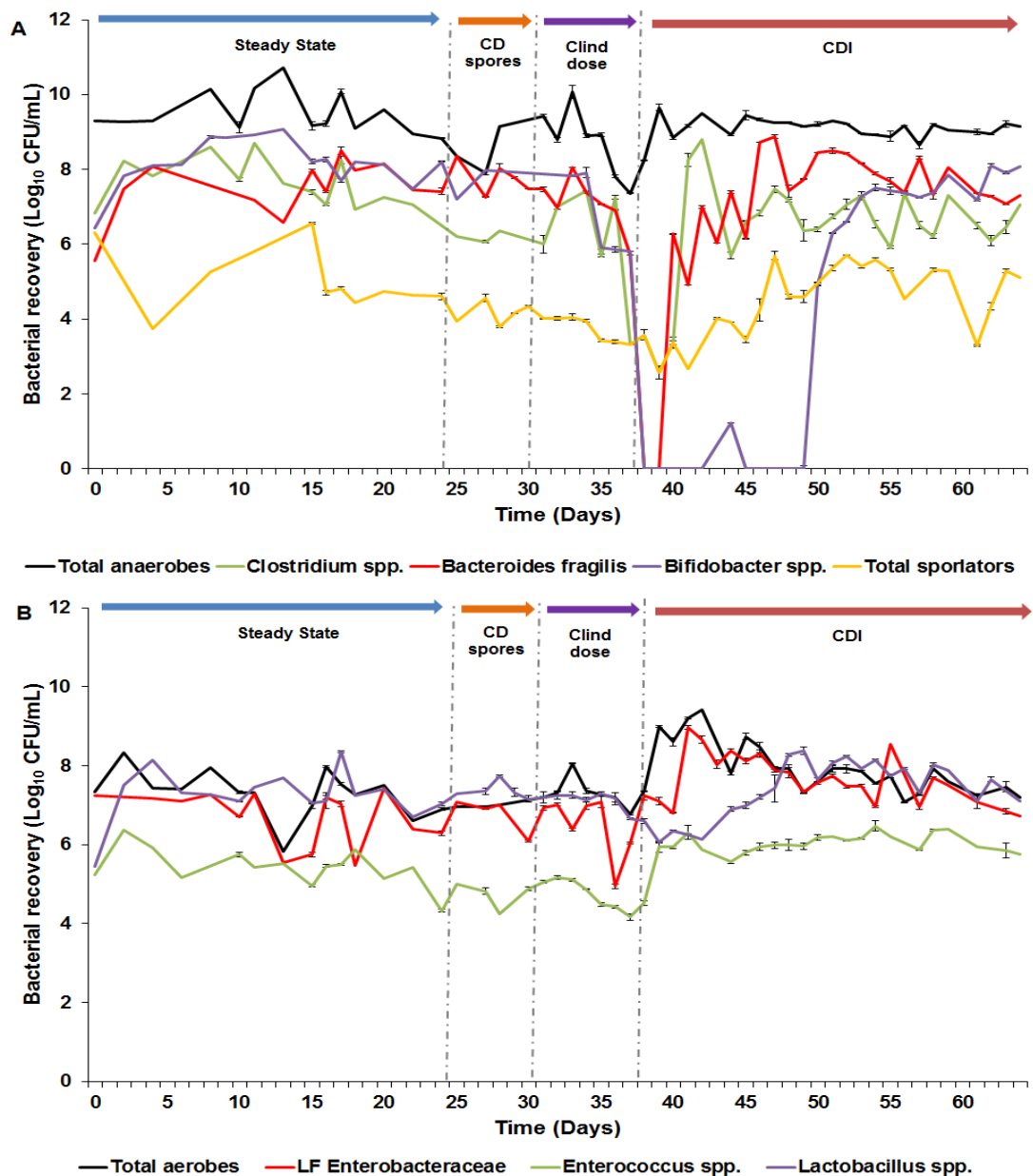
A.5 Models characterising the niche generated by clindamycin



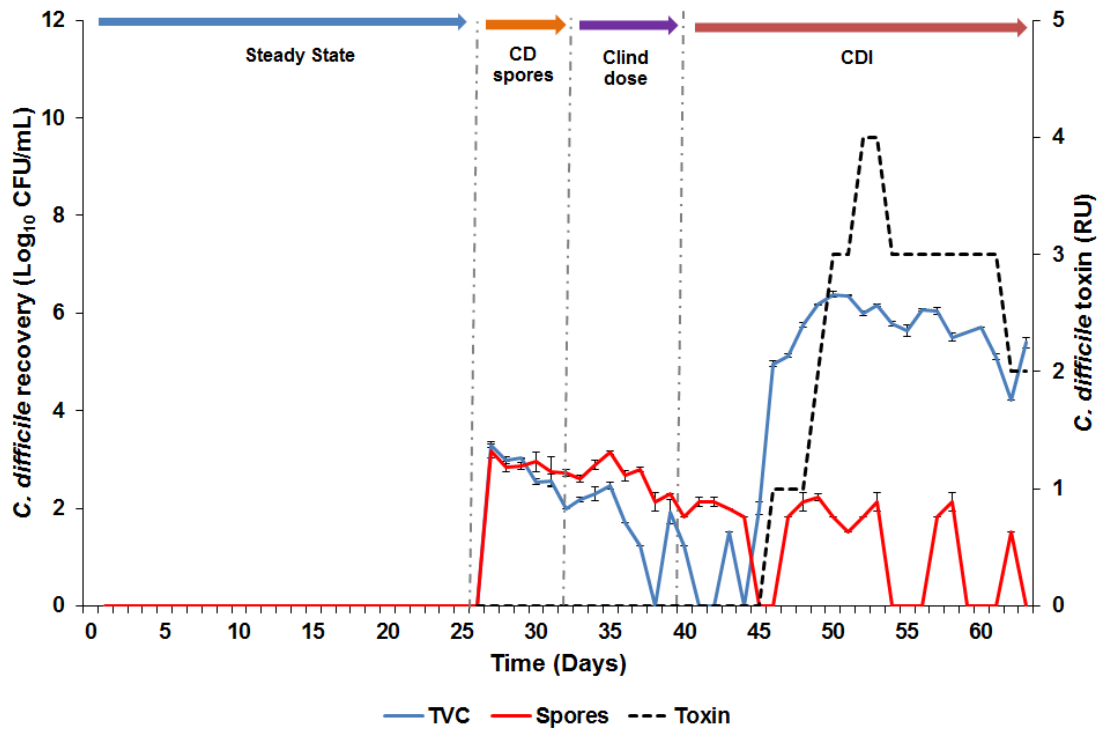
Enumeration of biofilm populations in a *C. difficile* naïve model during clindamycin treatment. (a) Enumeration of total anaerobes (black), *B. fragilis* gp. (red), *Clostridium* spp. (green), *Bifidobacterium* spp. (purple), and spores (yellow). (b) Enumeration of total facultative anaerobes (black), lactose fermenting (LF) Enterobacteriaceae (red), *Enterococcus* spp. (green), and *Lactobacillus* spp. (purple). Results show bacterial population changes in response to clindamycin therapy. Data shown are the mean log_{10} CFU/mL \pm standard error from three technical replicates per day of a single biological replicate. Clind – clindamycin



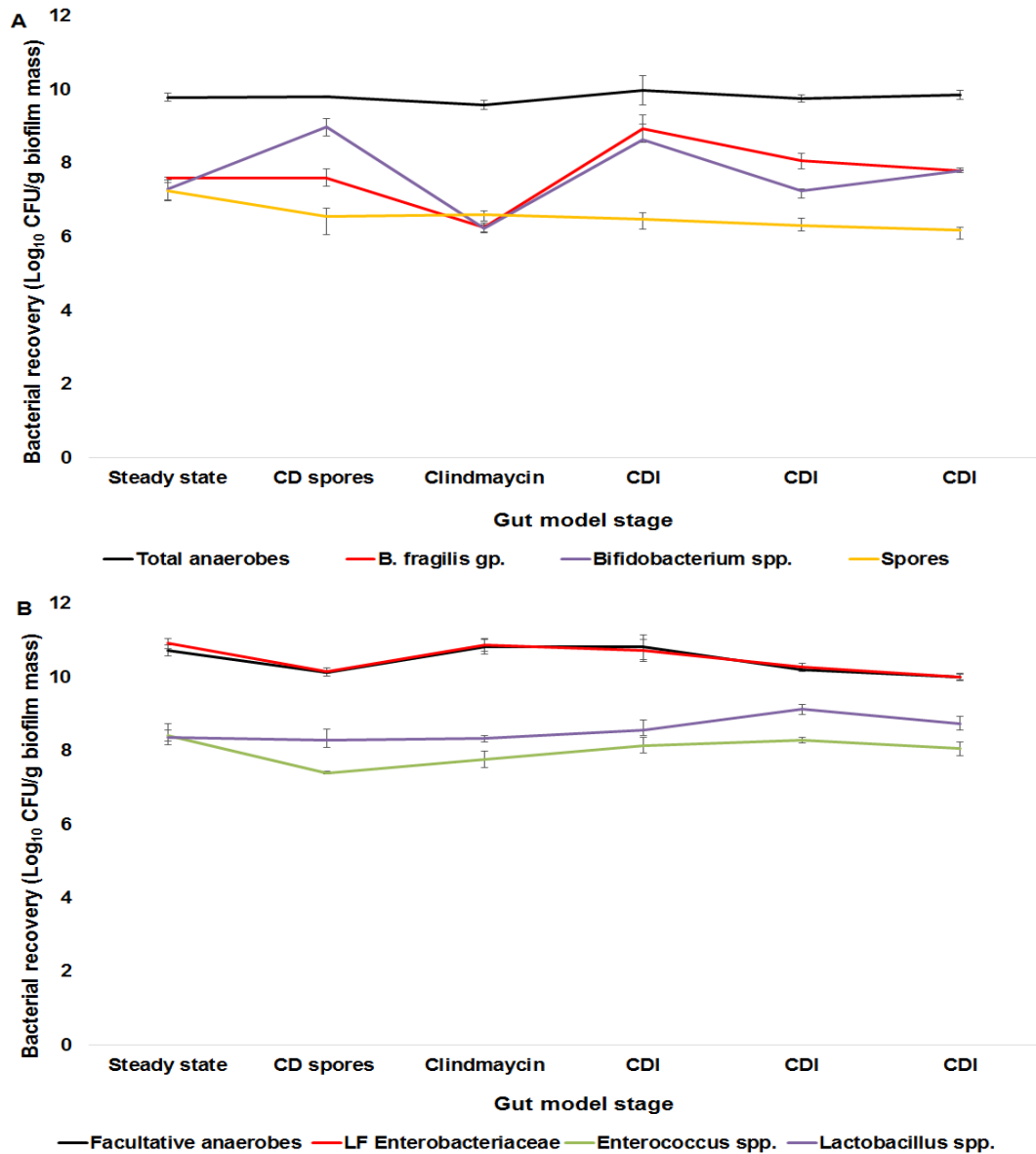
Enumeration of biofilm populations in a *C. difficile* naïve model during clindamycin treatment. (a) Enumeration of total anaerobes (black), *B. fragilis* gp. (red), *Clostridium* spp. (green), *Bifidobacterium* spp. (purple), and spores (yellow). (b) Enumeration of total facultative anaerobes (black), lactose fermenting (LF) Enterobacteriaceae (red), *Enterococcus* spp. (green), and *Lactobacillus* spp. (purple). Results show bacterial population changes in response to clindamycin therapy. Data shown are the mean log_{10} CFU/g biofilm mass \pm standard error from three technical replicates at selected time points of a single biological replicate, at various stages throughout the model timeline. Clind – clindamycin



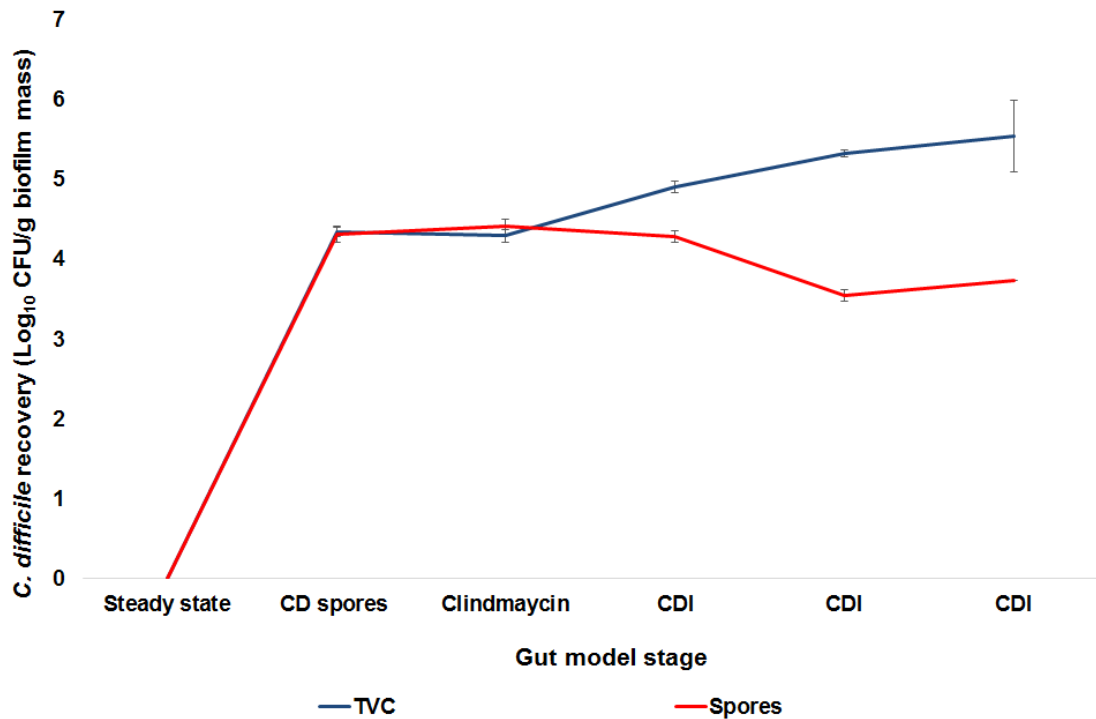
Enumeration of biofilm populations in a simulated *C. difficile* infection model during clindamycin treatment. (a) enumeration of total anaerobes (black), *B. fragilis* gp. (red), *Clostridium* spp. (green), *Bifidobacterium* spp. (purple), and spores (yellow). (b) Enumeration of total facultative anaerobes (black), lactose fermenting (LF) Enterobacteriaceae (red), *Enterococcus* spp. (green), and *Lactobacillus* spp. (purple). Results show bacterial population changes in response to clindamycin therapy. Data shown are the mean log_{10} CFU/mL \pm standard error from three technical replicates per day of a single biological replicate. Clind – clindamycin, CD- *C. difficile*, CDI – *C. difficile* infection



Enumeration of planktonic *C. difficile* total and spore counts recovered from the simulated *C. difficile* infection model. Bacterial enumeration of *C. difficile* total viable counts (TVC - blue) and spore counts (red). Data demonstrates detection of *C. difficile* spore germination, vegetative outgrowth and toxin. Data shown are the mean log₁₀ CFU/mL ± standard error from three technical replicates per day of a single biological replicate. Clind – clindamycin, CD- *C. difficile*, CDI – *C. difficile* infection



Enumeration of biofilm populations in a simulated *C. difficile* model during clindamycin treatment. (a) Enumeration of total anaerobes (black), *B. fragilis* gp. (red), *Clostridium* spp. (green), *Bifidobacterium* spp. (purple), and spores (yellow). (b) Enumeration of total facultative anaerobes (black), lactose fermenting (LF) Enterobacteriaceae (red), *Enterococcus* spp. (green), and *Lactobacillus* spp. (purple). Results show bacterial population changes in response to clindamycin therapy. Data shown are the mean \log_{10} CFU/g biofilm mass \pm standard error from three technical replicates at selected time points of a single biological replicate, at various stages throughout the model timeline. Clind – clindamycin, CD- *C. difficile*, CDI – *C. difficile* infection.



Enumeration of *C. difficile* total and spore counts recovered from the biofilm in the simulated *C. difficile* infection model. Bacterial enumeration of *C. difficile* total viable counts (TVC - blue) and spore counts (red). Data demonstrates the persistence of *C. difficile* cells in the biofilm through clindamycin therapy. Data shown are the mean log₁₀ CFU/g biofilm mass \pm standard error from three technical replicates at selected time points of a single biological replicate, at various stages throughout the model timeline. Clind – clindamycin, CD – *C. difficile*, CDI – *C. difficile* infection, TVC – total viable counts.

A.6 *C. difficile luxS* mutagenesis using homologous recombination by allele exchange.

The following *C. difficile* mutagenesis was performed using the method described in Faulds-Pain and Wren (2013).

Bacterial strains and growth conditions

C. difficile PCR ribotype 027 strain R20291 was grown for 48 hours anaerobically on CBA. Chemically competent *Escherichia coli* TOP10 (Invitrogen, UK), used as a cloning host, and the conjugal donor *E. coli* CA434 (supplied by Dr Anthony Buckley, University of Leeds), were cultured aerobically on Luria-Bertani (LB) agar, supplemented with chloramphenicol (15 µg/mL) and kanamycin (25 µg/mL), where appropriate. Mutated *C. difficile* was routinely grown on BHISC agar plates supplemented with 5% egg yolk and 15 µg/mL thiamphenicol, 250 µg/ mL D-cycloserine and 8 µg/ mL cefoxitin , where appropriate.

Knockout plasmid construction

Primers were designed based on the *C. difficile* R20291 genome sequence from the Artemis genome browser (Version 16.0.0, Wellcome Trust Sanger Institute) and all primers used are listed in Table 1. CLC Genomics Workbench (version 7.5.1) was used for the *in silico* design of the four primers (2 x homology arm 1 primers and 2 x homology arm 2 primers) required to generate the knockout (KO) *luxS* gene (Figures 1 and 2). To increase the frequency of recombination events, primers were designed to amplify approximately 1200 bp up- and downstream of the *luxS* gene. Homology arm 1 (HA1) primers were designed to amplify 1355 bp in total, including the first 12 bp of the *luxS* gene to incorporate the promoter sequence and start codon. Homology arm 2 (HA2) primers were designed to amplify a total of 1414 bp, including 15 bp of the *luxS* gene to incorporate the stop codon and an additional 50 bp of the gene due to any potential overlap with a promoter sequence of the adjacent gene to prevent downstream polar effects. Both HA1 and HA2 contained sequences to match the restriction sites for plasmid integration (green, Figure 2) and an overlapping complementary region of 25 bp (red, Figure 2). Additional primers were designed to amplify the entire KO construct and the primer binding site located outside of the HA regions. Primer binding position is represented in Figure 1.

Table 1. Oligonucleotides and respective binding sites and sequences

Oligonucleotide	Binding site	Sequence (5'-3')
CDR luxS KO HA1 F	Primer set to amplify upstream and start of CDR-luxS –homology arm 1.	GCGTGACGTCGACTCTAGAGGATCCGTGAGATATCTGTAAT TAATCAACT
CDR luxS KO HA1 R		TTATCTAAAACATCTTTTGCATATTTTTTCCATTATTTAATC CT
CDR luxS KO HA2 F	Primer set to amplify upstream and start of CDR-luxS –homology arm 2.	AATGGAGGATTAATAATGGAAAAAATATGCAAAAGATG TTTTA
CDR luxS KO HA2 R		TGATTACGAATTCGAGCTCGGTACCCACCTTCATCAAATG TCAT
Forward primer for pMTL82151	Primer set to confirm homology arm insertion into plasmid	CAGGAAACAGCTATGACC
Reverse primer for pMTL82151		TGTA AACGACGGCCAGT
CDR_LuxS F	KO confirm primer set(outside HA region)	GCTGTGCTTTAACTTCAATGCTTA
CDR_LuxS R		CTCCTATTGCATCTACACCTAGACC
CDR_LuxS F	KO confirm primer set(inside HA region)	ACAATGTCACACACTTCTTC
CDR_LuxS R		ACA ACTGCCAATAATACAAT

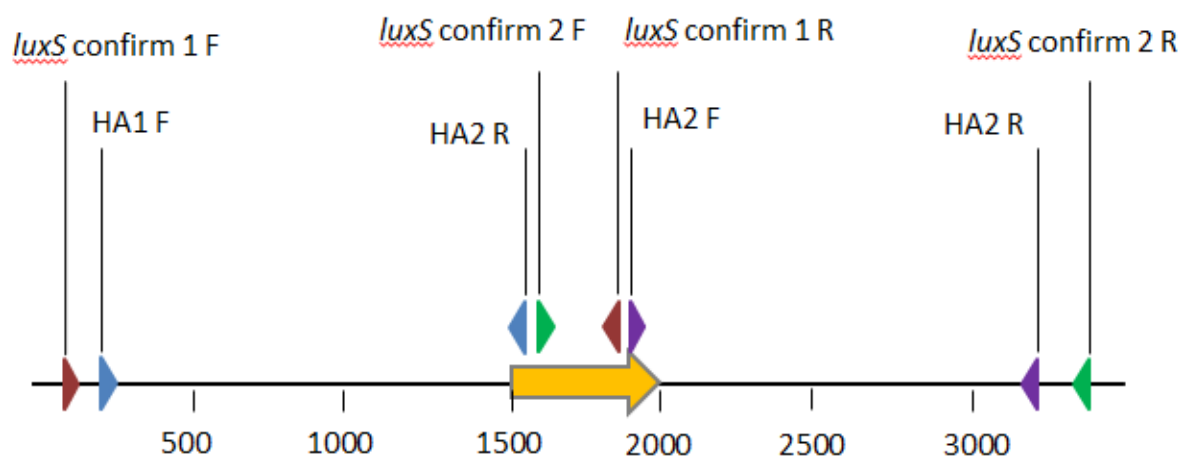


Figure 1. The graphical representation of the *C. difficile luxS* gene (yellow arrow) and the different primer binding sites. Homology arm 1 (HA 1) forward and reverse primers (blue) were designed to amplify the region approximately 1200 bp before and including the start codon. Homology arm 2 (HA2) forward and reverse primers (purple) were designed to amplify the region approximately 1200 bp downstream and including the stop codon. Primers located outside of the homology regions (*luxS* confirm 1F- red and *luxS* confirm 2R- green) were designed to amplify the region spanning both homology arms and the *luxS* gene.

Using the extracted genomic DNA from *C. difficile* and the primers for HA1 and HA2, HA1 and HA2 regions were amplified using PCR (Prime Thermal Cycler, 5PRIMEG/02, Thechne), see Table 2 for reaction and program parameters. PCR products were run on a 1.2 % agarose gel (gel electrophoresis in TBE buffer, run at 120V for 1 hour) to confirm the product size and then they were purified from PCR reaction mix using the QIAquick PCR Purification kit (Qiagen, Germany). HA1 and HA2 fragments were joined using the Gibson Assembly® (New England Biolabs) (2.5 µL each HA purified fragment, 5 µL Gibson master mix for 50°C for 1 hour) and the product amplified using primers HA1 (F) and HA2 (R) (Table 1). The HA PCR product was run on a 0.8% agarose gel (100V for 2 hours) to confirm an approximately 2700 bp size product.

The shuttle vector pMTL82151 was enzyme digested using restriction enzymes BamH-HF and Kpn1-HF (New England Biolabs)(1 µL each enzyme, 1 µL plasmid, 5 µL NE buffer made up to 50 µL with PCR grade water and kept at 37°C for 1 hour before the reaction was stopped with the addition of gel loading dye). Shuttle vector pMTL83151 was initially used but failed to conjugate into *C. difficile*. The cut pMTL82151 plasmid was then run on a 0.8% agarose gel (80V for 2 hours) before extraction with the QIAquick Gel Extraction kit (Qiagen, Germany) and eluted in 30 µL PCR grade water. The pMTL82151 *luxS* KO construct was assembled using the Gibson Assembly® kit (2 µL HA purified construct, 5 µL Gibson master mix for 50°C for 1 hour) (Figure 2 and Figure 3).

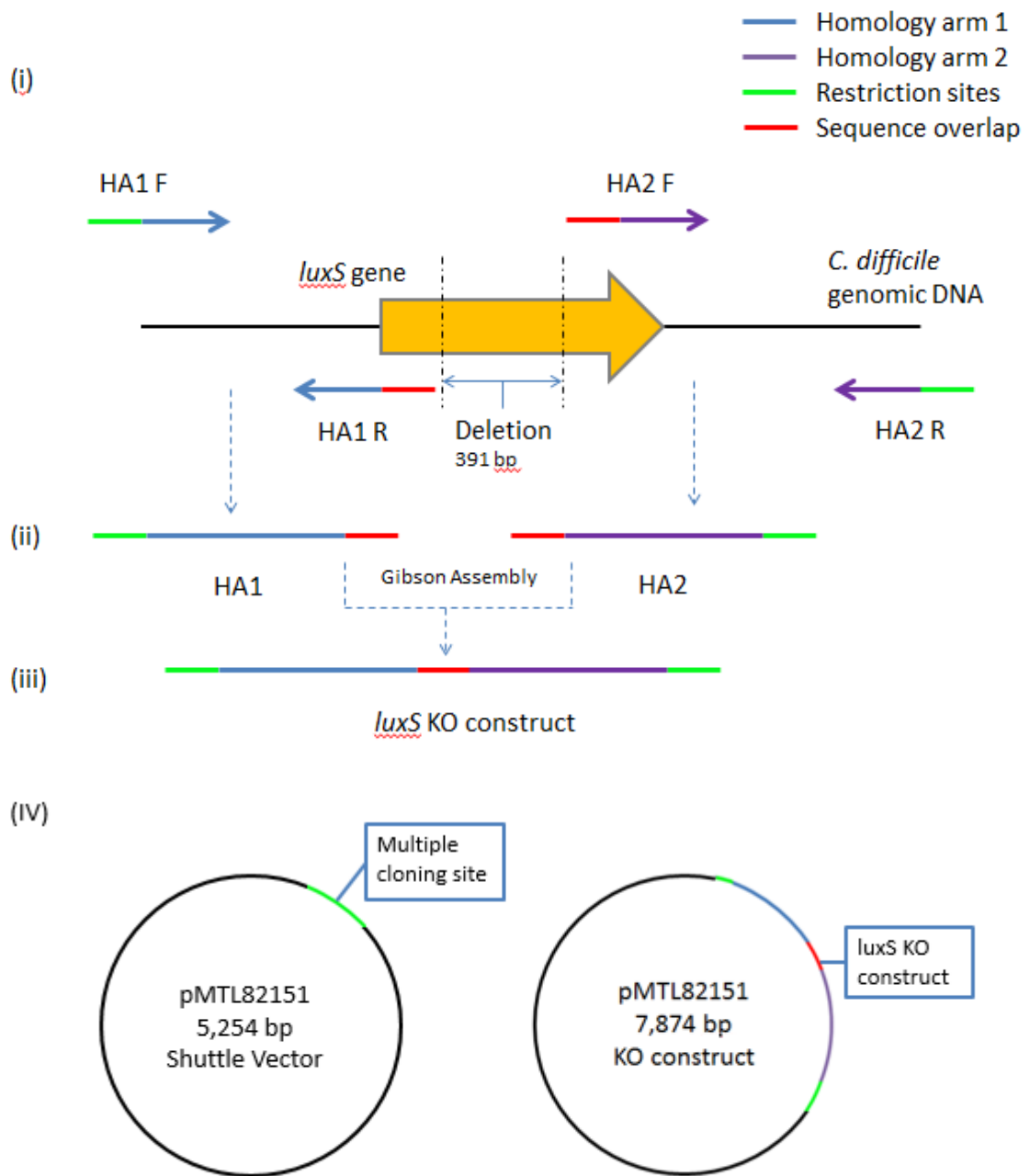


Figure 2. Graphical representation of the mutagenesis of the *C. difficile luxS* gene. (i) The primer binding sites for homology arm 1 (HA1 forward and reverse primers) and the primer binding sites for homology arm 2 (HA2 forward and reverse primers). Both sets of primers consist of a region of homology with the *C. difficile* genome (HA1 – blue arrow, HA2 – purple arrow) and either a region of homology with the plasmid restriction site (green) or an overlapping sequence (red). (ii) Once both homology arms have been amplified, the HA1

and HA2 PCR products are purified and assembled into a single construct (iii) using the Gibson assay and mediated by the overlapping sequence (red). (iv) The shuttle vector pMTL82151 is then enzyme digested at the multiple cloning site with restriction enzymes matching the sequence on the KO construct (green). The KO construct is then inserted into the cut plasmid using the Gibson assay to create a pMTL82151 plasmid carrying a mutated *luxS* gene.

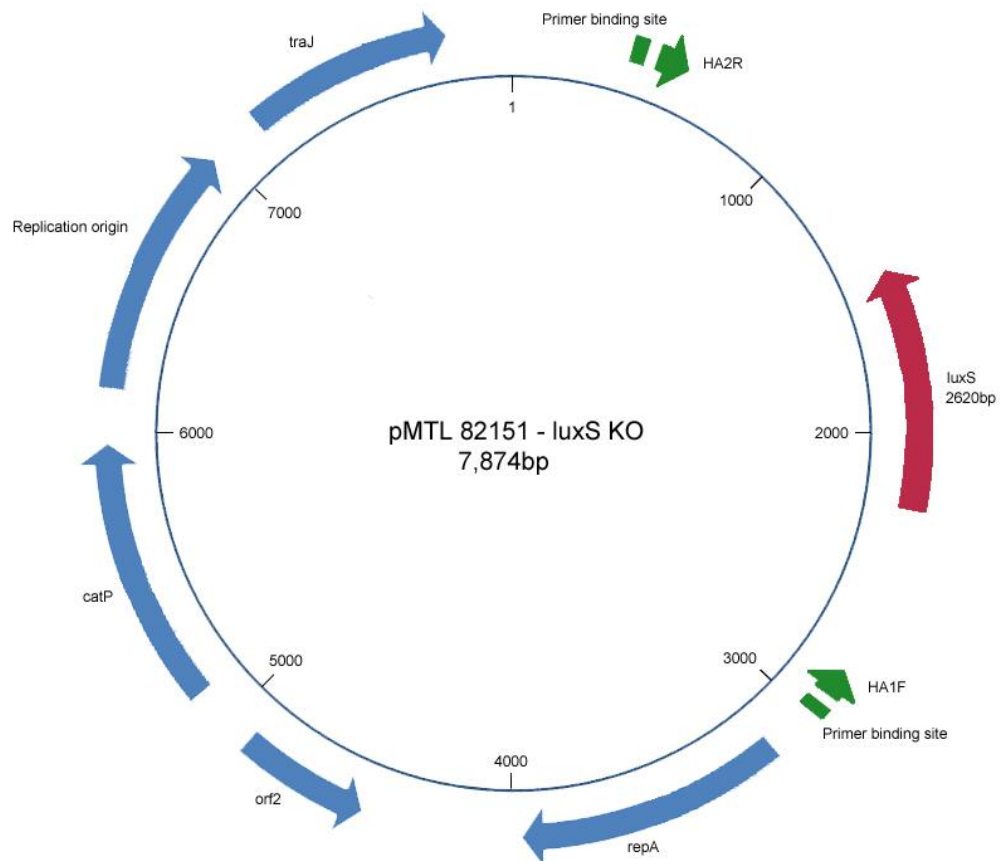


Figure 3. *In silico* schematic of the pMTL82151 shuttle vector with the *luxS* KO homology recombination construct inserted into the multiple cloning site. The green bars represent the restriction binding sites; the green arrows indicate the homology arm binding sites and direction. The red arrow illustrates the mutated *luxS* gene with a 391 bp deletion. Blue arrows represent genes present on the plasmid and include the regulatory protein A (*repA*), the putative plasmid replication protein (*orf2*), chloramphenicol acetyltransferase (*catP*), the replication origin and the protein transfer (*traJ*).

Transformation

The pMTL82151 *luxS* KO construct was then transformed into *E. coli* TOP10 cells and 100 μ L plated onto LB agar plates supplemented with chloramphenicol (15 μ g/ mL) and incubated aerobically at 37°C for 24 hours to select for transformed cells. *E. coli* TOP10 was retained at room temperature overnight and was concentrated by centrifugation (16 000g for 3 mins) and plated onto fresh LB agar plates supplemented with chloramphenicol (15 μ g/ mL) and incubated aerobically at 37°C for 24 hours. Putative colonies were plated onto fresh supplemented LB agar and after overnight incubation, and were then grown in 10 mL LB broth supplemented with chloramphenicol (15 μ g/ mL) overnight at 37°C. 3 mL of the overnight culture was then centrifuged (16 000g, 5 mins) and the supernatant discarded. The plasmid was extracted from the remaining pellet using the QIAprep Spin Miniprep kit (Qiagen, Germany). The homology construct within the plasmid was then amplified using plasmid primers flanking the insert region (Table 1). The PCR product was run on a 1% gel (120V for 2.5 hours) to confirm the size of an approximately 3000 bp and the construct was confirmed by sequencing.

The plasmid was then transferred to heat-competent *E. coli* CA434 cells. 3 μ L of the plasmid was added to *E. coli* CA434 cells, gently mixed and left on ice for 20 mins followed by heat shock at 42°C for 30s and then placed at -20°C for 5 mins. 1 mL of 37°C SOC (Invitrogen, UK) was added and left to gently shake for 6 hours. 100 μ L of the solution was then plated onto LB agar supplemented with chloramphenicol (15 μ g/ mL) and kanamycin (25 μ g/ mL). Clones were confirmed by plasmid extraction, PCR and gel electrophoresis, as above.

Table 2. PCR reaction composition and respective PCR program settings for the different PCR amplification steps.

Description	PCR reaction	PCR program settings
HA1 and HA2 amplification	25 µL Phusion® high-fidelity PCR master mix 0.5 µL of each primer, final concentration 2.5 µM 2 µL <i>C. difficile</i> template DNA 0.5 µL DMSO 21.5 µL PCR grade water	Initial denaturation 95°C for 5 mins Amplification x 30 cycles Denaturation 95°C for 30s Anneal 50°C for 30s Extension 68°C for 90s Elongation 72°C for 10 mins
Homology arm assembly	25 µL Phusion® high-fidelity PCR master mix 2 µL HA construct from the Gibson Assembly 0.5 µL of HA1 (F) primer 0.5 µL of HA2 (R) primer 0.5 µL DMSO 21.5 µL PCR grade water	Initial denaturation 95°C for 5 mins Amplification x 30 cycles Denaturation 95°C for 30s Anneal 50°C for 30s Extension 68°C for 120s Elongation 72°C for 10 mins
KO construct confirm	10 µL Phusion® high-fidelity PCR master mix 1µL pMTL82151 plasmid containing KO construct 0.3 µL of pMTL forward primer 0.3 µL of pMTL reverse primer 0.5 µL DMSO 7.9 µL PCR grade water	Initial denaturation 95°C for 5 mins Amplification x 30 cycles Denaturation 95°C for 30s Anneal 50°C for 30s Extension 68°C for 170s Elongation 72°C for 10 mins

Conjugation

Wild type *C. difficile* was grown in BHISC broth for 24 hours anaerobically. Overnight cultures of *E. coli* CA434 harbouring the KO plasmid in LB broth supplemented with chloramphenicol and kanamycin (15 µg/ mL and 25 µg/ mL,

respectively), were centrifuged at 16 000 g for 2 mins and the pellet gently washed in 1 mL PBS before centrifuging again as above, and the supernatant discarded. The *E. coli* pellet was then transferred to the anaerobic cabinet where it was gently resuspended in 200 μ L of the *C. difficile* culture. This step is best carried out using a 1 mL pipette tip to avoid breaking the conjugation pili on the *E. coli*. The resultant solution was then dotted onto 4 pre-reduced BHISC agar plates (supplemented with 5% egg yolk) and incubated anaerobically for 24 hours. All growth was scraped off the culture plates and resuspended in pre-reduced PBS. This was then plated out neat or 1:10 dilution on pre-reduced BHISC agar (supplemented with 5% egg yolk, 15 μ g/mL thiamphenicol, 250 μ g/mL D-cycloserine and 8 μ g/mL ceftiofur) and incubated for 3 days anaerobically. The largest colonies after 3 days growth were restreaked onto fresh supplemented BHISC media, as above, and this process was repeated three times to allow for the first crossover event to occur. The second crossover event was mediated by restreaking the cells from the selective plates on to non-selective media (BHISC supplemented with 5% egg yolk) and incubated anaerobically for 24 hours. This step was repeated five times before colonies were patch plated on non-selective (BHISC supplemented with 5% egg yolk) and selective (BHISC supplemented with 5% egg yolk and 15 μ g/mL thiamphenicol) media. *C. difficile* colonies with growth on non-selective media and no growth on selective media were indicative of double crossovers. These clones were checked by PCR to look for mutants and wild type revertants and the former was sent for sequencing to confirm no errors at the gene loci. The mutants contained a 391 bp deletion in the *luxS* gene, however, start and stop codons were still present, thus preventing polar effects of downstream genes.